

THE ROLE OF THE NMDA RECEPTOR AND REVERSE SODIUM
CALCIUM EXCHANGER IN CALCIUM DYSREGULATION IN
GLUTAMATE-EXPOSED NEURONS

Matthew K Brittain

Submitted to the faculty of the University Graduate School
in partial fulfillment of the requirements
for the degree of
Doctor of Philosophy
in the Department of Pharmacology and Toxicology,
Indiana University

June 2012

Accepted by the Faculty of Indiana University, in partial fulfillment of the requirements for the degree of Doctor of Philosophy.

Nickolay Brustovetsky, Ph. D., chairman

Theodore R. Cummins, Ph. D.

Doctoral Committee

Richard M. Nass, Ph. D.

Grant D. Nicol, Ph. D.

Michael R. Vasko, Ph. D.

April 16, 2012

DEDICATION

This thesis is dedicated to my wife, Nicole, for her unwavering love and sacrifice throughout the long hours and many years of work, and for her willingness to take care of our son when I was traveling to complete my dissertation during the final 18 months. Without her support and confidence in me, this dream of mine would never have been realized. I would also like to dedicate this thesis to my son, Benjamin, for his sacrifice during the first year and a half of his life, as I was absent a significant portion of that time.

ACKNOWLEDGEMENTS

First of all I would like to thank my research mentor Dr. Nickolay Brustovetsky. He has been steadfast in his commitment to develop me into a quality scientist. He has challenged me and engaged in countless hours of conversations to push my critical thinking and scientific understanding to new intellectual levels. This has been vital for me to not only critically evaluate scientific literature but also to be a critic of my own work. Dr. Brustovetsky has also helped me identify areas in which I was deficient and aided me in developing them. Although difficult at times, this will be and has been an immeasurable benefit in my development as a scientist. Throughout my tenure under Dr. Brustovetsky's guidance, he has helped me publish and submit grant applications. I have gained an enormous amount of respect for this process and have learned what it takes to develop a scientific story. Even though, Dr. Brustovetsky and I, have had our differences, I honestly consider him to be a close friend.

In addition to Dr. Brustovetsky, I would be remiss if I did not thank Tatiana Brustovetsky. She taught me the skills needed to master fluorescence imaging of cultured neurons. She was also willing to help troubleshoot issues that occurred throughout my research. She also, without reservation, made sure that everything in the lab was in perfect order so that our research could continue without hindrance. I want to especially thank Tatiana for her work on a weekly basis to provide uniformed and consistent cultured neurons for my scientific study. Without her help none of my research would have been possible.

I also must give credit to my doctoral research committee for their guidance and suggestion in directing my research focus and hypothesis. Through their critical evaluation of my data and scientific thinking, I was able to adjust and develop a complete, cohesive thesis. I would especially like to thank Dr. Theodore Cummins for acting as the chair of my committee. He helped guide me through the final stages of my thesis preparation and was a calming, steady voice of reason and understanding during difficult decisions.

Also, I want to thank both Dr. Juan Gonzalez and Dr. James Williams. Dr. Gonzalez is a mentor and friend who was very supportive before and throughout my doctoral studies. I consider Juan to be a very close friend and an endless source of knowledge. Also throughout my time at Indiana University, Dr. Williams has become a very close friend, and one that I have relied heavily on to help push me when dealing with difficult outside issues. He has been a source of endless prayer and guidance, keeping me focused on my goals and what is important in life. Thank you to both of these individuals for I could not have accomplished this endeavor without them in my corner.

Finally, I must give praise to my Lord and savior, Jesus Christ, for giving me the drive and support to take on and finish this endeavor. Only through His power was any of this possible.

ABSTRACT

Matthew K. Brittain

THE ROLE OF THE NMDA RECEPTOR AND REVERSE SODIUM CALCIUM EXCHANGER IN CALCIUM DYSREGULATION IN GLUTAMATE-EXPOSED NEURONS

Introduction: During glutamate excitotoxicity, overstimulation of glutamate receptors leads to sustained elevation in cytosolic Ca^{2+} ($[\text{Ca}^{2+}]_c$), or delayed Ca^{2+} dysregulation (DCD), which is causally linked to cell death. There are two major hypothetical mechanisms for DCD: the continuous activation of N-methyl-D-aspartate-subtype of the ionotropic glutamate receptors (NMDAR) and the reversal of the plasmalemmal $\text{Na}^+/\text{Ca}^{2+}$ exchanger. However, the contribution of each of these mechanisms in DCD is not completely established.

Major results: Neurons exposed to excitotoxic glutamate produced DCD, an increase in cytosolic Na^+ ($[\text{Na}^+]_c$), and plasma membrane depolarization. MK801 and memantine, noncompetitive NMDAR inhibitors, added after glutamate, completely prevented DCD; however AP-5, a competitive NMDAR inhibitor, failed to do so. The NMDAR inhibitors had no effect on lowering elevated $[\text{Na}^+]_c$ or on restoring plasma membrane potential, which are conditions suggesting NCX_{rev} could be involved. In experiments inducing NCX_{rev} , MK801 and memantine completely inhibited Ca^{2+} dysregulation after glutamate while AP-5 did not. Inhibition of NCX_{rev} , either with KB-R7943 or by preventing the increase in $[\text{Na}^+]_c$, failed to avert DCD. However, NCX_{rev} inhibition combined with

NMDAR blocked by AP-5 completely prevented DCD. Overall, these data suggested that both NMDAR and NCX_{rev} are essential for glutamate-induced DCD, and inhibition of only one mechanism is insufficient to prevent collapse of calcium homeostasis.

Based on the data above, we investigated a NMDA receptor antagonist currently in clinical trials for reducing the effects of glutamate excitotoxicity, ifenprodil. Ifenprodil is an activity-dependent, NMDAR inhibitor selective for the NR2B subunit. We found that ifenprodil not only inhibited the NR2B-specific NMDAR, but also inhibited NCX_{rev} . If ifenprodil is combined with PEAQX, a NMDAR inhibitor selective for the NR2A subunit, low concentrations of both inhibitors completely prevent DCD.

Conclusion: The inhibition of a single Ca^{2+} influx mechanism is insufficient in preventing DCD, which requires simultaneous inhibition of both the NMDAR and NCX_{rev} . These findings are critical for the correct interpretation of the experimental results obtained with these inhibitors and for better understanding of their neuroprotective actions.

Nickolay Brustovetsky, Ph. D., chairman

TABLE OF CONTENT

List of Figures	xiii
List of Abbreviations.....	xx
I. INTRODUCTION.....	1
A. Historical background on “Glutamate excitotoxicity”	4
B. Calcium homeostasis and “delayed calcium dysregulation”	7
C. Possible mechanism(s) for glutamate-induced delayed calcium dysregulation.....	10
1. Continuous-activation of glutamate receptors.....	10
2. Failure of the plasmalemmal sodium calcium exchanger (NCX).....	24
3. Failure of the mitochondrial calcium accumulation	32
D. Cell death caused by calcium dysregulation	37
E. Hypothesis and specific aim.....	38
II. MATERIALS AND METHODS	43
A. Materials	43
B. Cell culturing	43
C. Fluorescence imaging of cultured neurons	44
1. Measurements of cytosolic calcium concentration ($[Ca^{2+}]_c$)	45
2. Measurements of cytosolic sodium concentration ($[Na^+]_c$).....	50
3. Measurements of mitochondrial membrane potential ($\Delta\psi$): Rhodamine 123	52
4. Measurements of nicotinamide adenine dinucleotide (NADH) redox state	54

5. Measurements of Reactive Oxygen Species (ROS): dihydroethidium.....	55
6. Measurements of plasma membrane potential: Annine-6plus	56
7. Measurements of changes in cytosolic pH: BCECF-AM.....	57
D. Calcium and sodium fluorescence signal converted to concentration.....	58
E. Isolation and purification of brain mitochondria	60
F. Measurements of mitochondrial respiration and Ca ²⁺ uptake.....	61
G. Patch-clamp electrophysiology	62
H. Cellular respirometry.....	63
I. Western blotting	63
J. Glutamate measurements	64
K. Statistics.....	65
III. RESULTS	66
A. What are the effects of prolonged glutamate exposure on cultured hippocampal neurons from rats?	66
1. Prolonged glutamate exposure causes cytosolic Ca ²⁺ dysregulation and mitochondrial depolarization	66
2. Prolonged glutamate exposure causes the “uncoupling” of the respiratory chain and oxidative phosphorylation	70
3. Prolonged glutamate exposure causes an increase in the presence of superoxide radicals in cytosol	73
4. Prolonged glutamate exposure causes an increase in both cytosolic Ca ²⁺ and Na ⁺ simultaneously	76
5. Prolonged glutamate exposure causes a decrease in cytosolic pH	78

B. What is the contribution of the reverse mode of the Na ⁺ /Ca ²⁺ exchanger on glutamate-induced delayed calcium dysregulation?	81
1. KB-R7943 inhibits the reverse mode of the Na ⁺ /Ca ²⁺ exchanger, but it fails to protect neurons against glutamate-induced delayed calcium dysregulation	82
C. What is the contribution of the NMDA receptors on glutamate-induced delayed calcium dysregulation?	103
1. NMDA receptor antagonists are inconsistent concerning their ability to prevent glutamate-induced delayed calcium dysregulation; however all fail to prevent glutamate-induced increase in cytosolic sodium.....	107
2. Antagonizing ionotropic glutamate receptors has not effect on glutamate-induced increase in cytosolic Na ⁺ and plasmalemmal depolarization	111
3. MK801 and memantine, glutamate receptor antagonists, inhibit the reverse mode of the Na ⁺ /Ca ²⁺ exchanger	122
4. Tested NMDA receptor antagonists have no adverse effects on the forward mode of the Na ⁺ /Ca ²⁺ exchanger	140
5. Combined inhibition of the reverse of the Na ⁺ /Ca ²⁺ exchanger and the NMDA receptor completely prevented glutamate-induced delayed calcium dysregulation	142
D. Does ifenprodil inhibit both the NMDA receptor and the reverse mode of the Na ⁺ /Ca ²⁺ exchanger?	150

1. Ifenprodil and PEAQX, selective NMDA receptor antagonists, differentially block calcium influx induced by NMDA	153
2. Ifenprodil and PEAQX, selective NMDA receptor antagonists, differentially block calcium influx induced by glutamate	158
3. Ifenprodil, an NR2B-containing NMDA receptor antagonist, inhibits the reverse mode of the Na ⁺ /Ca ²⁺ exchanger	162
IV. DISCUSSION	166
A. Inhibition of the reverse mode of the Na ⁺ /Ca ²⁺ exchanger alone fails to prevent glutamate-induced delayed calcium dysregulation	166
1. Glutamate exposure results in “uncoupling” of the respiratory chain and oxidative phosphorylation	168
2. KB-R7943 inhibits Complex I on the mitochondrial respiratory chain	170
3. Experiments with isolated mitochondria confirm that KB-R7943 inhibits Complex I on the respiratory chain and thus, depolarize the mitochondria and reduce its ability to accumulate calcium	171
B. Inhibition of the NMDA receptor alone fails to prevent glutamate- induced delayed calcium dysregulation, but simultaneous inhibition of both the NMDA receptor and the reverse mode of the Na ⁺ /Ca ²⁺ exchanger strongly prevented this phenomenon.....	174
1. MK801 and memantine inhibit both the NMDA receptor and the reverse mode of the Na ⁺ /Ca ²⁺ exchanger and thus, prevent glutamate- induced delayed Ca ²⁺ dysregulation	177

2. Tested NMDA receptor antagonists produce mixed results concerning the NMDA receptor importance in glutamate-induced delayed calcium dysregulation	178
3. The reverse mode of the Na ⁺ /Ca ²⁺ exchanger is sufficient to produce glutamate-induced delayed Ca ²⁺ dysregulation	179
C. Ifenprodil inhibits both the N2R-containing NMDA receptor and the reverse mode of the Na ⁺ /Ca ²⁺ exchanger confirming our hypothesis that both routes of Ca ²⁺ influx are sufficient for producing glutamate-induced delayed calcium dysregulation	180
1. Ifenprodil and PEAQX, NR2B- and NR2A- containing NMDA receptor antagonists, respectively, have differential inhibitor abilities depending on age of neurons	181
2. Ifenprodil, not PEAQX, inhibit the reverse mode of the Na ⁺ /Ca ²⁺ exchanger	181
3. Ifenprodil inhibit both the NMDA receptor and the reverse mode of the Na ⁺ /Ca ²⁺ exchanger confirms results suggesting that both Ca ²⁺ influx routes are sufficient to produced glutamate-induced delayed calcium dysregulation	184
V. SUMMARY AND CONCLUSIONS	186
V. REFERENCES	189
CURRICULUM VITAE	

LIST OF FIGURES

Figure 1. Pictorial scheme of the electron transport chain and oxidative phosphorylation located on the inner mitochondrial membrane.....	33
Figure 2. Scheme represents the central hypothesis and specific aims of this thesis.....	42
Figure 3. Glutamate induces dysregulation in cytosolic calcium concentration and mitochondrial depolarization in cultured rat hippocampal neurons.....	67
Figure 4. Inhibition of the forward mode of the NCX or mitochondrial calcium accumulation results in immediate calcium dysregulation after glutamate exposure.....	69
Figure 5. Glutamate evoked NAD(P)H oxidation which was either coupled 3 (in the absence of external Ca^{2+}) or uncoupled (with external Ca^{2+}) from ATP synthesis.....	71
Figure 6. Increase in reactive oxygen species during glutamate exposure is a result of calcium accumulation by the mitochondria.....	74
Figure 7. Glutamate induces an increase in both in cytosolic calcium and sodium in cultured hippocampal neurons from rats.....	77
Figure 8. Inhibition of glutamate receptors and/or voltage-gated sodium 3channels fails to prevent glutamate-induced increase cytosolic sodium.....	79
Figure 9. Glutamate induces an increase in cytosolic proton concentration resulting in intracellular acidification in cultured hippocampal neurons.....	80

Figure 10. KB-R7943 accelerates delayed calcium deregulation and mitochondrial depolarization in cultured hippocampal neurons exposed to glutamate	83
Figure 11. MK801, an inhibitor of NMDA receptor, inhibits glutamate- and NMDA-induced calcium deregulation while CNQX, an inhibitor of AMPA/kainate receptors, is without effect.....	84
Figure 12. KB-R7943 inhibits gramicidin-induced increase in cytosolic Ca^{2+} concentration ($[Ca^{2+}]_c$) in cultured hippocampal neurons (A-C)	86
Figure 13. Gramicidin exposure results in conditions that are favorable for the reverse mode of the Na^+/Ca^{2+} exchanger (NCX) to occur.....	87
Figure 14. NCXrev currents obtained with cultured hippocampal neurons from rats.....	88
Figure 15. Patch-clamp recordings of NMDA-induced whole-cell currents obtained with cultured hippocampal neurons from rats.....	90
Figure 16. KB-R7943 inhibits NMDA-induced increases in cytosolic Ca^{2+}	91
Figure 17. KB-R7943 increases NAD(P)H fluorescence under resting conditions and suppressed glutamate-induced NAD(P)H oxidation similar to rotenone.....	93
Figure 18. KB-R7943 depolarizes mitochondria and this is accelerated by ultra-low concentration of FCCP in cultured hippocampal neurons.....	95
Figure 19. In cultured hippocampal neurons from rats, KB-R7943 depolarizes mitochondria in a Ca^{2+} -independent manner	96
Figure 20. KB-R7943-induces inhibition of cellular respiration.....	98

Figure 21. KB-R7943 depolarizes isolated brain mitochondria fueled with glutamate and malate, a mixture of Complex I substrates, but fails to depolarize mitochondria fueled with succinate, a Complex II substrate	100
Figure 22. KB-R7943 inhibits respiration of isolated brain mitochondria oxidizing malate plus glutamate, but fails to affect mitochondrial respiration supported by succinate	102
Figure 23. KB-R7943 hinders Ca^{2+} uptake by isolated brain mitochondria oxidizing glutamate and malate, but fails to inhibit Ca^{2+} uptake by mitochondria oxidizing succinate	104
Figure 24. MK801 and AP-5 inhibited NMDA-induced $[\text{Ca}^{2+}]_c$ increase (A, B), and MK801, but not AP-5, prevented glutamate-induced Ca^{2+} dysregulation (C, D)	106
Figure 25. MK801 and memantine but not AP-5 prevent sustained elevation in $[\text{Ca}^{2+}]_c$; however none of the tested inhibitors influence glutamate-induced $[\text{Na}^+]_c$ increase.....	108
Figure 26. Inhibition of voltage-gated calcium channel with ω -conotoxin and nifedipine have no effect on glutamate-induced calcium dysregulation	109
Figure 27. MK801 and memantine but not AP-5 prevent sustained elevation in $[\text{Ca}^{2+}]_c$, but none of the antagonists affect glutamate-induced $[\text{Na}^+]_c$ increase	110
Figure 28. NMDA receptor inhibitors antagonized NMDA-induced increases in $[\text{Ca}^{2+}]_c$	112

Figure 29. Patch-clamp recordings of NMDA-induced whole-cell currents recorded with cultured hippocampal neurons	114
Figure 30. NMDA-induced increases in $[Ca^{2+}]_c$. MK801, memantine, and AP-5 prevented sustained elevation in $[Ca^{2+}]_c$	115
Figure 31. KCl- and glutamate-induced plasma membrane depolarizations in cultured hippocampal neurons. Neither MK801, nor memantine, nor AP-5 prevent this membrane depolarization	116
Figure 32. NMDA-induced increases in $[Na^+]_c$. MK801, memantine, and AP-5 decrease $[Na^+]_c$	118
Figure 33. NMDA receptor antagonist prevent NMDA-induced increases in $[Ca^{2+}]_c$ and $[Na^+]_c$	119
Figure 34. The Na^+/K^+ ATPase reduce the cytosolic Na^+ concentration following the large Na^+ influx induced by NMDA stimulation	120
Figure 35. MK801, memantine, and AP-5 prevent NMDA-induced plasma membrane depolarizations in cultured hippocampal neurons	121
Figure 36. MK801 and memantine but not AP-5 inhibit gramicidin reversed Na^+/Ca^{2+} exchanger (NCX) leading to the increase in $[Ca^{2+}]_c$	123
Figure 37. MK801 and memantine but not AP-5 inhibit gramicidin-induced increase in cytosolic Ca^{2+} concentration ($[Ca^{2+}]_c$) in cultured hippocampal neurons	125
Figure 38. Inhibition of the NMDA receptor with MK801 has not effect on the increase in cytosolic Na^+ or plasma membrane depolarization induced by gramicidin	128

Figure 39. Low glutamate concentration induces sustained elevation in $[Ca^{2+}]_c$ under conditions of forward NCX shut down	129
Figure 40. Glutamate removal in the bath solution fails to prevent gramicidin-induced increase in $[Ca^{2+}]_c$	131
Figure 41. DL-TBOA inhibits the Na^+ /glutamate co-transporter, preventing endogenous glutamate release, has no effect on gramicidin-induced calcium dysregulation	132
Figure 42. Na^+ /NMDG ⁺ replacement induces an increase in sodium and calcium concentrations in cultured hippocampal neurons.....	133
Figure 43. Glutamate removal in the bath solution fails to prevent the increase in $[Ca^{2+}]_c$ induced by Na^+ /NMDG ⁺ replacement.....	135
Figure 44. Substitution of Na^+ with equimolar N-methyl-D-glucamine (NMDG ⁺) reverses Na^+ / Ca^{2+} exchanger (NCX) leading to the increase in $[Ca^{2+}]_c$. MK801 and memantine and to much lesser extent AP-5 inhibit the reverse NCX	137
Figure 45. MK801 and memantine but not AP-5 inhibit Na^+ /NMDG ⁺ replacement-induced increase in cytosolic Ca^{2+} concentration ($[Ca^{2+}]_c$) in cultured hippocampal neurons.....	138
Figure 46. The effects of Ni^{2+} , MK801, memantine, and AP-5 on NCX_{rev} -mediated ion currents recorded with cultured hippocampal neurons from rats.....	141
Figure 47. Tested NMDA receptor antagonists did not inhibit the forward mode of the Na^+ / Ca^{2+} exchanger	143

Figure 48. Glutamate-induced sustained elevation in $[Ca^{2+}]_c$ is inhibited by a combination of KB-R7943 and AP-5 but not by individual inhibitors applied separately..... 144

Figure 49. Glutamate-induced sustained elevation in $[Ca^{2+}]_c$ is inhibited by a combination of KB-R7943 and memantine (10 μ M) but not by individual inhibitors applied separately..... 146

Figure 50. Inhibition of forward and reverse Na^+/Ca^{2+} exchanger by eliminating Na^+ gradient across the plasma membrane permits complete inhibition of glutamate-induced calcium dysregulation by AP-5 148

Figure 51. EIPA but not MK801 inhibit the increase in $[Na^+]_c$ induced by glutamate 149

Figure 52. EIPA did not affect NMDA- and gramicidin-induced increases in $[Ca^{2+}]_c$ 151

Figure 53. Glutamate-induced sustained elevation in $[Ca^{2+}]_c$ is inhibited by a combination of EIPA and AP-5 but not by individual inhibitors applied separately 152

Figure 54. In “younger” neurons (6-8 DIV), ifenprodil completely inhibits Ca^{2+} influx induced by NMDA 154

Figure 55. In younger neurons, ifenprodil completely inhibits NMDA-induced increase in cytosolic Ca^{2+} whereas PEAQX was without effect..... 155

Figure 56. In “oldere” neurons (13-16 DIV), ifenprodil and PEAQX partially inhibits Ca^{2+} influx induced by NMDA. Combined application of ifenprodil and PEAQX completely block the $[Ca^{2+}]_c$ increase 156

Figure 57. In older neurons, ifenprodil and PEAQX partially inhibit NMDA-induced increase in cytosolic Ca^{2+} 157

Figure 58. NR2A and NR2B expression in cultured hippocampal neurons at 7 and 14 DIV 159

Figure 59. In “younger” neurons (6-8 DIV), ifenprodil but not PEAQX inhibit glutamate-induced sustained elevation in $[Ca^{2+}]_c$ 160

Figure 60. In “older” neurons (13-16 DIV), the combination of ifenprodil and PEAQX but not individual inhibitors applied separately completely prevent glutamate-induced sustained elevation in $[Ca^{2+}]_c$ 161

Figure 61. AP-5 inhibits NMDA-induced $[Ca^{2+}]_c$ increase (A,B) but fails to inhibit $[Ca^{2+}]_c$ increases mediated by the reverse Na^+/Ca^{2+} exchanger (C-F) or prevent glutamate-induced Ca^{2+} dysregulation (G,H)..... 163

Figure 62. Ifenprodil but not PEAQX inhibit the increases in $[Ca^{2+}]_c$ mediated by reversal of Na^+/Ca^{2+} exchanger triggered by gramicidin or by $Na^+/NMDG^+$ replacement..... 165

LIST OF ABBREVIATIONS

- AMPA: α -amino-3-hydroxy-5-methyl-4-isoxazolepropionic acid
- AP-5: (2*R*)-amino-5-phosphonopentanoate
- ASIC: calcium-permeable acid-sensing ion channels
- ATP: adenosine-5'-triphosphate
- BAPTA: 1,2-bis(*o*-aminophenoxy)ethane-*N,N,N',N'*-tetraacetic acid
- $[Ca^{2+}]_c$: cytosolic calcium concentration
- CNQX: 6-cyano-7-nitroquinoxaline-2,3-dione
- CycD: cyclophilin-D
- DCD: delayed Ca^{2+} dysregulation
- DIV: days in vitro
- ER: endoplasmic reticulum
- FCCP: carbonyl cyanide-*p*-trifluoromethoxyphenylhydrazone
- Glu: glutamate
- GluR: glutamate receptor
- GPCR: G-protein-coupled receptor
- iGluR: ionotropic glutamate receptor
- KA: kainite
- KB-R7943: 2-[2-[4-(4-nitrobenzyloxy)phenyl]ethyl]isothiourea
methanesulfonate
- K_d : dissociation constant
- mGluR: metabotropic glutamate receptor
- MK-801: Dizocilpine

- mNCX: mitochondrial NCX
- mPTP: mitochondrial permeability transition pore
- Mtc: mitochondria
- $[\text{Na}^+]_c$: cytosolic sodium concentration
- NADH: nicotinamide adenine dinucleotide
- NBQX: 2,3-dihydroxy-6-nitro-7-sulfamoyl-benzo[f]quinoxaline-2,3-dione
- NCKX: potassium-dependent NCX
- NCX: sodium calcium exchanger
- NCX_{fwd} : NCX in the forward mode
- NCX_{rev} : NCX in the reverse mode
- NHE: Na^+ - H^+ exchanger
- NMDG⁺: N-methyl-D-glucamine
- NMDA: *N*-methyl-*D*-aspartate
- NMDAR: *N*-methyl-*D*-aspartate receptor
- NR2A: a subunit of the NMDA receptor
- NR2B: a subunit of the NMDA receptor
- PARP-1: poly (ADP-ribose) polymerase-1
- Rh123: Rhodamine 123
- ROS: reactive oxygen species
- VGCC: voltage-gated calcium channels

I. INTRODUCTION

Delayed calcium dysregulation (DCD) is a sustained elevation in cytosolic calcium concentration (Nicholls & Budd, 1998; Tymianski *et al.*, 1993b) which is a hallmark of glutamate excitotoxicity (Manev *et al.*, 1989; Tymianski *et al.*, 1993b; Thayer & Miller, 1990; Budd & Nicholls, 1996). Glutamate excitotoxicity occurs when neurons are over exposed to glutamate resulting in neuronal death due to Ca^{2+} dependent proteases and phospholipases. Excitotoxicity is manifested in many common neuronal traumas ranging from stroke and spinal cord injuries to traumatic brain injury, and it is also found in many neurodegenerative diseases such as Parkinson's disease, Alzheimer's disease, multiple sclerosis, and Huntington's disease (Bramlett & Dietrich, 2004; Hazell, 2007; Salinska *et al.*, 2005; Kim *et al.*, 2010). This thesis research has the potential to help countless individuals suffering from these neuronal diseases. Ischemic stroke, alone, is a devastating condition that can lead to irreversible brain damage and death. Ischemic stroke affects over 700,000 people a year, and roughly every 3 minutes someone dies of a stroke, making it the third leading cause of death in the United States (AHA, 2007). In recent years, individuals at high risk of having a stroke have been encouraged to implement many preventive measures to reduce the incidents of stroke (Lipton, 2004; Gwag *et al.*, 2007), but little progress has been made on treatment options to diminish the neuronal death that occurs due to a stroke (Sacco *et al.*, 2007). One of the main obstacles in the developing effective treatments to reduce neuronal death that occur during a stroke is the lack of

knowledge about the precise mechanisms that contribute to brain damage on a cellular level which is a direct result of glutamate excitotoxicity.

During glutamate excitotoxicity, a persistent elevation of the major excitatory neurotransmitter, glutamate, occurs in the extracellular environment resulting in continuous activation of glutamate receptors (Tymianski *et al.*, 1993b). This persistent elevation of glutamate activates the ionotropic glutamate receptors setting in motion a series of cytosolic calcium fluctuations, ultimately resulting in a sustained elevation of cytosolic calcium (Choi, 1988; Manev *et al.*, 1989). There is a well documented causal relationship between the elevation in cytosolic calcium and eventual neuronal death (Manev *et al.*, 1989; Choi & Hartley, 1993; Tymianski *et al.*, 1993b). This was shown in a series of experiments where low cytosolic Ca^{2+} was stabilized during glutamate exposure by chelating it with BAPTA (Tymianski *et al.*, 1993c; Tymianski *et al.*, 1994). The stabilization of low cytosolic Ca^{2+} concentration significantly increased the survival rate of neurons exposed to excitotoxic glutamate. Over the past several decades, many researchers have studied the mechanism(s) of glutamate-induced calcium dysregulation, and many hypotheses have been proposed to combat this debilitating phenomenon.

During glutamate excitotoxicity, overstimulation of glutamate receptors leads to sustained elevation in cytosolic Ca^{2+} ($[\text{Ca}^{2+}]_c$), which is causally linked to cell death. There are two major hypothetical mechanisms for DCD: the continuous activation of *N*-methyl-*D*-aspartate-subtype of the ionotropic glutamate receptors and the reversal of the plasmalemmal $\text{Na}^+/\text{Ca}^{2+}$ exchanger,

an important calcium extrusion mechanism. In this thesis, data is provided that merges two of the main competing hypotheses for the root cause of glutamate-induced delayed calcium dysregulation.

The data in this thesis shows that if calcium influx is blocked through both the activated *N*-methyl-*D*-aspartate (NMDA) receptor (Tymianski *et al.*, 1993b) and the ion flow reversal of the sodium/calcium exchanger (NCX_{rev}) (Kiedrowski, 1999; Hoyt *et al.*, 1998), one can prevent glutamate-induced DCD. The NMDA receptor is a subtype of the ionotropic glutamate receptor family which is specifically activated by NMDA. This receptor is important for normal neuronal synaptic transmission (McBain & Mayer, 1994). However, during prolonged glutamate exposure, the NMDA receptor fails to deactivate and becomes continuously active (Nowak *et al.*, 1984; Planells-Cases *et al.*, 2006) allowing a continuous influx of calcium from the extracellular environment. On the other hand, the sodium/calcium exchanger, or NCX, is a high-capacity calcium extrusion mechanism which is vital in maintaining low calcium homeostatic concentrations (Carafoli *et al.*, 2001). Under normal conditions where there is a large Na⁺ gradient across the plasma membrane and the plasma membrane is at a negative potential NCX extrudes one intracellular Ca²⁺ ion for three extracellular Na⁺ ions (Yu & Choi, 1997), but during excitotoxic glutamate exposure, conditions become favorable for the reversal of the NCX (Yu & Choi, 1997; Wolf *et al.*, 2001; Bindokas & Miller, 1995). The reversal of the NCX potentially allows entry of large amounts of calcium from the extracellular environment. Thus, by inhibiting the NMDA receptor or reverse NCX separately,

an insignificant reduction in the sustained calcium levels is achieved, but if both of these mechanisms are blocked simultaneously, complete inhibition of calcium dysregulation is accomplished (Brittain *et al.*, 2012).

Also throughout this research several off-target effects of commonly used drugs were discovered, which brings into question conclusions previously published when using these drugs. Only by determining these off-target effects has a better understanding been gained of how Ca^{2+} influx through the NMDA receptor and reverse NCX are actually working together to bring about calcium dysregulation. This insight into the mechanisms that lead to excitotoxic calcium dysregulation could eventually be translated into novel therapeutics that have the potential to help millions of people struggling with these debilitating diseases resulting from loss of neuronal function due to prolonged glutamate exposure.

A. Historical background on “Glutamate excitotoxicity”

Throughout the 1940's many medical professionals and scientists viewed glutamate as a “wonder drug” that treated many cognitive ailments (Weil-Malherbe, 1950). Several papers were published looking at benefits of taking glutamate orally. These benefits ranged from reducing psychomotor seizures to increasing mental alertness and attention to increasing one's energy level (Price *et al.*, 1943). Also a series of papers by Zimmerman *et al.*, showed that glutamate was given to children as a way to increase their IQ (Zimmerman *et al.*, 1947; Zimmerman *et al.*, 1948). Glutamate was also given intravenously to treat hypoglycemic coma (Mayer-Gross & Walker, 1947).

Then in 1954 a paper was published by a former member of Pavlov's Institute in Leningrad, Takashi Hayashi (Hayashi, 1954). Based on previous publications showing an increase in cognitive ability induced by glutamate, Hayashi was trying to improve on the condition response reflex in canines by adding glutamate directly to the canine's brain. The research found that glutamate did not produce the intended response of increased conditioning but resulted in seizures (Hayashi, 1954). This was the first negative results published concerning the effects of glutamate.

Another study three years later also looked at the possible cognitive benefits of glutamate on the offspring of mice, however, this research determined that administration of glutamate to the dame resulted in damage to the inner layer of the retina in the offspring (Lucas & Newhouse, 1957). Then in 1969, based on Lucas and Newhouse's work (Lucas & Newhouse, 1957), a scientist named John W. Olney confirmed that glutamate-induced retina lesions and also observed lesions in the brain. He followed up this work by repeating his experiments in primates and found similar lesions on the brains of Rhesus monkeys after treatment with glutamate (Olney & Sharpe, 1969). Olney was the first to use the term "*Excitotoxicity*" to refer to the destruction of the neurons by glutamate (Olney, 1969; Olney & Ho, 1970). Olney proposed that this phenomenon was governed either by sustained neuronal depolarization leading to a lethal exhaustion of the cell's energy reserves or a lethal disturbance in the internal environment (Olney *et al.*, 1971).

Throughout the 1970's and 1980's, several scientists observed an ionic dependence in regard to glutamate excitotoxicity. It was first suggested that the an elevation of cytosolic Na^+ was the mechanism by which excitotoxic neuronal death was initiated, and glutamate exposure induced this influx of Na^+ by increasing membrane conductance (Baker *et al.*, 1973; Baker & Glitsch, 1973; Hablitz, 1982). This observation suggested that the presence of extracellular Na^+ was necessary for cell death to occur. This notion of Na^+ being the primary ion responsible for excitotoxicity was contested in the early 1980's by Simon *et al.* (1984) and by a series of papers by Choi, DW (Choi *et al.*, 1987; Choi, 1987). They suggested that Ca^{2+} , not Na^+ , influx was resulting in excitotoxic neuronal death. Simon observed an accumulation of Ca^{2+} persisting in neurons of the hippocampus following an ischemic insult (Simon *et al.*, 1984). From this observation he proposed that toxic effects induced by glutamate were not dependent on an influx of extracellular Na^+ but rather on the influx of extracellular Ca^{2+} .

This was confirmed by Dennis W. Choi in the 1980's, who showed that excitotoxic neuronal death was more dependent on the presence of extracellular Ca^{2+} than on extracellular Na^+ (Choi, 1985). This line of experimentation was further confirmed by Kass & Lipton (1986), and it was hypothesized that the Ca^{2+} influx was through the *N*-methyl-*D*-aspartate (NMDA) receptor was responsible for excitotoxic neuronal death (Choi *et al.*, 1987).

B. Calcium homeostasis and “delayed calcium dysregulation”

Calcium plays a fundamental role in cellular physiology and biochemistry, and it is one of the most highly regulated ions within neurons with resting cytosolic concentrations maintained at roughly 100 nM. When neurons are stimulated, Ca^{2+} can increase to between 1 to 100 μM (Nicholls, 1986). This increase is normally accomplished through Ca^{2+} influx from the extracellular environment which has a Ca^{2+} concentration of roughly 1.8 mM. Once Ca^{2+} enters the neuron, it is quickly removed by either Ca^{2+} extrusion or accumulation mechanisms, and it is brought back to the resting concentrations (Nicholls, 1986). The tight regulation of Ca^{2+} is important since in many instances Ca^{2+} acts as a second messenger during signal transduction, and calcium has been found to be an important component during cell-to-cell communication by aiding in the release of neurotransmitters (England, 1986). Also, many enzymes require Ca^{2+} ions to activate. It is known that an uncontrolled and sustained elevation of free cytosolic Ca^{2+} concentration ($[\text{Ca}^{2+}]_c$), also known as Ca^{2+} dysregulation, is causally linked to neuronal death found in stroke and many neuronal diseases (Manev *et al.*, 1989; Choi & Hartley, 1993; Tymianski *et al.*, 1993b). For these reasons the maintenance of low $[\text{Ca}^{2+}]_c$ is essential.

Calcium dysregulation transpires when an imbalance between calcium influx and calcium extrusion/accumulation occurs. Calcium influx mechanisms include the activation of glutamate receptors (GluR) and opening of voltage-gated Ca^{2+} channels. GluR consist of both ionotropic and metabotropic receptors. Metabotropic glutamate receptors (mGluR) stimulation does not result

in immediate channel activation. Thus mGluR are thought not having immediate impact on Ca^{2+} fluctuation (Xu *et al.*, 2007). On the other hand, ionotropic glutamate receptors (iGluR) are ion channels that are activated directly by glutamate allowing an immediate Ca^{2+} influx. iGluR consist of three primary receptor subtypes: *N*-methyl-*D*-aspartate receptor (NMDA receptor), α -amino-3-hydroxy-5-methyl-4-isoxazolepropionic acid receptor (AMPA receptor), and kainate receptor (KA receptor) (Xu *et al.*, 2007). Of these three receptor subtypes, sustained activation of the NMDA receptor is considered most vital to Ca^{2+} dysregulation (Tymianski *et al.*, 1993b). However, it is well known that magnesium, a natural blocker of the NMDA receptor, causes rapid inhibition of the NMDA receptor (Nowak *et al.*, 1984), this makes the NMDA receptor activation as the solo calcium influx mechanism less likely. Ca^{2+} influx is countered by Ca^{2+} removal. This is accomplished by Ca^{2+} extrusion mechanisms such as the $\text{Na}^+/\text{Ca}^{2+}$ exchanger and the Ca^{2+} ATPase and by Ca^{2+} accumulation by the endoplasmic reticulum (ER) and the mitochondria (Mtc) (Nicholls, 1986).

Under normal conditions neurons are excited by a synaptic release of glutamate that travels across the synaptic cleft and interacts with the GluR, resulting in receptor activation leading to $\text{Ca}^{2+}/\text{Na}^+$ influx and plasma membrane depolarization. Glutamate is then quickly cleared from this cleft by the Na^+/Glu co-transporter, allowing the GluR to become inactive and resting conditions to be restored (Bellocchio *et al.*, 2000; Grewer *et al.*, 2008). But during a stroke or severe head trauma, blood flow to a region of the brain is stopped (Won *et al.*, 2002). This prevents oxygen and glucose from reaching these neurons, resulting

in a failure of cellular bioenergetics. It has been theorized that this bioenergetics failure ultimately causes ATP depletion which prevents the Na⁺/K⁺ ATPase pumps from maintaining the Na⁺ gradient across the plasma membrane. This Na⁺ gradient is necessary for the Na⁺/Glu co-transporters to function. The failure or possible reversal of the Na⁺/Glu co-transporters allows a build-up of glutamate in the synaptic cleft (Davalos *et al.*, 1997; Castillo *et al.*, 1997) which is responsible for the initiation of glutamate excitotoxicity and eventually Ca²⁺ dysregulation. During experiments where neuronal cultures are deprived of oxygen and glucose, extracellular glutamate rises from 0.1µM to between 1.5 and 2.5µM within 60 minutes (Goldberg & Choi, 1993). Glutamate levels have also been measured in the cerebral spinal fluid of patients following a stroke and measure between 2 and 8µM (Benveniste *et al.*, 1984; Castillo *et al.*, 1999; Lancelot *et al.*, 1997).

Ca²⁺ dysregulation is the hallmark of glutamate excitotoxicity (Manev *et al.*, 1989; Tymianski *et al.*, 1993b; Thayer & Miller, 1990; Budd & Nicholls, 1996). Throughout literature this Ca²⁺ dysregulation is referred to as “delayed calcium dysregulation” or simply DCD, referring to the distinct or classical manner in which cytosolic calcium becomes dysregulated (Nicholls & Budd, 1998; Tymianski *et al.*, 1993b). This classical manner consists of three distinct steps following exposure to glutamate: (i) an initial spike in cytosolic calcium concentration ([Ca²⁺]_c), followed by (ii) a transient decrease in [Ca²⁺]_c. This transient decrease in [Ca²⁺]_c is near the resting concentrations but is still slightly elevated. Then after some delay (iii) a larger, sustained elevation of [Ca²⁺]_c.

occurs. This secondary increase in $[Ca^{2+}]_c$ is referred to as delayed calcium dysregulation. The precise mechanism(s) resulting in the onset of this glutamate-induced delayed calcium dysregulation still remains elusive.

C. Possible mechanism(s) for glutamate-induced delayed calcium dysregulation

Excitotoxicity and delayed calcium dysregulation has been studied since the late 1950's, thus several hypotheses have been suggested for the underlying mechanism of calcium dysregulation with little success.

1. Continuous-activation of glutamate receptors

Glutamate receptors (GluR) are transmembrane receptors expressed in both the central and peripheral nervous systems (Dingledine *et al.*, 1999). These receptors bind the major excitatory neurotransmitter, glutamate. Glutamate is the most abundant neurotransmitter in the body and can be found in over 50% of all neurons (Dingledine *et al.*, 1999). There are two basic types of glutamate receptors, ionotropic GluR (iGluR) and metabotropic GluR (mGluR). mGluR, unlike iGluR, are not ion channels. However, important to the overall neuronal function, the mGluR appear to have a minimal role in the onset of glutamate-induced delayed calcium dysregulation (Tymianski *et al.*, 1993b).

On the other hand, iGluR are transmembrane, ligand-gated ion channels that open in response to glutamate. There are three subtypes of the iGluR; they are referred to by the name of the chemical compound that binds to the receptor

more selectively than glutamate. When iGluRs are activated, the ion channel opens allowing ions to flow freely down their respective electrochemical gradients. iGluRs play a critical role in the normal neuronal synaptic transmission because glutamate is the major excitatory neurotransmitter, and it is released into the synaptic cleft in response to neuronal depolarization during the propagation of an action potential (McEntee & Crook, 1993; Okubo *et al.*, 2010). Under normal circumstances glutamate is released when the presynaptic neuron becomes depolarized (usually due to receiving a signal from an adjacent neuron) and diffuses across the synaptic cleft, interacting with GluRs on the postsynaptic neuron (Palmada & Centelles, 1998). This interaction results in neuronal depolarization, and the process begins again as the signal is passed to other neurons. Then the postsynaptic neurons normally return to their pre-excited state following the removal of glutamate from the synaptic cleft (Bellocchio *et al.*, 2000; Grewer *et al.*, 2008).

It has been hypothesized that if the glutamate remains elevated in the synaptic cleft the iGluR remain active. This will allow a continuous influx of calcium from the extracellular environment into the cytosol leading to Ca^{2+} dysregulation (Tymianski *et al.*, 1993b).

(a.) *NMDA subtype of the ionotropic glutamate receptor (NMDA receptor)*

The *N*-methyl-*D*-aspartate receptor (NMDA receptor) is an iGluR, which can be specifically activated by NMDA. When activated, the NMDA receptor allows Na^+ , Ca^{2+} , and K^+ to flow down their respective electrochemical gradients,

but the receptors appear to be more permeable to Ca^{2+} than the other ions (MacDermott *et al.*, 1986). Calcium influx, along with plasma membrane depolarization, occurs as a result of the activation of the NMDA receptors primarily on the postsynaptic neurons; this process is known to play a critical role in synaptic transmission and overall synaptic plasticity, which is a mechanism for learning and memory (McEntee & Crook, 1993; Okubo *et al.*, 2010). Thus, widespread and irreversible inhibition of this receptor would be detrimental to normal function of neurons and the central nervous system (Ikonomidou *et al.*, 1999; Lipton, 2004).

The NMDA receptor is widely expressed in all neurons in both the central and peripheral nervous systems. It appears to have particularly high expression in the hippocampus, cortex, and striatum (Monyer *et al.*, 1994). Interestingly, these regions of the brain also correspond to those regions most susceptible to a prolonged elevation in glutamate (Nicholls, 2004), suggesting a possible link between NMDA receptor density and excitotoxic neuronal death.

A feature that distinguishes the NMDA receptors from the other iGluR, AMPA and kainate receptors is that the NMDA receptor is both ligand-gated and voltage-dependent (Nowak *et al.*, 1984). The voltage-dependence of the NMDA receptor is due to an endogenous magnesium block that prevents ion flow through the channel when the plasma membrane is at resting potential (Nowak *et al.*, 1984). When the plasma membrane becomes depolarized, the magnesium is expelled from the ion channel, and if the proper ligands are present, the channel will be activated. Studies have suggested that a slight kinetic delay in

the activation of the NMDA receptor in comparison to the other iGluRs (AMPA and kainate receptors) allows the plasma membrane to depolarize enough to expel this endogenous inhibitor (Johnson & Ascher, 1987; Lester *et al.*, 1990; Dingledine *et al.*, 1999).

This kinetic delay in NMDA receptor activation is a result of the structural differences of the NMDA receptor compared to other iGluR. The NMDA receptor is a heterotetrameric split between NR1 and NR2 subunits, requiring co-agonists (McBain & Mayer, 1994). The NR1 subunit binds the co-agonist glycine, where the NR2 subunit binds the excitatory neurotransmitter, normally glutamate. This structure of the NMDA receptor requires the binding of two different ligands and thus slows the activation kinetics of the NMDA receptor in comparison to the other iGluR: AMPA and kainate receptors. Along with the slower kinetic activation, the NMDA receptor is also slower to close (Johnson & Ascher, 1987; Lester *et al.*, 1990). Thus overall, the length of time that NMDA receptor is activated is longer in comparison to the other iGluR (Dingledine *et al.*, 1999). These differences in the NMDA receptor kinetics allows the NMDA receptor to remain open longer than the other iGluRs, which is part of the reason why many researchers hypothesize that NMDA receptor plays a central role in the Ca²⁺ dysregulation.

There are eight different isoforms of the NR1 subunit, and they are ubiquitously expressed in neurons (Stephenson, 2006). Also, all the NR1 isoforms are derived from alternate splicing of the *GRIN1* gene, which, yields the functional isoforms by slight modification of the three short exon cassettes in the

N-terminal (N1) and C-terminal (C1, C2) domains of the subunit protein (Hollmann *et al.*, 1993; Janssens & Lesage, 2001). These slight modifications in the N- and C- terminals are functionally identical in the protein subunits. In other words, because the isoforms are ubiquitously expressed in neurons and lack any functional differences, they are not seen as possible targets for regulating the NMDA receptor during excitotoxic events.

In contrast to the NR1 subunit, the localization of the four NR2 isoforms differs throughout the central nervous system (Stephenson, 2006). The NR2A and NR2B subunits are abundant in the cortex, striatum, and hippocampal regions, whereas the NR2C is concentrated in the cerebellum and NR2D is located in sub-cortical areas (Ishii *et al.*, 1993; Goebel & Poosch, 1999; Sun *et al.*, 2000). The localization of these isoforms indicates greater importance to the NR2A and NR2B isoforms because the regions of the brain where they are abundant are the regions most susceptible to excitotoxic injury (Nicholls, 2004). These regional differences are one of the reasons that some efforts have been made to design specific antagonists to block these subunits; further details will be provided later on in this section.

Also important to note is that the NR2A and NR2B subunits abundance and localization are developmentally dependent. During the embryonic and early post-natal developmental stages, the NR2B subunit is the most prominent, but as the neurons mature, the expression of the NR2A subunits increases, and eventually the NR2A subunits outnumber the NR2B subunits (Brewer *et al.*, 2007; Liu *et al.*, 2004). This shift in dominance is prevalent enough that NR2B

knockout mice are not viable, whereas NR2A knockouts are viable with only some developmental issues. This shift between the subunits is known as the NR2B-NR2A developmental switch (Barth & Malenka, 2001; Flint *et al.*, 1997; Lu *et al.*, 2001). This NR2B-NR2A developmental switch must take into account, and careful note needs to be made of the age of the animal that is being sacrificed and days *in vitro* (DIV) when analyzing the data, particularly if a specific NMDA receptor subunit is being blocked.

Many of these characteristics of the NMDA receptor described above have led researchers to hypothesize that the NMDA receptor might be involved in Ca²⁺ dysregulation following excitotoxic glutamate exposure. The hypothesis is that glutamate exposure results in plasma membrane depolarization, which removes the endogenous blocker, Mg²⁺. This allows the NMDA receptor, once it binds both the co-agonists, glutamate and glycine, to become continuously activated (Nowak *et al.*, 1984; Planells-Cases *et al.*, 2006) allowing uncontrolled Ca²⁺ influx to occur (Tymianski *et al.*, 1993b). This Ca²⁺ influx overwhelms the homeostatic Ca²⁺ extrusion and accumulation mechanisms, and thus sustained exposure to excitotoxic glutamate leads to delayed Ca²⁺ dysregulation (DCD) (Nicholls & Budd, 1998; Tymianski *et al.*, 1993b).

Several antagonists have been designed to block the activation of the NMDA receptor, but the research that was performed in this thesis focused on just a few of these. The antagonists that will be focused on in this research are memantine, MK-801 (Dizocilpine), AP5, Ifenprodil, and PEAQX. These

antagonists have different characteristics that we used to distinguish the contribution of the NMDA receptor in Ca²⁺ dysregulation.

- Memantine is a low-affinity, voltage-dependent, non-competitive antagonist of the NMDA receptor (Kornhuber *et al.*, 1989; Rogawski & Wenk, 2003; Robinson & Keating, 2006). It was first synthesized in 1968 and since then has been used extensively in laboratory research. Memantine is one of a growing number of NMDA receptor antagonists that are currently being used clinically or are being tested in clinical trials (Villoslada *et al.*, 2009; Schifitto *et al.*, 2007; Corbett, 2007). Memantine is approved to treat individuals with moderate to severe Alzheimer's disease (Mount & Downton, 2006). Patients have shown some moderate improvements in cognitive function, mood, a reduction of aggressive behavior, and the ability to perform daily activities, with few reporting side effects once the blood levels of the drug are in the therapeutic range (Mount & Downton, 2006). Memantine is considered to be the first Alzheimer's disease medication to focus on inhibiting the glutamatergic system, which is thought to help reduced unwanted and abnormal brain activity.
- (5S,10R)-(+)-5-methyl-10,11-dihydro-5H-dibenzo[a,b]cyclohepten-5,10-imine, or MK801 is a high-affinity, voltage-dependent, non-competitive antagonist of the NMDA receptor. Currently, MK-801 is solely used in the laboratory setting. Researchers thought that MK-801 would be used clinically as an anti-convulsant, but during animal testing, researchers found lesions on the brains of rats (Olney *et al.*, 1989). It also resulted in a schizophrenic-like psychosis

in rats, and it is currently used as a model to study schizophrenia (Rung *et al.*, 2005). MK-801 is one of the most potent and efficacious NMDA receptor antagonist, and thus it is still one of the most widely used NMDA receptor inhibitors for studying the glutamatergic component for possible treatments of diseases that are excitotoxic in nature. The issue with clinical use of MK-801 is that it irreversibly blocks the NMDA receptor, preventing the NMDA receptor from functioning which is needed for long-term potentiation (learning and memory) (Coan *et al.*, 1987; Lipton, 2004). MK-801 has some use as a recreational drug, putting individuals into a dissociative state, similar to phencyclidine (PCP) but with longer lasting effects (Carlezon, Jr. & Wise, 1996; Herberg & Rose, 1989; Beardsley *et al.*, 1990). The risk of over-dosing with MK-801 is extremely high and little is known about the long-term effect.

- (2*R*)-amino-5-phosphonopentanoate or AP-5, unlike memantine and MK-801, is a competitive antagonist of the NMDA receptor (Clements & Westbrook, 1994); meaning AP-5 binds to the glutamate binding site on the NR2 subunit (Morris, 1989). The effects of AP-5 are reversible with a short half-life. The rapid interaction and dissociation of AP-5 on the NMDA receptor has made it an ideal drug for studying the effects of the NMDA receptor on long-term potentiation (Morris, 1989). As a competitive antagonist of the NMDA receptor, AP-5 has the potential to be used to out-compete glutamate during excitotoxic events. However, results obtained using AP-5 have been mixed in prevent calcium dysregulation during prolonged glutamate exposure.

- Ifenprodil is a clinically promising, non-competitive NMDA receptor antagonist. This inhibitor is different from the NMDA receptor inhibitors listed above because it is specific for the NR2B subunit of the NMDA receptor (Reynolds & Miller, 1989). The NR2B subunit, as previously described, is highly expressed in the regions of the brain most affected by excitotoxic events (Ishii *et al.*, 1993; Goebel & Poosch, 1999; Sun *et al.*, 2000; Nicholls, 2004) and also has a developmental component with more prominence during the embryonic and early post-natal stages (Barth & Malenka, 2001; Flint *et al.*, 1997; Lu *et al.*, 2001). This selectivity is thought to be useful to target the affected regions while having minimal impact on the rest of the brain. Another attribute that makes ifenprodil interesting as a drug is that it is activity-dependent (Mott *et al.*, 1998; Kew *et al.*, 1996). Many studies have shown that the stronger the stimulus, the greater the inhibitory response. With further investigation this increased response seems to be tied to the acidification that accompanies glutamate exposure. Several clinical trials using ifenprodil as drug have been performed, but many have been abandoned due to high risk/benefit ratio arising from adverse cardiovascular consequences at higher doses (Small & Buchan, 1997).
- PEAQX is similar to ifenprodil in that it is a subunit-specific NMDA receptor antagonist, but it differs in that it is a competitive, NR2A-specific NMDA receptor inhibitor (Frizelle *et al.*, 2006). The NR2A subunit shares similar brain region specificity to the NR2B subunit, but as the NR2B becomes less dominant during development, while the NR2A subunit expression increases

in what is known as the NR2B-NR2A developmental switch (Barth & Malenka, 2001; Flint *et al.*, 1997; Lu *et al.*, 2001). Few studies has been done using this inhibitor, but some researchers see promise as possible a anti-convulsant (Auberson *et al.*, 2002). PEAQX, like all NMDA receptor antagonists, interfere with long-term potentiation. This is interference with long-term potentiation is critical because it would prevent those one's ability to learn while under the influence of these drugs. From a clinical relevance standpoint, PEAQX is not dissimilar from ifenprodil in that toxicity issues arise with higher doses.

(b.) *AMPA and Kainate receptors*

The AMPA and kainate receptors are transmembrane ionotropic glutamate receptors that play a critical role in mediating the fast synaptic transmissions and neuronal plasticity in the central nervous system. The activation kinetics of the AMPA and kainate receptors are more rapid in comparison to the NMDA receptor; this is due to the AMPA receptor and the kainate receptor only requiring one agonist, glutamate (Bortolotto *et al.*, 1999). Also, unlike the NMDA receptor, AMPA and kainate receptors do not have a voltage-dependent component for activation (Mayer, 2005). It is thought that this slight difference in activation rate for these non-NMDA receptor iGluRs actually contributes to the plasma membrane depolarization which aids in the NMDA receptor expelling the Mg⁺ block (Bortolotto *et al.*, 1999). This is vital for normal cell-cell communication.

(1.) *alpha-amino-3-hydroxy-5-methyl-4-isoxazolepropionic acid receptor (AMPA receptor)*

The AMPA receptor is an ion channel, that when activated is permeable to sodium and potassium and sometimes calcium. The driving force for these ions to move through the open channel is their electrochemical gradient, similar to when the NMDA receptor is activated (Honore *et al.*, 1982; Mayer, 2005). The AMPA receptor is the most abundant receptor found in the nervous system, and it is found indiscriminately throughout nearly all the regions of the brain. The AMPA receptor is named from the artificial derivative of glutamate, AMPA that is a specific agonist for this receptor. This receptor does not require a co-agonist to become activated (Mayer, 2005).

The AMPA receptor is a heterotetrameric ion channel. Most AMPA receptors consist of symmetric “dimer of dimers” of GluR2 and either GluR1, 3, or 4 subunits (Shi *et al.*, 1999; Song & Huganir, 2002). This receptor has binding sites on each of the four subunits for the agonist to bind. The AMPA receptor becomes partially active when only two of the four sites are occupied (Platt, 2007), and it is fully activated when all four binding site are bound to the agonist (Rosenmund *et al.*, 1998). Once the receptor is activated; it goes through a rapid desensitization, and the ion channel closes (Platt, 2007). This stops the flow of ions across the plasma membrane with respect to this channel. The rapid activation and inactivation makes the AMPA receptor an ideal candidate for the fast excitatory synaptic transmission found in the central nervous system.

The ionic permeability of the AMPA receptor is altered by the combination of the dimer subunits that make-up the ion channel. Most AMPA receptors have a GluR2 dimer as part of the channel construction. The GluR2 dimer subunits are thought to be the most influential in regard to calcium permeability. When the GluR2 subunit is not present in the AMPA receptor, it is permeable to calcium, sodium, and potassium when activated, but when the GluR2 subunit is present, which is found in most cases, the channel becomes impermeable to Ca^{2+} ions. This is due to a very common mutation that occurs to the GluR2 subunit, where a non-charged amino acid is replaced with a positively charged amino acid. The positively-charged amino acid is then located in such a way that the activated channel becomes energetically unfavorable for the calcium ions to flow through the channel. Due to the abundance of the GluR2 subunit expression in the AMPA receptor and this common mutation, few scientist theorize that the AMPA receptor is critical for calcium dysregulation that occurs following glutamate excitotoxicity (Kim *et al.*, 2001; Mayer, 2005). The activation of the AMPA receptor, however, could play a critical role in the increase of intracellular Na^+ and the depolarization of the plasma membrane that is observed during prolonged glutamate exposure.

Several antagonists have been designed to specifically inhibit the AMPA receptor. The most commonly used AMPA receptor antagonists are 6-cyano-7-nitroquinoxaline-2,3-dione (CNQX) and 2,3-dihydroxy-6-nitro-7-sulfamoylbenzo[f]quinoxaline-2,3-dione (NBQX). CNQX is selective for both non-NMDA ionotropic GluR, AMPA and Kainate receptors, whereas NBQX is more specific

for the AMPA receptor (Pitt *et al.*, 2000; Yamaguchi *et al.*, 1993). These antagonists have been used by researcher to try to determine the impact that the activated AMPA receptor has on glutamate excitotoxicity. By inhibiting the AMPA receptor it has been shown the that AMPA receptor has a minimal impact on Ca^+ dysregulation (Brustovetsky *et al.*, 2011) or the increase in Na^+ in the cytosol or plasma membrane depolarization induced by prolonged glutamate exposure (Kirischuk *et al.*, 2007).

(2.) *Kainate receptor (KA receptor)*

The kainate receptor is an iGluR that is selective for sodium and potassium (Huettner, 2003). In comparison to the other iGluR, NMDA and AMPA receptors, little is known about the kainate receptor. It is known that there are five different kainate receptor subunits, GRIK1-5. These subunits form the ion channel in either a homo- or hetero- tetramer structure. It has been shown that some of these combinations when activated have a minimal permeability to calcium. The KA receptor contribution to increasing intracellular Ca^{2+} is negligible in comparison the AMPA and NMDA receptors. The contribution of the KA receptor is also limited by its minimal expression in the brain (Huettner, 2003; Dingledine *et al.*, 1999).

Kainate receptor has both pre- and post-synaptic role in neurotransmission with both excitatory and inhibitory functions. The excitatory component of the KA receptors is postsynaptic and is due to its activation by glutamate. The kinetics of this activation of the KA receptor is very rapid, similar

to the activation kinetics of AMPA receptor (Huettner, 2003). This rapid activation contributes to plasma membrane depolarization which aids in the expelling of the endogenous magnesium of block of the NMDA receptor. Also, similar to the AMPA receptor, the receptor closing kinetics of the kainate receptor is also very rapid. Thus, it is thought that due to this rapid closing, the KA receptors makes only a minimal contribution to the ion fluctuation during glutamate exposure (Dingledine *et al.*, 1999).

Unlike the NMDA and AMPA receptors, the kainate receptor can inhibit neuronal function. This inhibition occurs by modulating the release of the main inhibitory neurotransmitter, gamma-aminobutyric acid, or GABA on presynaptic neurons. GABA is released into the synaptic cleft and interacts with GABA receptors resulting in inhibition of the postsynaptic neuron (Huettner, 2003).

The glutamate receptor antagonist, CNQX, is used to prevent KA receptors activation (Kirischuk *et al.*, 2007). This inhibitor also blocks the AMPA receptor, hindering researchers ability to monitor the specific contribution of the kainate receptors during glutamate exposure (Pitt *et al.*, 2000; Yamaguchi *et al.*, 1993). Another more specific KA receptor antagonist, NS102, has been developed. However, specifically blocking the kainate receptors during excitotoxic glutamate exposure has no effect on either Ca^{2+} or Na^{+} influx.

In addition to iGluR there are other ion channels that may contribute to triggering and subsequent maintenance of DCD following exposure to glutamate. Recently, the transient receptor potential channel TRPM7 was proposed to play a

pivotal role in excitotoxicity associated with oxygen/glucose deprivation (OGD) (Aarts *et al.*, 2003). Subsequently, it was suggested that TRP channels are essential for DCD in glutamate-treated neurons (Chinopoulos *et al.*, 2004). However, in the latter study TRP channels were implicated in DCD based on the inhibitor action of 2-aminoethoxydiphenyl borate (2-APB) and La^{3+} , both of which demonstrated a wide variety of effects (Chinopoulos & Adam-Vizi, 2006) including La^{3+} antagonism at NMDA receptor (Reichling & MacDermott, 1991) and 2-APB-induced inhibition of the cyclosporine A-insensitive permeability transition in isolated brain mitochondria (Chinopoulos *et al.*, 2003). In addition to TRP channels, a subpopulation of AMPA receptors which lack the GluR2 subunit and are highly permeable to Ca^{2+} may contribute to the disturbance of calcium homeostasis in ischemia accompanied by glutamate excitotoxicity (Kwak & Weiss, 2006). However minimal expression of this AMPA receptor limits the likelihood of this hypothesis. Another possibility is the Ca^{2+} -permeable acid-sensitive ion channels (ASICs), which could be activated by acidification that occurs in ischemic brain, are also potentially important routes for Ca^{2+} influx into neurons (Xiong *et al.*, 2004).

2. The plasmalemmal sodium calcium exchanger (NCX)

The plasmalemmal sodium calcium exchanger, or NCX, is an important Ca^{2+} extrusion mechanism necessary for calcium recovery following normal neuronal excitation (DiPolo & Beauge, 2006; Carafoli *et al.*, 2001; Yu & Choi, 1997). The $\text{Na}^+/\text{Ca}^{2+}$ exchanger is an antiporter that uses the energy from the

electrochemical gradient of sodium to transport Ca^{2+} out of the cytosol. Three extracellular Na^+ ions are transported down the electrochemical gradient of sodium into the neuron in exchange for one intracellular Ca^{2+} ion being transported against the electrochemical gradient of calcium out of the neuron (Blaustein & Lederer, 1999).

Two forces comprise the electrochemical gradient; one force is a large difference between concentrations of a particular ion across a membrane. In this case, Na^+ has a 150mM concentration in the extracellular environment compared to 10mM concentration in the intracellular environment. The second force is the charge difference across the membrane that occurs due to this concentration disparity. The resting plasma membrane potential is maintained near -70 mV. This would suggest that positively charged ions, such as Na^+ and Ca^{2+} , would be drawn towards the negative, intracellular side of the plasma membrane. Thus, when the NCX exchanges Na^+ for Ca^{2+} , the charge difference between three Na^+ ions and one Ca^{2+} ion is plus one charge towards the inside of the plasma membrane. Both of these forces are favorable for Ca^{2+} to be transported out of the cell (Mayer & Westbrook, 1987; Yamaguchi & Ohmori, 1990; Tsuzuki *et al.*, 1994).

The $\text{Na}^+/\text{Ca}^{2+}$ exchanger as an extrusion mechanism is highly effective during large concentration changes, like those that occur during glutamate exposure (Kiedrowski *et al.*, 1994). It is effective because NCX has a low affinity for Ca^{2+} , meaning that Ca^{2+} is only loosely bound so it can rapidly bind and be released. Also as described above, the large electrochemical gradient of sodium

results in rapid transport of these ions; in other words, NCX has high capacity. This low affinity and high capacity of the NCX allows up to five thousand Ca^{2+} ions per exchanger to be transported across the membrane per second (Carafoli *et al.*, 2001). Thus for the NCX to be effective, a large concentrations of Ca^{2+} is needed. The low affinity and high capacity characteristics distinguish NCX from another calcium extrusion mechanism, Ca^{2+} ATPase, which uses ATP to pump Ca^{2+} out of the neuron. Ca^{2+} ATPase is a high-affinity, low-capacity transport, removing 10 to 50 Ca^{2+} ions from the cytosolic per second. Thus, it binds Ca^{2+} more tightly than the NCX making the turn over rate much slower. For this reason the Ca^{2+} ATPase is more suited for minor changes in the overall $[\text{Ca}^{2+}]_c$, and thus it is thought to have a minimal role in glutamate-induced delayed calcium dysregulation (Tymianski *et al.*, 1993b; Carafoli *et al.*, 2001).

Three main isoforms of the $\text{Na}^+/\text{Ca}^{2+}$ exchanger exist in the brain: NCX1, NCX2, and NCX3 (Sakaue *et al.*, 2000; Kiedrowski *et al.*, 2004). All three isoforms are functionally similar but have differing expression throughout the brain. In cultured hippocampal neurons, NCX1 is considered the dominant isoform, whereas NCX3 can be found, but it is less expressed. NCX1 is also the dominant isoform of the exchanger in cortical neurons (Sakaue *et al.*, 2000; Kiedrowski *et al.*, 2004). NCX2 is predominantly expressed in glial cells (Thurneysen *et al.*, 2002a; Thurneysen *et al.*, 2002b), and has minimal localization in neurons (Minelli *et al.*, 2007). Although the NCX3 is less expressed in neurons than NCX1, NCX3 appears to be essential for the maintenance of calcium homeostasis during ischemic insults (Jefferis *et al.*, 2007;

Secondo *et al.*, 2007), while the reversal of NCX1 has been suggested to have a role in ischemic related calcium dysregulation (Luo *et al.*, 2007a). Overall, evidence suggests that both NCX1 and NCX3 may play a role in glutamate-induced Ca^{2+} dysregulation (Luo *et al.*, 2007b; Luo *et al.*, 2007a; Bano *et al.*, 2005).

(a.) *Ion reversal of the $\text{Na}^+/\text{Ca}^{2+}$ exchanger (NCX_{rev})*

Under normal conditions the $\text{Na}^+/\text{Ca}^{2+}$ exchanger transports Ca^{2+} out of the neuron; this is considered the forward mode (Blaustein & Lederer, 1999). This forward mode is dependent on the electrochemical gradient of the sodium ions (Mayer & Westbrook, 1987; Yamaguchi & Ohmori, 1990; Tsuzuki *et al.*, 1994). During prolonged neuronal exposure to the excitatory neurotransmitter, glutamate, these conditions break down (Mayer & Westbrook, 1987; Tymianski *et al.*, 1994; Yamaguchi & Ohmori, 1990).

The Na^+ gradient and plasma membrane polarization are the two conditions that directly affect the probability that the NCX can properly function (Kiedrowski *et al.*, 1994). The NCX under normal conditions runs in the forward mode and thus extrudes calcium from the cytosol. Under excitotoxic conditions, the NCX can stop functioning and even reverse the flow of ions across the plasma membrane (Hoyt *et al.*, 1998; Kiedrowski, 1999). Plasma membrane depolarization is known to prevent the NCX from functioning in the forward mode (Yu & Choi, 1997). This loss of function alone is detrimental in reducing the cytosolic Ca^{2+} concentration. Secondary to the loss of NCX function, if the

plasma membrane depolarization is combined with a large increase in cytosolic Na^+ , the probability that the ion flow of the $\text{Na}^+/\text{Ca}^{2+}$ exchanger reverses increases (Kiedrowski *et al.*, 1994). This $\text{Na}^+/\text{Ca}^{2+}$ exchanger reversal allows the $\text{Na}^+/\text{Ca}^{2+}$ exchanger to transport intracellular Na^+ to the outside of the cell in exchange for extracellular Ca^{2+} . The loss of function of the NCX and possible reversal not only fails to counteract Ca^{2+} influx induced by excitotoxic glutamate, but may also contribute to Ca^{2+} dysregulation (Hoyt *et al.*, 1998; Kiedrowski, 1999).

The isoform NCX1 is the most prominent isoform of the $\text{Na}^+/\text{Ca}^{2+}$ exchanger (Sakaue *et al.*, 2000; Kiedrowski *et al.*, 2004); studies has suggested that the reversal of this isoform (NCX1) might contribute to Ca^{2+} dysregulation during ischemic events (Luo *et al.*, 2007a). A few attempts to prevent NCX_{rev} have been made by knocking out the NCX1. These attempts revealed that the NCX1 isoform is essential in development, and no viable knockout mice have been produced. A viable heterozygous $\text{Na}^+/\text{Ca}^{2+}$ exchanger isoform 1 ($\text{NCX1}^{+/-}$) knockdown mouse has been produced. The $\text{NCX1}^{+/-}$ knockdown has roughly 70% less NCX1 isoform (Luo *et al.*, 2007b). In experiments with excitotoxic glutamate exposure in these mice there is an immediate Ca^{2+} dysregulation. This result support the notion that NCX is an essential Ca^{2+} extrusion mechanism needed to maintain homeostatic calcium levels (DiPolo & Beauge, 2006; Carafoli *et al.*, 2001; Yu & Choi, 1997).

Even though reduction of the expression of the $\text{Na}^+/\text{Ca}^{2+}$ exchanger was detrimental to cell survival and increased the risk of Ca^{2+} dysregulation,

preventing the reverse mode of the NCX is an attractive target for blocking glutamate-induced delayed Ca^{2+} dysregulation. Thus a few inhibitors have been designed to specifically block the reverse mode of NCX. The most widely used and well known NCX_{rev} inhibitor is KB-R7943 (Namekata *et al.*, 2006; Kiedrowski, 2007; Chen *et al.*, 2007; Dietz *et al.*, 2007; Araujo *et al.*, 2007).

2-[2-[4-(4-nitrobenzyloxy)phenyl]ethyl]isothiourea methanesulfonate (KB-R7943) is an isothiourea derivative. KB-R7943 has been the most widely used antagonist to block the reverse mode of NCX since being introduced in 1996. Originally, it was designed as a selective inhibitor of NCX isoform 1 (NCX1) operating in the reverse mode, but later, KB-R7943 was shown to also inhibit NCX isoforms 2 (NCX2) and 3 (NCX3) in the reverse mode with higher affinity to NCX3 (Iwamoto *et al.*, 1996; Amran *et al.*, 2003). Some positive results have been observed concerning KB-R7943 protection following ischemic insult, but the exact mechanism by which this neuronal protection is achieved is controversial (Schroder *et al.*, 1999; Breder *et al.*, 2000; Li *et al.*, 2000; MacGregor *et al.*, 2003; Luo *et al.*, 2007b). This is due, in part, to the ability of KB-R7943 to inhibit L-type voltage-gated Ca^{2+} channels in dorsal column slices (Ouardouz *et al.*, 2005) which can affect Ca^{2+} dysregulation. In permeabilized HeLa cells, KB-R7943 also has been shown to inhibit mitochondrial Ca^{2+} uptake (Santo-Domingo *et al.*, 2007). KB-R7943 also blocked transient receptor potential (TRP) channels expressed in HEK-293 cells (Kraft, 2007). In addition, some investigators reported that KB-R7943 blocks NMDA receptor (Sobolevsky & Khodorov, 1999), while other investigators did not find compelling evidence for

that result (Hoyt *et al.*, 1998; Czyz *et al.*, 2002). Overall KB-R7943 has several non-specific inhibitor targets that affect glutamate induced Ca^{2+} dysregulation. Thus when using KB-R7943 as an inhibitor for NCX_{rev} these non- NCX_{rev} inhibitions maybe responsible for the neuronal protection that is observed.

To further complicate the role of NCX_{rev} in glutamate excitotoxicity, is the suggestion that not only the reversal of the $\text{Na}^+/\text{Ca}^{2+}$ exchanger contributes to DCD, but another K^+ dependent form of NCX (NCKX) may also reverse its ion flow and contribute to DCD (Czyz & Kiedrowski, 2002; Kiedrowski, 2004; Lee *et al.*, 2002; Lytton *et al.*, 2002), and the reverse NCKX may not be inhibited by KB-R7943 or other NCX_{rev} inhibitors (Czyz & Kiedrowski, 2002).

(b.) *Increase in cytosolic sodium, Na^+/H^+ exchanger (NHE)*

Studies have been performed determining that Ca^{2+} influx through the $\text{Na}^+/\text{Ca}^{2+}$ exchanger in the reverse mode contributes to DCD, and it is known that for NCX_{rev} to occur there must be a rapid increase in cytosolic sodium (Mayer & Westbrook, 1987; Yamaguchi & Ohmori, 1990; Tsuzuki *et al.*, 1994). Thus it is possible that if one could inhibit this increase $[\text{Na}^+]_c$, NCX_{rev} would also be prevented. Different mechanisms have been proposed for Na^+ entry into the neuron following glutamate exposure. Only minimal amounts of Na^+ actually enter the neuron through the activation of ionotropic glutamate receptors or voltage-gated Na^+ channels (Kirischuk *et al.*, 2007), and nearly all the sodium is brought into the neurons through the activity of the Na^+/H^+ exchanger (Luo *et al.*, 2007b; Kintner *et al.*, 2010; Luo *et al.*, 2005).

The Na⁺-H⁺ exchanger, or NHE, is an antiporter that is highly sensitive to changes in intracellular pH (Yao *et al.*, 1999). NHE exchanges one intracellular proton (H⁺) for one extracellular Na⁺ ion. The NHE has eight different known isoforms, NHE1-8 (Counillon & Pouyssegur, 2000), but only NHE1, 5, 6, and 7 are found in mammals (Orlowski & Grinstein, 1997). Of those found in mammals, only NHE 5, 6, and 7 are expressed in the brain, with NHE5 thought to be prominent in hippocampal neurons (Counillon & Pouyssegur, 2000; Goyal *et al.*, 2003; Bevensee *et al.*, 1997; Orlowski & Grinstein, 1997; Avkiran, 2001; Karmazyn *et al.*, 1999).

The main function of NHE is to exchange Na⁺ ions for protons (H⁺) in an effort to maintain the cytosolic pH around 7.35 (Kintner *et al.*, 2004). During glutamate exposure, it has been proposed that acidification occurs due to the increased activity of the Ca²⁺ ATPase and the Na⁺/K⁺ ATPase, resulting in the intracellular pH dropping from ~7.5 to ~6.6 (Wu *et al.*, 1999).

Based on what is known about the pH sensitivity of the Na⁺/H⁺ exchanger, the acidification that occurs during excitotoxic glutamate exposure will result in immediate activation of the NHE in its attempt to maintain normal H⁺ levels (Yao *et al.*, 1999; Trapp *et al.*, 1996; Schneider *et al.*, 2004). This could explain the massive influx of Na⁺ ions observed during glutamate exposure. Over the past ten years, a lab at the University of Wisconsin in Madison, WI headed by D. Sun, PhD, has published several manuscripts in regards to sodium increase following an ischemic insult and the possible link between this increase in Na⁺ and the reversal of the NCX (Kintner *et al.*, 2004; Kintner *et al.*, 2010; Luo *et al.*, 2005).

3. Failure of the mitochondrial calcium accumulation

In addition to calcium influx through the NMDA receptor and NCX_{rev} , mitochondrial failure might contribute to delayed calcium dysregulation. Accumulation of Ca^{2+} in mitochondria contributes to clearance of elevated $[\text{Ca}^{2+}]_c$ (Kiedrowski & Costa, 1995). The inner mitochondrial membrane has a Ca^{2+} uniporter, that allows Ca^{2+} influx into the mitochondria driven by a large mitochondrial membrane potential (Bernardi, 1999). The large mitochondrial membrane potential is produced by the mitochondrial respiratory chain. The respiratory chain is a series of four Complexes (I-IV) located on the inner mitochondrial membrane in which oxidation/reduction reactions shuttle electrons from a higher energy state to a lower energy state (Hatefi, 1985). A pictorial scheme of the respiratory chain is shown in Figure 1. The excess energy between reactions is used to pump protons from the mitochondrial matrix to the inner mitochondrial membrane space. This buildup of protons constitutes the proton motive force which is used by ATP synthase to convert ADP to ATP. This process is known as oxidative phosphorylation. The strength of the proton motive force also regulates the rate at which the respiratory chain occurs (Hatefi, 1985). As the proton motive force builds, it becomes greater than the excess energy released between reactions as the electrons are being shuttled from Complex to Complex (Hatefi, 1985). When this occurs, the respiratory chain shuts down. Thus, the respiratory chain and oxidative phosphorylation are tightly coupled in the sense that the cellular need for energy dictates the rate of respiration.

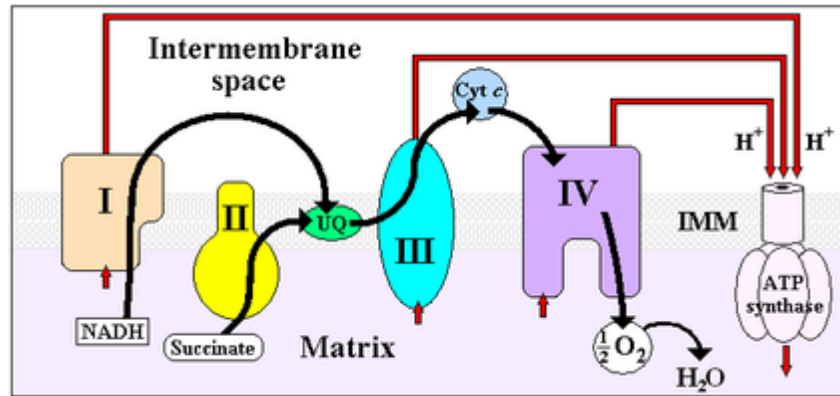


Figure 1. **Pictorial scheme of the electron transport chain and oxidative phosphorylation located on the inner mitochondrial membrane.** The electron transport chain is comprised of four Complexes (Delldot et al., 2007):

- Complex I, NADH dehydrogenase
- Complex II, succinate dehydrogenase
- Complex III, cytochrome c reductase
 - cytochrome c
- Complex IV, cytochrome c oxidase

These four Complexes (the electron transport chain) are coupled with oxidative phosphorylation by the proton motive force. The proton motive force is created by the pumping of protons out of the mitochondrial matrix into the inner mitochondrial membrane space by the electron transport chain. This proton gradient is then used by the ATP synthase to produce ATP by oxidative phosphorylation.

The proton motive force is the large mitochondrial membrane potential that drives Ca^{2+} accumulation. An excessive Ca^{2+} influx into mitochondria may trigger activation of a non-selective permeability transition pore (PTP) in the inner mitochondrial membrane (Zoratti & Szabo, 1995). The activation of the PTP leads to mitochondrial depolarization and swelling (Brustovetsky *et al.*, 2009), inhibiting oxidative phosphorylation, and causing a failure of mitochondrial Ca^{2+} uptake (Bernardi *et al.*, 2006) critically affecting the cell's ability to maintain calcium homeostasis (Bernardi & Petronilli, 1996). The mitochondrial membrane depolarization occurs because the proton motive force is being uncontrollably dissipated through the PTP rather than through ATP synthase. Thus, if the induction of the PTP occurs, the respiratory chain and oxidative phosphorylation becomes uncoupled because the proton motive force is dissipated through the PTP rather than through oxidative phosphorylation resulting in a possible depletion of ATP.

Cyclosporine A (CsA) is the most widely used antagonist of the PTP (Broekemeier *et al.*, 1989). Inhibition of the PTP occurs due to the binding of CsA to mitochondrial cyclophilin D (CyD), a mitochondrial matrix peptidyl-prolyl cis-trans isomerase (Halestrap & Davidson, 1990). In isolated mitochondria CsA makes mitochondria resistant to Ca^{2+} and suppresses PTP activation (Kushnareva *et al.*, 2005). Thus, PTP inhibition increases mitochondrial calcium accumulation and may improve maintenance of cellular Ca^{2+} homeostasis (Chalmers & Nicholls, 2003).

In early studies with cultured neurons exposed to excitotoxic glutamate, CsA was found to be protective against DCD and excitotoxic neuronal death (Nieminen *et al.*, 1996). However, CsA binds to both CyD and cytosolic cyclophilin A leading to the inhibition of calcineurin (Liu *et al.*, 1991), which is a protein phosphatase with various targets. FK506, an inhibitor of calcineurin which does not inhibit the PTP, produced some protective results (Ruiz *et al.*, 2000; Butcher *et al.*, 1997). Thus, it is unclear whether PTP inhibition or calcineurin inhibition is responsible for the protective effects of CsA. N-methyl-isoleucine-4-cyclosporin (NIM811) and D-methyl-alanine-3-ethyl-valine-4-cyclosporin (Debio 025) are new CsA derivatives and more specific inhibitors of the PTP, which do not inhibit calcineurin (Waldmeier *et al.*, 2002; Hansson *et al.*, 2004). The extent to which these inhibitors protect against DCD is unknown.

The presence of CyD strongly correlates to the susceptibility of brain mitochondria to the opening of Ca²⁺-induced PTP (Brustovetsky *et al.*, 2003). Brain mitochondria isolated from homozygous cyclophilin D knockout mice (Ppif^{-/-} mice) were less prone to opening of PTP (Baines *et al.*, 2005). In addition, cultured cortical neurons derived from these mice have increased resistance to glutamate-triggered DCD and cell death (Schinzel *et al.*, 2005). Ppif^{-/-} mice demonstrate a significant decrease in brain infarct size after acute middle cerebral artery occlusion, supporting the importance of CyD-dependent PTP in an ischemic injury model (Schinzel *et al.*, 2005). These results strongly suggest an important role for the CyD-dependent PTP in neuronal injury associated with

stroke-related insults. However, the bioenergetics consequences of PTP activation in neurons have yet to be fully investigated.

Ca²⁺ influx into glutamate-treated neurons is known to result in ROS generation (Duan *et al.*, 2007). In experiments with isolated mitochondria, activation of PTP also results in an increased ROS generation (Schonfeld & Reiser, 2007). On the other hand, the increased ROS generation might be involved in activation of the PTP and perpetuating mitochondrial injury. However, the link between PTP and the increase in ROS generation in glutamate-treated neurons remains unknown. The mechanisms and consequences of elevated ROS generation in these neurons require investigation.

In addition to possible activation of the PTP, increased ROS generation is involved in oxidative DNA damage (Rajesh *et al.*, 2003). This damage activates DNA repair mechanisms, including poly (ADP-ribose) polymerase-1 (PARP-1), an enzyme that repairs single-stranded DNA breaks (Bryant *et al.*, 2005). The PARP-1-catalyzed DNA repair reaction uses NAD⁺ as a substrate (Duan *et al.*, 2007). This could lead to a deficit of NADH, a main substrate for the mitochondrial respiratory chain responsible for the generation of mitochondrial membrane potential ($\Delta\psi$). Whereas most NADH is located inside of mitochondria (Duchen & Biscoe, 1992), PARP-1 is predominantly a cytosolic enzyme (Di *et al.*, 2001). Therefore, NADH (or its oxidized form NAD⁺) has to escape from mitochondria to be used in PARP-1-catalyzed reactions. The PTP seems the only conceivable route for NADH/NAD⁺ escape from mitochondria

because there are no known transports on the inner mitochondria membrane. It is not clear to what extent an increase in $[Ca^{2+}]_c$ following exposure of neurons to glutamate causes NADH/NAD⁺ escape from mitochondria versus reversible NADH oxidation. Recently, PARP-1 was found in mitochondria (Du *et al.*, 2003) suggesting that oxidative stress and mitochondrial PARP-1-activation could trigger NADH depletion within mitochondria without the need for escape. In this case, inhibition of ROS generation with potent cell-permeable antioxidants could diminish PARP-1 activation within mitochondria and prevent NADH depletion and a failure of bioenergetics.

D. Cell death caused by calcium dysregulation

Excitotoxicity is neuronal death induced by glutamate (Olney, 1969; Olney & Ho, 1970). This neuronal death can be either apoptotic or necrotic depending on the intensity and duration of glutamate exposure. During a stroke or traumatic brain injury, neurons located at the epicenter or core of the trauma are most likely to have a high exposure to glutamate resulting in necrosis rather than apoptosis. Neurons located farther away from the core in the penumbra region have a much lower exposure to glutamate, and thus tend to have more apoptotic neuronal death characteristics (Choi, 1996; Hou & MacManus, 2002). The common factor between both of these forms of neuronal death is the dysregulation in cytosolic calcium.

The elevation of $[Ca^{2+}]_c$ initiates several detrimental processes. Some of these processes are directly activated by calcium, while others are indirect

consequences of Ca^{2+} influx into the mitochondria. Increased free cytosolic Ca^{2+} activates many Ca^{2+} -dependent degradation enzymes including calpains, Ca^{2+} -dependent proteases (Goll *et al.*, 2003). The activation of calpains results in the degrading of a variety of intracellular proteins, including cytoskeleton proteins, membrane receptors, and metabolic enzymes (Chan & Mattson, 1999; Nixon, 2003). Calpains may also play an important role in the activating of caspases which initiate the apoptotic pathway. Also, this increase in free cytosolic Ca^{2+} increases the activity of phospholipase A_2 , a calcium-dependent lipase, which degrades vital membrane phospholipids. This breakdown of phospholipids can disrupt membranes of the intracellular organelles (Bonventre, 1997). The activation of calpains or phospholipase can result in neuronal death.

In addition to the direct activation of calcium-dependent proteases and phospholipases, Ca^{2+} dysregulation leads to mitochondrial dysfunction and an increase in cytosolic reactive oxygen species (ROS) (Duan *et al.*, 2007). An increase in ROS will result in DNA damage leading to cell senescence and eventually cell death.

Besides the increase in ROS, calcium uptake by the mitochondria results in increased permeability in the mitochondrial membrane possibly leading to the release of the apoptotic protein cytochrome c. The release of cytochrome c may occur when the mitochondria swell, which occurs during glutamate exposure, leading to the rupture of the outer mitochondrial membrane (Buki *et al.*, 2000). Cytochrome c would initiate the apoptotic pathway by activating pro-apoptotic proteins, ultimately resulting in neuronal death.

E. Hypothesis and specific aim

The evidence presented above shows that glutamate induces calcium dysregulation (Budd & Nicholls, 1996), and the consequence of this calcium dysregulation is neuronal death (Choi & Hartley, 1993). The mechanism(s) that leads to Ca^{2+} dysregulation is not yet well understood, but calcium influx from the extracellular environment plays a critical role. Several possible mechanisms for calcium influx have been studied, but no single mechanism has been identified as the solo contributor of DCD. However, it appears likely that the NMDA receptor (Tymianski *et al.*, 1993b), and the $\text{Na}^+/\text{Ca}^{2+}$ exchanger in the reverse mode (Kiedrowski, 1999; Hoyt *et al.*, 1998) may have a critical role in this calcium influx induced by glutamate. The prolonged exposure of neurons to the major excitatory neurotransmitter, glutamate, causes sustained stimulation of glutamate receptors and results in a massive Ca^{2+} influx and significant elevation of $[\text{Ca}^{2+}]_c$ (Tymianski *et al.*, 1993b). This increase in $[\text{Ca}^{2+}]_c$ can be extruded from the cytosol by plasmalemmal Ca^{2+} -ATPase or by NCX operating in the forward mode (Guerini *et al.*, 2005). In addition, Ca^{2+} can be accumulated by mitochondria or by the endoplasmic reticulum (ER) (Bernardi, 1999). The Ca^{2+} -ATPase has low transport capacity (Tymianski *et al.*, 1993b) and, thus, cannot counteract the massive Ca^{2+} influx that occur when neuron are exposure to a prolonged elevation of glutamate. The ER accumulates calcium through the Ca^{2+} ATPase located on the ER. Thus, a similar limitation is created due to the low transport capacity of the Ca^{2+} ATPase. On the other hand, the NCX has high Ca^{2+} transport capacity and, therefore, can effectively clear elevated $[\text{Ca}^{2+}]_c$ (Carafoli

et al., 2001). However, during glutamate excitotoxicity there is an increase in $[Na^+]_c$ and the plasma membrane depolarization. These conditions prevent the NCX from operating and can result in the reversal of NCX that, instead of removing Ca^{2+} , now brings more Ca^{2+} into the cell (Kiedrowski *et al.*, 1994).

In addition, the mitochondria play a significant role in reducing the elevated cytosolic Ca^{2+} (Herrington *et al.*, 1996). However, mitochondrial Ca^{2+} uptake capacity is limited because of induction of the permeability transition pore (PTP) that precludes further Ca^{2+} accumulation (Chalmers & Nicholls, 2003; Li *et al.*, 2009). On the other hand, the extracellular space is practically an infinite source of Ca^{2+} and, therefore, attenuating Ca^{2+} entry from the outside of the cell seems the most effective way to protect neurons exposed to glutamate. However, this requires precise knowledge about Ca^{2+} entry mechanisms into neurons exposed to glutamate and warrants extensive research in this direction. Thus, the focus of this thesis is determining the Ca^{2+} influx mechanisms that lead to glutamate-induced calcium dysregulation, particular the role of the NMDA receptor and the reverse NCX.

Central hypothesis: Glutamate-induced delayed calcium dysregulation occurs due to Ca^{2+} influx through both the NMDA receptor and the reverse mode of the $\text{Na}^+/\text{Ca}^{2+}$ exchanger and that inhibition of both of these calcium influx mechanisms are necessary to prevent this delayed calcium dysregulation in hippocampal neurons. (Figure 2 is a visual representation of the central hypothesis and specific aims.)

Specific Aim 1: Determine if the reverse mode of $\text{Na}^+/\text{Ca}^{2+}$ exchanger is essential in delayed calcium dysregulation induced by glutamate in neurons.

Specific Aim 2: Determine if the activation of the NMDA receptor is essential in delayed calcium dysregulation induced by glutamate in neurons.

Specific Aim 3: Establish whether both NMDA receptor and the reverse mode of $\text{Na}^+/\text{Ca}^{2+}$ exchanger have to be inhibited to prevent glutamate-induced delayed calcium dysregulation in neurons.

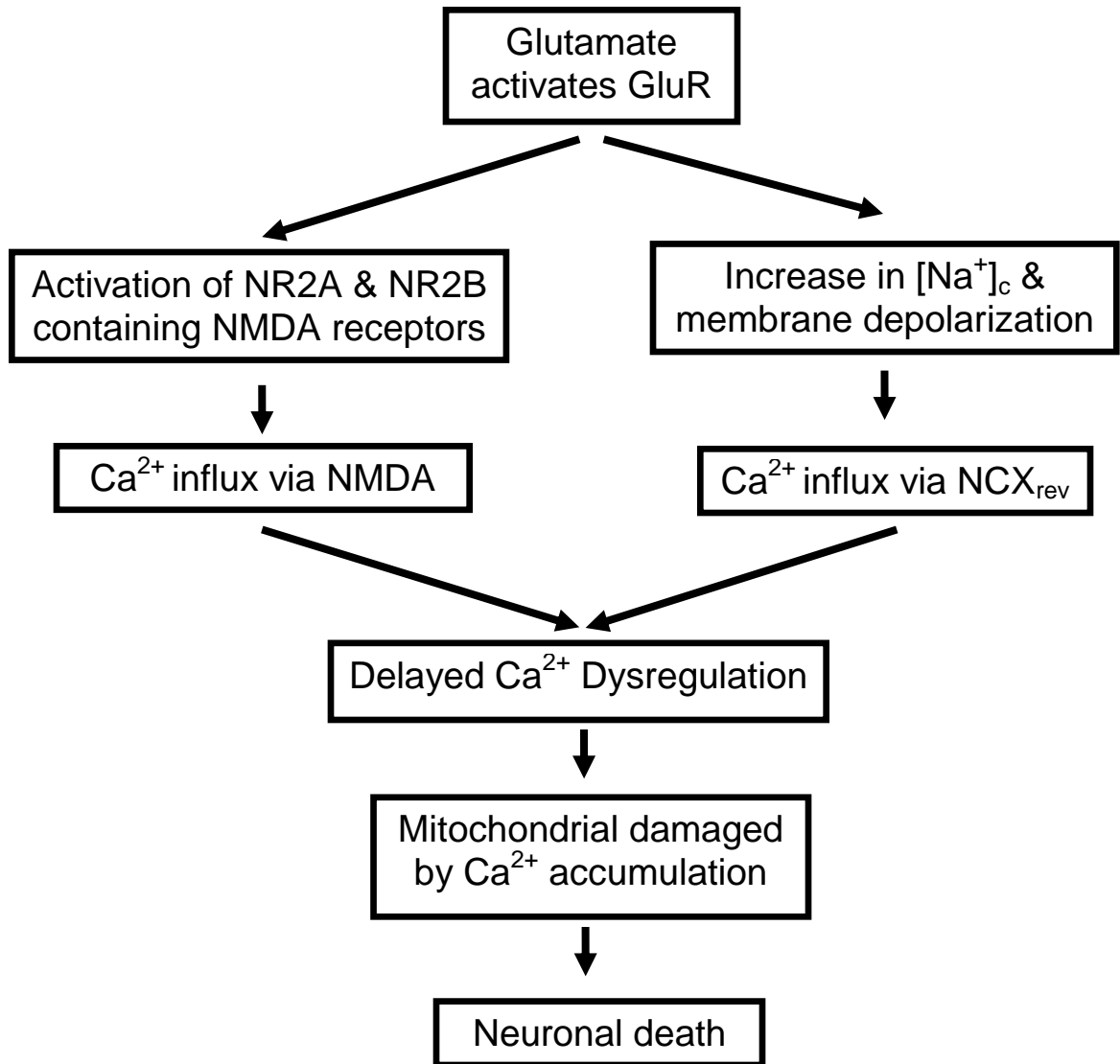


Figure 2. **Scheme represents the central hypothesis and specific aims of this thesis.** Calcium influx occurs through both the activation of the NMDA receptor and through the reverse mode of the sodium calcium exchanger. It requires simultaneous inhibition of both calcium influx mechanisms to prevent calcium dysregulation induced by glutamate.

II. MATERIALS AND METHODS

A. Materials

Glutamate, NMDA, glycine, rotenone, FCCP, and gramicidin were purchased from Sigma (St. Louis, MO). Fura-2FF-AM and Fura-2-AM were bought from Teflabs (Austin, TX) and Fluo-4FF-AM was purchased from Invitrogen (Carlsbad, CA). SBF1 and Sodium GreenTM were both purchased from Invitrogen. D-(-)-2-Amino-5-phosphonopentanoic acid (AP-5) and KB-R7943 were from Tocris (Ellisville, MO). KB-R7943 solutions were prepared daily and only used fresh on the day of the experiment. MK801 was purchased from Calbiochem (San Diego, CA). Memantine, ifenprodil, and PEAQX were all from Sigma (St. Louis, MO), and 5-(N-ethyl-N-isopropyl)amiloride (EIPA) was from MP Biomedicals (Irvine, CA). Aninone-6plus was kindly provided by Dr. Michael Rubart (Indiana University School of Medicine, Indianapolis).

B. Cell culturing

Primary cultures of hippocampal neurons were prepared from postnatal day 1 rat pups according to Institutional Animal Care and Use Committee (IACUC) approved protocol. For fluorescence measurements, neurons were plated on glass-bottomed Petri dishes without pre-plated glial (Dubinsky, 1993). The hippocampus was removed, minced, and incubated for 20 minutes at 37°C in L-15 containing 3 mg/mL papain and 3 mg/mL bovine serum albumin (BSA). After gentle trituration in growth medium, the cell suspension was layered on L-

15 containing 100 mg/ml BSA and centrifuged at 500 rpm for 5 min. The pellet was resuspended in growth medium minimum essential medium (MEM) without glutamine containing 27.75 mM glucose, 10% NuSerum (Collaborative Research), 50 U/ml penicillin, and 50µg/mL streptomycin, 335 mOsm. 500,000-cell aliquots were added to the polylysine-coated, glass-bottomed, 35 mm Petri dishes (Dubinsky, 1993). For all platings, 35µg/ml uridine plus 15µg/ml 5-fluoro-2'-deoxyuridine were added 24 hours after plating to inhibit proliferation of non-neuronal cells. Neuronal cultures were maintained in a 5% CO₂ atmosphere at 37°C in Earl's MEM supplemented with 10% NuSerum (BD Bioscience, Bedford, MA), 27 mM glucose and 26 mM NaHCO₃ (Dubinsky *et al.*, 1995).

C. Fluorescence imaging of cultured neurons

In our experiments, cultured hippocampal neurons from rats grown for 12-14 days *in vitro* (12-14 DIV) were used. Where indicated, in some experiments, younger neurons were used; for these experiments the cultured hippocampal neurons from rats were grown for 6-8 days *in vitro* (6-8 DIV). This distinction of younger and older was based upon the difference in expression of the NR2A/NR2B subunits of the NMDA receptor (Brewer *et al.*, 2007). This is supported by western blot.

For all experiments, at the time of the experiments neurons were rinsed twice with standard bath solution: 139 mM NaCl, 3 mM KCl, 0.8 mM MgCl₂, 1.8 mM CaCl₂, 10 mM NaHEPES, 5 mM glucose, 65 mM sucrose, as used previously in studies of DCD and excitotoxicity (Dubinsky *et al.*, 1995; Wang &

Thayer, 1996; White & Reynolds, 1996; Kushnareva *et al.*, 2005). The pH was adjusted to 7.36-7.38 using 1 M NaOH. Osmolarity of the bath solution was measured with an osmometer (Osmette II™, Precision Systems Inc., Natick, MA). The osmolarity ranged from 320 to 340 mOsm. Fluorescence imaging was performed with a Nikon Eclipse TE2000-U inverted microscope used a Nikon objective Plan Fluor 20X 0.45 NA and a back-thinned EM-CCD Hamamatsu C9100-12 camera (Hamamatsu Photonic Systems, Bridgewater, NJ) controlled by Simple PCI software 6.1 (Compix Inc., Sewickley, PA). The excitation light was delivered by a Lambda-LS system (Sutter Instruments, Novato, CA) and a Lambda 10-2 optical filter changer (Sutter Instruments, Novato, CA) controlled the excitation filters. To minimize photobleaching and phototoxicity, the images were taken every 15 seconds.

1. Measurements of cytosolic calcium concentration ($[Ca^{2+}]_c$)

(a.) *Fura-2-AM*

Fura-2-AM is a high-affinity, ratiometric, calcium-sensitive fluorescent dye with dissociation constant (K_d) near the typical basal calcium levels in mammalian cells (~100 nM) (Grynkiewicz *et al.*, 1985). The fluorescence measurements from a ratiometric dye are based on the use of a ratio between two fluorescence intensities. Ratiometric indicators undergo a shift in excitation or emission spectrum upon binding a specific substrate; for example, when Fura-2 is bound to calcium, it has a different excitation wavelength than the unbound indicator. This method allows correction of artifacts due to bleaching, changes in

focus, or variations in laser intensity, and the ratio calculation amplifies the changes in signal intensity. This signal amplification occurs because as the indicator concentration of the bound form increases, the concentration of the unbound form decreases. Thus the difference between emission fluorescence intensities of the two excitation wavelengths increase as the substrate concentration increases. Another important feature is that Fura-2 displays a high selectivity for Ca^{2+} binding relative to Mg^{2+} . Nevertheless, calcium binding is slightly effected by physiological levels of Mg^{2+} ; the K_d for Ca^{2+} of Fura-2 is ~ 135 nM in Mg^{2+} free Ca^{2+} buffer and ~ 224 nM in the presence of 1 mM Mg^{2+} (endogenous Mg^{2+} concentration) (Miyawaki *et al.*, 1997). The buffers used in experiments for this thesis contain 1 mM Mg^{2+} (unless otherwise indicated), thus the K_d of 224 nM was used for calcium concentration calculations. Fura-2-AM is a cell-permeant acetoxymethyl (AM) ester. Once Fura-2-AM crosses the plasma membrane, nonspecific esterases, present in most cells, hydrolyze the acetoxymethyl ester into formaldehyde and acetic acid, liberating the Ca^{2+} -sensitive indicator and significantly reducing permeability of Fura-2. This traps the indicator inside the cells, resulting in an extremely low leakage rate of the polyanionic indicator, and thus stabilizes the final intracellular indicator concentration. For calcium imaging with Fura-2, neurons are loaded with $2.6\mu\text{M}$ Fura-2AM at 37°C for 60 minutes. The excitation filters, 340 ± 5 and 380 ± 7 nm, were controlled by a Lambda 10-2 optical filter changer (Sutter Instruments, Novato, CA). Fluorescence was recorded from individual neurons through a 505 nm dichroic mirror at 535 ± 25 nm. The changes in $[\text{Ca}^{2+}]_c$ were monitored by

following Fura-2 F_{340}/F_{380} ratio, after the background was subtracted from fluorescence signals.

For all calcium sensitive dyes, the maximum and minimum signal is need to convert fluorescence signal into calcium concentration. The method used to for this conversion will be discussed later on in this section. To determine the maximum signal neurons are exposure to 5 μ M ionomycin plus 5 μ M FCCP. Following the collection of the maximum signal, the minimum signal was collected by exposing the neurons to a calcium free bath solution containing 10 mM Mg^+ plus 10 mM digitonin.

(b.) *Fura-2FF-AM*

Fura-2FF-AM is a low-affinity, ratiometric, calcium-sensitive fluorescent dye allowing one to monitor changes in cytosolic calcium during excitotoxic events (dynamic range ~0.5 to 50 μ M). This increases the dynamic range in comparison to Fura-2, allowing monitoring of changes in cytosolic calcium concentration during glutamate excitotoxicity. Fura-2FF-AM is a difluorinated derivative of Fura-2 with a K_d of 5.5 μ M (Miyawaki *et al.*, 1997). Because Fura-2FF-AM is a derivative of Fura-2, it has similar properties in that it is relatively insensitive to endogenous Mg^{2+} , and has excitation wavelengths that are the same as Fura-2, 340 \pm 5 and 380 \pm 7 nm. Fluorescence was recorded from individual neurons through a 505 nm dichroic mirror at 535 \pm 25 nm. The changes in $[Ca^{2+}]_c$ were monitored by following Fura-2FF F_{340}/F_{380} ratio, after the background was subtracted from the fluorescence signals. For calcium imaging with Fura-2FF,

neurons are loaded with 2.6 μ M Fura-2FF-AM at 37°C for 60 minutes. Fura-2FF-AM, like Fura-2-AM, is a cell-permeant acetoxymethyl ester. Nonspecific esterases present in the cell hydrolyze the acetoxymethyl ester to formaldehyde and acetic acid, liberating the Ca²⁺-sensitive indicator. This prevents significant leakage of the indicator, resulting in a stable intracellular concentration.

(c.) *Fluo-4-AM*

Fluo-4-AM is a green-fluorescent, calcium-sensitive dye. Similar to Fura-2, Fluo-4 has a high calcium binding affinity and is highly selective for calcium. The calcium binding affinity is similar to that of Fura-2 with a K_d of 345 nM. This low nanomolar K_d allows one to monitor accurately changes in basal [Ca²⁺]_c within the range of 35 nM to 3.5 μ M (Grynkiewicz *et al.*, 1985; Gee *et al.*, 2000). Another important feature of this Ca²⁺-sensitive dye is that calcium free Fluo-4 is essentially non-fluorescent, but exhibits strong fluorescence enhancement with no spectral shift upon binding Ca²⁺. The change in fluorescence intensity between the Ca²⁺ bound and unbound indicator is nearly a 100-fold difference for Fluo-4. This strong intensity change is important because unlike Fura-2 and Fura-2FF, Fluo-4 has only a single excitation wavelength at 488 nm (Gee *et al.*, 2000). This prevents the intensification properties of the ratiometric dyes, which is accomplished through the ratio calculation of the two different excitation wavelengths of the bound and unbound indicator. In experiments where Fluo-4 was used to monitor changes in [Ca²⁺]_c, the neurons were loaded with 2.5 μ M Fluo-4-AM for 30 minutes at 37°C. A single excitation wavelength at 480 \pm 20 nm

was used, and fluorescence was recorded from individual neurons through a 505 nm dichroic mirror at 535 ± 25 nm. The changes in fluorescence are expressed as F/F_0 , after the background was subtracted from the fluorescence signals. Calculating F/F_0 essentially allows one to gain the signal correction benefits of a ratio calculation out of a single wavelength measurement. The F_0 notation is the background-subtracted prestimulus fluorescence level. If this ratio intensity is used in place of the absolute intensity, then variations in cell thickness, total dye concentration, laser intensity, and focus are canceled out. This is similar to a ratiometric fluorescent dye without the amplification benefit. Another benefit of calculating F/F_0 , is that the initial point for each trace (individual neurons) starts at or near one, making it easier to compare traces from different experiments.

(d.) *Fluo-4FF-AM*

Fluo-4FF-AM is a green-fluorescent, low-affinity, calcium-sensitive indicator with a K_d of $9.7\mu\text{M}$ (Gee *et al.*, 2000; Grynkiewicz *et al.*, 1985). This allows one to monitor changes in cytosolic Ca^{2+} from 1 to $100\mu\text{M}$. This is a similar range to Fura-2FF. Fluo-4FF is an analog of Fluo-4, and thus, it retains many of the basic properties of Fluo-4. It has a single excitation wavelength maximum at 494 nm with emission wavelength maximum at 518 nm (Gee *et al.*, 2000). In experiments where Fluo-4FF is used, neurons were loaded with $2.5\mu\text{M}$ Fluo-4FF-AM for 30 minutes at 37°C . A single excitation wavelength at 480 ± 20 nm was used, and fluorescence was recorded from individual neurons through a 505 nm dichroic mirror at 535 ± 25 nm. The changes in fluorescence are

expressed as F/F_0 , after the background was subtracted from the fluorescence signals. By calculating F/F_0 rather than absolute fluorescence, one is able to correct for arbitrary signal variations. Similar to the other calcium indicators, fluo-4FF-AM is a cell-permeant acetoxymethyl ester, which becomes trapped inside the cell following ester hydroxylation.

2. Measurements of cytosolic sodium concentration ($[Na^+]_c$)

(a.) *SBFI-AM*

SBFI-AM is a ratiometric, sodium-sensitive fluorescent indicator. It is derived from benzofuran isophthalate with an acetoxymethyl ester to increase cell permeability. SBFI is relatively unaffected by changes in pH within the range of 6.5 and 7.5, which is important in the study of excitotoxicity because of the cellular acidification that occurs during glutamate exposure. The selectivity for sodium over potassium for SBFI is relatively high with roughly an 18-fold preference for Na^+ . However, the presence of K^+ has an effect on the affinity of SBFI for Na^+ . The K_d for SBFI in regard to Na^+ in the absence of K^+ is 3.8 mM, but the K_d for Na^+ in the presence of physiological concentrations of potassium is 11.3 mM. All of the experiments in this thesis contain K^+ , thus the K_d that has been used is 11.3 mM (Harootunian *et al.*, 1989). In experiments using SBFI, neurons were loaded with 9 μ M of the Na^+ -sensitive fluorescent dye SBFI-AM at 37°C for 60 minutes. The excitation filters 340 \pm 5 and 380 \pm 7 nm were used. Fluorescence was recorded through a 505 nm dichroic mirror at 535 \pm 25 nm. The changes in $[Na^+]_c$ were calculated as F_{340}/F_{380} after subtracting the background

from both channels. SBFI is a ratiometric dye, thus the benefits of the ratio calculation concerning data correction and signal amplification apply to this indicator.

For all sodium sensitive dyes, the maximum and minimum signal is need to convert fluorescence signal into calcium concentration. The method used to for this conversion will be discussed later on in this section. To determine the maximum signal neurons are exposure to 5 μ M gramicidin. Following the collection of the maximum signal, the minimum signal was collected by exposing the neurons to a calcium free bath solution containing 10 mM Mg⁺ plus 10 mM digitonin.

(b.) *Sodium Green*TM

Sodium GreenTM is a cell-permeant, visible light-excitation, sodium-sensitive indicator with a peak excitation and emission wavelengths of 507 nm and 532 nm, respectively (Harootunian *et al.*, 1989). Similar to SBFI, Sodium GreenTM exhibits a greater selectivity towards Na⁺ rather than K⁺, 41-fold preference for Na⁺. The K_d for this indicator is affect by potassium, which is also similar to SBFI. The K_d for Sodium GreenTM in a K⁺-free bath solution is 6 mM and 21 mM in a bath solution containing physiologically relevant K⁺ concentrations (Harootunian *et al.*, 1989). All experiments in this thesis contain physiological potassium concentrations. In experiments with Sodium GreenTM, neurons were loaded with 2 μ M Sodium GreenTM for 30 minutes at 37°C. Then the neurons were washed for 5 minutes to allow excess dye to leak out of the

cell. This process prevents a massive loss of dye during the experiment. The excitation wavelength used during the experiments was 480 ± 20 nm and fluorescence was recorded from individual neurons through a 505 nm dichroic mirror at 535 ± 25 nm. The changes in $[Na^+]_c$ were monitored by following Sodium GreenTM F/F_0 . The F/F_0 calculation aids in correcting variations in total dye concentrations between cells, changes in focus that can occur during the experiment, and photo bleaching of the dye that occurs due to repeated excitation.

3. Measurements of mitochondrial membrane potential ($\Delta\psi$): Rhodamine 123

Rhodamine 123 is a fluorescent indicator that is used to monitor changes in mitochondrial membrane potential. Rhodamine 123 is a cell-permeant, cationic, green-fluorescent dye that is readily sequestered by active mitochondria without cytotoxic effects (Kubin & Fletcher, 1982). Rhodamine 123 is cationic or positively charged, and it collects in the mitochondria due to strong mitochondrial membrane potential. Rhodamine 123, similar to other green-fluorescent indicators, has only a single excitation and emission wavelength. The excitation filter 480 ± 20 nm was used, and fluorescence was recorded through a 505 nm dichroic mirror at 535 ± 25 nm. The excitation light at 480 nm was attenuated by a quartz-neutral density filter to 10%. The changes in mitochondrial membrane potential were monitored by following Rhodamine 123 F/F_0 after background subtraction. Rhodamine 123 is unusual in that it is a proximity-sensitive dye. When Rhodamine 123 is in close proximity to itself it quenches the signal. The

caveat to this property is that one must have a high enough concentration of the dye so that the signal can be detected by the microscope. To this end Rhodamine 123 can be used in two different modes, a quenching or non-quenching mode. Each mode has different usages in this thesis.

(a.) *Rhodamine 123 - quenching mode*

Rhodamine 123 in quenching mode is used during experiments with whole cells assays. In these experiments neurons are loaded with 1.7 μ M Rhodamine 123 for 30 minutes at 37°C. At this concentration the mitochondria accumulate enough of the indicator that the fluorescence becomes quenched, and the baseline signal is at a minimum. Thus as the mitochondria become depolarized, Rhodamine 123 leaks out of the mitochondria, lowering the concentration enough to allow fluorescence to be detected. This results in an increase in Rhodamine 123 signal as the mitochondria become depolarized (Brustovetsky *et al.*, 2011). In cases where the mitochondria are depolarized for an extended period of time, the signal may begin to decrease; this rarely indicates mitochondrial repolarization. It is most likely that the dye is diffusing out of the cell, and the concentration is dropping below the level of detection. An easy way to determine which case is occurring is to simply depolarize the mitochondria at the end of the experiment with 1 μ M FCCP. If the signal has a dramatic increase, which would indicate that the mitochondria did repolarize. No change in the fluorescent signal would indicate a simple diffusion of the dye.

(b.) *Rhodamine 123 - non-quenching mode*

Rhodamine 123 in the non-quenching mode is used in experiments with isolated brain nonsynaptic mitochondria. Isolated mitochondria were placed into the glass-bottomed 35mm Petri dish and continuously perfused with a standard incubation medium supplemented with 0.2 μ M Rhodamine 123 (Brustovetsky *et al.*, 2011). During these experiments, the mitochondria were perfused using a ValveBank 8 perfusion system (AutoMate Scientific, San Francisco, CA). At this concentration of Rhodamine 123, the mitochondria can accumulate enough indicator to produce a strong fluorescent signal. As the mitochondria become depolarized Rhodamine 123 leaks out of the mitochondria, becoming diluted. This low concentration is not high enough to produce a strong signal. The non-quenching mode is opposite of the quenching mode in that when the mitochondria have a high membrane potential there is a strong fluorescence (Brustovetsky *et al.*, 2011). Then as the mitochondria become depolarized the fluorescence signal dims. In these experiments, one can monitor mitochondrial repolarization; this is due to the bath solution containing 0.2 μ M Rhodamine 123. Thus as the mitochondria repolarizes, they will accumulate a high enough concentration of Rhodamine 123 to produce a visible signal.

4. Measurements of nicotinamide adenine dinucleotide (NAD(P)H) redox state

NADH measurements in cultured hippocampal neurons from rats were performed using auto-fluorescence of NAD(P)H. Auto-fluorescence can be used when monitoring NAD(P)H redox state due to the different fluorescence

properties of the reduced state, NAD(P)H and the oxidized form, NAD(P)⁺ at the excitation wavelength, 360 nm (Brustovetsky *et al.*, 2011). The reduced form, NAD(P)H, fluoresce but the oxidized form, NAD(P)⁺, has no fluorescence. Using this change in fluorescence, one is able to monitor changes in redox state of NAD(P)H during excitotoxicity. The excitation filter used was 360±20 nm, and emission recording was through a 400 nm dichroic mirror at 460±25 nm. The excitation light was attenuated by a quartz-neutral density filter to 10%. For these experiments the microscope used a Nikon objective Plan Fluor 40X 0.45 NA. The changes in NAD(P)H redox state were calculated as F/F_0 , after background subtraction. Because this measurement relies on auto-fluorescence rather than a fluorescence dye, the signal is easily reversed. The only caveat to this is if there is a significant loss of or dilution of NAD(P)⁺. This could be due to NAD(P)⁺ leakage out of the mitochondria as a result of the induction of the mitochondrial permeability transition pore, or it could be due to NAD(P)⁺ degradation by Parp-1 in the cellular attempt to repair single strand breaks in the DNA.

5. Measurements of Reactive Oxygen Species (ROS): dihydroethidium

Neurons were loaded with superoxide radical sensitive indicator dihydroethidium (DHE, 4µM). This dye was added directly to bath solution at the onset of the experiment. The excitation and emission are similar to Rhodamine 123 with an excitation filter of 480±20 nm, and the emission was recorded through a 505 nm dichroic mirror at 535±25 nm. The superoxide indicator

dihydroethidium, also called hydroethidine, exhibits blue-fluorescence in the cytosol until oxidized. When it becomes oxidized, the oxidized form intercalates within the cell's DNA, staining its nucleus a bright fluorescent red. Dihydroethidium is a cumulative indicator, meaning once it is oxidized and intercalates with the DNA, it cannot be reversed (Eruslanov & Kusmartsev, 2010; Peshavariya *et al.*, 2007). Thus the baseline for this dye is constantly increasing due to the background ROS. The changes in reactive oxygen species were calculated as F/F_0 , after background subtraction. The F/F_0 calculation aids in correcting variations in total dye concentrations between cells, changes in focus that can occur during the experiment, and photo bleaching of the dye that occur due to repeated excitation.

6. Measurements of plasma membrane potential: Annine-6plus

A voltage sensitive fluorescent indicator, Annine-6plus (Fromherz *et al.*, 2008), was used to determine the changes in plasmalemmal membrane potential. Neurons were loaded with 4 μ M Annine-6plus for 5 minutes at room temperature. The short loading time allows the majority of this indicator to be incorporated into the plasma membrane rather than intracellular organelle membranes. The excitation wavelength that was used for these experiments was 488 \pm 20 nm, and the emission fluorescence was recorded from individual neurons through a long pass 570 nm filter. The changes in plasma membrane potential were monitored by following Annine-6plus F_{480} and expressed as F/F_0 . These calculations were made following subtraction of the background signal.

This signal is not reversible. For this dye to work a significant concentration must accumulate in the membrane to produce a signal. Then, as the membrane becomes depolarized, the indicator is released from the membrane, resulting in reduced fluorescence. Thus once the dye is released into the bath solution, the needed concentration to produce a signal no longer exists. Thus if the plasma membrane repolarizes, the amount of dye that membrane can accumulate from the bath solution is not sufficient to produce a visible signal.

7. Measurements of changes in cytosolic pH: BCECF-AM

BCECF-AM (2',7'-bis-(2-carboxyethyl)-5-(and-6)-carboxyfluorescein) is a ratiometric pH sensitive indicator. BCECF is an ideal indicator for physiological systems because it has a pK_a of 7.0, which is near the physiological pH range of 6.8 to 7.4. The pK_a is the acid dissociation constant, which is the measurement of the probability that a specific molecule will either be protonated or deprotonated at a specific pH (Rink *et al.*, 1982). This is relevant for a pH sensitive indicator because near the pK_a a molecule is in equilibrium between protonated and deprotonated states. Thus as the pH changes this dye will either gain or lose protons and change fluorescence correspondingly. In experiments where pH is monitored, neurons are loaded with 1.3 μ M BCECF-AM for 30 minutes at 37°C. BCECF-AM is an acetoxymethyl ester, which increases its cell permeability. Once BCECF enters the neuron, nonspecific esterases present in the cell hydrolyze the acetoxymethyl ester to formaldehyde and acetic acid. This essentially traps the indicator inside the neurons; also, BCECF has 4-5 negative

charges at physiological pH, aiding intracellular retention. The excitation filters 460 ± 5 and 488 ± 20 nm were used. Fluorescence was recorded through a 505 nm dichroic mirror at 535 ± 25 nm. The changes in cytosolic pH were calculated as F_{460}/F_{488} after subtracting the background from both channels. Similar to fura and SBFI, BCECF is a ratiometric indication; this allowing for correction of artifacts due to bleaching, changes in focus, or variations in laser intensity, and the ratio calculation amplifies the changes in signal intensity.

In some experiments, neurons were co-loaded with two different indicators. This allows for simultaneous monitoring of two different conditions. This is significant because it allows one to definitively observe multiple conditions within the same system without any variation that can occur between experiments. Any experiments that use this technique of co-loaded dyes will be noted in the figure legend.

D. Calcium and sodium fluorescence signal converted to concentration

Cytosolic Ca^{2+} concentrations ($[\text{Ca}^{2+}]_c$) and cytosolic Na^+ concentrations ($[\text{Na}^+]_c$) were calculated using the Grynkiewicz method (Grynkiewicz *et al.*, 1985) from the ratio or F/F_0 signals following the background subtraction. To perform this calculation, following the experiment calibration points must have been made. These points consist of the maximum and minimum signal. If these calibration points have been collected, the fluorescence signal can be converted to an approximate ion concentration using the K_d from the specific dye that was

used. This conversion is done using the following equation (Grynkiewicz *et al.*, 1985).

$$[\text{ion}] = K_d \left(\frac{F - F_{\min}}{F_{\max} - F} \right)$$

This conversion calculation must be taken as an approximation of the cytosolic ion concentration (Stanika *et al.*, 2009). Two assumptions exist concerning this calculation method. The first is that K_d used for the indicator acts the same inside the cellular environment as it does in an experimentally calculating it in a non-cellular environment. The cellular environment, in which these dyes are monitoring fluctuations in ion concentrations, is complex, and thus slight variations in the actual K_d could greatly affect the actual concentration in comparison to the calculated concentration. The second assumption is that minimum and maximum calibration points are accurate. The minimal calibration point is where the ion of interests is completely prevented from interacting with the indicators, however, this results in an incomplete quenching of the signal, and the process of saturating the signal for max fluorescence is also imperfect (Stanika *et al.*, 2009). When using indicators with high K_d values, the amount of ions that is needed to completely saturate the signal sometimes exceeds the content in the bath solution. This makes it difficult to produce a maximum fluorescence signal.

E. Isolation and purification of brain mitochondria

Brain mitochondria were isolated in mannitol-sucrose medium and purified on a discontinuous Percoll gradient as described previously in Brustovetsky *et al.* (2002). An adult rat brain was rapidly removed according to an IACUC-approved protocol and immediately put into ice-cold isolation medium containing 225 mM mannitol, 75 mM sucrose, 0.1% bovine serum albumin (BSA, free fatty acid-free), 1 mM EGTA, and 10 mM HEPES, pH 7.4. The tissue was washed with the isolation medium, dissected and homogenized with 20 mL of the isolation medium in a Dounce-type homogenizer. The homogenate was centrifuged at 2,000 g for 10 min at 2°C. The supernate was then centrifuged at 12,000 g for 10 min. The pellet was re-suspended in 20 mL of the medium containing 225 mM mannitol, 75 mM sucrose, 0.1 mM EGTA, and 10 mM HEPES, pH 7.4 and centrifuged again at 12,000 g for 10 min at 2°C. The pellet was re-suspended again to a final volume of 2 mL in the medium containing 394 mM sucrose, 1 mM EGTA, 10 mM HEPES, pH 7.4, and layered over pre-formed discontinuous Percoll gradient consisting of a bottom layer of 4 mL of 40% Percoll in 320 mM sucrose, 1 mM EGTA, 10 mM HEPES, pH 7.4, and a top layer of 4 mL of 26% Percoll in the same medium. The gradient was spun at 31,000 g for 28 min in a Beckman SW-41 rotor. The mitochondrial fraction appearing in the interface between two Percoll layers was transferred into a fresh tube, diluted 1:5 with medium containing 394 mM sucrose, 0.1 mM EGTA, 10 mM HEPES, pH 7.4 and centrifuged at 31,000 g for 20 min. The pellet was re-suspended in 0.5 mL of the latter medium and kept on ice. Mitochondrial protein was determined by the

Bradford method (Bradford, 1976) using BSA as a standard. This method was described previously in Brustovetsky *et al.* (2002).

F. Measurements of mitochondrial respiration and Ca²⁺ uptake.

The mitochondrial respiratory rates were measured as described previously in Li *et al.* (2008) at 37°C under continuous stirring in the closed 0.3 ml thermostated chamber using a Clark-type oxygen electrode in the standard incubation medium containing 125 mM KCl, 10 mM HEPES, pH 7.4, 0.5 mM MgCl₂, 3 mM KH₂PO₄, 10 μM EGTA, supplemented with 3 mM pyruvate and 1 mM malate or with 3 mM succinate plus 3 mM glutamate. Here and in other experiments, glutamate was used to prevent oxaloacetate inhibition of succinate dehydrogenase (Lehninger *et al.*, 1993). Mitochondrial Ca²⁺ uptake was measured as described previously in Storozhevyykh *et al.* (2010) with a miniature Ca²⁺-selective electrode in a 0.3 ml chamber at 37°C under continuous stirring. A decrease in the external Ca²⁺ concentration indicated mitochondrial Ca²⁺ uptake. The incubation medium was supplemented with 0.1% bovine serum albumin (BSA, free from fatty acids), 0.1 mM ADP, and 1 μM oligomycin. In all experiments with isolated mitochondria, the concentration of mitochondrial protein in the chamber was 0.2 mg/ml. All data traces shown are representative of at least three separate experiments.

G. Patch-clamp electrophysiology

Whole-cell patch-clamp recordings were conducted at room temperature using a HEKA EPC-10 double amplifier. Data were acquired using the Pulse program (HEKA Electronic, Lambrecht/Pfalz, Germany). Fire-polished electrodes (0.9—1.3 M Ω) were fabricated from 1.7 mm capillary glass (VMR Scientific, West Chester, PA) using a Sutter P-97 puller (Novato, CA, USA). When examining NMDA-induced currents, the composition of the electrode (“intracellular”) solution was as follows: 140 mM CsF, 10 mM NaCl, 1.1 mM EGTA, and 10 mM HEPES, pH 7.3 was adjusted with CsOH. The external solution was the same as in the fluorescence imaging experiments, except Mg²⁺ was omitted. The NCX-mediated ion currents were recorded using voltage ramp protocol as described previously in Convery & Hancox (1999). The composition of the electrode solution used for recording voltage ramp currents mediated by NCX was as follows: 20 mM KCl, 100 mM K-aspartate, 20 mM tetraethylammonium-Cl, 10 mM HEPES, 0.01 mM K-EGTA, 4.5 mM MgCl₂, and 4 mM Na-ATP, pH 7.3 adjusted with KOH (Smith *et al.*, 2006). The external solution used for recording ramp currents was as follows: 129 mM NaCl, 10 mM CsCl (to block K⁺ channels), 3 mM KCl, 0.8 mM MgCl₂, 1.8 mM CaCl₂, 5 mM glucose, 10 mM Na-HEPES, pH 7.2, 65 mM sucrose, 0.01 mM nifedipine (to block voltage-gated Ca²⁺ channels), 0.02 mM ouabain, 0.001 mM TTX (to block Na⁺ channels). Cover slips containing hippocampal neurons were placed into an RC-26 Open Diamond Bath perfusion chamber (Warner Instruments, LLC, Hamden, CT). The bath solution was removed using a Masterflex[®] C/L[®] Single

Channel Variable Speed peristaltic pump (Cole-Parmer Instrument Company, Vernon Hills, IL). A SF-77B Perfusion Fast-Step system (Warner Instruments, LLC, Hamden, CT) was used to deliver drugs focally onto isolated hippocampal neurons in whole-cell configuration. The drug delivery 3-barrel tube was placed near the neuron, and its positioning was calibrated before each experiment. The position of the drug delivery tube was controlled manually by a stepper motor, which could change the positioning in about 20 milliseconds. This method was previously described in Brustovetsky *et al.* (2011).

H. Cellular respirometry

Oxygen consumption rate (OCR) of cultured hippocampal neurons (10 DIV) was measured using Seahorse XF24 flux analyzer (Seahorse Bioscience, Billerica, MA) following the manufacturer's instructions. Neurons were grown in the assay plates at 5×10^5 cells per well. Before measuring, the growth medium was replaced by the standard bath solution supplemented with 10 mM glucose and 15 mM pyruvate (Brustovetsky *et al.*, 2011).

I. Western blotting

Cultured hippocampal neurons were solubilized with a solution containing 50 mM Tris-HCl, pH 7.35, 2 mM EDTA, 5 mM dithiothreitol, and 1% Nonidet P-40, and supplemented with a Proteinase Inhibitor Cocktail (Roche, Indianapolis, IN). Aliquots of this solution were mixed with NuPAGE® LDS sample buffer (Invitrogen, Carlsbad, CA), supplemented with a 1× NuPAGE® reducing agent

(Invitrogen) and incubated at 70°C for 15 minutes. 3-8% Tris-Acetate gels for α -spectrin and 7% Tris-Acetate gels (Invitrogen) for NCXs were used in electrophoresis (5 μ g protein/lane for α -spectrin and 5-50 μ g protein/lane for NR2A and NR2B). After electrophoresis, proteins were transferred to Hybond™-ECL™ nitrocellulose membrane (Amersham Biosciences, Piscataway, NJ). Blots were incubated for an hour at room temperature with one of the following primary antibodies: rabbit polyclonal antibody against NR2B or rabbit polyclonal antibody against NR2A (Millipore, Temecula, CA) at 1:2000 dilution with 5% non-fat dry milk and 0.15% Triton X-100 in phosphate-buffered saline (PBS), pH 7. Blots were developed using goat anti-rabbit IgG (1:20000) coupled with horseradish peroxidase (Jackson ImmunoResearch Laboratories, West Grove, PA) and Supersignal West Pico chemiluminescent reagents (Pierce, Rockford, IL). Molecular weight marker HiMark™ Pre-Stained Standards (15 μ l) (Invitrogen) were used to determine molecular weights of the bands. Western blots were quantified using Quantity One® software (Bio-Rad Laboratories, Hercules, CA), and densitometry data were expressed in arbitrary units (a.u.) for the corresponding bands.

J. Glutamate measurements

The glutamate concentrations were measured in the neuronal bath solutions following gramicidin application or Na⁺/NMDG⁺ replacement. Glutamate concentrations were quantified as previously described in Wang *et al.* (2010). Briefly, glutamate was determined using the Amplex Red glutamic

acid/glutamate oxidase assay kit (Invitrogen) according to the manufacturer's instructions. This assay utilizes the production of H₂O₂ that occurs during oxidation of glutamate to α -ketoglutarate by glutamate oxidase to fuel conversion of Amplex Red to the highly fluorescent resorufin by horseradish peroxidase. Samples were incubated with the Amplex Red enzyme mixture for 30 minutes before fluorescence was measured using an excitation of 530 nm and emission of 590 nm in a Victor³ V plate reader (Perkin Elmer, Shelton, CT).

K. Statistics

Statistical analysis of the experimental results consisted of unpaired *t*-test or one-way ANOVAs followed by Bonferroni's *post hoc* test (GraphPad Prism[®] 4.0, GraphPad Software Inc., San Diego, CA). Every experiment was performed using at least three different preparations of isolated mitochondria or three separate neuronal platings. All data are mean \pm SEM of at least 3 independent experiments. In most of the experiments dealing with changes in ion fluctuation as a result of a particular stimulus, area under the curve (Chang *et al.*, 2006) was calculated using GraphPad Prism[®] 4.0 software. The initial point was used as the baseline. These data were used to compare multiple conditions with the same experimental set-up.

III. RESULTS

The debilitating effects of neuronal death resulting from glutamate-induced delayed calcium dysregulation (DCD) are experienced by thousands of individuals each year (AHA, 2007). This neuronal death is a result of prolonged neuronal exposure to glutamate which leads to a sustained excitation of the neurons, manifested in a dysregulation in cytosolic calcium concentration ($[Ca^{2+}]_c$) (Nicholls & Budd, 1998). $[Ca^{2+}]_c$ is normally maintained at low levels (~100 nM) by homeostatic calcium extrusion and calcium accumulation mechanisms. However, during excitotoxic glutamate exposure, these mechanisms fail and an uncontrolled elevation of $[Ca^{2+}]_c$ occurs. A causal relationship between this elevation in $[Ca^{2+}]_c$ and neuronal death has been established (Manev *et al.*, 1989; Choi & Hartley, 1993), but the root cause of this calcium dysregulation is not yet well understood.

A. What are the effects of prolonged glutamate exposure on cultured hippocampal neurons from rats?

1. Prolonged glutamate exposure causes cytosolic Ca^{2+} dysregulation and mitochondrial depolarization

Figure 3 shows a representative experiment of pseudo-color (Figure 3A, C) images of cultured hippocampal neurons from rats co-loaded with Fura-2FF-AM and Rhodamine 123 (Rh123), respectively. Fluorescent imaging using Fura-2FF allows one to follow changes in $[Ca^{2+}]_c$ in real-time, as seen in

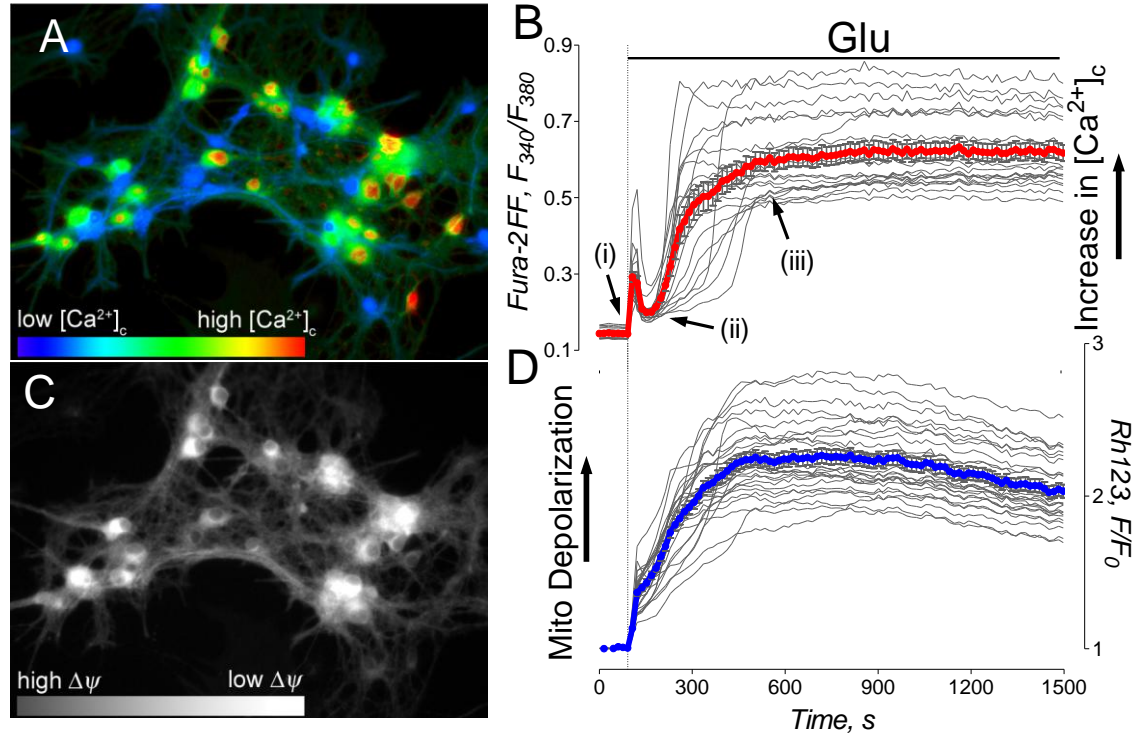


Figure 3. **Glutamate induces dysregulation in cytosolic calcium concentration and mitochondrial depolarization in cultured rat hippocampal neurons.** Neurons were co-load with Fura-2FF-AM (A, B) and Rhodamine 123 (C, D) to follow cytosolic calcium concentration ($[Ca^{2+}]_c$) and mitochondrial membrane potential ($\Delta\psi$), respectively. In panel A, a representative pseudo color Fura-2FF ratio F_{340}/F_{380} image demonstrates changes in $[Ca^{2+}]_c$ in individual neurons following exposure to 25 μ M glutamate plus 10 μ M glycine. (In all experiments throughout this thesis, where glutamate is used glycine is also present.) In panel C, the co-pseudo color Rhodamine 123 fluorescence image that was taken from the same field, demonstrating changes in $\Delta\psi$ follow glutamate exposure. Panels B and D are the corresponding traces representing the changes in $[Ca^{2+}]_c$ and $\Delta\psi$, respectively. Here and in all other experiments, the thin gray lines are the individual neurons found within the field of interest. The thicker red line found in panel B and the thicker blue line found in panel D are the cumulative averages of the thin gray lines from that particular trace. The colored line represents one experiment. The numerals (i, ii, iii) found in panel B represent the three distinct stages of $[Ca^{2+}]_c$ found during classical delayed calcium dysregulation that occur following exposure to excitotoxic glutamate.

corresponding traces in Figure 3B. Fura-2FF is expressed in a F_{340}/F_{380} ratio. Figure 3D is the corresponding trace of Rhodamine 123 expressed as F/F_0 ratio, allowing one to follow mitochondrial membrane potential in real-time. Co-loading the neurons with these fluorescent dyes permits the monitoring of multiple conditions simultaneously within a field of interest. Figure 3B is a good example of classical delayed calcium dysregulation induced by excitotoxic glutamate exposure. The numerals (i, ii, iii) show the three distinct transitions that $[Ca^{2+}]_c$ goes through in delayed Ca^{2+} dysregulation. Immediately following the addition of glutamate, (i) a large influx of Ca^{2+} is observed. This Ca^{2+} influx is due to the activation of ionotropic glutamate receptors, particularly the NMDA receptor. This initial spike can be prevented by inhibiting the NMDA receptor with an NMDA receptor antagonist. The initial influx of Ca^{2+} from the extracellular environment is followed by (ii) a transient decrease to a lower yet still elevated level of $[Ca^{2+}]_c$. Ca^{2+} levels never reach baseline, and this transition, depending on the age and health of the neurons, can last a few seconds as seen in this trace, to several minutes followed by (iii) a large, sustained increase in $[Ca^{2+}]_c$ (Nicholls & Budd, 2000; Brustovetsky *et al.*, 2010).

The reduction in $[Ca^{2+}]_c$ is due to the normal Ca^{2+} extrusion/accumulation mechanisms that maintain low resting calcium levels. The two essential mechanisms are Ca^{2+} extrusion by the Na^+/Ca^{2+} exchanger (NCX) and Ca^{2+} accumulation by the mitochondria. These mechanisms are essential for maintaining low levels of $[Ca^{2+}]_c$, and they are necessary to reduce the initial influx in calcium seen during glutamate exposure. In Figure 4A and B, Na^+ from

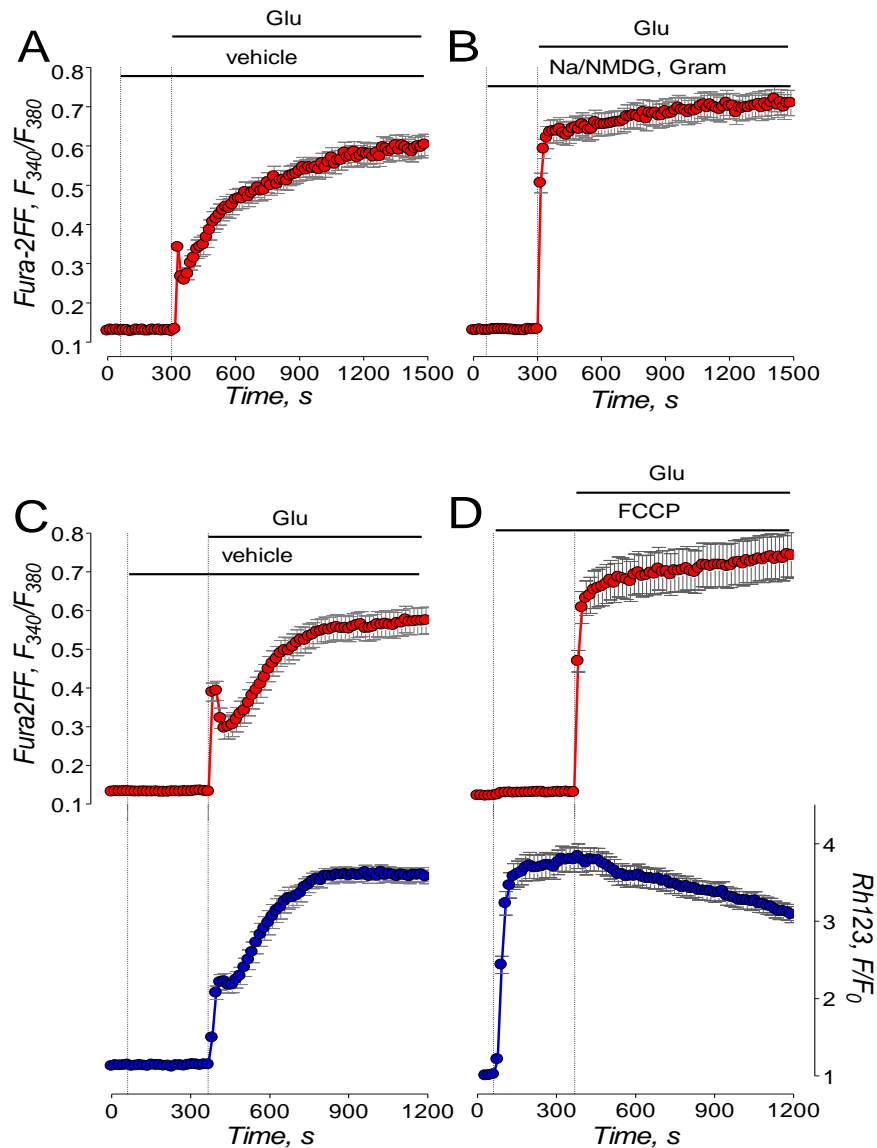


Figure 4. **Inhibition of the forward mode of the NCX or mitochondrial calcium accumulation results in immediate calcium dysregulation after glutamate exposure.** In panel A, B, neurons were loaded with Fura-2FF-AM (thick red line) to follow cytosolic calcium concentration ($[Ca^{2+}]_c$). Where indicated 25 μ M glutamate plus 10 μ M glycine were added. In panel B, Na⁺ in the bath solution was replaced with NMDG⁺, shutting down the NCX. In panel C, D, neurons were co-loaded with Fura-2FF-AM (thick red line) and Rhodamine 123 (thick blue line) to follow cytosolic calcium concentration ($[Ca^{2+}]_c$) and mitochondrial membrane potential ($\Delta\psi$), respectively. In panel D, the neurons were exposed to 5 μ M FCCP to depolarize the mitochondria, preventing mitochondria Ca²⁺ accumulation. The traces are expressed as F_{340}/F_{380} for Fura-2FF and F/F_0 for Rhodamine 123.

the extracellular bath solution was replaced with N-methyl-D-glucamine (NMDG⁺), a large organic cation. This prevented the NCX from extruding Ca²⁺. When glutamate is added, immediate calcium dysregulation occurs. Likewise, in Figure 4C and D, the mitochondria were depolarized with carbonyl cyanide-*p*-trifluoromethoxyphenylhydrazone (FCCP), a proton ionophore. This mitochondrial depolarization prevented the mitochondria from accumulating Ca²⁺. Thus, when the neurons are exposed to glutamate, immediate Ca²⁺ dysregulation is observed. This influx and removal of Ca²⁺ in the cytosol occurs during normal neuronal excitation, in which the neurons are exposed to a stimulus only briefly. However, during excitotoxicity, glutamate exposure is sustained. This prolonged exposure to glutamate results in failure of these counteracting Ca²⁺ extrusion/accumulation mechanisms which leads to the sustained Ca²⁺ dysregulation.

2. Prolonged glutamate exposure causes the “uncoupling” of the respiratory chain and oxidative phosphorylation

The observed mitochondrial depolarization is most likely a result of the respiratory chain and oxidative phosphorylation becoming uncoupled. To test this hypothesis, we examined autofluorescence of NAD(P)H in cultured hippocampal neurons exposed to glutamate. In the presence of external Ca²⁺ (1.8 mM), glutamate produced a gradual decrease in NAD(P)H fluorescence, reflecting NAD(P)H oxidation and conversion into NAD(P)⁺, which does not fluoresce (Chance & Williams, 1956) (Figure 5A). This NAD(P)H oxidation

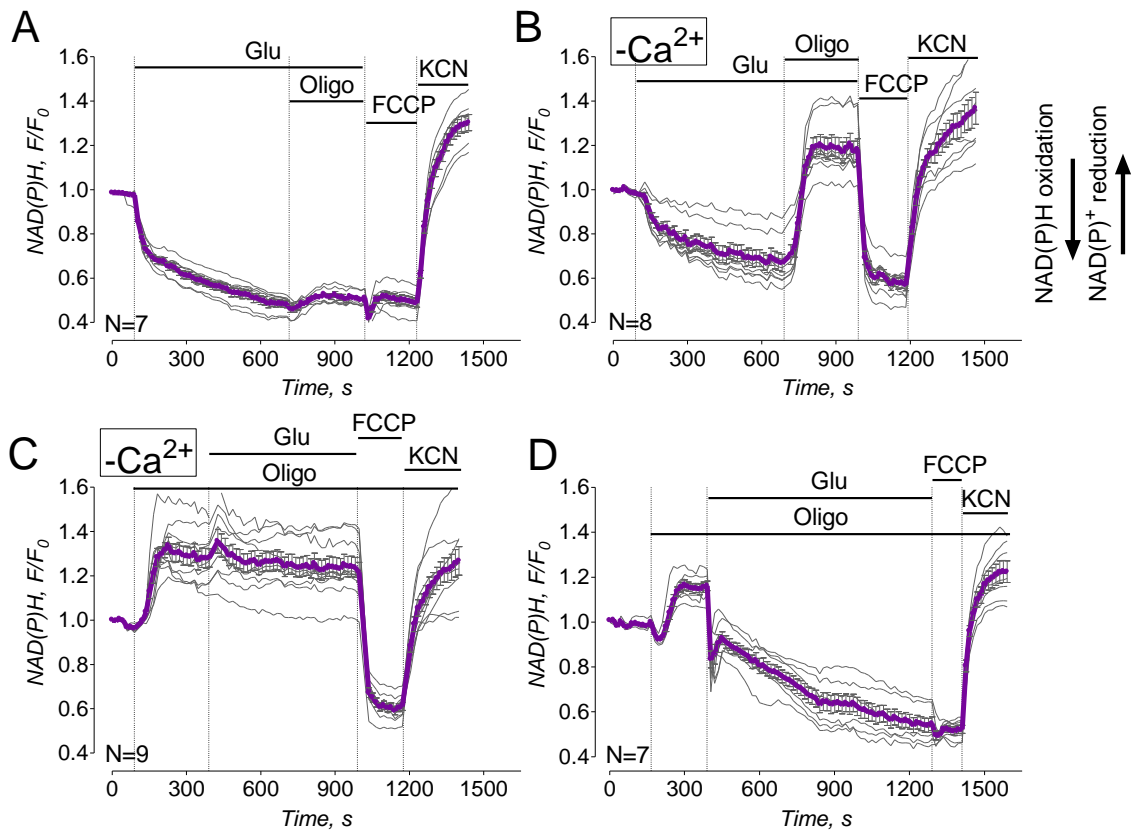


Figure 5. **Glutamate evoked NAD(P)H oxidation which was either coupled (in the absence of external Ca^{2+}) or uncoupled (with external Ca^{2+}) from ATP synthesis.** In A and D, bath solution was with 1.8 mM Ca^{2+} ; in B and C, bath solution was nominally Ca^{2+} -free. Where indicated, 25 μM glutamate (Glu, plus 10 μM glycine), 1 μM oligomycin (Oligo), 1 μM FCCCP, or 10 mM KCN were applied to neurons. Thin, grey traces show signals from individual neurons from the same dish while thick, purple traces show averaged signals (mean \pm SEM) for NAD(P)H F/F_0 . In A-D, each experiment was performed five times. The total number of examined neurons was 38 (A), 37 (B), 40 (C), and 44 (D).

could be due to accelerated electron flow in the respiratory chain associated with the increased mitochondrial plasma membrane potential dissipation in response to augmented ATP synthesis.

Alternatively, NAD(P)H oxidation could be due to accelerated electron flow resulting from the uncoupling of respiration and ATP synthesis in mitochondria. Oligomycin (1 μ M), an inhibitor of the mitochondrial ATP synthase, failed to recover NAD(P)H, suggesting that the decrease in NAD(P)H was not due to augmentation of ATP synthesis (Figure 5A). FCCP, a protonophore that depolarized mitochondria and, hence, accelerated electron flow in the respiratory chain, failed to influence NAD(P)H, suggesting that the NAD(P)H pool had already been maximally oxidized (Figure 5A). On the other hand, KCN, an inhibitor of cytochrome oxidase, stopped electron flow in the entire respiratory chain, leading to recovery of NAD(P)H (Figure 5A).

Omitting Ca²⁺ from the bath solution did not prevent oxidation of NAD(P)H induced by glutamate (Figure 5B). However, in this case oligomycin produced a strong increase in NAD(P)H, indicating that oxidation and ATP synthesis were tightly coupled and mitochondria were healthy. FCCP strongly decreased NAD(P)H, whereas KCN added after FCCP recovered NAD(P)H. In the absence of external Ca²⁺, oligomycin added prior to glutamate increased NAD(P)H and completely prevented NAD(P)H oxidation following the application of glutamate (Figure 5C). In the bath solution with 1.8 mM Ca²⁺, oligomycin added prior to glutamate also increased NAD(P)H, indicating tight coupling of oxidative phosphorylation under resting conditions (Figure 5D). Interestingly, glutamate

added after oligomycin still produced oxidation of NAD(P)H, suggesting uncoupling between mitochondrial oxidation and ATP synthesis. Moreover, in the presence of oligomycin, glutamate caused accelerated NAD(P)H oxidation. In the presence of oligomycin, ATP supply for plasma membrane Ca^{2+} -ATPase could be depleted, leading to less Ca^{2+} extruded from the cytosol. Additionally, by inhibiting ATP synthesis oligomycin hyperpolarizes mitochondria.

Mitochondrial hyperpolarization accelerates Ca^{2+} uptake because mitochondrial membrane potential is a driving force for Ca^{2+} uptake (Bernardi, 1999). Correspondingly, elevated cytosolic Ca^{2+} could be taken up by mitochondria faster, resulting in more rapid depolarization, more robust activation of electron flow in the respiratory chain, and faster NAD(P)H oxidation. At the end of the experiment, FCCP failed to further decrease NAD(P)H, while KCN produced robust NAD(P)H recovery (Figure 5D) by inhibiting Complex VI in on electron transport chain.

3. Prolonged glutamate exposure causes an increase in the presence of superoxide radicals in cytosol

During glutamate exposure, researchers observed an increase in reactive oxygen species (ROS) in the cytosol in response to mitochondrial depolarization (Castilho *et al.*, 1999). In Figure 6, the neurons were loaded with a superoxide radical indicator, dihydroethidium (DHE) to test whether similar results are observed in the neuronal cultures. DHE exhibits blue-fluorescence in the cytosol until it is oxidized. Once DHE is oxidized, it is incorporated in the DNA staining

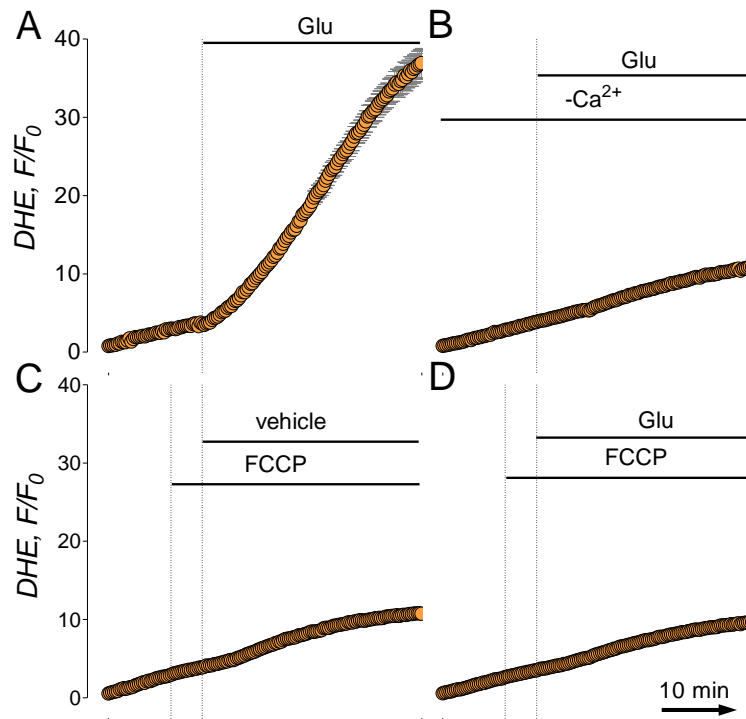


Figure 6. Increase in reactive oxygen species during glutamate exposure is a result of calcium accumulation by the mitochondria. In this figure, neurons were load with 4 μ M dihydroethidium (DHE), a superoxide radical indicator. DHE allows one to monitor changes in cytosolic reactive oxygen species (ROS) concentration. The excitation of 480 \pm 20 nm was used. Fluorescence was recorded through a 505 nm dichroic mirror at 535 \pm 25 nm. The slow increase in fluorescence prior to any experimental manipulations shows the basal level of ROS in the cytosol. When DHE is oxidized by superoxide radicals it becomes incorporated into the DNA. This is irreversible, and thus, over time a stead increase fluorescent signal is observed. Where indicated 25 μ M glutamate and 10 μ M glycine were added. In panel A, glutamate exposure resulted in an increase in ROS concentration in the cytosol. Panel B, calcium was removed from the bath solution, preventing calcium influx due to glutamate exposure. In the absences of Ca²⁺ influx, glutamate exposure had no effect on cytosolic ROS levels. In panel C, 1 μ M FCCP was added to depolarize the mitochondria, resulting in no changes to ROS concentrations. In panel D, FCCP depolarized the mitochondria preventing mitochondrial calcium uptake. These experiments indicate that it is necessity of mitochondrial calcium uptake for an elevation in ROS concentrations during glutamate exposure.

the nucleus to a bright red-fluorescence. This change in fluorescence spectrum allows one to monitor the change in ROS concentration in the cytosol (Bucana *et al.*, 1986). In Figure 6A, glutamate exposure resulted in a rapid increase in cytosolic ROS concentration. As previously published, this increase in ROS is dependent on an increase in cytosolic calcium (Castilho *et al.*, 1999). In Figure 6B, calcium was removed from the external bath solution preventing an increase in cytosolic calcium. When there is no increase in cytosolic calcium, glutamate exposure has no effect on changes of ROS concentrations. These experiments (Figure 6A,B) confirm that changes in ROS concentration in the cytosol are Ca^{2+} dependent.

The presence of elevated calcium in the cytosol alone would not increase the ROS concentration. This elevated $[\text{Ca}^{2+}]_c$ must interact with something resulting in either an increase in ROS production or a decrease in ROS detoxification or both. We know that the increase in $[\text{Ca}^{2+}]_c$ results in mitochondrial depolarization, and research has suggested that mitochondrial depolarization results in an increase in ROS (Castilho *et al.*, 1999). Thus, mitochondrial depolarization could cause this observed increase in ROS. In Figure 6C, the mitochondria were depolarized by the addition of 1 μM FCCP. This mitochondrial depolarization without the increased $[\text{Ca}^{2+}]_c$ failed to produce increased ROS concentrations.

In Figure 6D, the mitochondria were depolarized by the addition of FCCP prior to the addition of glutamate. As previously described in Figure 4, the addition of FCCP results in mitochondrial depolarization, and thus the

mitochondria no longer have the ability to accumulate calcium (Wang & Thayer, 1996; Bernardi, 1999). Regardless, the addition of glutamate results in an increase in $[Ca^{2+}]_c$, but the mitochondria will not be affected. Based on the above controls with no increase in ROS concentrations, one can conclude that calcium must be taken up by the mitochondria to cause an increase in ROS concentration during excitotoxicity.

4. Prolonged glutamate exposure causes an increase in both cytosolic Ca^{2+} and Na^+ simultaneously

We have shown that glutamate exposure indeed results in a robust increase in $[Ca^{2+}]_c$ and that increase in $[Ca^{2+}]_c$ hampers the ability of the mitochondria to accumulate calcium. This ultimately hinders the neurons from maintaining low calcium levels. In addition to mitochondrial calcium accumulation, the Na^+/Ca^{2+} exchanger (NCX) is vital to maintaining low $[Ca^{2+}]_c$ levels (Figure 4A,B). The NCX is known to use the large Na^+ gradient across the plasma membrane to exchange three Na^+ ions for one Ca^{2+} ion (Blaustein & Lederer, 1999). Thus, if the Na^+ gradient collapses, the NCX may lose the ability to function properly.

In Figure 7, changes in $[Ca^{2+}]_c$ and cytosolic Na^+ concentration ($[Na^+]_c$) were followed simultaneously using Ca^{2+} -sensitive fluorescent dye Fluo-4FF and Na^+ -sensitive dye SBFI. Neurons were co-loaded with both Fluo-4FF and SBFI, then 25 μ M glutamate and 10 μ M glycine were added where indicated. The increase in $[Na^+]_c$ was suspected to be caused by activation of the AMPA

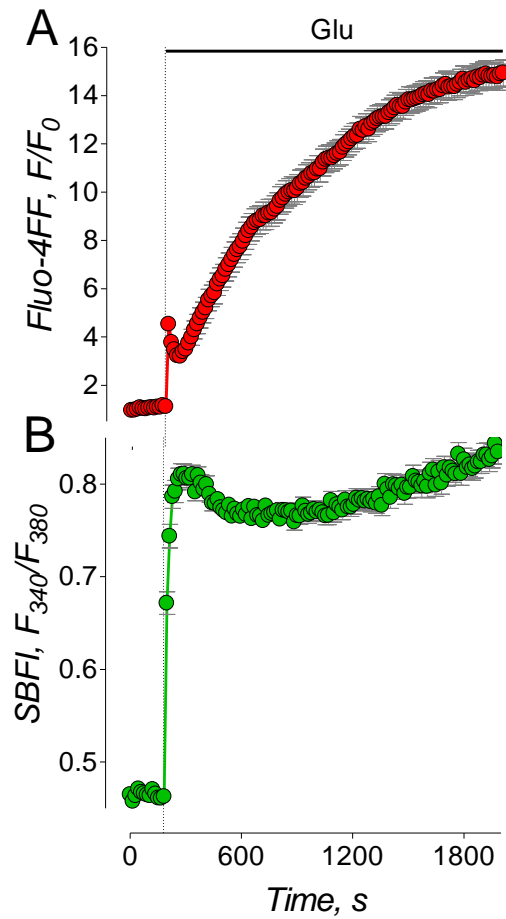


Figure 7. **Glutamate induces an increase in both in cytosolic calcium and sodium in cultured hippocampal neurons from rats.** Neurons were co-load with Fluo-4FF (A) and SBFI (B) to follow changes in cytosolic calcium (thick red line) and sodium (thick green line) levels, respectively. Where indicated, 25 μ M glutamate plus 10 μ M glycine was added. Fluo-4FF signal is express as F/F_0 while SBFI is expressed as F_{340}/F_{380} . The back ground signal was subtracted from both the Fluo-4FF and SBFI signals prior to final ratio calculations.

and kainate receptors (ionotropic glutamate receptors) or by the opening of the voltage-gated Na⁺ channels. Thus, to test this hypothesis (Figure 8), neurons were loaded with SBFI and 100µM CNQX, or 1µM tetrodotoxin (TTX), or the combination of CNQX and TTX was added prior to the addition of glutamate, none of which prevented the glutamate-induced increase in cytosolic Na⁺. Recently, the Na⁺/H⁺ exchanger (NHE) has been suggested to play a central role in the increase in cytosolic Na⁺ in neurons following oxygen glucose deprivation (Kintner *et al.*, 2004; Kintner *et al.*, 2010). The role of the NHE in the increase in cytosolic Na⁺ induced by glutamate is further investigated later on in this thesis.

5. Prolonged glutamate exposure causes a decrease in cytosolic pH

The NHE normally aids in the maintenance of the cytosolic pH, ~7.35. However, during glutamate exposure cytosolic acidification has been observed. In Figure 9, a proton-sensitive fluorescent dye, BCECF-AM, was used to monitor changes in the intracellular proton concentration. The concentration of protons can be expressed as pH, $\text{pH} = -\lg([\text{H}^+])$. In Figure 9A, varying pH bath solutions were used to produce a calibration curve to determine the sensitivity of BCECF. Throughout this experiment 3µM nigericin, a K⁺/H⁺ ionophore, was present to equilibrate the extracellular and intracellular pH. Based on this experiment, this fluorescent dye was shown to detect minor changes in pH within the needed dynamic range. In Figure 9B, 25µM glutamate plus 10µM glycine were added where indicated resulting in immediate acidification. At the conclusion of the experiment, the bath solution was replaced with a standard solution with a pH of

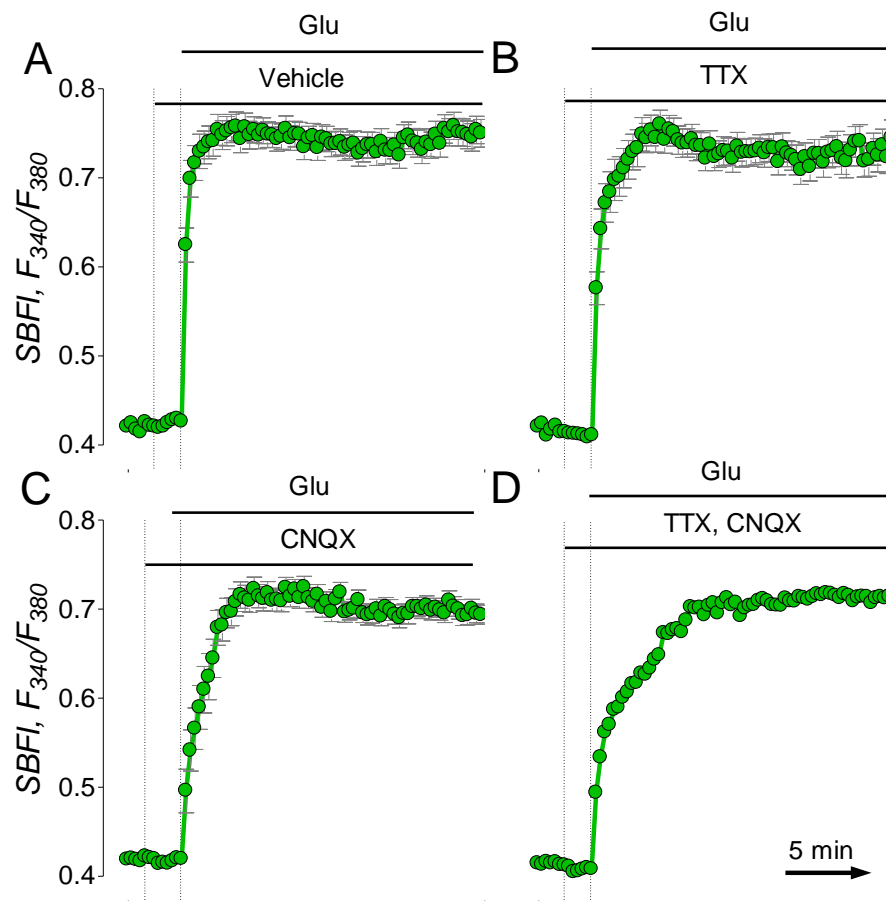


Figure 8. Inhibition of glutamate receptors and/or voltage-gated sodium channels fails to prevent glutamate-induced increase cytosolic sodium. In these experiments, the neurons were loaded with 9 μ M SBFI, a Na⁺-sensitive dye to monitor changes in cytosolic sodium. Where indicated 25 μ M glutamate plus 10 μ M glycine was added resulting an increase in cytosolic Na⁺ (A). 1 μ M TTX (B), 100 μ M CNQX (C), or the combination of both inhibitors at their respective concentrations (D) failed to prevent this increase in cytosolic Na⁺.

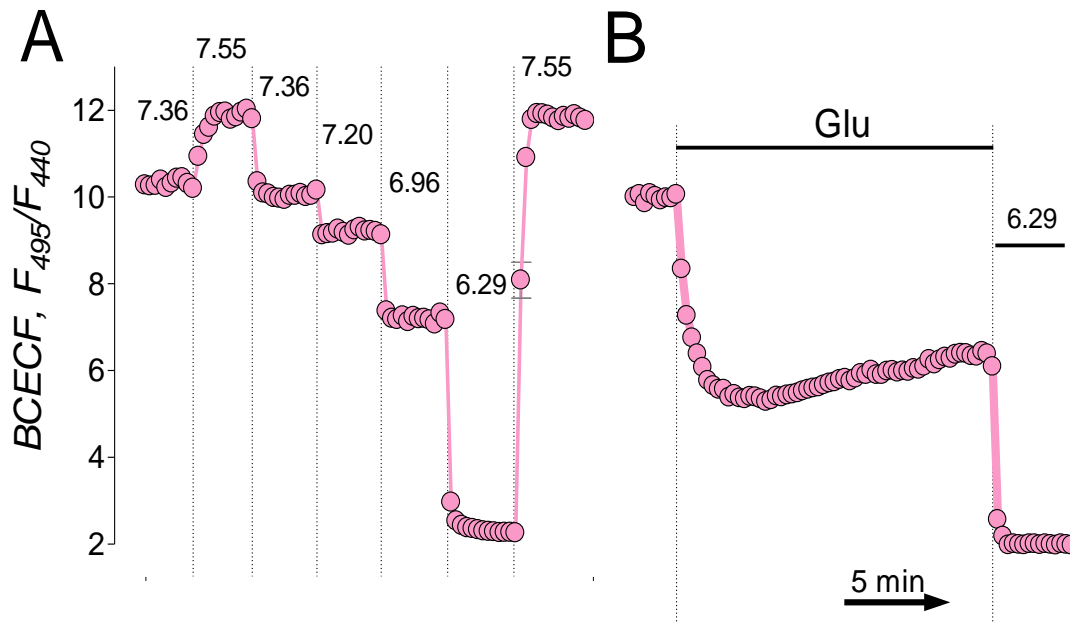


Figure 9. Glutamate induces an increase in cytosolic proton concentration resulting in intracellular acidification in cultured hippocampal neurons. Neurons were loaded with a proton sensitive dye BCECF-AM and monitor using excitation wavelengths 460 ± 5 and 488 ± 20 nm. The traces are expressed as F_{488}/F_{460} following background subtraction, where the thick pink line is the average of the individual neurons. In panel A, several different bath solutions with varying pHs. This was used to determine the sensitive and possibly build a calibration curve for BCECF. Throughout this experiment in panel A, a K^+/H^+ ionophore, nigericin $3\mu M$, was present to equalize that proton concentration across the plasma membrane. Panel B represents the change in intracellular proton concentration following the addition of glutamate $25\mu M$ and glycine $10\mu M$ where indicated. Where indicated in panel B, the bath solution at a pH of 6.29 with $3\mu M$ nigericin was added to calibrate this experiment to the calibration curve in panel A.

6.29 supplemented with nigericin; this point along with the initial pH measurement was used to calibrate this experiment to the calibration curve. The change in proton concentration was similar to other published data (Wu *et al.*, 1999; Hartley & Dubinsky, 1993; Wang *et al.*, 1994). The glutamate-induced acidification has been suggested to be due to the increased activity of the Ca²⁺ ATPase removing calcium from the cytosol. Ca²⁺ ATPase activity produces 2 protons for every calcium ion extruded.

B. What is the contribution of the reverse mode of the Na⁺/Ca²⁺ exchanger on glutamate-induced delayed calcium dysregulation?

During normal physiological conditions, the Na⁺/Ca²⁺ exchanger (NCX) removes calcium from the cytosol in exchange for extracellular sodium (DiPolo & Beauge, 2006; Carafoli *et al.*, 2001; Yu & Choi, 1997). The energy used to transport these ions is the large gradient of sodium across the plasma membrane and the plasma membrane polarization (Mayer & Westbrook, 1987; Yamaguchi & Ohmori, 1990; Tsuzuki *et al.*, 1994). However during the prolonged neuronal exposure to glutamate, there is a large sustained influx of Na⁺ into the cytosol and the plasma membrane becomes depolarized (Mayer & Westbrook, 1987; Tsuzuki *et al.*, 1994). Studies have shown that under these conditions, the NCX will stop functioning as a Ca²⁺ extrusion mechanism and could possibly reverse ion flow bringing calcium into the cytosol. The reverse mode of the Na⁺/Ca²⁺ exchanger (NCX_{rev}) has been proposed as a major contributor to glutamate-induced calcium dysregulation (Kiedrowski, 1999; Hoyt *et al.*, 1998).

1. KB-R7943 inhibits the reverse mode of the Na⁺/Ca²⁺ exchanger, but it fails to protect neurons against glutamate-induced delayed calcium dysregulation

Since its introduction, KB-R7943 remains the only commercially available NCX_{rev} inhibitor, and thus, it is the most widely used inhibitor of NCX_{rev}. In our experiments, KB-R7943 (15μM) failed to protect cultured hippocampal neurons against DCD (Figure 10A,B). Moreover, KB-R7943 accelerated the onset of DCD and mitochondrial depolarization induced by 25μM glutamate and completely prevented a recovery of [Ca²⁺]_c after glutamate removal (Figure 10B). Here and in other experiments, 100% of neurons responded to KB-R7943 by accelerating DCD and by depolarizing mitochondria. Recently, we introduced a parameter: *the time from the beginning of glutamate exposure to completion of the DCD* (t_{DCD}) to provide a statistical analysis of DCD (Brustovetsky *et al.*, 2009; Li *et al.*, 2009). The statistical analysis revealed that KB-R7943 significantly accelerated the onset of DCD in cultured neurons exposed to 25μM glutamate (Figure 10): t_{DCD} without KB-R7943 was 817±27 seconds while t_{DCD} with 15μM KB-R7943 was 398±38 seconds (mean±SEM, $p<0.01$, unpaired t -test, N=5, five independent experiments, 113 neurons total in the control with vehicle, 0.2% DMSO, and 108 neurons with KB-R7943 were analyzed). In contrast to KB-R7943, MK801 (10μM), an inhibitor of the NMDA receptor, completely inhibited glutamate-induced calcium deregulation, whereas CNQX, an inhibitor of AMPA/kainate receptors, was practically without effect (Figure 11).

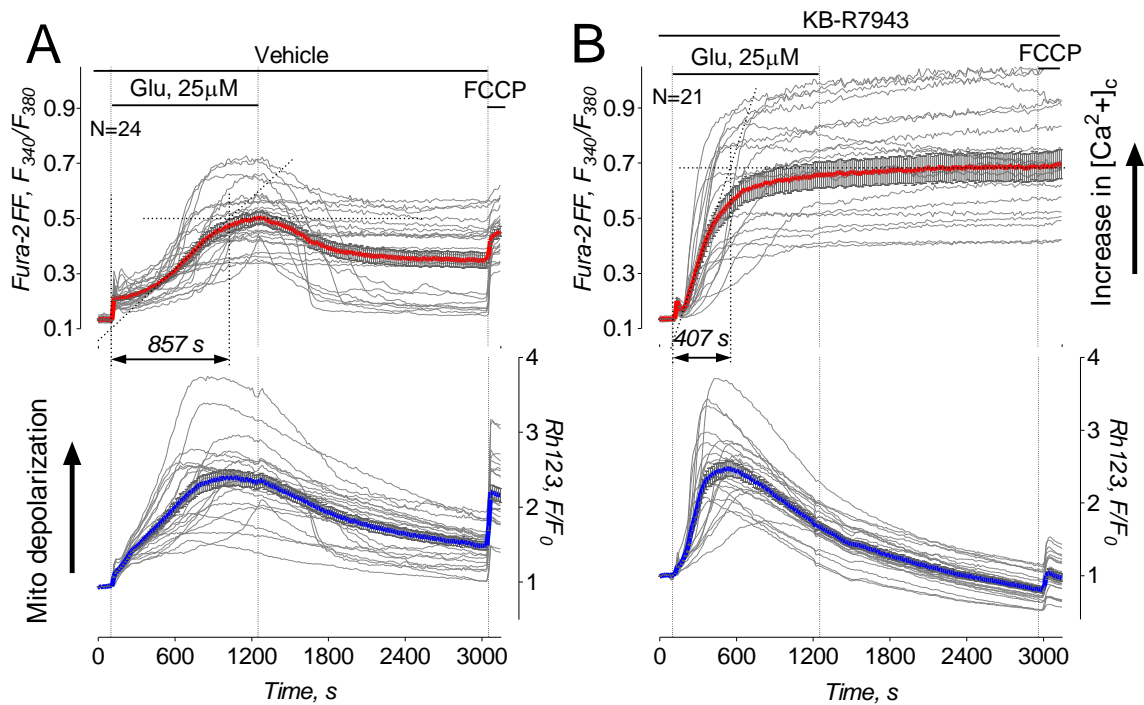


Figure 10. **KB-R7943 accelerates delayed calcium deregulation and mitochondrial depolarization in cultured hippocampal neurons exposed to glutamate.** Here and in all other similar illustrations, thin, grey traces show signals from individual neurons while thick, red traces show averaged signals (mean \pm SEM) for Fura-2FF ratio F_{340}/F_{380} (upper panels) and thick, blue traces for Rhodamine 123 (Rh123) F/F_0 (lower panels), respectively. Neurons were derived from postnatal day one (PN1) Sprague-Dawley rat pups and were 12-14 days *in vitro* on the day of the experiment. In A and B, neurons were treated with 25 μ M glutamate (Glu). In both cases, glutamate was applied in combination with 10 μ M glycine. In A, 0.2% DMSO was applied to neurons as a vehicle. In B, 15 μ M KB-R7943 was applied to neurons as indicated. Here and in other similar experiments, 1 μ M FCCP was applied at the end of experiments to completely depolarize mitochondria in the Ca^{2+} -free bath solution. (These experiments were preformed in collaboration with Tatiana Brustovetsky, MS.)

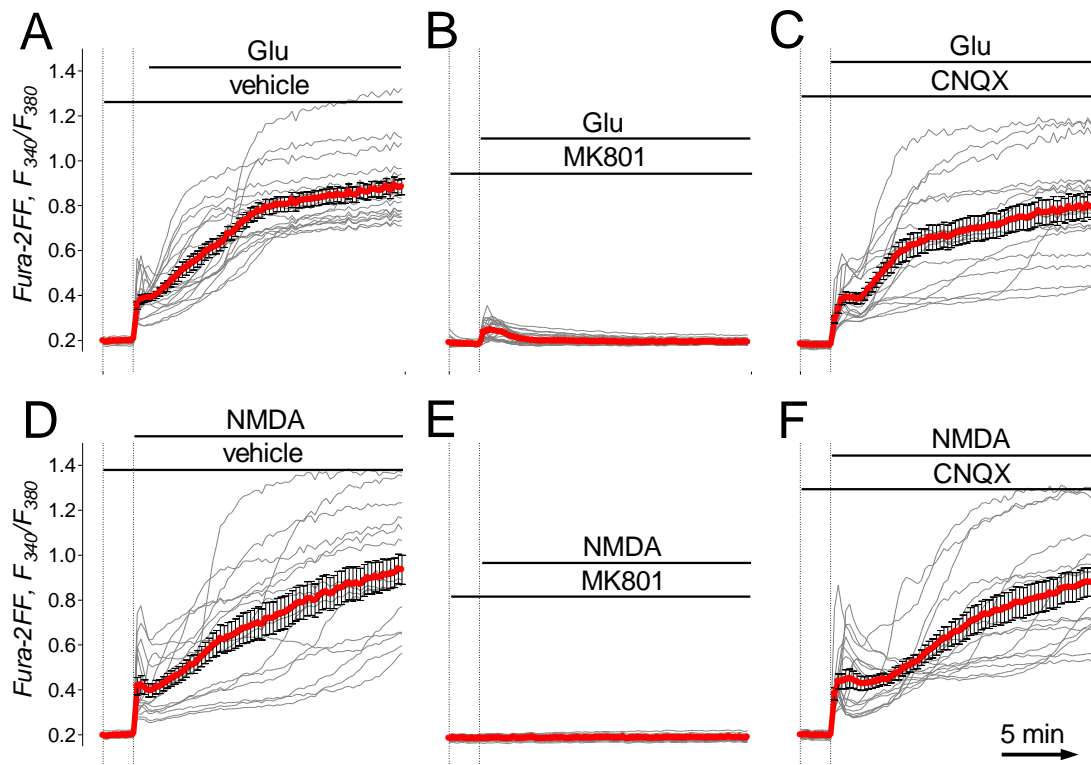


Figure 11. **MK801, an inhibitor of NMDA receptor, inhibits glutamate- and NMDA-induced calcium deregulation while CNQX, an inhibitor of AMPA/kainate receptors, is without effect.** Neurons were loaded with 2.6 μ M Fura-2FF to monitor changes in cytosolic Ca²⁺ concentrations. Where indicated, 30 μ M glutamate (plus 10 μ M glycine) or 30 μ M NMDA (plus 10 μ M glycine) as a stimulus. 10 μ M MK801 or 20 μ M CNQX were added to antagonist either the NMDA receptor or AMPA/kainate receptors, respectively.

(a.) *KB-R7943 inhibits the reverse mode of the Na⁺/Ca²⁺ exchanger*

Despite failing to prevent DCD in our experiments, KB-R7943 (15 μ M) inhibited an increase in $[Ca^{2+}]_c$ induced by gramicidin, an ionophore for monovalent cations which does not transport Ca^{2+} on its own (Figure 12A,C). Gramicidin collapses the Na^+ gradient across the plasma membrane (Figure 13A) and depolarizes cells (Figure 13B), resulting in a reversal of NCX (Czyz & Kiedrowski, 2002). The exact cause of variations in the delay of gramicidin-induced calcium deregulation evident in individual neurons treated with KB-R7943 (Figure 12C) is unknown, but it might be due to different expressions of various proteins involved in calcium signaling and, correspondingly, due to different resistances of individual cells to Ca^{2+} overload. The replacement of Na^+ for a large monovalent cation, N-methyl-D-glucamine ($NMDG^+$) in the bath solution prevented the gramicidin-induced increase in $[Ca^{2+}]_c$ indicating that this increase is depended on Na^+ (Figure 12B). $NMDG^+$ cannot be transported through the NCX, essentially turning off both the forward and reverse modes of the NCX. Using the calcium imaging protocol, we determined $IC_{50}=5.7\pm 2.1\mu M$ (mean \pm SEM, N=3 independent experiments) for KB-R7943-induced inhibition of NCX_{rev} (Figure 12D,E).

In addition to calcium imaging, we used the electrophysiological patch-clamp technique to evaluate the effect of KB-R7943 on NCX_{rev} activity in cultured hippocampal neurons. Figure 14 shows measurements of whole-cell outward ion currents obtained in response to repeated application of the voltage ramp protocol shown in Figure 14A. KB-R7943 (15 μ M) inhibited ion currents produced

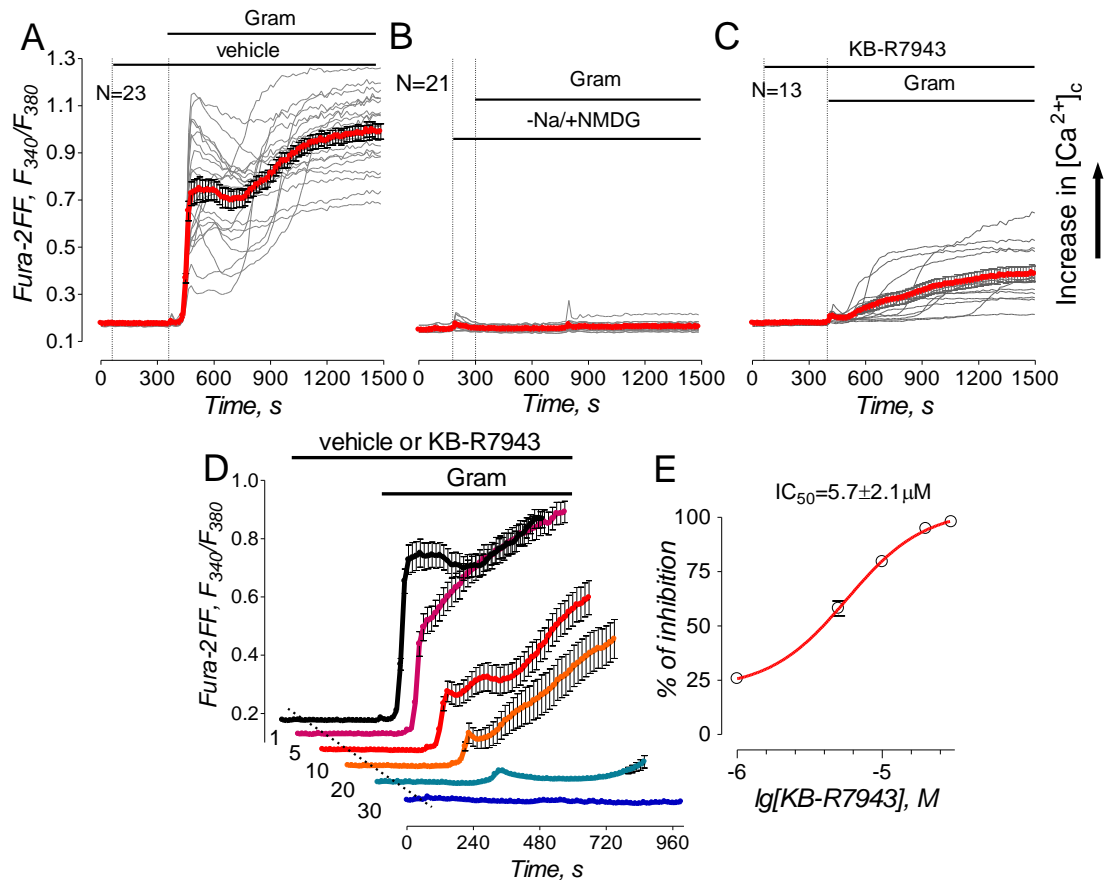


Figure 12. KB-R7943 inhibits gramicidin-induced increase in cytosolic Ca^{2+} concentration ($[Ca^{2+}]_c$) in cultured hippocampal neurons (A-C). In A, 0.2% DMSO was applied to neurons as a vehicle. In A-C, 5 μ M gramicidin (Gram) and 15 μ M KB-R7943 were applied as indicated. In B, where indicated, Na in the bath solution was replaced with NMDG. In A-C, bath solution was supplemented with 5 μ M nifedipine, a blocker of voltage-gated Ca^{2+} channels, and 1 mM ouabain, an inhibitor of the Na^+/K^+ -ATPase. In A-C, each experiment was performed in triplicate with the total number of examined neurons 51 (A), 56 (B), and 41 (C). In D, traces are averages \pm SEM from individual experiments (N=18-24 neurons per experiment) performed in triplicate. Where indicated, vehicle (veh, 0.2% DMSO, black trace) or various concentrations of KB-R7943 (1-30 μ M) were applied and present in the bath solution until the end of the experiment. Gramicidin (Gram, 5 μ M) was applied as indicated. The activity of NCX_{rev} was evaluated by measuring the area under the curve for 90 seconds following the onset of $[Ca^{2+}]_c$ elevation, the dose-dependence graph was plotted, and IC_{50} was calculated using GraphPad Prism[®] 4.0 (GraphPad Software Inc., San Diego, CA).

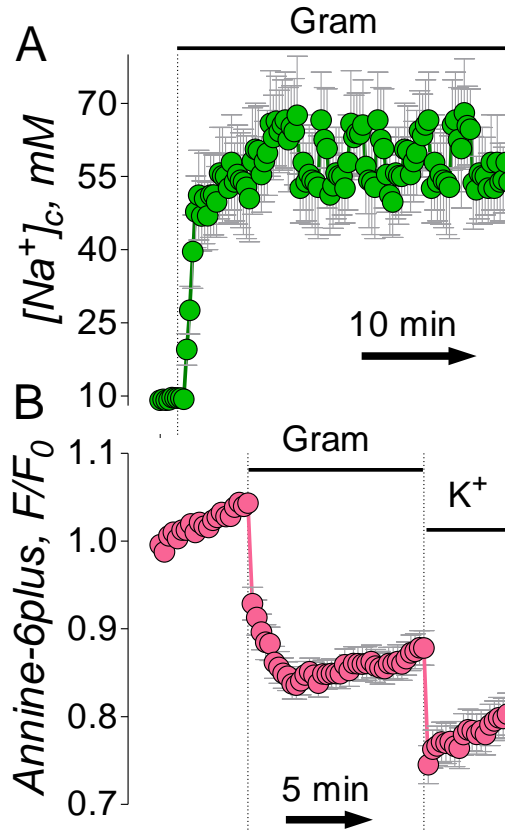


Figure 13. **Gramicidin exposure results in conditions that are favorable for the reverse mode of the Na^+/Ca^{2+} exchanger (NCX) to occur.** In panel A, the neurons are loaded with a Na^+ -sensitive dye, SBFI to monitor changes in cytosolic Na^+ concentrations and in panel B the neurons are loaded with a voltage-sensitive dye, Annine-6plus, to monitor changes in plasma membrane potential. Where indicated the neurons were exposure $5\mu M$ gramicidin.

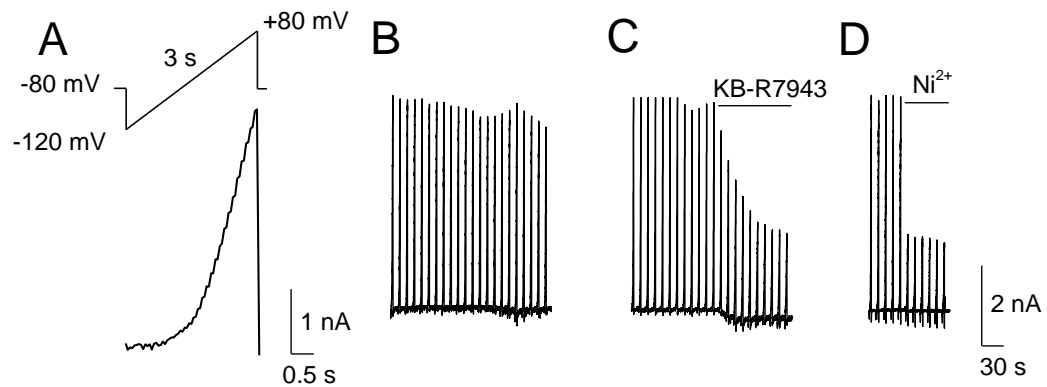


Figure 14. **NCX_{rev} currents obtained with cultured hippocampal neurons from rats.** In A, the ascending voltage ramp protocol used in these experiments and associated currents obtained with and without KB-R7943 (B, C) and Ni²⁺ (D). Where indicated, KB-R7943, 15 μM, or Ni²⁺, 5 mM, were applied. For further details, see Materials and Methods. (These experiments were performed in collaboration with Patrick L. Sheets, Ph.D. and Theodore R. Cummins, Ph.D.)

in response to the voltage ramp protocol (Figure 14B,C). Previously, it has been shown that this type of ion current is mediated by NCX in forward mode at negative voltages (i.e. -120 mV) and by NCX in reverse mode (NCX_{rev}) at positive voltages (i.e. +80 mV) (Convery & Hancox, 1999; Watanabe & Kimura, 2000). For comparison, we evaluated Ni²⁺-sensitivity of the ramp currents (Figure 14D), which has been previously attributed to NCX activity (Smith *et al.*, 2006; Reppel *et al.*, 2007). Overall, these results suggested that KB-R7943 inhibited NCX_{rev} in cultured hippocampal neurons.

(b.) *KB-R7943 inhibits the NMDA receptor*

There is a dispute in the literature concerning KB-R7943 and its ability to inhibit the NMDA receptor. Thus, we used the electrophysiological patch-clamp technique to evaluate the effect of KB-R7943 on NMDA receptor activity in cultured hippocampal neurons. KB-R7943 dose-dependently and reversibly blocked ion currents elicited by NMDA (Figure 15A,B). As a positive control, MK801, an inhibitor of NMDA receptor (Clifford *et al.*, 1989), completely blocked NMDA-induced ion current (Figure 15C). Additionally, for the first time we demonstrated that KB-R7943 dose-dependently inhibited NMDA-induced increases in [Ca²⁺]_c with IC₅₀=13.4±3.6µM (mean±SEM, N=3 independent experiments) (Figure 16) confirming the inhibition of NMDA receptor observed in electrophysiological experiments (Figure 15A,B). Thus, our experiments showed that KB-R7943 inhibited NMDA receptor in addition to inhibiting NCX_{rev}.

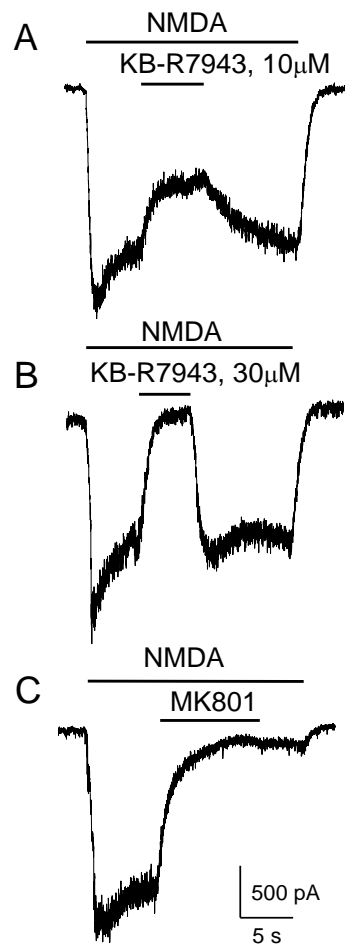


Figure 15. Patch-clamp recordings of NMDA-induced whole-cell currents obtained with cultured hippocampal neurons from rats. The effects of 10 μ M or 30 μ M KB-R7943 (A, B), and 20 μ M MK801 (C). In all experiments, 30 μ M NMDA (plus 10 μ M glycine) were applied as indicated. Holding voltage was -100 mV. For further details, see Materials and Methods. (These experiments were performed in collaboration with Patrick L. Sheets, Ph.D. and Theodore R. Cummins, Ph.D.)

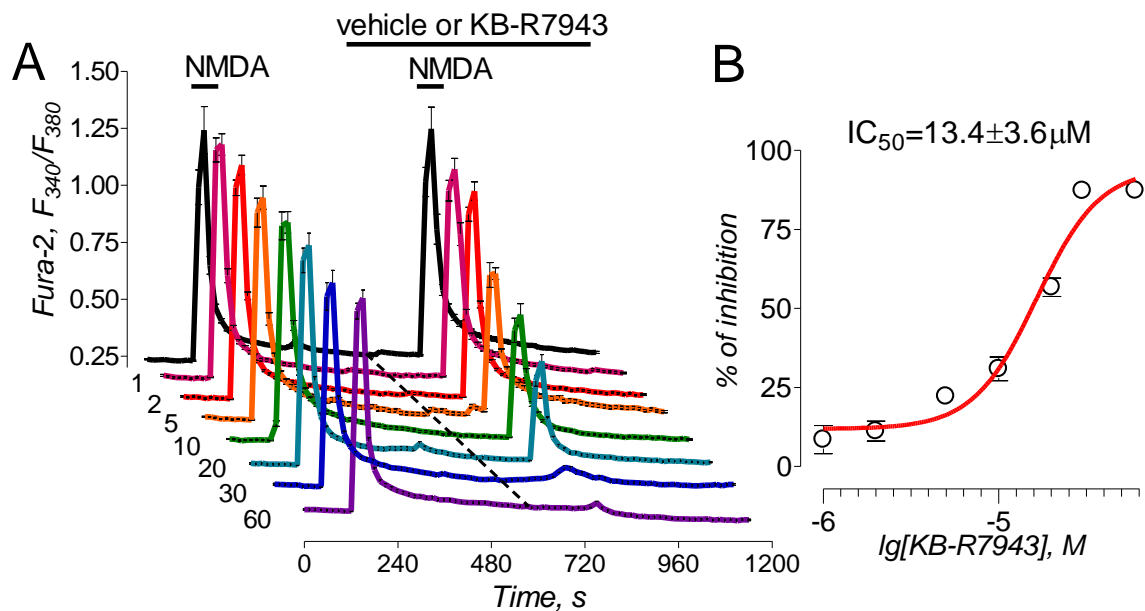


Figure 16. **KB-R7943 inhibits NMDA-induced increases in cytosolic Ca^{2+} .** Traces are averages \pm SEM from individual experiments (N=19-26 neurons per experiment) performed in triplicate. Where indicated, vehicle (veh, 0.2% DMSO, black trace) or various concentrations of KB-R7943 (2-60 μM) were applied and present in the bath solution until the end of the experiment. NMDA (30 μM , plus 10 μM glycine) was applied twice for 30 seconds as indicated. The activity of NMDA receptors was evaluated by measuring amplitude of the increases in Fura-2 F_{340}/F_{380} ratio triggered by the second application of NMDA. The dose-dependence graph was plotted, and IC_{50} was calculated using GraphPad Prism[®] 4.0 (GraphPad Software Inc., San Diego, CA).

(c.) *KB-R7943 exposure causes mitochondrial depolarization in neurons*

We previously demonstrated that KB-R7943 depolarized mitochondria (Storozhevykh *et al.*, 2010). Mitochondrial depolarization inhibits Ca^{2+} uptake by the organelles (Bernardi, 1999) and strongly contributes to collapse of calcium homeostasis in cultured neurons (Pivovarova *et al.*, 2004). Therefore, it is possible that mitochondrial depolarization produced by KB-R7943 could interfere with ability of the drug to alter $[\text{Ca}^{2+}]_c$ (Figure 10). The mechanism of KB-R7943-induced mitochondrial depolarization demonstrated in our previous work (Storozhevykh *et al.*, 2010) remained unclear.

We hypothesized that KB-R7943 depolarizes mitochondria by inhibiting electron flow in the mitochondrial respiratory chain, and to test this we examined autofluorescence of NAD(P)H in cultured hippocampal neurons exposed to glutamate. Rotenone (1 μM), an inhibitor of Complex I, prevented NAD(P)H oxidation by the NAD(P)H dehydrogenase (Complex I). This was manifested in the increased NAD(P)H fluorescence (Figure 17B) resembling the effect of oligomycin (see Figure 5D). However, in the presence of rotenone, the effects of glutamate, FCCP, and KCN were greatly diminished because of inhibited Complex I and strongly suppressed electron flow in the respiratory chain (Figure 17B). Similar to rotenone and oligomycin, KB-R7943 (15 μM) increased NAD(P)H fluorescence (Figure 17C). In contrast to oligomycin (Figure 5D) and similar to

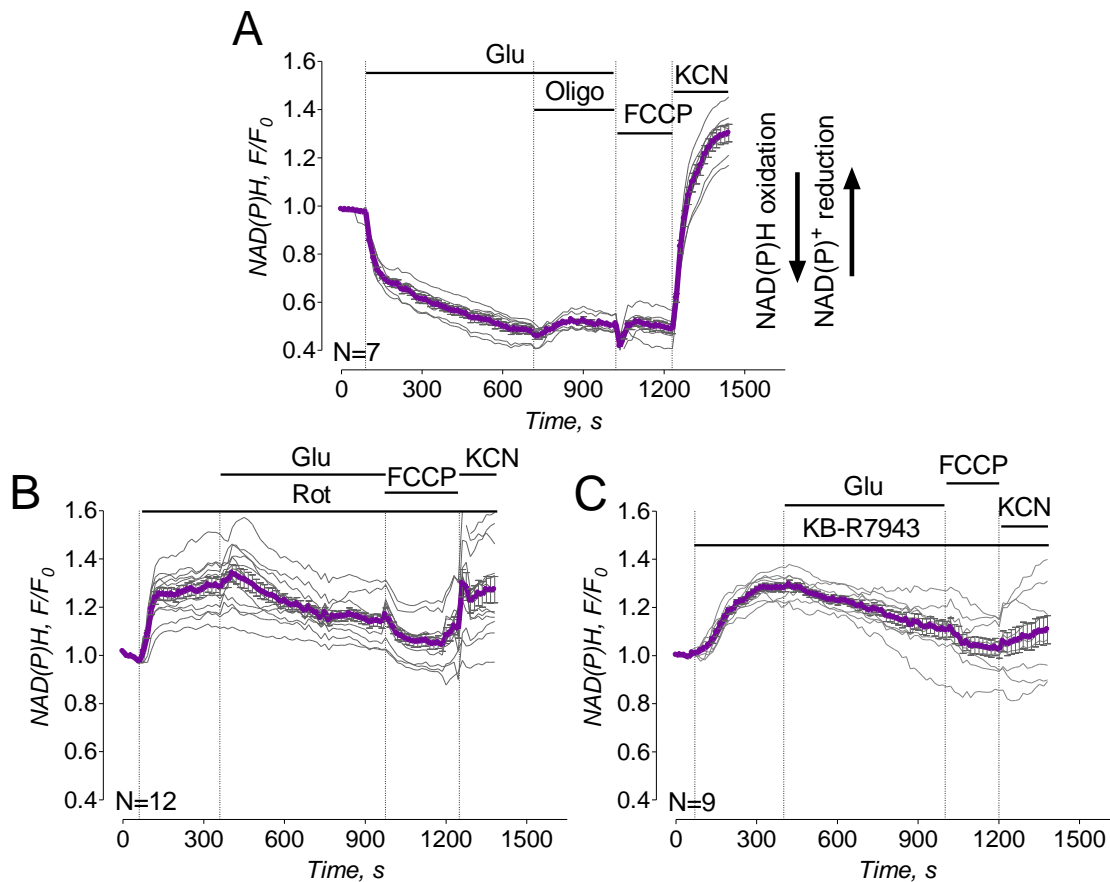


Figure 17. **KB-R7943 increases NAD(P)H fluorescence under resting conditions and suppressed glutamate-induced NAD(P)H oxidation similar to rotenone.** Where indicated, 25 μ M glutamate (Glu, plus 10 μ M glycine), 1 μ M oligomycin (Oligo), 1 μ M rotenone, 1 μ M FCCP, or 10 mM KCN were applied to neurons. In C, 15 μ M KB-R7943 was applied as indicated. Thin, grey traces show signals from individual neurons from the same dish while thick, purple traces show averaged signals (mean \pm SEM) for NAD(P)H F/F_0 . Each experiment was performed five times.

rotenone (Figure 17B), the increase in NAD(P)H induced by KB-R7943 (Figure 17C) was almost insensitive to glutamate, FCCP, and KCN. This strongly suggested that KB-R7943, like rotenone, inhibited Complex I in the respiratory chain.

Consistent with Complex I inhibition, KB-R7943 depolarized neuronal mitochondria which otherwise maintained a stable membrane potential (Figure 18A,B). Depolarization occurred gradually with some lag. In the experiments with cultured neurons, Rhodamine 123 (Rh123) was used in the quenching mode. Mitochondrial depolarization caused a release of dye from mitochondria accompanied by an increase in Rhodamine 123 fluorescence due to Rhodamine 123 unquenching. However, the decrease in Rhodamine 123 fluorescence following the initial fluorescence increase (Figure 18B) most probably was not due to mitochondrial re-polarization but rather due to dye leakage out of the cells. Following mitochondrial depolarization, $[Ca^{2+}]_c$ was gradually increased probably due to impaired Ca^{2+} extrusion and sequestration mechanisms. A slight increase in proton permeability of the inner mitochondrial membrane produced with ultra-low concentration of FCCP (2.5 nM) did not depolarize mitochondria on its own but significantly accelerated depolarization in the presence of KB-R7943 (Figure 18C,D).

Importantly, KB-R7943-induced mitochondrial depolarization did not depend on Ca^{2+} (Figure 19A) and occurred without external Ca^{2+} (Figure 19B) as well. During glutamate exposure calcium enters the neuron and is accumulated by the mitochondria. This Ca^{2+} accumulation results in mitochondrial

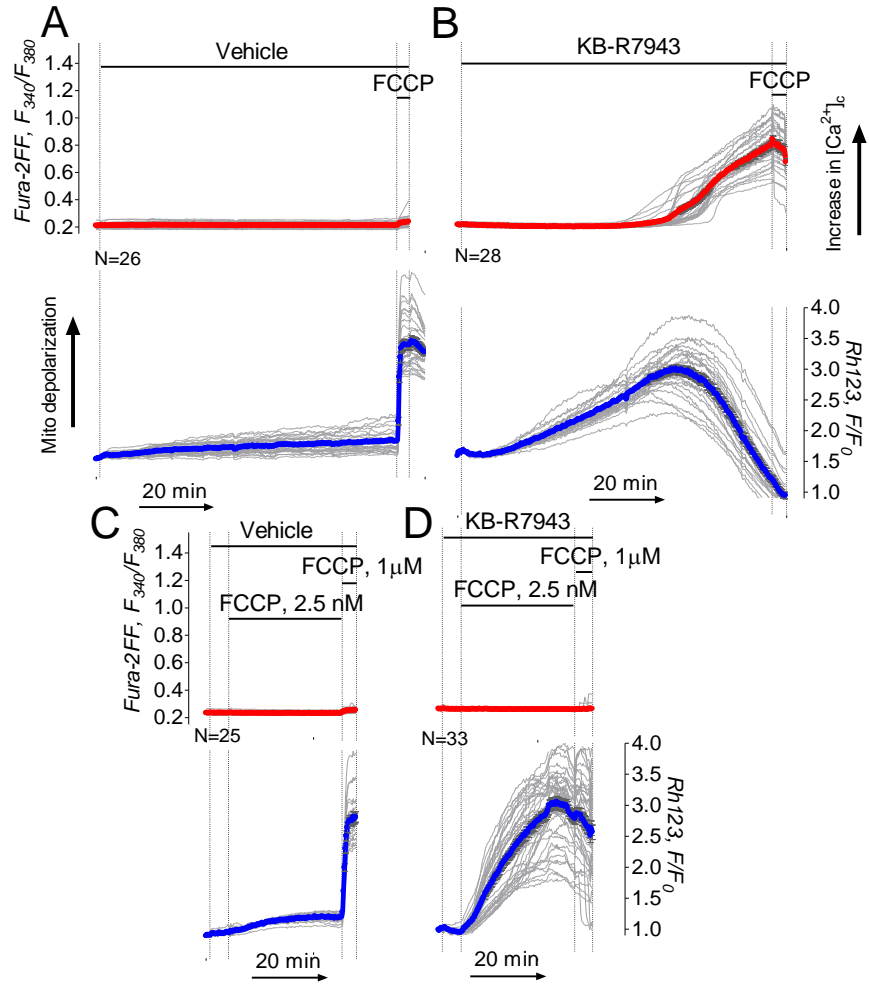


Figure 18. **KB-R7943 depolarizes mitochondria and this is accelerated by ultra-low concentration of FCCP in cultured hippocampal neurons.** In A and C, 0.2% DMSO was applied to neurons as a vehicle. In B and D, 15 μ M KB-R7943 was applied as indicated. In C and D, 2.5 nM FCCP was applied as indicated. In A-D, each experiment was performed three times. The total number of examined neurons was 81 (A), 79 (B), 84 (C), and 91 (D).

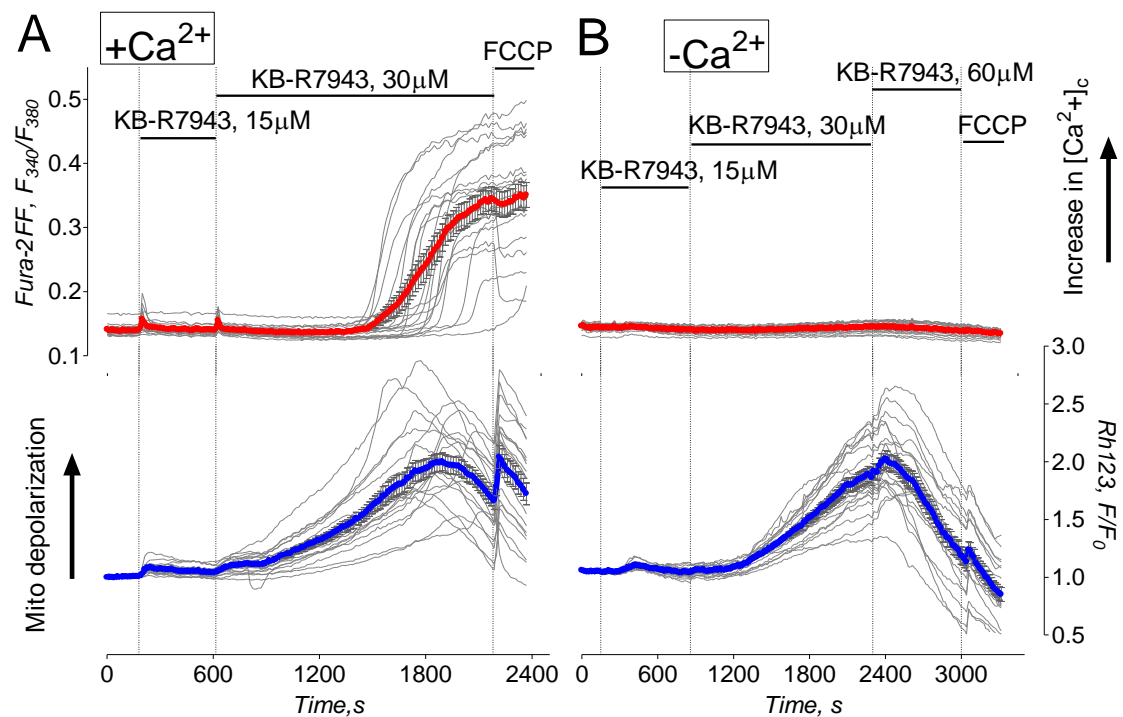


Figure 19. In cultured hippocampal neurons from rats, KB-R7943 depolarizes mitochondria in a Ca²⁺-independent manner. In A and B, 15μM or 30μM KB-R7943 was applied as indicated. In B, Ca²⁺ was omitted from the bath solution throughout this experiment. FCCP, 1μM.

depolarization. Thus it was important to determine if calcium has a role in the mitochondrial depolarization induced by KB-R7943. Overall, these data suggested that KB-R7943 depolarized mitochondria by most likely inhibiting Complex I of the respiratory chain and that this inhibition might be responsible for mitochondrial depolarization.

(d.) KB-R7943 inhibits respiration in a dose-dependent manner

An increase in NAD(P)H (Figure 17C) accompanied by mitochondrial depolarization (Figure 18B,D) suggested an inhibition of electron transport in the respiratory chain and suppression of respiration. We evaluated the effect of KB-R7943 on neuronal respiration using Seahorse XF24 flux analyzer (Seahorse Bioscience, Billerica, MA). The Seahorse technology allows precise measurements of oxygen consumption by as low as $2-6 \times 10^5$ cells. In our experiments, oligomycin inhibited respiration coupled with ATP synthesis while 2,4-dinitrophenol (2,4-DNP), a protonophore, uncoupled oxidation and phosphorylation in mitochondria. This resulted in maximal oxygen consumption rate (OCR), reflecting the activity of the respiratory chain. KB-R7943 dose-dependently inhibited both basal and 2,4-DNP-stimulated respiration (Figure 20) with $IC_{50}=11.4 \pm 2.4 \mu M$ for 2,4-DNP-stimulated respiration (mean \pm SEM, N=3 independent experiments). Thus, the inhibition of 2,4-DNP-stimulated respiration confirmed inhibition of the electron transport in the respiratory chain by KB-R7943.

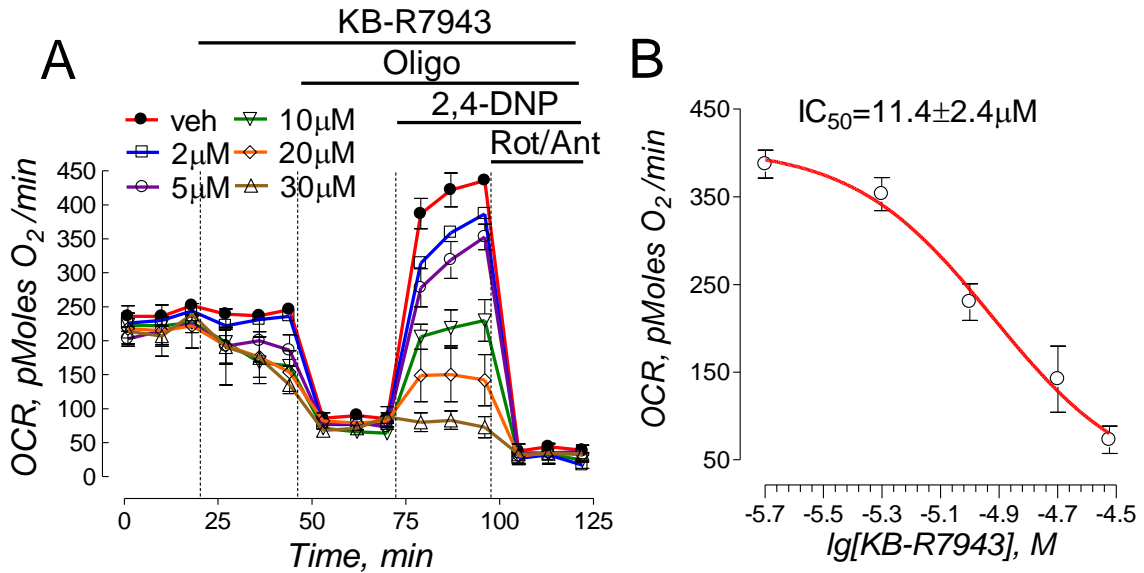


Figure 20. KB-R7943-induces inhibition of cellular respiration. In A, oxygen consumption rate (OCR) was measured in triplicate with a Seahorse XF24 flux analyzer. KB-R7943 (2-30 μ M), oligomycin (Oligo, 1 μ M), 2,4-dinitrophenol (2,4-DNP, 50 μ M), and a combination of rotenone (Rot, 1 μ M) and antimycin A (Ant, 1 μ M) were applied to neurons as indicated. 0.2% DMSO was used as a vehicle (veh). At the beginning of the experiment, basal respiration was measured prior to addition of KB-R7943. After KB-R7943 was applied, it was present in the bath solution until the end of the experiment. In B, the dose-dependence graph was plotted and IC₅₀ was calculated using GraphPad Prism[®] 4.0 (GraphPad Software Inc., San Diego, CA).

(e.) *KB-R7943 inhibits Complex I on the respiratory chain*

To test our hypothesis about inhibition of Complex I with KB-R7943, we performed experiments with isolated brain mitochondria. First, we evaluated the effect of KB-R7943 on mitochondrial membrane potential in individual mitochondria attached to a cover slip (Shalbuyeva *et al.*, 2007). In these experiments, Rh123 was used in the non-quenching mode in which a decrease in Rh123 fluorescence reflected mitochondrial depolarization. Figure 21A,B shows representative images demonstrating fluorescence of Rh123-loaded isolated mitochondria with high membrane potential (A) and depolarized with 1 μ M FCCP (B). In these experiments, KB-R7943 depolarized mitochondria supplied with malate and glutamate, oxidative substrates for Complex I (Figure 21C-E), but did not depolarize mitochondria supplied with succinate plus glutamate (Figure 21F,G). Here and in other experiments, glutamate was used to prevent oxaloacetate inhibition of succinate dehydrogenase (Lehninger *et al.*, 1993). This strongly suggests specific inhibition of Complex I. In addition, KB-R7943 inhibited mitochondrial respiration when mitochondria oxidized malate plus glutamate (Figure 22A) but failed to influence mitochondrial respiration when mitochondria oxidized succinate in the presence of glutamate (Figure 22B). Interestingly, respiration of isolated brain mitochondria appeared to be less sensitive to KB-R7943 than mitochondrial respiration *in situ* in live cells (Figure 20). The reason for that is not clear. Figure 22C and D summarize the respirometry data and show statistical analyses of mitochondrial respiratory rates. Finally, KB-R7943 inhibited mitochondrial Ca²⁺ uptake when mitochondria

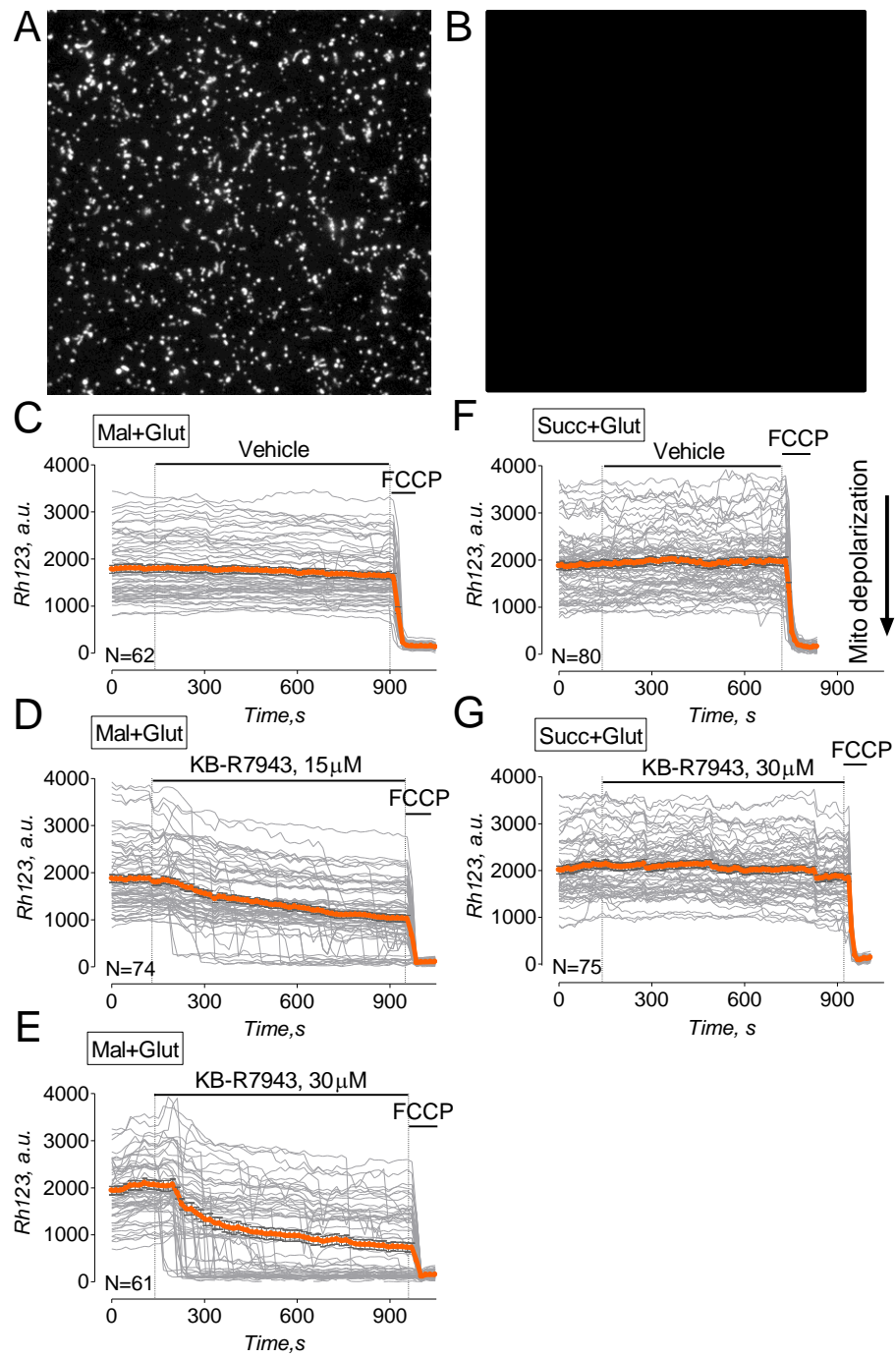


Figure 21.

Figure 21. **KB-R7943 depolarizes isolated brain mitochondria fueled with Complex I substrates, but fails to depolarize mitochondria fueled with a Complex II substrate.** In A and B, representative images of isolated mitochondria prior to (A) and after depolarization with 1 μ M FCCP (B). Mitochondria were attached to cover slip and loaded with 0.2 μ M Rh123 during continuous perfusion (Shalbuyeva *et al.*, 2007). In C-E, mitochondria were perfused with the standard mitochondrial incubation medium supplemented with 1 mM malate plus 3 mM glutamate (Mal+Glut). Here and in other experiments with succinate, glutamate was used to prevent oxaloacetate inhibition of succinate dehydrogenase (Oestreicher *et al.*, 1969; Lehninger *et al.*, 1993). In F and G, mitochondria were perfused with the standard mitochondrial incubation medium supplemented with 3 mM succinate plus 3 mM glutamate (Succ+Glut). In C and F, 0.2% DMSO was applied as a vehicle. In D, E, and G, KB-R7943 was applied as indicated. Rh123 fluorescence is expressed in arbitrary units (a.u.). Thin, grey traces demonstrate signals from individual mitochondria while thick orange traces demonstrate averaged signals (mean \pm SEM) for Rh123 fluorescence expressed in arbitrary units (a.u.). In C-G, each experiment was performed three times. (These experiments were preformed in collaboration with Tatiana Brustovetsky, MS.)

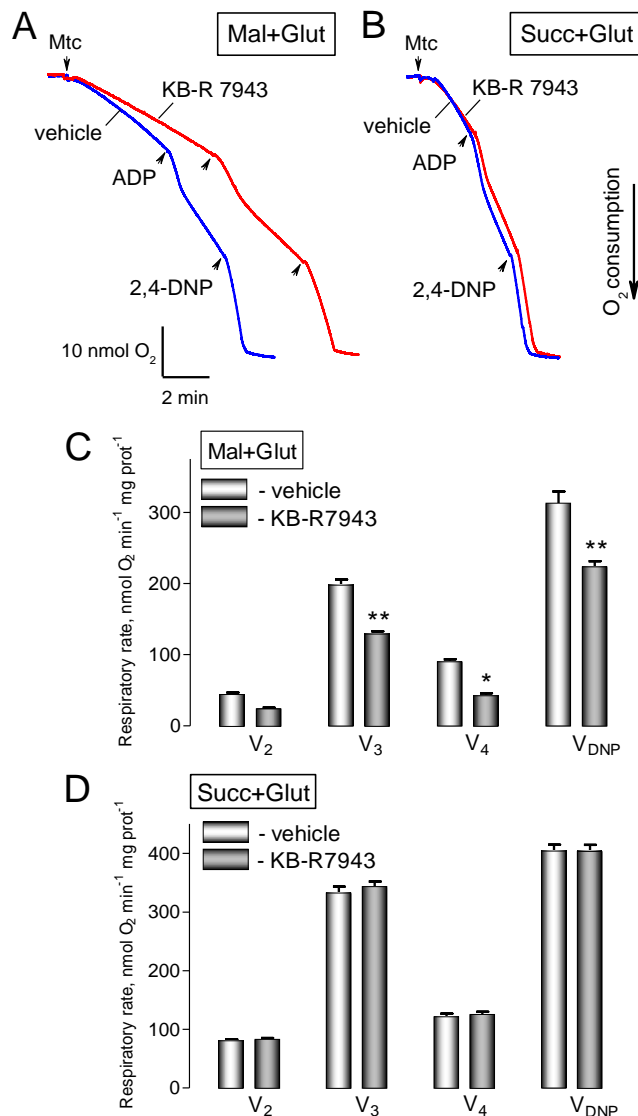


Figure 22. KB-R7943 inhibits respiration of isolated brain mitochondria oxidizing malate plus glutamate, but fails to affect mitochondrial respiration supported by succinate. In A and B, representative respiratory traces obtained with and without 30 μ M KB-R7943 are shown. The traces are overlapped for comparison. In A, the standard incubation medium was supplemented with 1 mM malate and 3 mM glutamate; in B, with 3 mM succinate plus 3 mM glutamate. ADP (100 μ M) and 2,4-dinitrophenol (2,4-DNP, 80 μ M) were applied as indicated. 0.2% DMSO was applied as a vehicle. Mtc, mitochondria. V₂, V₃, V₄, and V_{DNP} are respiratory rates prior to ADP addition, with added ADP, after ADP depletion, and with 2,4-DNP, respectively. Blue traces show experiments with vehicle; red traces - with KB-R7943. In C, data are mean \pm SEM, N=4, * p <0.01, ** p <0.001 comparing respiratory rates without and with KB-R7943. (These experiments were preformed in collaboration with Nickolay Brustovetsky, PhD.)

were incubated with malate plus glutamate (Figure 23A-C) but failed to inhibit Ca^{2+} uptake when mitochondria were incubated with succinate plus glutamate (Figure 23D,E). Moreover, after inhibition with KB-R7943 the Ca^{2+} uptake could be restored by addition of succinate (Figure 23C). Thus, experiments with isolated mitochondria confirmed that KB-R7943 inhibited Complex I and demonstrated possible ramifications of this inhibition: a decrease in respiration, mitochondrial depolarization, and suppression of mitochondrial Ca^{2+} uptake.

C. What is the contribution of the NMDA receptors on glutamate-induced delayed calcium dysregulation?

During prolonged glutamate exposure the plasmalemmal depolarization results in the elimination of the voltage-dependent Mg^{2+} block of the NMDA receptor (Nowak *et al.*, 1984) which then allows the NMDA receptor to remain constitutively active and permits continuous Ca^{2+} influx. This continuous Ca^{2+} influx has been shown to be a key factor in Ca^{2+} dysregulation (Tymianski *et al.*, 1993b) since MK801, an NMDA receptor antagonist, completely prevents DCD (Brustovetsky *et al.*, 2010) (Figure 24C). However, another NMDA receptor antagonist, AP-5, failed to inhibit glutamate-induced calcium dysregulation (Figure 24D). Both MK801 and AP-5 completely prevent calcium influx when stimulated with NMDA (Figure 24A, B). This discrepancy brings into questions the contribution of the NMDA receptor to delayed calcium dysregulation.

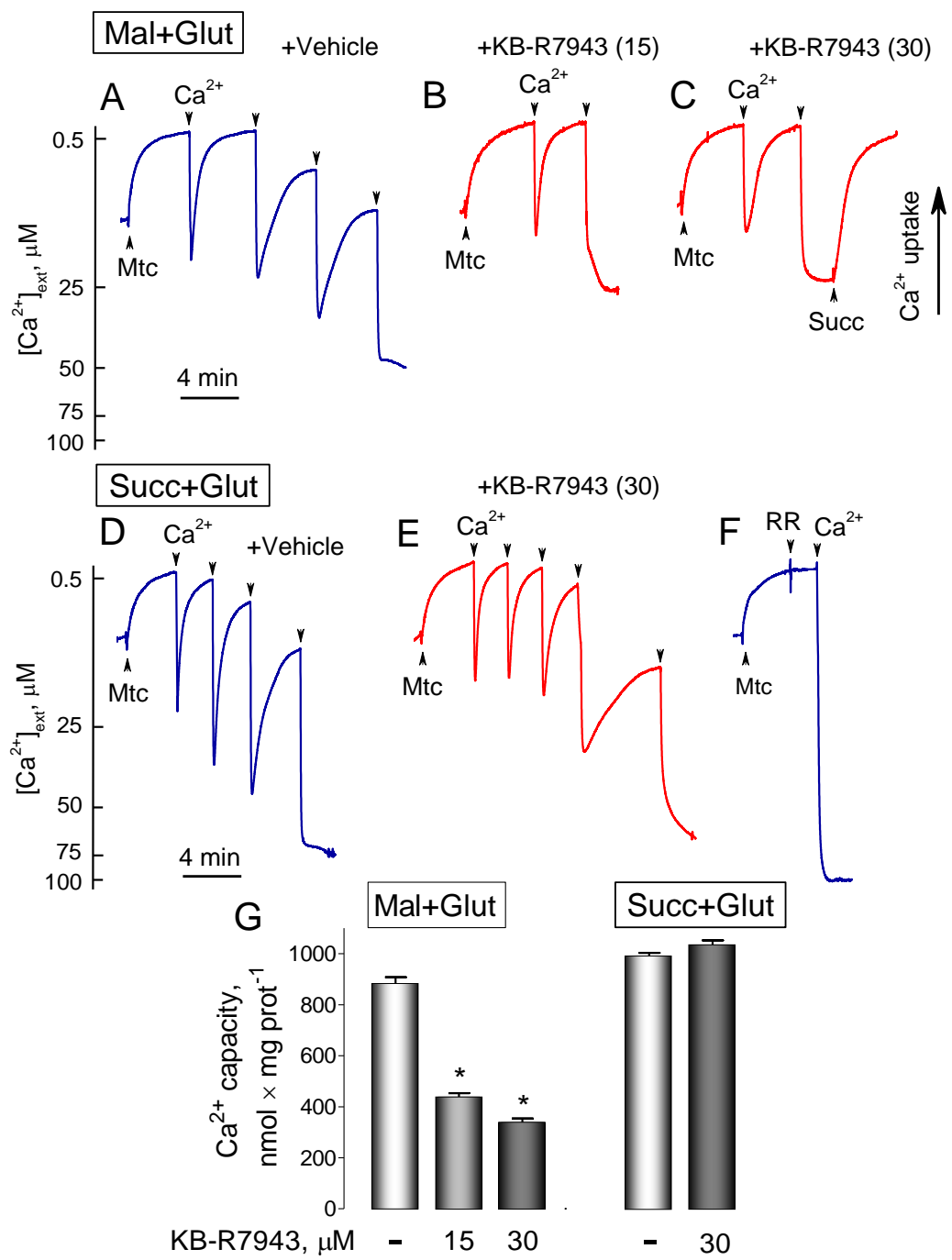


Figure 23.

Figure 23. **KB-R7943 hinders Ca^{2+} uptake by isolated brain mitochondria oxidizing glutamate and malate, but fails to inhibit Ca^{2+} uptake by mitochondria oxidizing succinate.** In A-F, $100\mu\text{M}$ Ca^{2+} was added to mitochondria as indicated. In A-C, the standard incubation medium was supplemented with 1 mM malate plus 3 mM glutamate; in D-F, with 3 mM succinate plus 3 mM glutamate. In all cases, the medium was supplemented with 0.1% BSA (free from free fatty acids), $100\mu\text{M}$ ADP, and $1\mu\text{M}$ oligomycin. In A and D, 0.2% DMSO was applied as a vehicle. In B, C, and E, KB-R7943 was added to the incubation medium prior to mitochondria. Numbers in the parentheses indicate KB-R7943 concentration in μM . In C, succinate (Succ, 3 mM) restored Ca^{2+} uptake by mitochondria fueled with glutamate plus malate and incubated with $30\mu\text{M}$ KB-R7943. In F, $1\mu\text{M}$ ruthenium red (RR) completely blocked Ca^{2+} uptake by mitochondria. Blue traces show experiments with vehicle; red traces - with KB-R7943. In G, data are mean \pm SEM, N=4, * p <0.001 comparing Ca^{2+} capacity without and with KB-R7943. (These experiments were performed in collaboration with Nickolay Brustovetsky, PhD.)

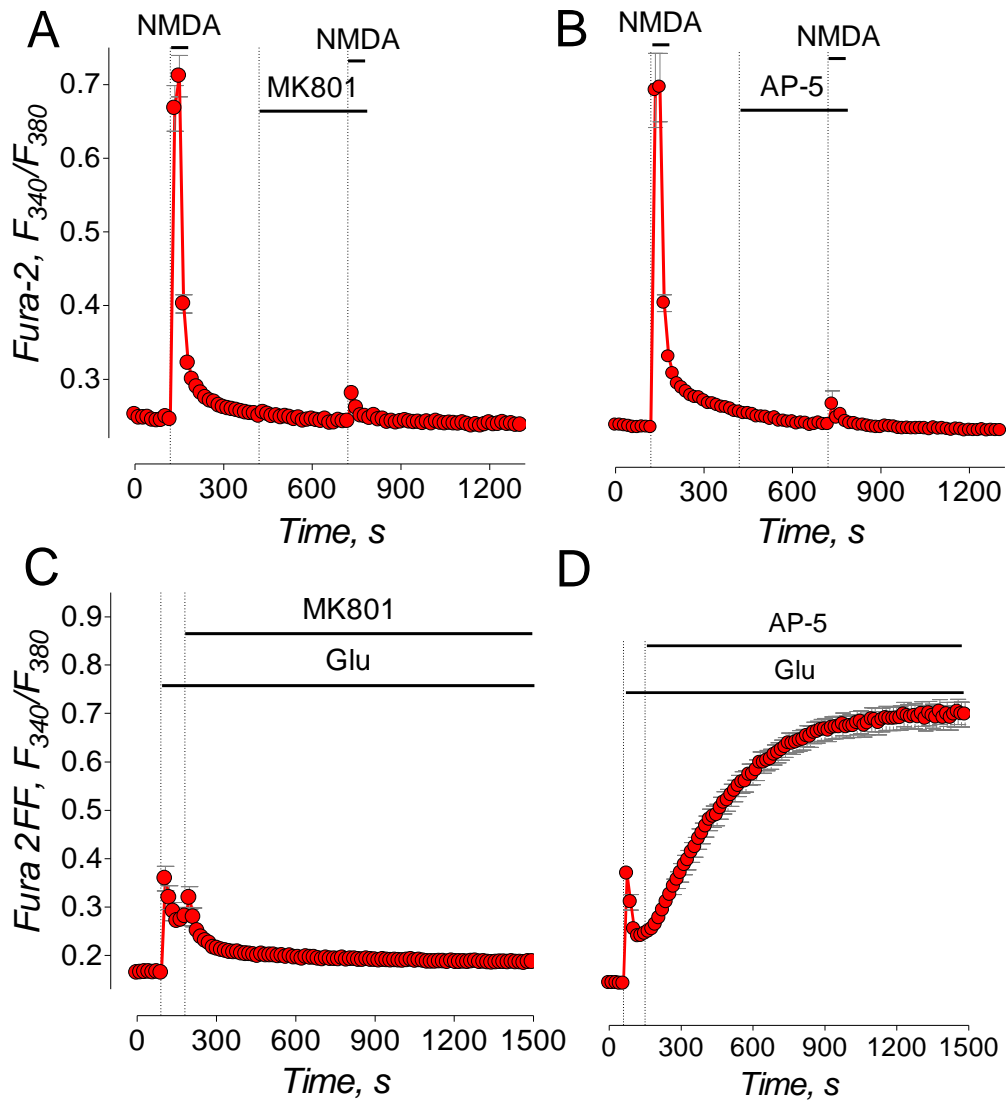


Figure 24. **MK801 and AP-5 inhibited NMDA-induced $[Ca^{2+}]_c$ increase (A, B), and MK801, but not AP-5, prevented glutamate-induced Ca^{2+} dysregulation (C, D).** Neurons were loaded with 2.6 μ M Fura-2 (A,B) or 2.6 μ M Fura-2FF-AM (C, D). In A and B, where indicated, neurons were treated with NMDA (30 μ M, plus 10 μ M glycine), MK801 (1 μ M), or AP-5 (20 μ M). In A, B, bath solution was supplemented with 1 μ M tetrodotoxin and 5 μ M nifedipine. In C and D, where indicated, neurons were treated with glutamate (Glu, 25 μ M, plus 10 μ M glycine), MK801 (1 μ M) or AP-5 (200 μ M).

1. NMDA receptor antagonists are inconsistent concerning their ability to prevent glutamate-induced delayed calcium dysregulation; however all fail to prevent glutamate-induced increase in cytosolic sodium

Prolonged exposure of neurons to glutamate resulted in a sustained elevation in $[Ca^{2+}]_c$, also known as delayed calcium dysregulation (DCD) (Tymianski *et al.*, 1993a) (Figure 25A). However, the contribution of the NMDA receptor in this calcium dysregulation is unknown, thus we asked if inhibition of the NMDA receptor would prevent glutamate-induced DCD? In these experiments, changes in $[Ca^{2+}]_c$ and cytosolic Na^+ concentration ($[Na^+]_c$) were followed simultaneously using Ca^{2+} -sensitive fluorescent dye Fluo-4FF and Na^+ -sensitive dye SBFI. Figure 25B-D show averaged Fluo-4FF and SBFI signals recorded from individual neurons and converted into $[Ca^{2+}]_c$ and $[Na^+]_c$. Neither nifedipine (5 μ M), nor ω -conotoxin (1 μ M), inhibitors of L- and N- types of voltage-gated Ca^{2+} channels (VGCC), respectively, affected glutamate-induced DCD (Figure 26). CNQX (10-100 μ M), an inhibitor of AMPA/kainate subtype of ionotropic glutamate receptors, also had no effect on glutamate-induced DCD (Figure 11) (Brustovetsky *et al.*, 2011). These data indicate that neither VGCC nor AMPA/kainate receptors contribute significantly to DCD in cultured hippocampal neurons exposed to glutamate.

Conversely, DCD was prevented by MK801 (1 μ M) or memantine (50 μ M) applied either prior to glutamate (Figure 27) or 90 seconds after glutamate (Figure 25B, C). Because we were interested in the mechanisms of DCD, in most of our experiments inhibitors were applied shortly after glutamate

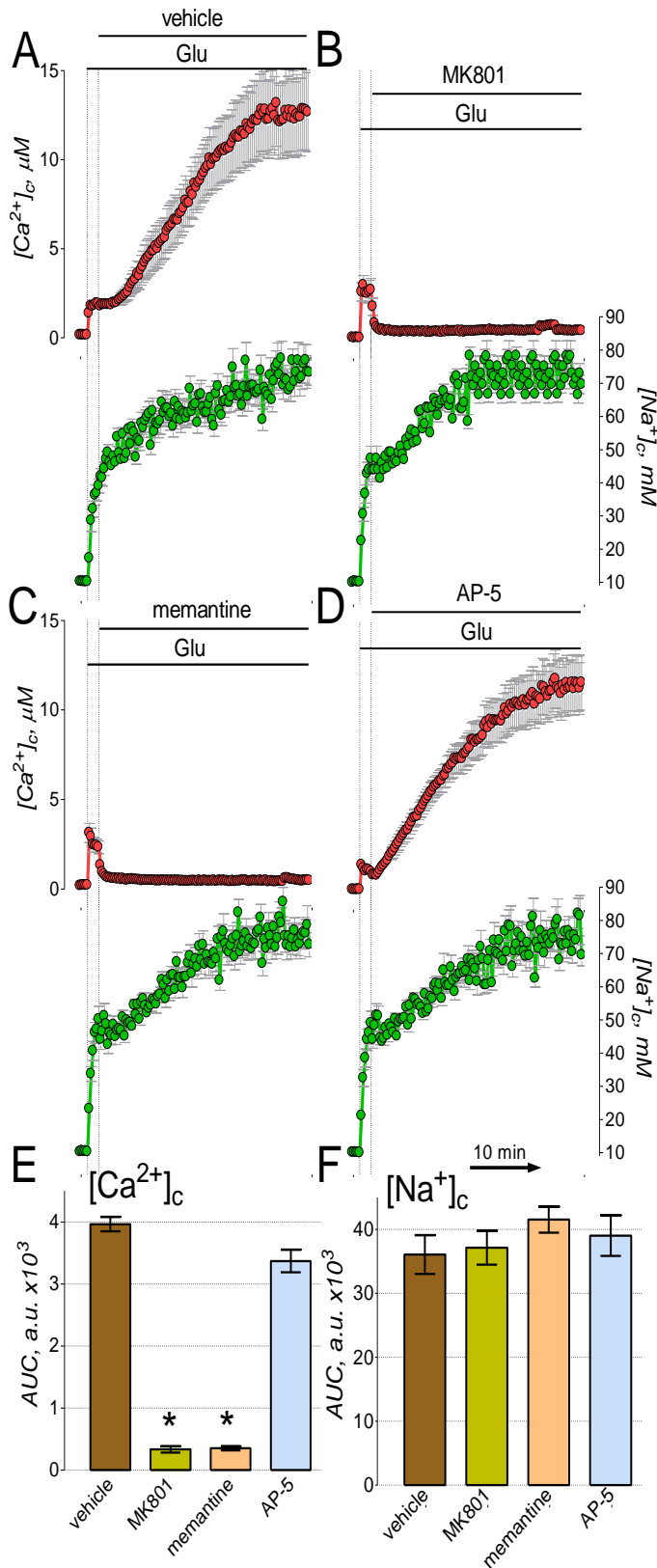


Figure 25. MK801 and memantine but not AP-5 prevent sustained elevation in $[Ca^{2+}]_c$; however none of the tested inhibitors influence glutamate-induced $[Na^+]_c$ increase. In all experiments, neurons were treated with 25 μM glutamate (Glu, plus 10 μM glycine) and 1 μM MK801, or 50 μM memantine, or 200 μM AP-5. Here and in all other experiments, 0.2% DMSO was used as a vehicle. The antagonists were added 90 seconds following glutamate application. In A-D, simultaneous measurements of $[Ca^{2+}]_c$ and $[Na^+]_c$ in hippocampal neurons loaded with a Ca^{2+} -sensitive fluorescent dye, Fluo-4FF (thick red line) and a Na^+ -sensitive dye, SBFI (thick green line). $[Ca^{2+}]_c$ and $[Na^+]_c$ were calculated using the Grynkiewicz method (Grynkiewicz *et al.*, 1985). Here and in other Figures, the traces show mean \pm s.e.m. from individual experiments (n=18-25 neurons per experiment). In E and F, statistical analyses of glutamate-induced $[Ca^{2+}]_c$ and $[Na^+]_c$ changes over time in dependence on the presence of different inhibitors. Data are mean \pm s.e.m., * $p < 0.01$ compared to vehicle, n=3.

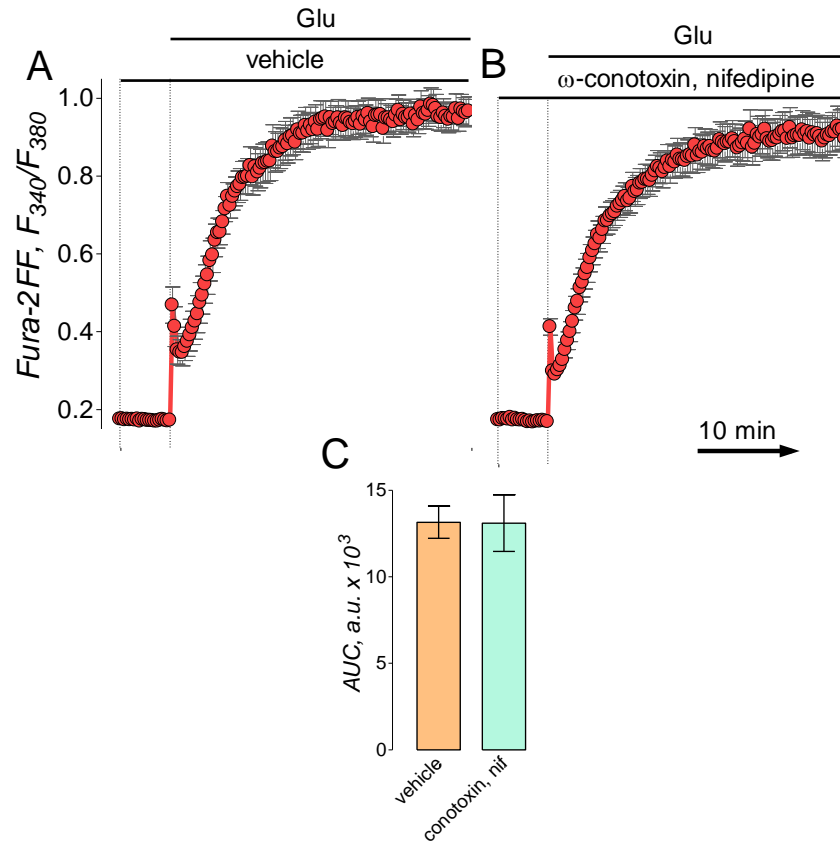


Figure 26. Inhibition of voltage-gated calcium channel with ω -conotoxin and nifedipine have no effect on glutamate-induced calcium dysregulation. Neurons were loaded with 2.6 μ M Fura-2FF-AM to follow changes in cytosolic calcium concentration ($[Ca^{2+}]_c$). Where indicated neurons were exposed to 25 μ M glutamate plus 10 μ M glycine. Panels A and B, corresponding traces representing the changes in $[Ca^{2+}]_c$, where indicated, (A.) vehicle (veh, 0.2% DMSO), or (B.) ω -conotoxin (1 μ M) and nifedipine (5 μ M) were applied. In C, statistical analysis of glutamate-induced $[Ca^{2+}]_c$ changes over time, depending on the presence of the inhibitors. Data are mean \pm SEM, * p <0.01 compared to vehicle, n=3.

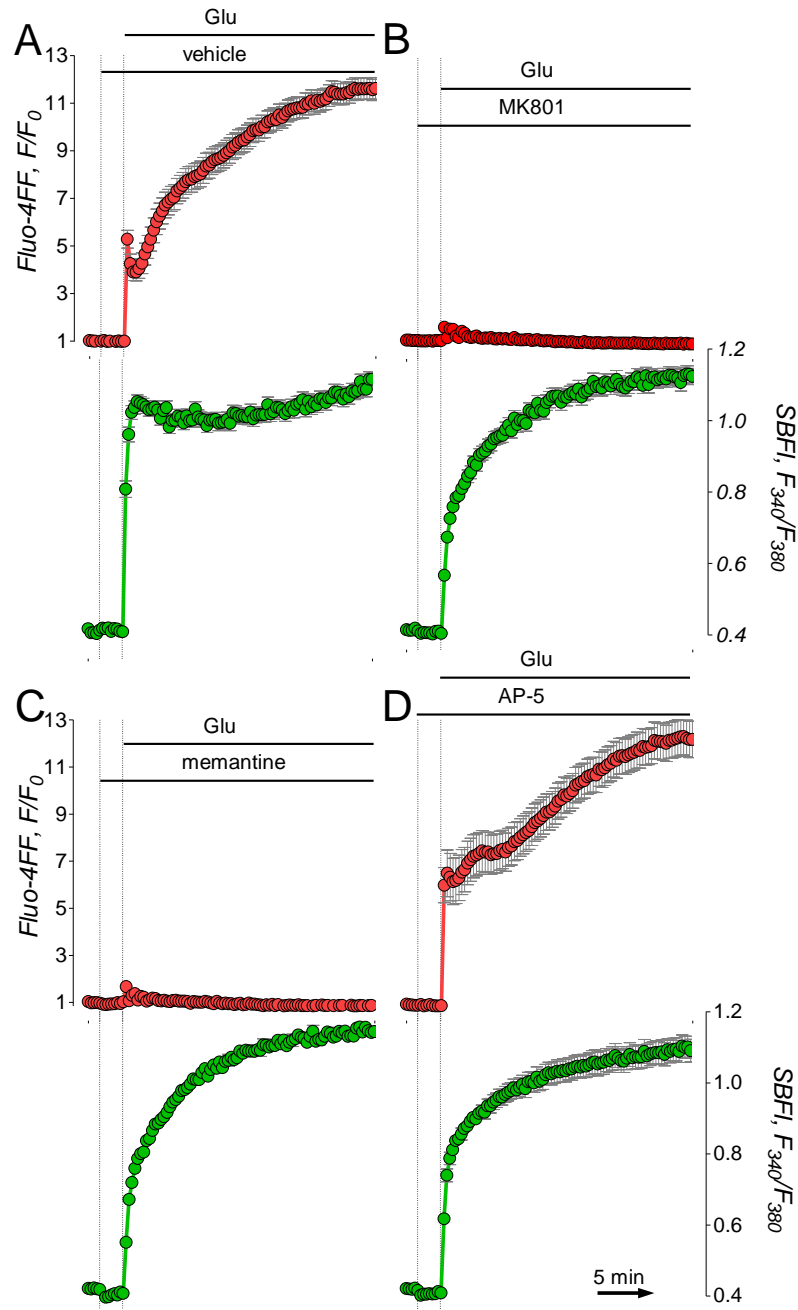


Figure 27. **MK801 and memantine but not AP-5 prevents sustained elevation in $[Ca^{2+}]_c$, but none of the antagonists affect glutamate-induced $[Na^+]_c$ increase.** In all experiments, neurons were treated with 25 μ M glutamate (Glu, plus 10 μ M glycine) and 1 μ M MK801, or 50 μ M memantine, or 200 μ M AP-5. Here and in all other experiments, 0.2% DMSO was used as a vehicle. The antagonists were added 120 seconds prior to the application of glutamate. In A-D, simultaneous measurements of $[Ca^{2+}]_c$ and $[Na^+]_c$ in hippocampal neurons loaded with a Ca^{2+} -sensitive fluorescent dye Fluo-4FF and a Na^+ -sensitive dye SBFI. Here and in other figures, the traces show mean \pm SEM from individual experiments (n=18-25 neurons per experiment).

just before onset of DCD. The strong inhibition of DCD with memantine or MK801 suggested that Ca^{2+} influx via NMDA receptor plays a major role in DCD consistent with the previous reports (Tymianski *et al.*, 1993b). Surprisingly, AP-5 (20-200 μM) failed to prevent DCD (Figure 25D and Figure 27D). Figure 25E shows a statistical analysis of the calcium imaging experiments. Here and in other figures, glutamate-induced changes in $[\text{Ca}^{2+}]_c$ over time were quantified by calculating the area under the curve (AUC) as it has been done previously (Chang *et al.*, 2006). All tested NMDA receptor antagonists completely inhibited NMDA-induced increases in $[\text{Ca}^{2+}]_c$ with $\text{IC}_{50}=0.2\pm 0.04\mu\text{M}$ for MK801, $3.6\pm 0.05\mu\text{M}$ for memantine, and $2.2\pm 0.03\mu\text{M}$ for AP-5, respectively (Figure 28), and inhibited NMDA-induced ion currents measured in whole-cell voltage-clamp experiments (Figure 29) suggesting complete inhibition of NMDA receptor. MK801 (1 μM), memantine (10 μM), and AP-5 (20 μM) also completely prevented DCD induced by 30 μM NMDA (plus 10 μM glycine) (Figure 30), indicating that all tested NMDA receptor antagonists were effective in inhibiting NMDA receptors. However, despite inhibition of NMDA receptor, AP-5, in contrast to MK801 and memantine, failed to prevent glutamate-induced DCD (Fig 25D).

2. Antagonizing ionotropic glutamate receptors has no effect on glutamate-induced increase in cytosolic Na^+ and plasmalemmal depolarization

In addition to DCD, glutamate produced sustained elevation in $[\text{Na}^+]_c$ (Figure 1A) and plasma membrane depolarization (Figure 31B). Figure 31A shows changes in Annine-6plus fluorescence following step-wise plasma

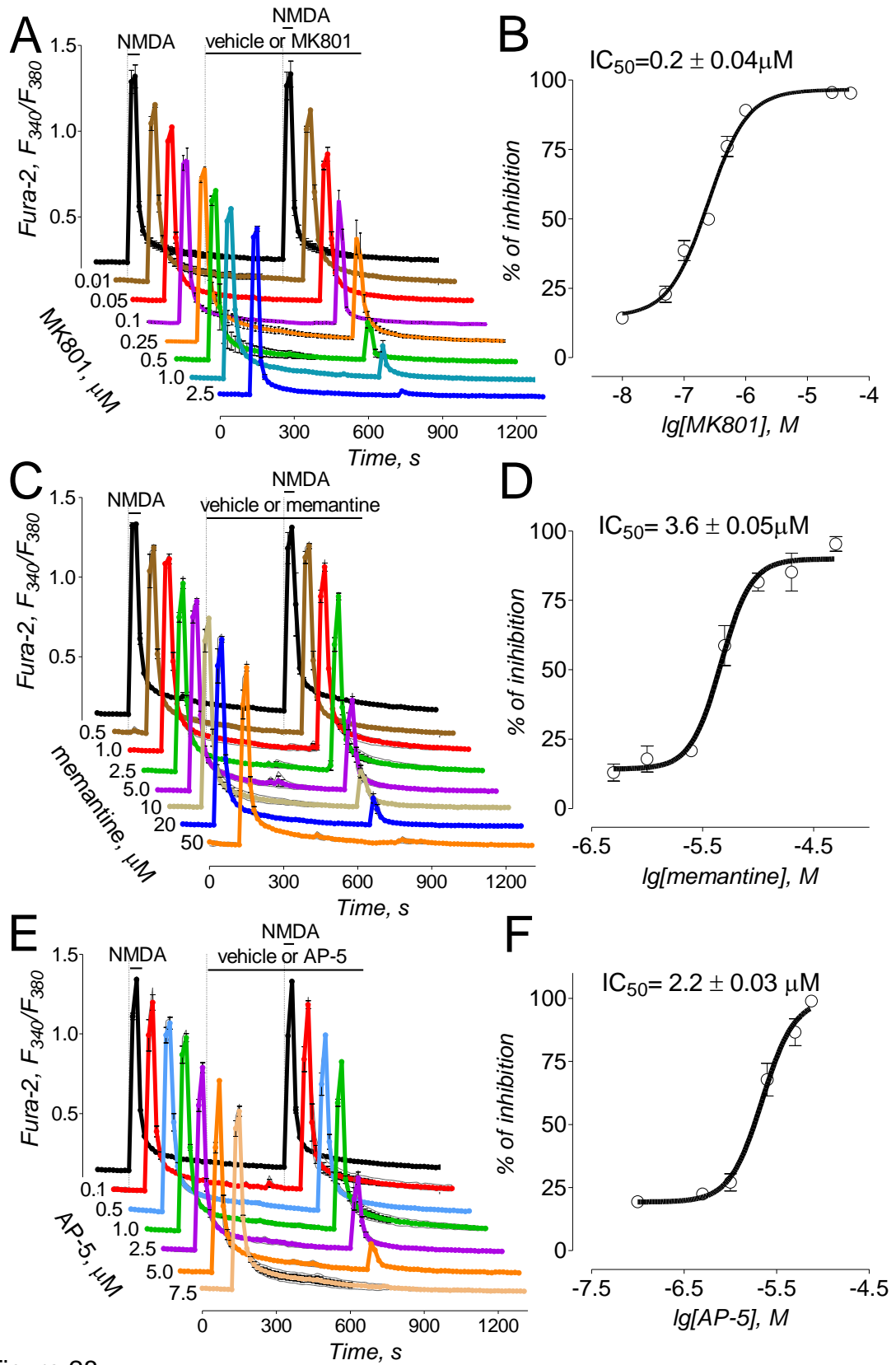


Figure 28.

Figure 28. **NMDA receptor inhibitors antagonize NMDA-induced increases in $[Ca^{2+}]_c$.** The bath solution was supplemented with 1 μ M tetrodotoxin and 5 μ M nifedipine. Neurons were loaded with 2.6 μ M Fura-2AM. Where indicated, vehicle (veh, 0.2% DMSO, black trace) or various concentrations of MK801 (0.01-2.5 μ M), memantine (0.5-50 μ M), and AP-5 (0.1-7.5 μ M) were applied and present in the bath solution until the end of the experiment. NMDA (30 μ M, plus 10 μ M glycine) was applied twice for 30 seconds as indicated. The activity of NMDA receptors was evaluated by measuring amplitude of the increases in Fura-2 F_{340}/F_{380} ratio triggered by the second application of NMDA. The dose-dependence graph was plotted, and IC_{50} was calculated using GraphPad Prism[®] 4.0 (GraphPad Software Inc., San Diego, CA).

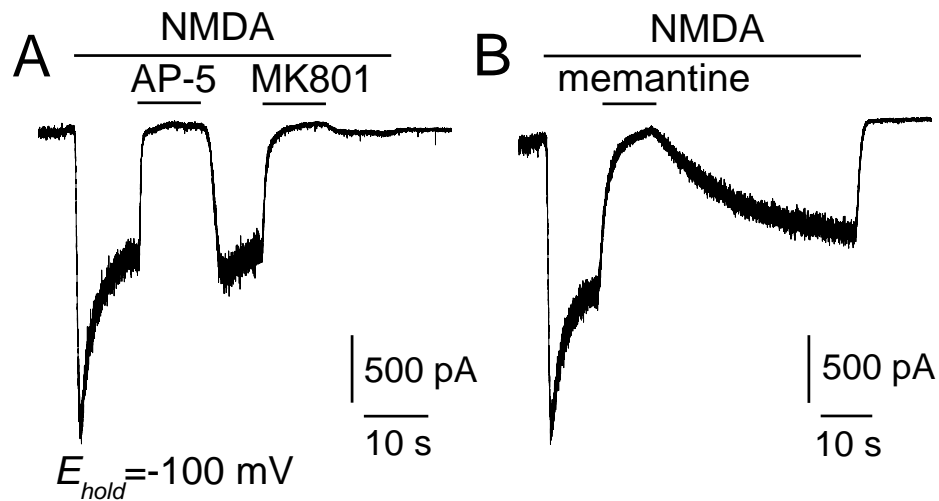


Figure 29. **Patch-clamp recordings of NMDA-induced whole-cell currents recorded with cultured hippocampal neurons.** The effects of 20 μM AP-5 and 10 μM MK801 (A), and 50 μM memantine (B). In all experiments, 30 μM NMDA (plus 10 μM glycine) were applied as indicated. Holding voltage (E_{hold}) was -100 mV. (These experiments were performed in collaboration with Patrick L. Sheets, Ph.D. and Theodore R. Cummins, Ph.D.)

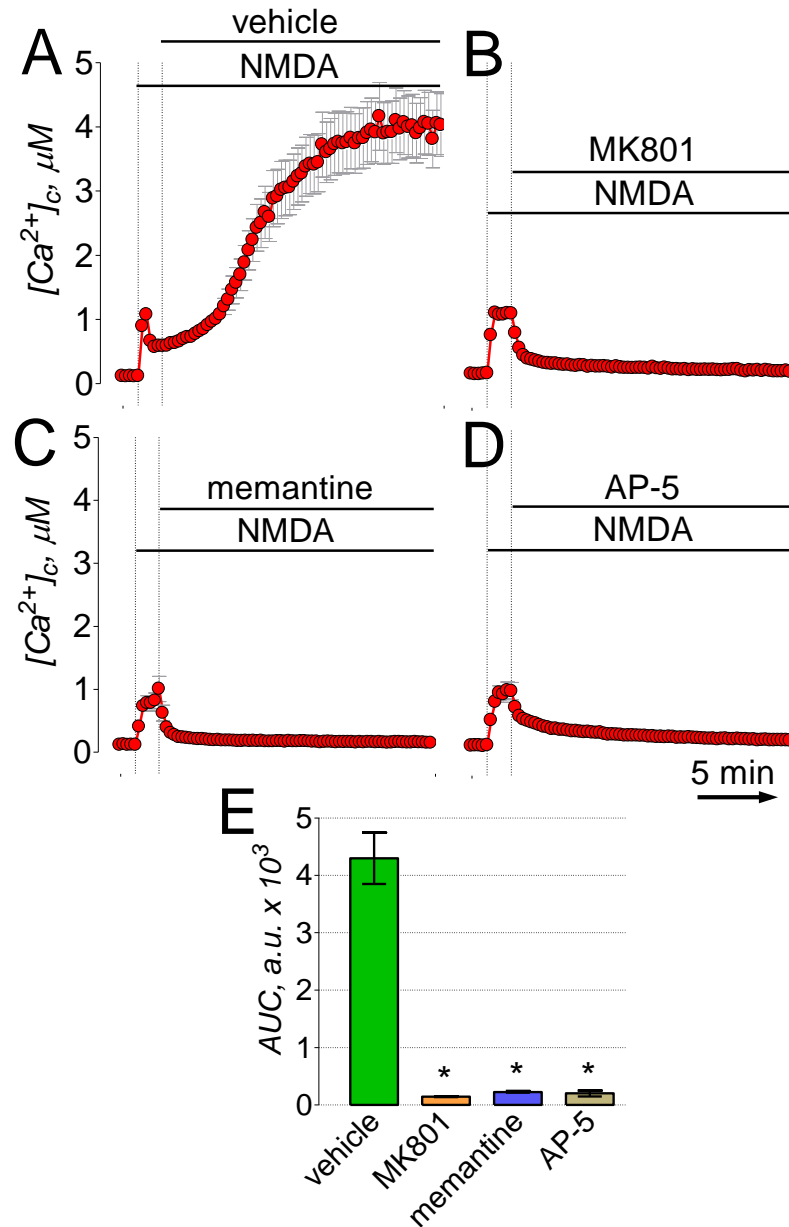


Figure 30. **NMDA-induced increases in $[Ca^{2+}]_c$. MK801, memantine, and AP-5 prevented sustained elevation in $[Ca^{2+}]_c$.** In all experiments, neurons were treated with 30 μM NMDA (plus 10 μM glycine) and 1 μM MK801, or 10 μM memantine, or 20 μM AP-5. Here and in all other experiments, 0.2% DMSO was used as a vehicle. The inhibitors were added 90 seconds following glutamate application. In A-D, measurements of $[Ca^{2+}]_c$ in hippocampal neurons loaded with a Ca^{2+} -sensitive fluorescent dye Fura-2FF. Here and in other figures, the traces show mean \pm SEM from individual experiments (n=18-25 neurons per experiment). The time scale shown in panel D is applicable to all traces in A-C. In E, statistical analysis of glutamate-induced $[Ca^{2+}]_c$ changes over time in dependence on the presence of different inhibitors. Data are mean \pm SEM, * $p < 0.01$ compared to vehicle, n=3.

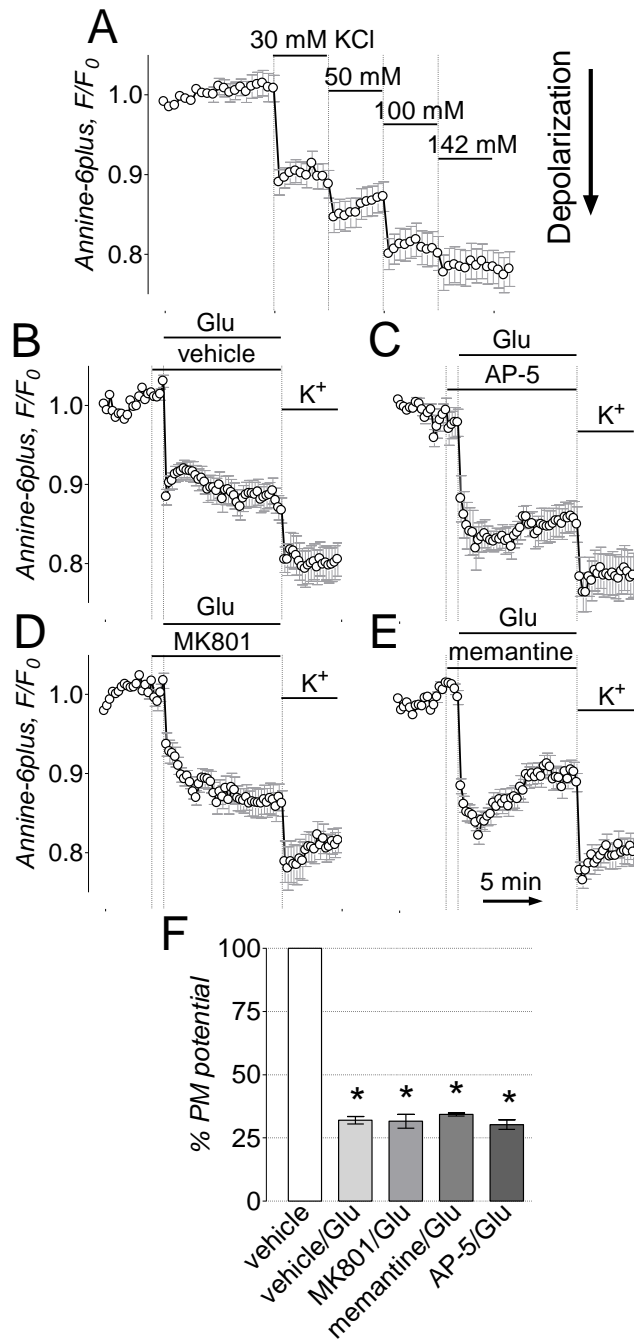


Figure 31. KCl- and glutamate-induced plasma membrane depolarizations in cultured hippocampal neurons. Neither MK801, nor memantine, nor AP-5 prevent this membrane depolarization. In A-E, the changes in plasma membrane potential were monitored by following Annine-6plus F_{480} and expressed as F/F_0 . Panel A shows changes in Annine-6plus fluorescence following step-wise plasma membrane depolarizations with increasing concentrations of KCl. In B-E, where indicated, neurons were treated with 25 μ M glutamate (Glu, plus 10 μ M glycine) and 200 μ M AP-5, or 1 μ M MK801, or 50 μ M memantine. At the end of the experiments, NaCl in the bath solution was replaced by 142 mM KCl to completely depolarize plasma membrane. The time scale shown in panel E is applicable to all traces in A-D. In F, statistical analysis of glutamate-induced plasma membrane depolarizations over time expressed as percentage of plasma membrane potential under resting conditions. Data are mean \pm s.e.m., * p <0.01 compared to vehicle, $n=3$.

membrane depolarization with increasing concentrations of KCl. MK801, memantine, and AP-5 neither attenuated the glutamate-induced increases in $[Na^+]_c$ (Figure 25B-D) nor prevented plasma membrane depolarization (Figure 31C-E). The changes in $[Na^+]_c$ were assessed similar to changes in $[Ca^{2+}]_c$ (Figure 25E) by calculating AUC (Figure 25F). The change in plasma membrane potential was evaluated by calculating the percentage of glutamate-induced decline in membrane potential compared to maximal depolarization produced by complete replacement of NaCl for KCl in the bath solution (Figure 31F). In contrast to glutamate-induced alterations in $[Na^+]_c$ and plasma membrane potential, MK801 (1 μ M), memantine (10 μ M), and AP-5 (20 μ M) significantly lowered $[Na^+]_c$ elevated after NMDA application (Figure 32). Similar results are observed when the NMDA receptor antagonists are added prior to glutamate (Figure 33). The addition of the NMDA receptor antagonist prior to glutamate is important to determine if the initial influx of Ca^{2+} and Na^+ through the NMDA receptor is necessary to induce DCD. The Na^+/K^+ ATPase is responsible for the reduction in $[Na^+]_c$ (Yuan *et al.*, 2005). In Figure 34, the Na^+/K^+ ATPase is blocked by 1 mM ouabain, and as a result of the inhibition of the Na^+/K^+ ATPase, the reduction in the Na^+ concentration is not observed (Figure 34C). All tested NMDA receptor antagonists completely prevented plasma membrane depolarization induced by 30 μ M NMDA (plus 10 μ M glycine) (Figure 35), confirming the effectiveness of the NMDA receptor inhibitors.

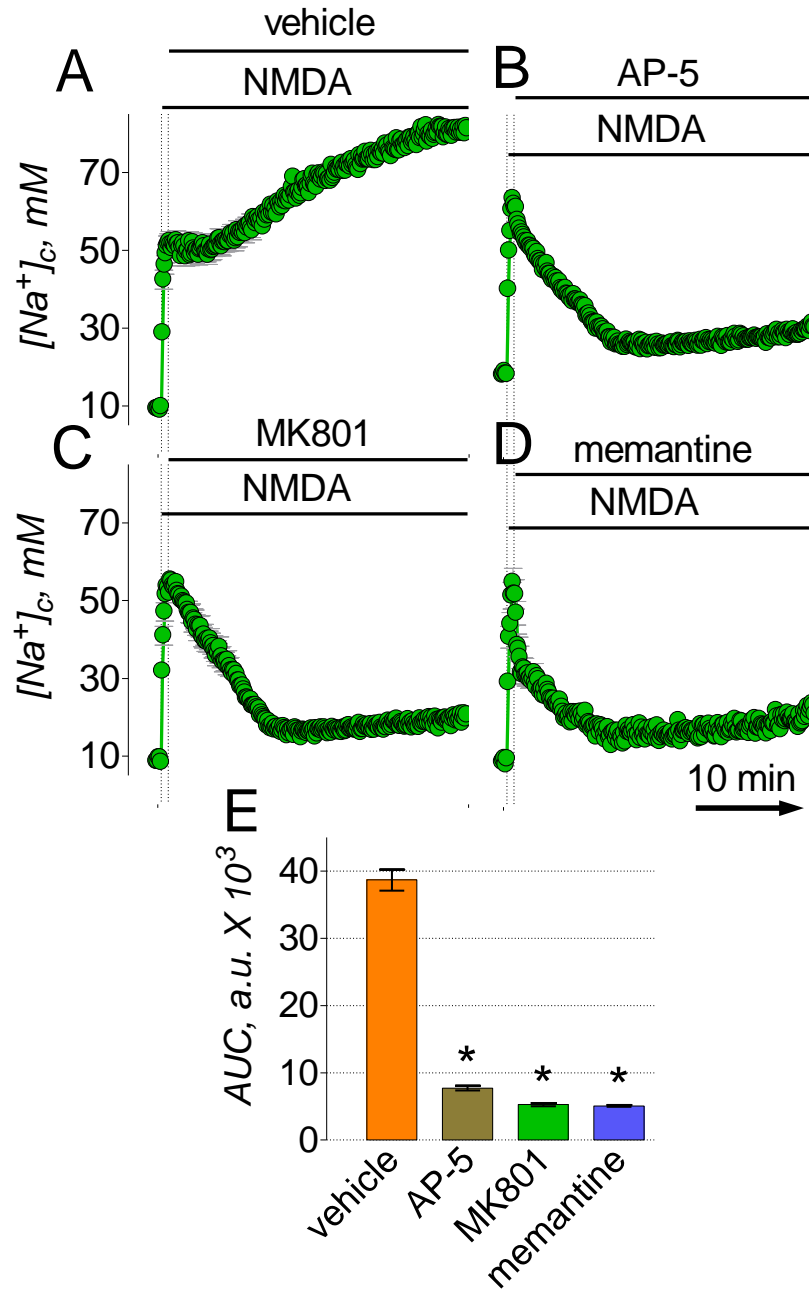


Figure 32. **Induced by NMDA, MK801, memantine, and AP-5 decrease $[Na^+]_c$.** In all experiments, neurons were treated with 30 μ M NMDA plus 10 μ M glycine (Glu) and 1 μ M MK801, or 10 μ M memantine, or 20 μ M AP-5. The antagonists were added 90 seconds following NMDA application. In A-D, measurements of $[Na^+]_c$ in hippocampal neurons loaded with a Na^+ -sensitive dye SBF1. The time scale shown in panel D is applicable to all traces in A-C. In E, statistical analyses of NMDA-induced $[Na^+]_c$ changes over time in dependence on the presence of different inhibitors. See text for details. Data are mean \pm SEM, * $p < 0.01$ compared to vehicle, $n=3$.

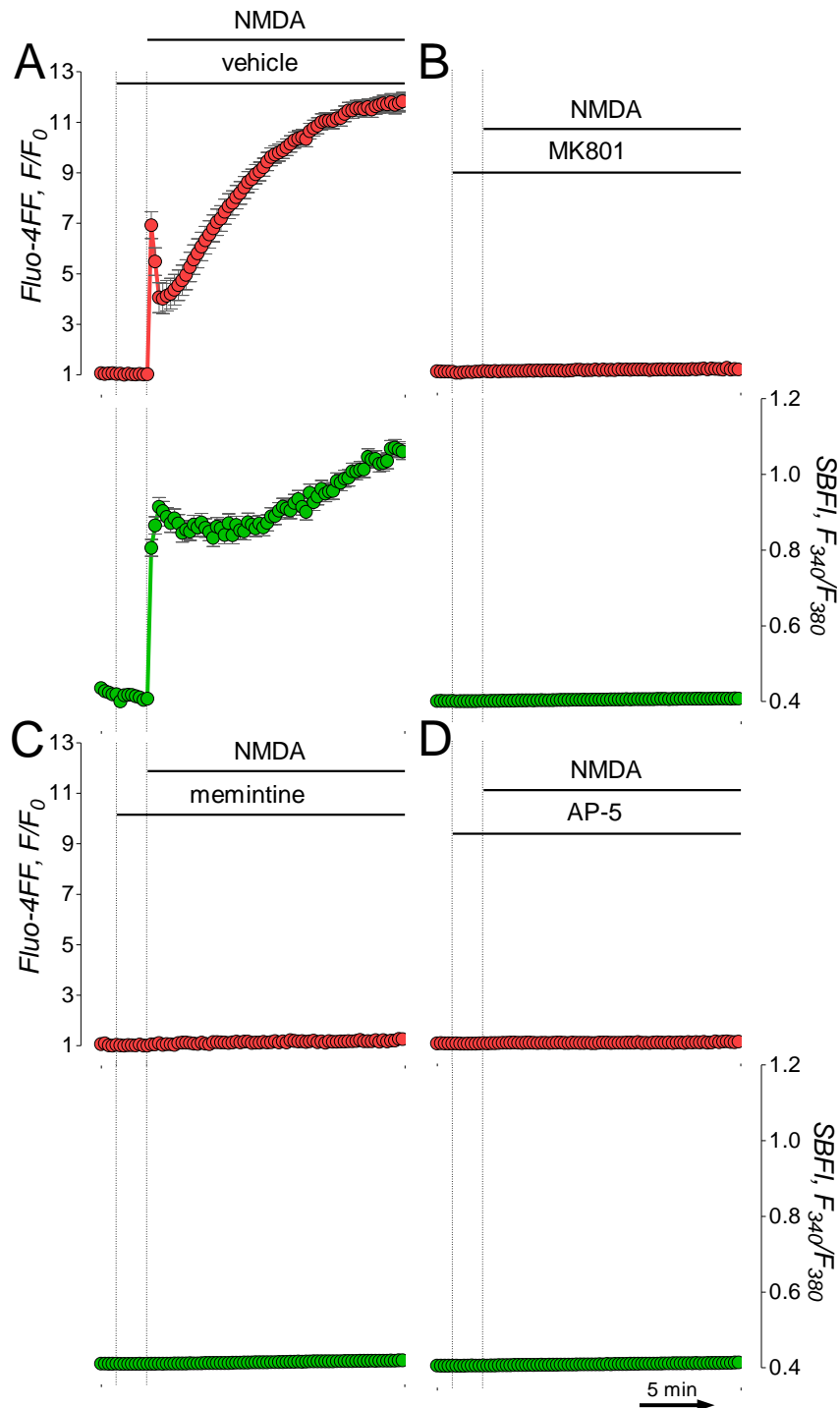


Figure 33. **NMDA receptor antagonists prevent NMDA-induced increases in $[Ca^{2+}]_c$ and $[Na^+]_c$.** In all experiments, neurons were treated with 30 μ M NMDA (plus 10 μ M glycine) and 1 μ M MK801, or 10 μ M memantine, or 20 μ M AP-5. The antagonists were added 120 seconds prior to the application of NMDA. In A-D, simultaneous measurements of $[Ca^{2+}]_c$ and $[Na^+]_c$ in hippocampal neurons loaded with a Ca^{2+} -sensitive dye Fluo-4FF and a Na^+ -sensitive dye SBFI.

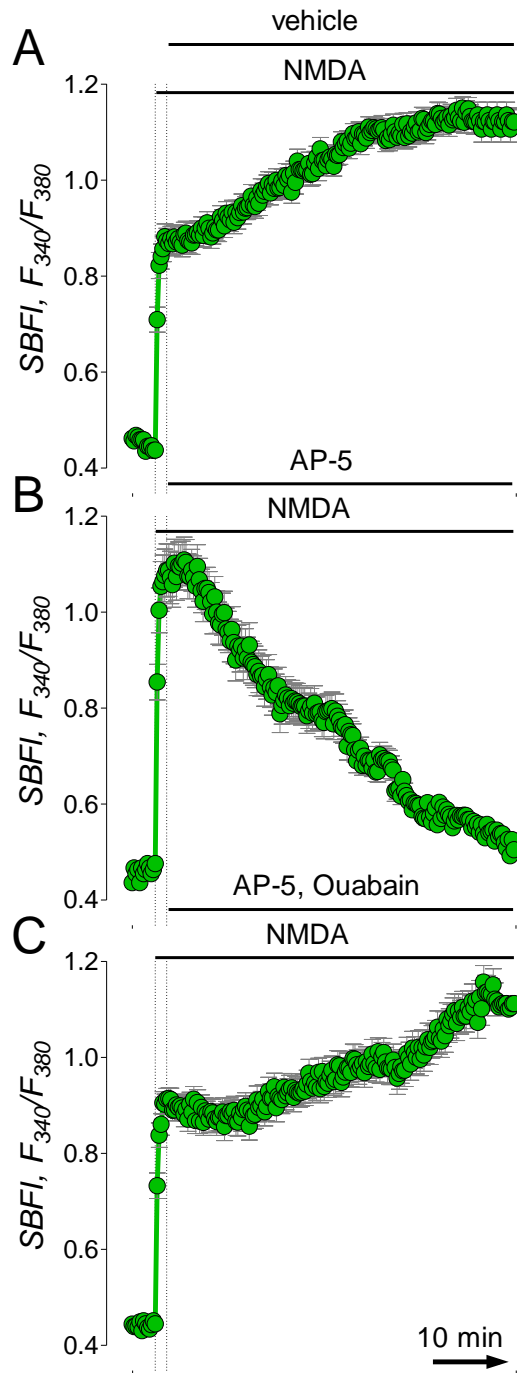


Figure 34. **The Na^+/K^+ ATPase reduce the cytosolic Na^+ concentration following the large Na^+ influx induced by NMDA stimulation.** The neurons were loaded with the sodium-sensitive dye, SBFI. Where indicated, the neurons were stimulated with $30\mu M$ NMDA plus $10\mu M$ glycine. Then, 90 seconds after the stimulation the neurons were treated with (A) vehicle (2% DMSO), (B) $20\mu M$ AP-5, or (C) $20\mu M$ AP-5 and 1 mM Ouabain.

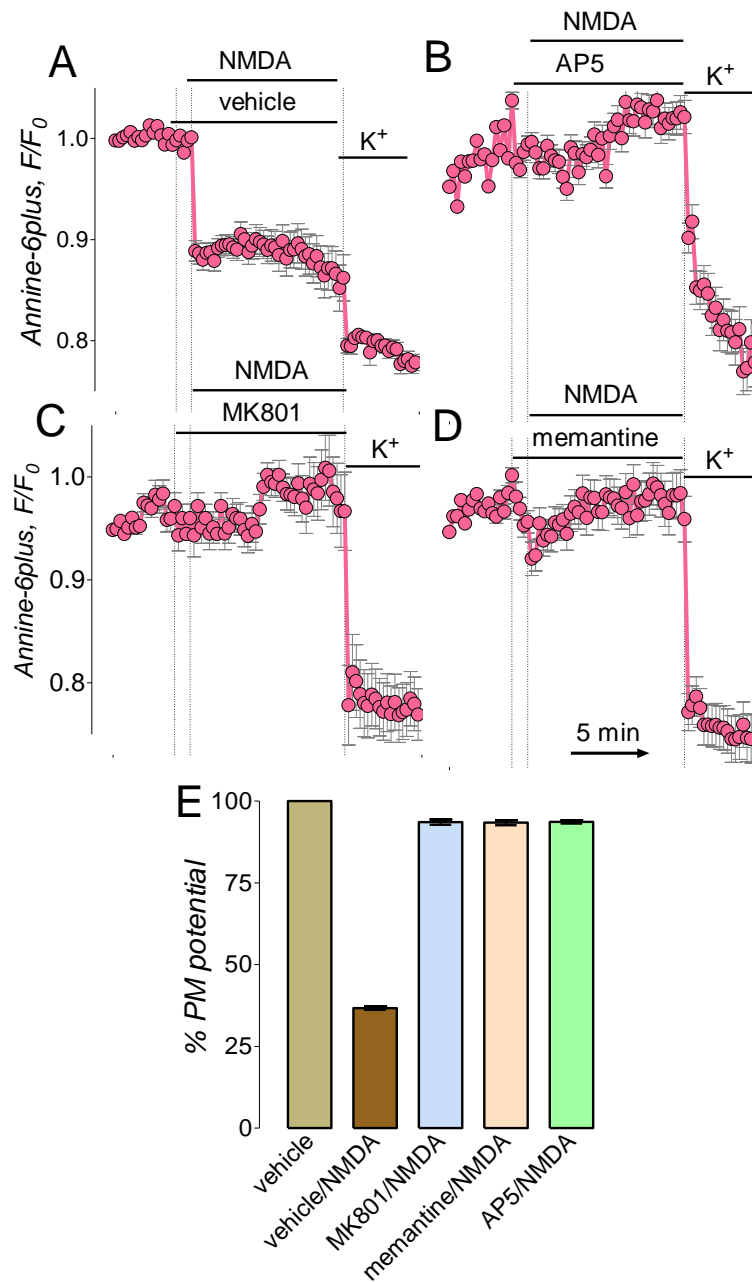


Figure 35. **MK801, memantine, and AP-5 prevent NMDA-induced plasma membrane depolarization in cultured hippocampal neurons.** In A-D, the changes in plasma membrane potential were monitored by following Annine-6plus F_{480} and expressed as F/F_0 . Panels A-D, where indicated, neurons were treated with $30\mu\text{M}$ NMDA (plus $10\mu\text{M}$ glycine) and $20\mu\text{M}$ AP-5, or $1\mu\text{M}$ MK801, or $50\mu\text{M}$ memantine. At the end of the experiments, NaCl in the bath solution was replaced by 142 mM KCl to completely depolarize plasma membrane. The time scale shown in panel D is applicable to all traces in A-D. In E, statistical analysis of glutamate-induced plasma membrane depolarization over time expressed as percentage of plasma membrane potential under resting conditions. Data are mean \pm SEM, * $p < 0.01$ compared to vehicle, $n=3$.

3. MK801 and memantine, glutamate receptor antagonists, inhibit the reverse mode of the Na⁺/Ca²⁺ exchanger

The increase in [Na⁺]_c and plasma membrane depolarization are the major pre-requisites for the reversal of NCX, which in the reverse mode brings Ca²⁺ into the cell in exchange for cytosolic Na⁺ (Kiedrowski *et al.*, 1994; Hoyt *et al.*, 1998). Thus, complete attenuation of the glutamate-induced DCD by MK801 and memantine suggested that either (i) NCX_{rev} was not involved in glutamate-induced DCD, or (ii) MK801 and memantine, also inhibited NCX_{rev}. In the following experiments, we tested whether MK801 and memantine inhibited NCX_{rev}. The reversal of NCX was triggered by treating neurons with gramicidin, a monovalent cation ionophore that increases plasma membrane permeability for Na⁺ and K⁺ but not for Ca²⁺ (Myers & Haydon, 1972). Gramicidin (5μM) induced Na⁺ influx into the cytosol and depolarized neurons (Figure 36A,B), providing conditions for NCX reversal and hence leading to the increase in [Ca²⁺]_c due to NCX_{rev} operation (Figure 36C) (Newell *et al.*, 2007; Brustovetsky *et al.*, 2011). Gramicidin applied with perfusion (1ml/min) also produced an increase in [Ca²⁺]_c (Figure 36D). MK801 and memantine completely inhibited gramicidin-induced increase in [Ca²⁺]_c (Figure 36E,F) with IC₅₀ 0.5±0.08μM and 17.1±0.24μM, respectively (Figure 37). AP-5, on the other hand, was potent (IC₅₀=2.8±0.7μM, Figure 37) but much less efficacious at blocking gramicidin-induced increase in [Ca²⁺]_c (Figure 36G).

To determine if the NMDA receptor antagonists blocked gramicidin from setting up conditions that are favorable for NCX_{rev}, gramicidin-induced plasma

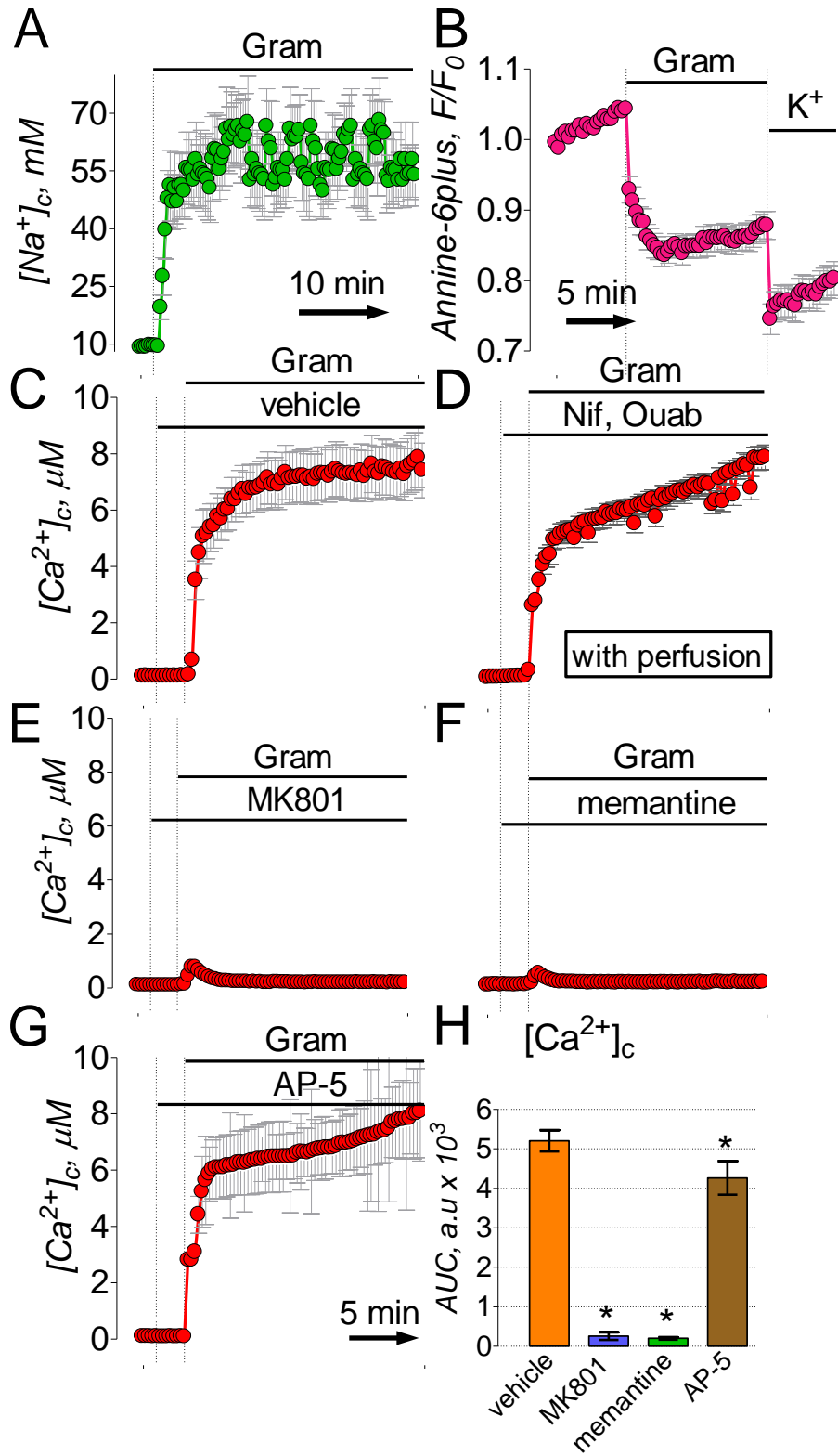


Figure 36.

Figure 36. **MK801 and memantine but not AP-5 inhibit gramicidin reversed Na⁺/Ca²⁺ exchanger (NCX) leading to the increase in [Ca²⁺]_c.** In A and B, gramicidin (5μM) produced an increase in [Na⁺]_c and plasma membrane depolarization, respectively. The changes in [Na⁺]_c were monitored by following SBFI F₃₄₀/F₃₈₀ ratio. The changes in plasma membrane potential were monitored by following Annine-6plus F/F₀. The changes in [Ca²⁺]_c were monitored by following Fura-2FF F₃₄₀/F₃₈₀ ratio. [Ca²⁺]_c and [Na⁺]_c were calculated using Grynkiewicz method (Grynkiewicz *et al.*, 1985). In A-F, where indicated, neurons were treated with 5μM gramicidin (Gram) and 1μM MK801, or 50μM memantine, or 200μM AP-5. In all experiments, bath solution was supplemented with 5μM nifedipine, a blocker of voltage-gated Ca²⁺ channels, and 1 mM ouabain, an inhibitor of the Na⁺/K⁺-ATPase. The time scale shown in panel F is applicable to all traces in C-E. In G, statistical analysis of glutamate-induced [Ca²⁺]_c changes over time in dependence on the presence of different inhibitors. Data are mean±SEM, **p*<0.01 compared to vehicle, n=3.

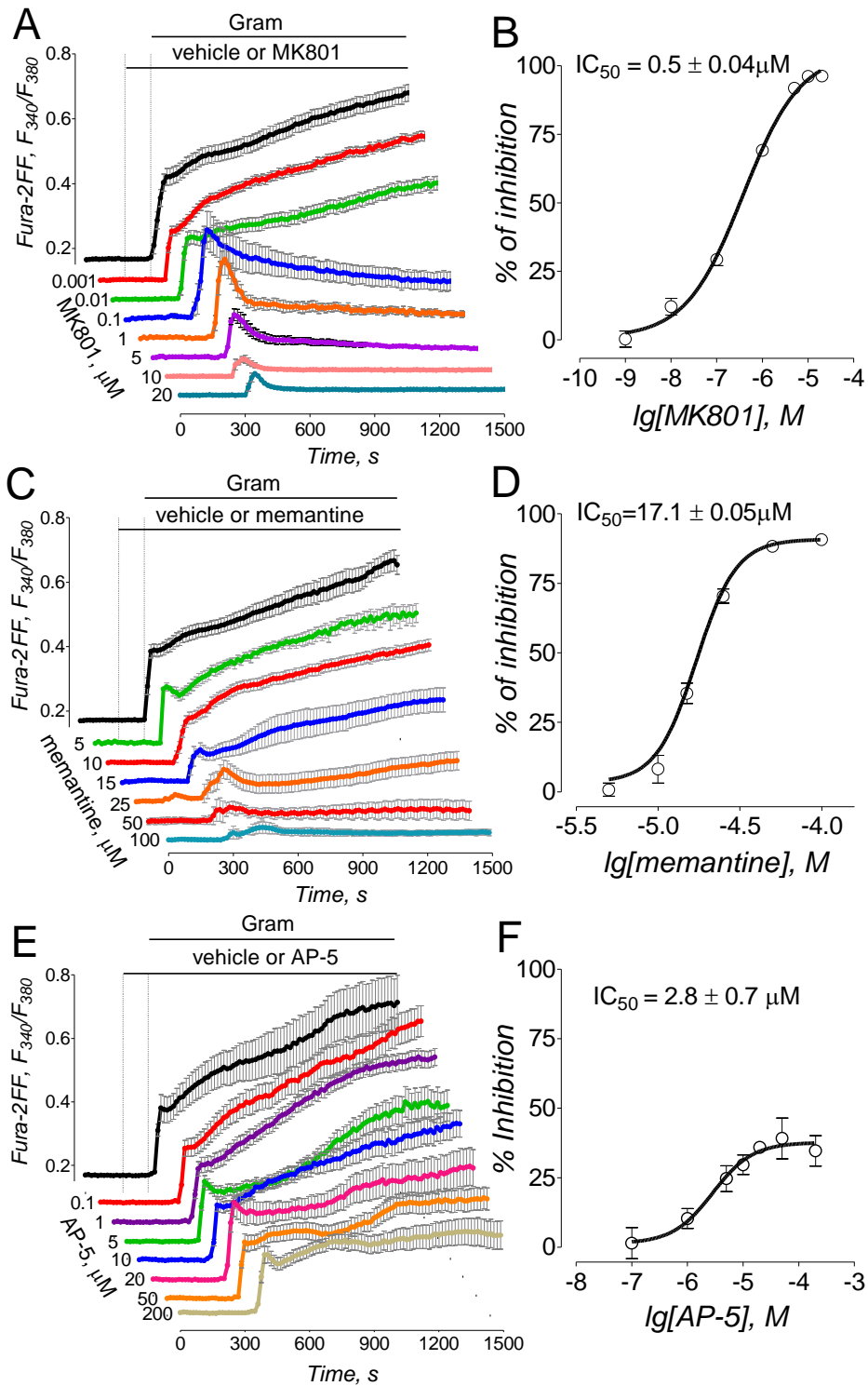


Figure 37.

Figure 37. MK801 and memantine but not AP-5 inhibit gramicidin-induced increase in cytosolic Ca^{2+} concentration ($[\text{Ca}^{2+}]_c$) in cultured hippocampal neurons. In A, C, and E, 5 μM gramicidin (Gram), MK801 (0.001-20 μM), memantine (5-100 μM), and AP-5 (0.1-200 μM) were applied as indicated. In all experiments, bath solution was supplemented with 5 μM nifedipine, a blocker of voltage-gated Ca^{2+} channels, and 1 mM ouabain, an inhibitor of the Na^+/K^+ -ATPase. The traces are averages \pm s.e.m. from individual experiments (n=18-25 neurons per experiment) performed in triplicate. Where indicated, vehicle (0.2% DMSO, black traces) or various concentrations of the inhibitors were applied and present in the bath solution until the end of the experiment. The activity of NCX_{rev} was evaluated by measuring the area under the curve for 15 minutes following the onset of $[\text{Ca}^{2+}]_c$ increase, the dose-dependence graph was plotted, and IC_{50} was calculated using GraphPad Prism[®] 4.0 (GraphPad Software Inc., San Diego, CA).

membrane depolarization and a change in $[Na^+]_c$ were monitored in the presences of the NMDA receptor antagonist MK801 (Figure 38). This shows that the NMDA receptor antagonist, MK801, has no effect on gramicidin, and the conditions are favorable for NCX_{rev} .

In addition to NCX reversal, the collapse of Na^+ gradient across the plasma membrane could trigger reversal of Na^+ -glutamate co-transporter and a release of endogenous glutamate. Indeed, we found $0.97 \pm 0.07 \mu M$ glutamate (mean \pm SEM, $n=6$) in the bath solution following 5 minutes exposure of neurons to $5 \mu M$ gramicidin compared to $0.18 \pm 0.07 \mu M$ glutamate ($n=11$) in the bath solution with untreated neurons. (These data acquired in collaboration with JM Brittain and R Khanna.) This glutamate concentration failed to induce sustained elevation in $[Ca^{2+}]_c$. However, gramicidin-induced collapse of Na^+ gradient most likely inhibited NCX operation in the forward mode and, thus, hindered Ca^{2+} extrusion from the cell. If the forward mode of NCX was turned off by replacing Na^+ in the bath solution by equimolar N-methyl-D-glucamine, $1 \mu M$ glutamate produced sustained elevations in $[Ca^{2+}]_c$ (Figure 39). Therefore, in the experiments with gramicidin we used a glutamate-pyruvate transaminase (GPT from pig heart, Roche, Indianapolis, IN) to eliminate glutamate from the bath solution. This enzyme catalyzes the glutamate-pyruvate transamination reaction producing alanine and oxaloacetate (Matthews *et al.*, 2000; Matthews *et al.*, 2003). The GPT ($25 \mu g/ml$ plus $2 mM$ pyruvate) applied together with gramicidin reduced glutamate concentration in the bath solution to $0.14 \pm 0.08 \mu M$ ($n=3$). In parallel calcium imaging experiments, GPT plus pyruvate slowed down

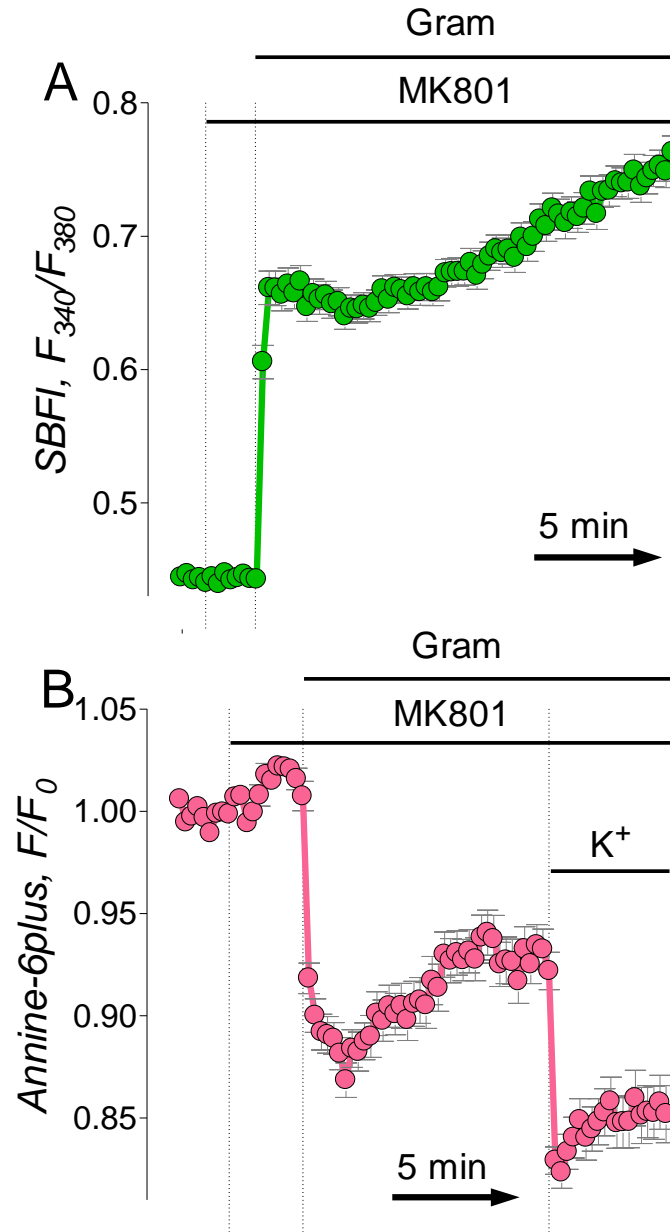


Figure 38. **Inhibition of the NMDA receptor with MK801 has no effect on the increase in cytosolic Na⁺ or plasma membrane depolarization induced by gramicidin.** Where indicated 5 μ M gramicidin was added. This addition results in the collapse of the Na⁺ gradient across the plasma membrane and the plasma membrane depolarization resulting in the reverse mode of the NCX. To determine if the MK801, an NMDA receptor antagonist interferes with these functions 5 μ M MK801 was added prior to the addition of gramicidin. In panel A, the neurons were loaded with 9 μ M SBF1 to monitor changes in cytosolic Na⁺ concentration, and panel B, loaded with a voltage-sensitive dye, annine-6plus (4 μ M), to monitor changes in plasma membrane potential.

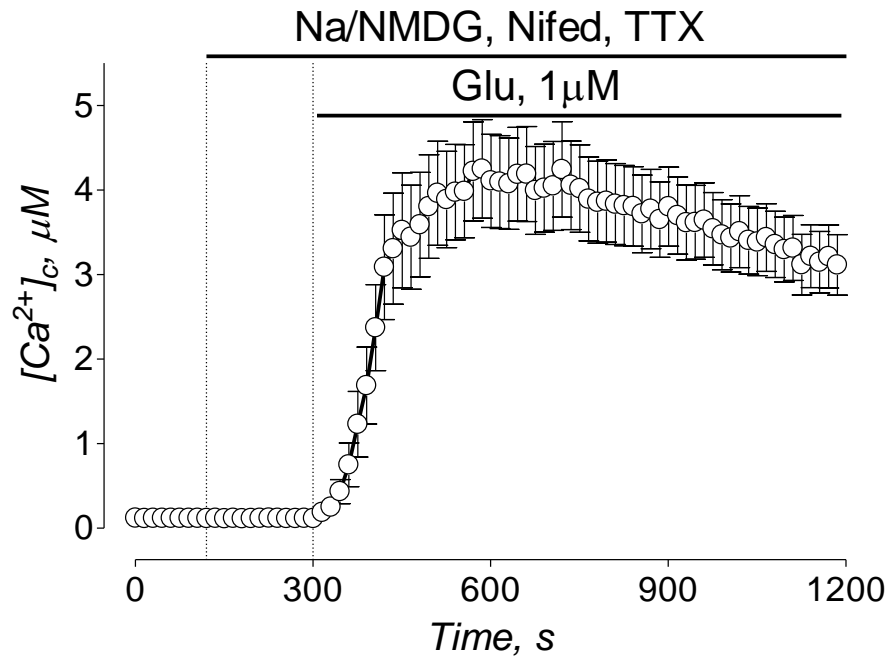


Figure 39. **Low glutamate concentration induces sustained elevation in $[Ca^{2+}]_i$ under conditions of forward NCX shut down.** In A, where indicated, Na^+ was replaced by equimolar N-methyl-D-glucamine ($NMDG^+$). Then, neurons were treated with $1\mu M$ glutamate (plus $10\mu M$ glycine). The trace shows $mean \pm SEM$ ($n=3$). In these experiments, the bath solution was supplemented with $5\mu M$ nifedipine and $1\mu M$ tetrodotoxin (TTX).

gramicidin-induced elevation in $[Ca^{2+}]_c$ but failed to prevent it (Figure 40).

Likewise, in Figure 41, DL-*threo*- β -Benzyloxyaspartate (DL-TBOA), an inhibitor of the Na^+ -glutamate co-transporter (Lebrun *et al.*, 1997), had minimal effect on gramicidin-induced increase in $[Ca^{2+}]_c$. DL-TBOA has been shown to prevent both forward and reverse modes of the Na^+ -glutamate co-transporters (Lebrun *et al.*, 1997). Thus, DL-TBOA would prevent any increase in extracellular glutamate (Bonde *et al.*, 2005). Presumably, gramicidin-induced increase in $[Ca^{2+}]_c$ involved Ca^{2+} influx via both NMDA receptors stimulated by the released glutamate and NCX_{rev} . Consequently, the partial inhibition of gramicidin-induced $[Ca^{2+}]_c$ increase by AP-5 could be due to inhibition of NMDA receptor (Figure 36G). However, gramicidin could damage mitochondria (Luvisetto & Azzone, 1989; Rottenberg & Koeppe, 1989) involved in Ca^{2+} buffering in neurons (Wang & Thayer, 1996). Therefore, alternatively, we triggered NCX reversal by replacing Na^+ in the bath solution with $NMDG^+$ replaced (Wu *et al.*, 2008).

Under resting conditions neurons maintain roughly 10 mM $[Na^+]_c$, while the extracellular environment is roughly 140 mM Na^+ . This large Na^+ gradient is one of the key driving forces that allow the NCX to remove Ca^{2+} from the cytosol. Thus, when the extracellular Na^+ is removed and replaced with the same concentration of a large monovalent cation, $NMDG^+$, the sodium gradient across the plasma membrane is reversed (Wu *et al.*, 2008). This results in an increased probability for the reverse mode of the NCX to occur. In Figure 42B, 1 mM ouabain and 5 μ M nifedipine were added at the beginning of the experiment.

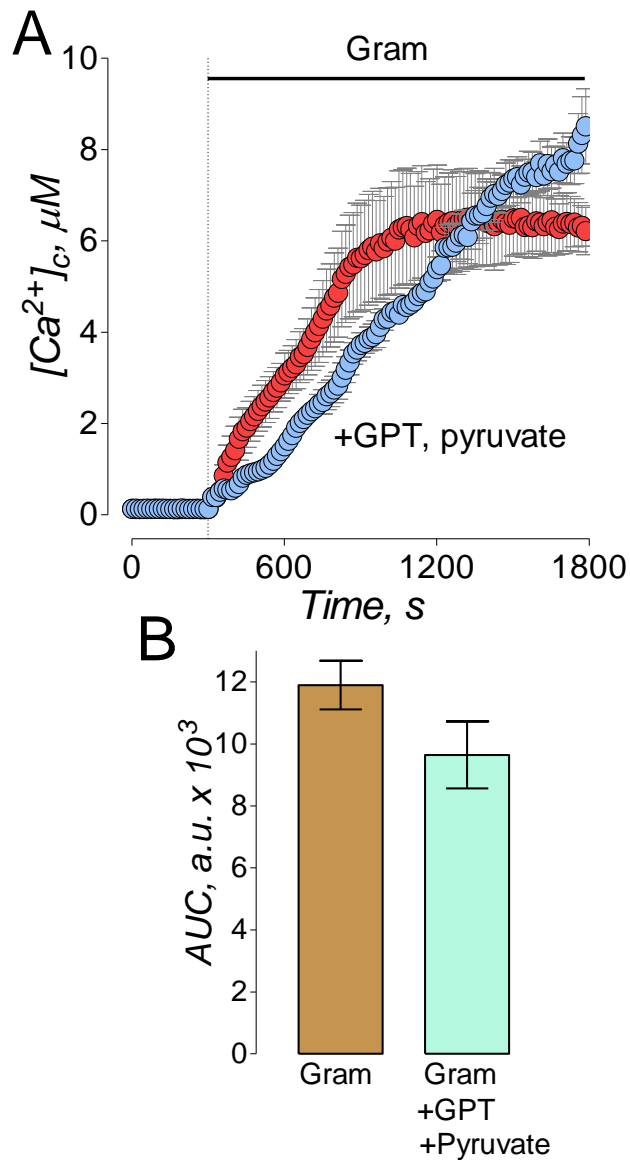


Figure 40. **Glutamate removal in the bath solution fails to prevent gramicidin-induced increase in $[Ca^{2+}]_c$.** In A, where indicated, neurons were treated with $5\mu M$ gramicidin. The trace with blue symbols illustrates experiment, in which bath solution was supplemented with $25\mu g/ml$ glutamate-pyruvate transaminase (GPT, Roche) plus 2 mM pyruvate; red symbols - without GPT and pyruvate. The traces show mean \pm SEM. In these experiments, the bath solution was supplemented with $5\mu M$ nifedipine and 1 mM ouabain. In B, statistical analysis of gramicidin-induced $[Ca^{2+}]_c$ changes over time in dependence on the presence of GPT plus pyruvate. Data are mean \pm SEM, $n=3$.

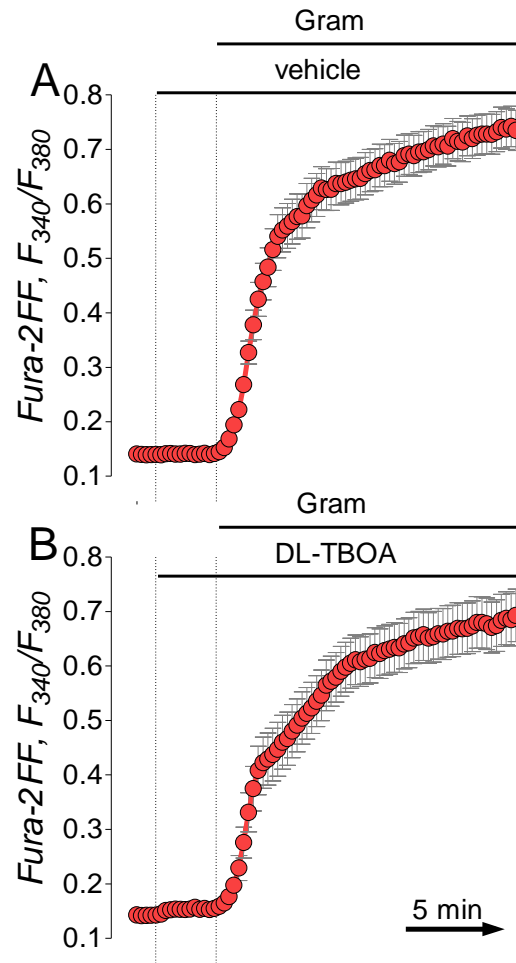


Figure 41. **DL-TBOA inhibits the Na⁺/glutamate co-transporter, preventing endogenous glutamate release, has no effect on gramicidin-induced calcium dysregulation.** Neurons were loaded with 2.6 μ M Fura-2FFAM to follow changes in cytosolic calcium concentration ($[Ca^{2+}]_c$). Where indicated, neurons were exposed to 5 μ M gramicidin and either vehicle (0.2% DMSO) or DL-TBOA (100 μ M). In these experiments, the bath solution was supplemented with 5 μ M nifedipine and 1 mM ouabain.

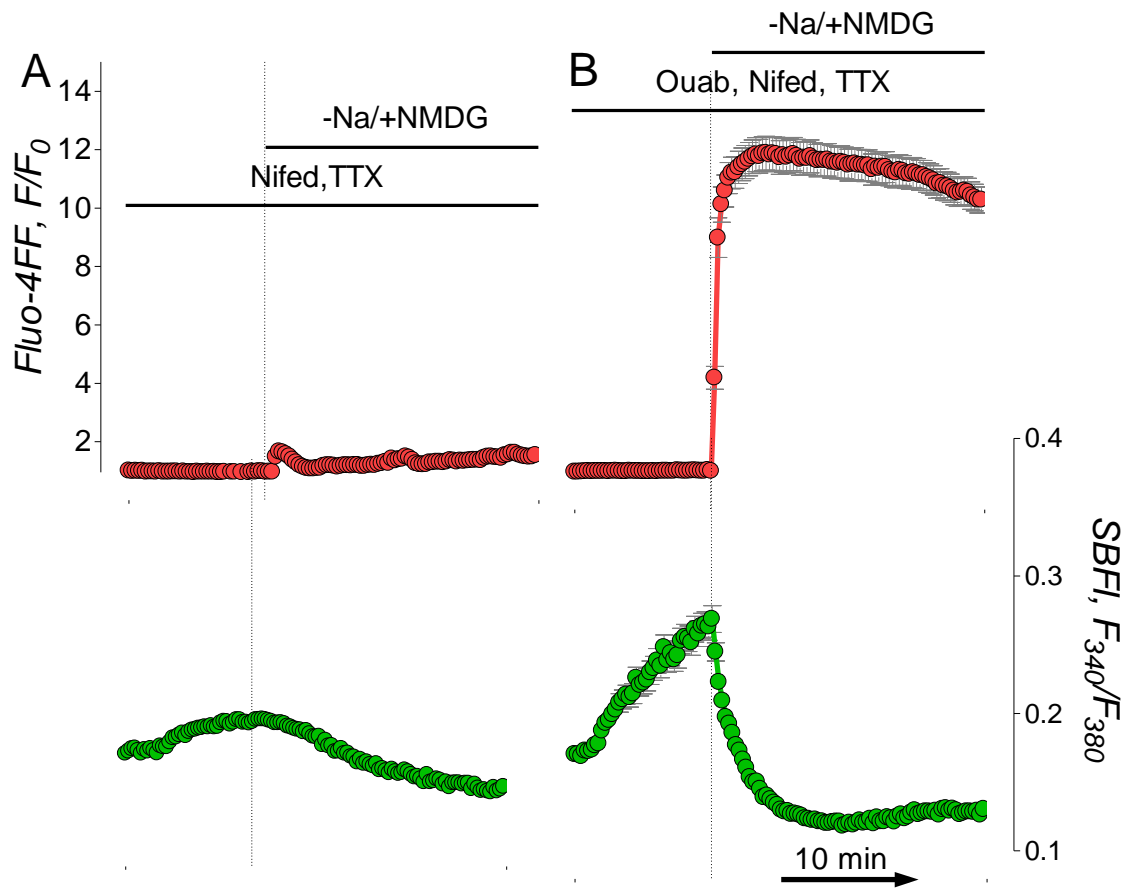


Figure 42. **Na⁺/NMDG⁺ replacement induces an increase in sodium and calcium concentrations in cultured hippocampal neurons.** In these experiments the bath solutions were supplemented with 1 μ M TTX and 5 μ M nifedipine. In panels B, 1 mM ouabain was added to induce an increase in cytosolic Na⁺. Where indicated, Na⁺ was replaced with equimolar NMDG⁺. Neurons were co-loaded with 9 μ M of Na⁺-sensitive fluorescent dye SBF1-AM and 2.6 μ M of Ca²⁺-sensitive dye Fluo-4FF-AM to monitor changes in cytosolic Na⁺ (Na⁺, lower panels) and Ca²⁺ (Ca²⁺, upper panels), respectively. The traces show mean \pm SEM.

Ouabain inhibits the Na^+/K^+ ATPase, resulting in a minimal increase in $[\text{Na}^+]_c$ (Figure 42D). Without the addition of ouabain, the $\text{Na}^+/\text{NMDG}^+$ replacement did not produce a rapid increase in $[\text{Ca}^{2+}]_c$ (Figure 42A and C). This need for an increase in Na^+ concentration was previously observed (Wu *et al.*, 2008).

Similar to gramicidin-induced calcium dysregulation, the NMDA receptor could be activated by the release of endogenous glutamate. During $\text{Na}^+/\text{NMDG}^+$ replacement, the Na^+ -glutamate co-transporter may reverse flow, allowing a buildup of extracellular glutamate. Using Amplex® Red Glutamic Acid/Glutamate Oxidase Assay Kit from Invitrogen, we determined that $1.2 \pm 0.2 \mu\text{M}$ glutamate (mean \pm SEM) in the bath solution 5 minutes after Na^+ was replaced with NMDG^+ . This endogenous glutamate concentration is elevated in comparison to $0.18 \pm 0.07 \mu\text{M}$ which was measured after 5 minutes of vehicle treatment (0.2% DMSO). However, when $25 \mu\text{g}/\text{mL}$ glutamate-pyruvate transaminase (GPT) plus 2 mM pyruvate was present to eliminate this endogenous glutamate from the bath solution, ($0.16 \pm 0.05 \mu\text{M}$, $n=3$ - experiments performed in collaboration with JM Brittain and R Khanna.) the levels returned to baseline (Matthews *et al.*, 2003; Matthews *et al.*, 2000). To test whether this endogenous glutamate affected the increase in $[\text{Ca}^{2+}]_c$ following the $\text{Na}^+/\text{NMDG}^+$ replacement, $25 \mu\text{g}/\text{mL}$ GPT plus 2 mM pyruvate was used in a series of experiments. The combination of GPT and pyruvate will prevent the buildup of endogenous glutamate, and thus, eliminate the possibility of NMDA receptor activation. The addition of GPT had a minimal effect ($\sim 25\%$ reduction in $[\text{Ca}^{2+}]_c$) on the calcium dysregulation induced by $\text{Na}^+/\text{NMDG}^+$ replacement (Figure 43). This suggests that observed increase

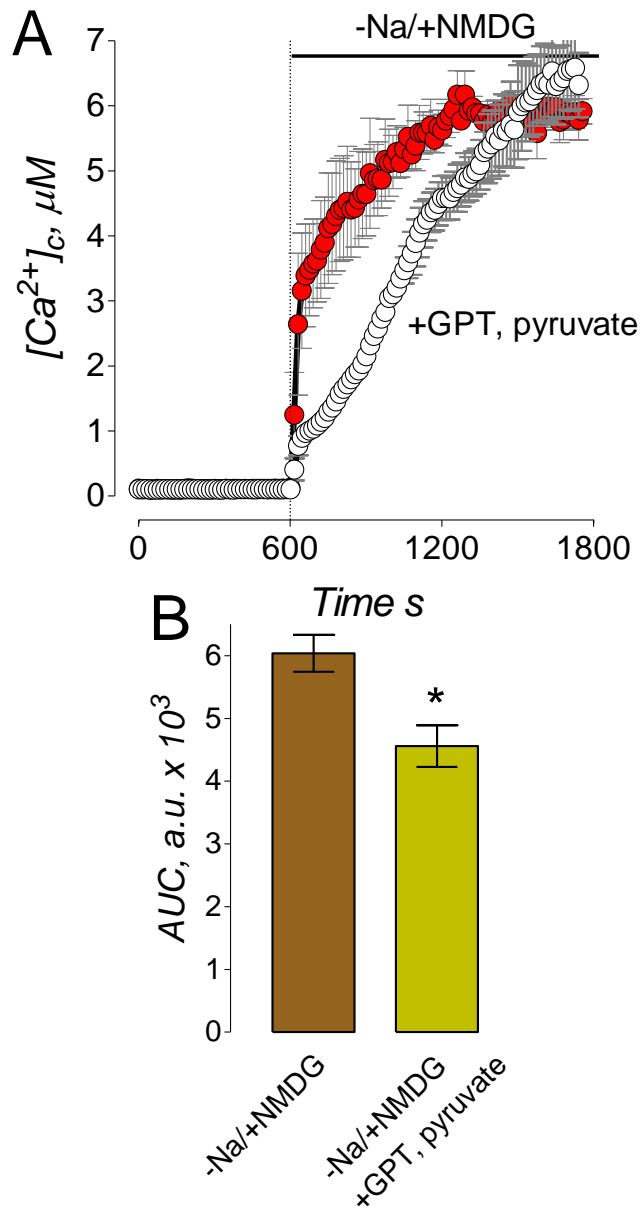


Figure 43. **Glutamate removal in the bath solution fails to prevent the increase in $[Ca^{2+}]_c$ induced by $Na^+/NMDG^+$ replacement.** In A, where indicated, Na^+ was replaced with NMDG in the bath solution following a 10 min exposure to 1 mM ouabain. The trace with white symbols illustrates experiment, in which bath solution was supplemented with 25 $\mu g/ml$ glutamate pyruvate transaminase (GPT, Roche) plus 2 mM pyruvate; gray symbols - without GPT and pyruvate. The traces show mean \pm SEM. In these experiments, the bath solution was supplemented with 1 μM TTX, 5 μM nifedipine, and 1 mM ouabain. In B, statistical analysis of $Na^+/NMDG^+$ replacement-induced $[Ca^{2+}]_c$ changes over time in dependence on the presence of GPT plus pyruvate. Data are mean \pm SEM, * $p < 0.05$ compared to the experiment without GPT and pyruvate, $n=3$.

in cytosolic Ca^{2+} is mostly due to calcium influx through the reverse mode of the NCX. However, it is possible to see a minimal decrease in $[\text{Ca}^{2+}]_c$ with AP-5 due to NMDA receptor inhibition that would have been activated by this endogenous glutamate release.

Gramicidin induces calcium dysregulation via Ca^{2+} influx through NCX_{rev} ; however, the integrity of the mitochondria is in question. Thus, Figure 44 represents experiments where neurons were loaded with a Ca^{2+} -sensitive dye, Fura-2FF, and NCX_{rev} was induced with a $\text{Na}^+/\text{NMDG}^+$ replacement. These neurons were treated with ouabain for 5 minutes before Na^+ was replaced with NMDG^+ . This resulted in immediate calcium dysregulation, mostly due to Ca^{2+} influx through NCX_{rev} . In Figure 44B and C, MK801 ($1\mu\text{M}$) and memantine ($50\mu\text{M}$), respectively, completely prevented calcium dysregulation induced by this replacement with an IC_{50} of $0.4\pm 0.02\mu\text{M}$ for MK801 (Figure 45A and B) and an IC_{50} of $17.7\pm 0.1\mu\text{M}$ for memantine (Figure 45C and D). In contrast, AP-5 inhibited the calcium dysregulation induced by the $\text{Na}^+/\text{NMDG}^+$ replacement to a much lesser extent (~25% inhibition) in comparison to MK801 and memantine (Figure 44D). The IC_{50} for AP-5 is $4.3\pm 1.1\mu\text{M}$ for inhibition of $\text{Na}^+/\text{NMDG}^+$ -induced Ca^{2+} dysregulation (Figure 45E and F). As previously mentioned, the AP-5-induced inhibition is most likely due to inhibition of the NMDA receptor. During the $\text{Na}^+/\text{NMDG}^+$ replacement, the NMDA receptor is minimally activated by a buildup of endogenous glutamate released by the Na^+ -glutamate co-transporter. This activation would allow some influx of calcium through the NMDA receptor, and the presence of AP-5 would prevent that from

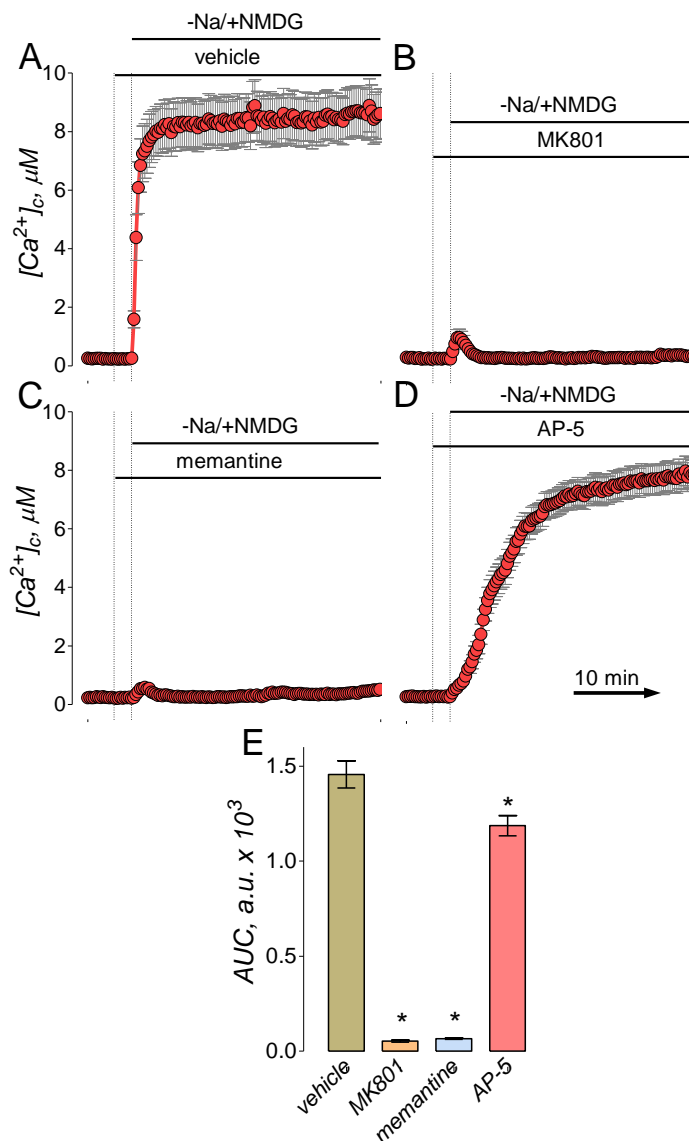


Figure 44. **Substitution of Na⁺ with equimolar N-methyl-D-glucamine (NMDG⁺) reverses Na⁺/Ca²⁺ exchanger (NCX) leading to the increase in [Ca²⁺]_c. MK801 and memantine and to much lesser extent AP-5 inhibit the reverse NCX.** The changes in [Ca²⁺]_c were monitored by following Fura-2FF F₃₄₀/F₃₈₀ ratio. [Ca²⁺]_c was calculated using Grynkiewicz method (Grynkiewicz *et al.*, 1985). In A-D, where indicated, NaCl in the bath solution was replaced by 139 mM NMDG and neurons were treated with 1 μM MK801, or 50 μM memantine, or 200 μM AP-5. In all experiments, bath solution was supplemented with 5 μM nifedipine, a blocker of voltage-gated Ca²⁺ channels, and 1 mM ouabain, an inhibitor of the Na⁺/K⁺-ATPase. The time scale shown in panel F is applicable to all traces in C-E. In E, statistical analysis of glutamate-induced [Ca²⁺]_c changes over time in dependence on the presence of different inhibitors. Data are mean ± SEM, **p* < 0.01 compared to vehicle, *n* = 3.

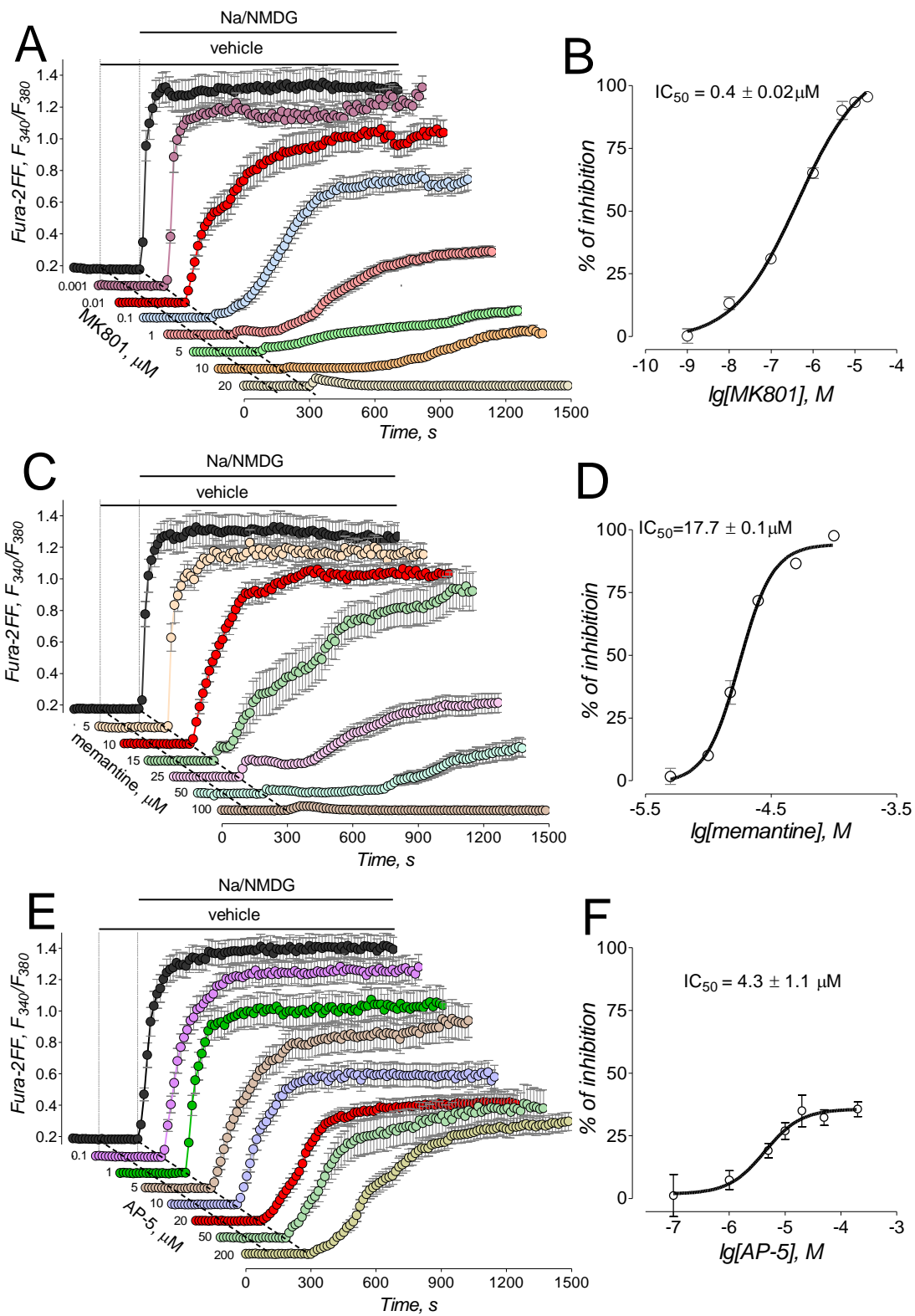


Figure 45.

Figure 45. **MK801 and memantine but not AP-5 inhibit Na⁺/NMDG⁺ replacement-induced increase in cytosolic Ca²⁺ concentration ([Ca²⁺]_c) in cultured hippocampal neurons.** In A, C, and E, Na⁺ was replaced for an equal molar of NMDG, MK801 (0.001-20 μM), memantine (5-100 μM), and AP-5 (0.1-200 μM) were applied as indicated. In all experiments, bath solution was supplemented with 5 μM nifedipine, a blocker of voltage-gated Ca²⁺ channels, and 1 mM ouabain, an inhibitor of the Na⁺/K⁺-ATPase. The traces are averages ± s.e.m. from individual experiments (n=18-25 neurons per experiment) performed in triplicate. Where indicated, vehicle (0.2% DMSO, black traces) or various concentrations of the inhibitors were applied and present in the bath solution until the end of the experiment. The activity of NCX_{rev} was evaluated by measuring the area under the curve for 15 minutes following the onset of [Ca²⁺]_c increase, the dose-dependence graph was plotted, and IC₅₀ was calculated using GraphPad Prism[®] 4.0 (GraphPad Software Inc., San Diego, CA).

occurring, slightly altering the overall calcium dysregulation induced by $\text{Na}^+/\text{NMDG}^+$ replacement. Overall, our data suggest that both MK801 and memantine, in addition to inhibiting NMDA receptor, strongly inhibited NCX_{rev} whereas AP-5 inhibited NMDA receptor but failed to inhibit NCX_{rev} .

In electrophysiological whole-cell, voltage-clamp experiments, repetitive voltage ramp protocols produced ion currents mediated predominantly by the NCX_{rev} (Convery & Hancox, 1999; Watanabe & Kimura, 2000). These currents were strongly attenuated by 5 mM Ni^{2+} (Figure 46B,C) and by 10 μM KB-R7943, both are NCX_{rev} inhibitors (Iwamoto *et al.*, 1996; Kimura *et al.*, 1987). These currents were also inhibited by 10 μM MK801 and by 50 μM memantine, but not by 50 μM AP-5 (Figure 46D,E) consistent with calcium imaging experiments with NCX reversal induced by gramicidin (Figure 36C-F) and by $\text{Na}^+/\text{NMDG}^+$ replacement (Figure 44). Thus, electrophysiological data confirmed that MK801 and memantine inhibited NCX_{rev} , whereas AP-5 was practically without effect.

4. Tested NMDA receptor antagonists have no adverse effects on the forward mode of the $\text{Na}^+/\text{Ca}^{2+}$ exchanger

In this thesis, evidence has been presented that MK801 and memantine block the reverse mode of the $\text{Na}^+/\text{Ca}^{2+}$ exchanger. This attribute could be helpful in understanding and combating calcium dysregulation induced by excitotoxic glutamate. However, if these NMDA receptor antagonists are interacting with the NCX , the interaction could be detrimental if they inhibit not only the reverse mode of NCX (NCX_{rev}) but also the forward mode of the NCX

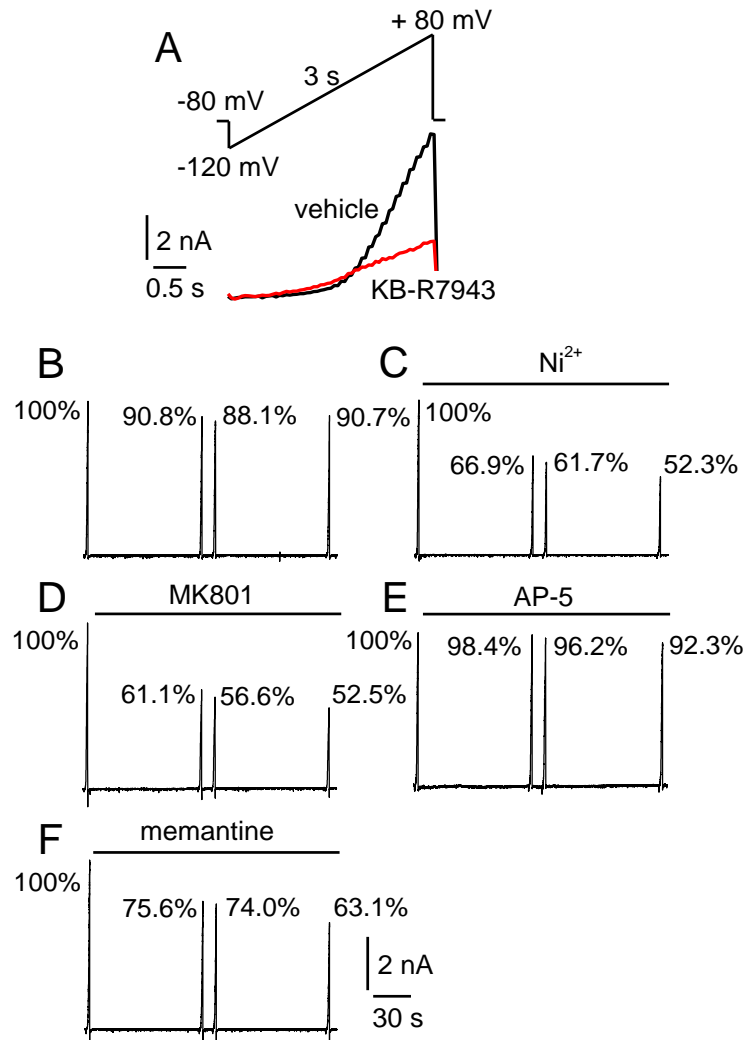


Figure 46. **The effects of Ni^{2+} , MK801, memantine, and AP-5 on NCX_{rev} -mediated ion currents recorded with cultured hippocampal neurons from rats.** In A, the ascending voltage ramp protocol employed in these experiments and associated current obtained with and without $10\mu\text{M}$ KB-R7943. In B-F, the effects of 5 mM Ni^{2+} (C), $10\mu\text{M}$ MK801 (D), $50\mu\text{M}$ AP-5 (E) and $50\mu\text{M}$ memantine (F) on NCX_{rev} -mediated ion currents. The effects of the inhibitors were calculated as percentage from the peak current without inhibitor taken as 100%. The time scale shown in panel F is applicable to all traces in B-E. (These experiments were preformed in collaboration with Patrick L. Sheets, Ph.D. and Theodore R. Cummins, Ph.D.)

(NCX_{fwd}). The forward mode of the NCX is necessary for normal maintenance of cytosolic calcium levels (DiPolo & Beauge, 2006; Carafoli *et al.*, 2001), and it is essential in reducing [Ca²⁺]_c following neuronal excitation (Kiedrowski *et al.*, 1994). To determine if the tested NMDA receptor antagonists inhibit the NCX_{fwd}, neurons were treated with a Ca²⁺ ionophore, ionomycin (5μM). This allows Ca²⁺ from the extracellular space to enter the neuron, resulting in an increase in [Ca²⁺]_c (Figure 47A). Conversely, if the NCX is shut off by removing Na⁺ from the bath solution, ionomycin induces an immediate increase in cytosolic calcium (Figure 47B). Testing the NMDA receptor antagonists under similar conditions, we observed no adverse effects concerning NMDA receptor antagonists inhibition of NCX_{fwd} (Figure 47C-E).

5. Combined inhibition of the reverse mode of the Na⁺/Ca²⁺ exchanger and the NMDA receptor completely prevented glutamate-induced delayed calcium dysregulation

In the following experiments, we evaluated the role of NCX_{rev} in glutamate-induced DCD. Despite numerous off-target effects, KB-R7943 remains one of the most efficacious and widely used NCX_{rev} inhibitors. Previously, we found that KB-R7943 inhibited NCX_{rev} in hippocampal neurons with IC₅₀=5.7±2.1μM (Brustovetsky *et al.*, 2011). In our experiments with glutamate-treated neurons, KB-R7943 (10μM) failed to prevent DCD (Figure 48A,B). KB-R7943 also inhibits NMDA receptor with IC₅₀=13.4±3.6μM (Figure 16) (Brustovetsky *et al.*, 2011), which is much higher than the IC₅₀ for MK801 (0.2±0.04μM) and memantine

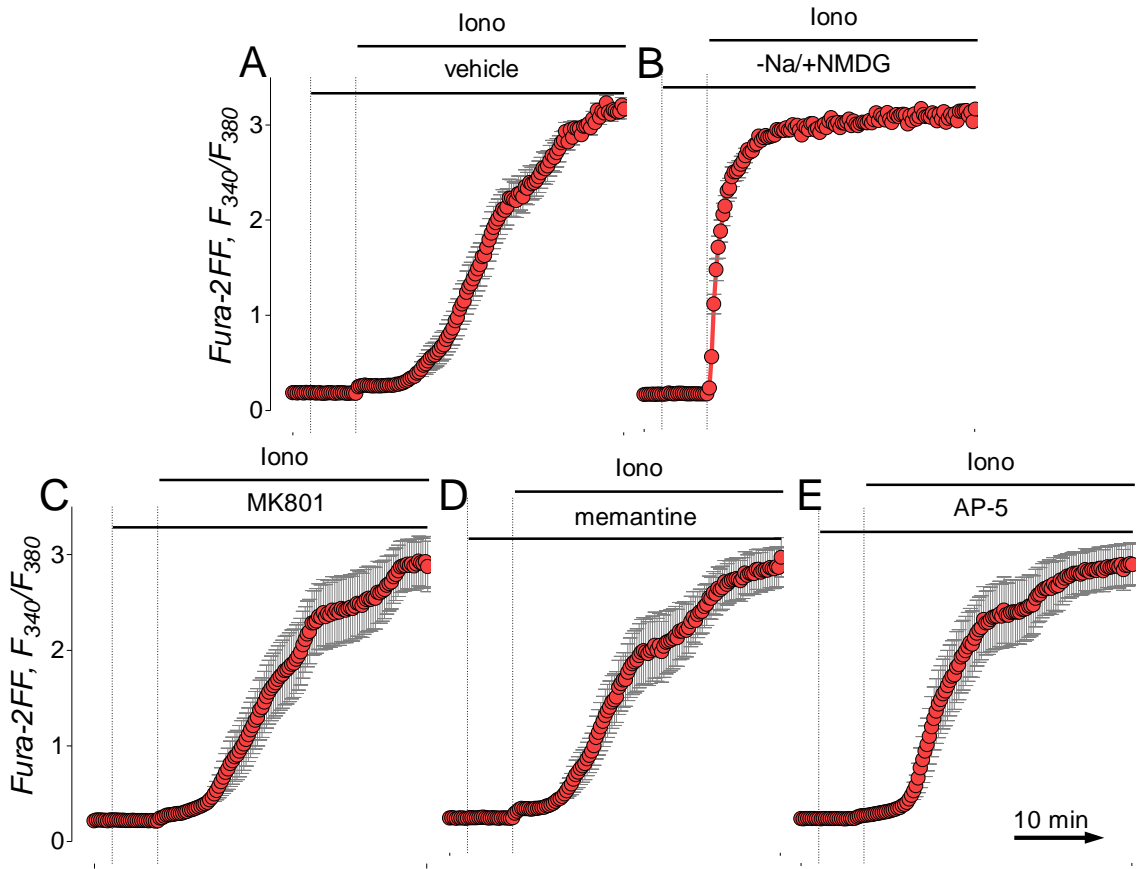


Figure 47. **Tested NMDA receptor antagonists did not inhibit the forward mode of the $\text{Na}^+/\text{Ca}^{2+}$ exchanger.** Neurons were loaded with the Ca^{2+} -sensitive dye Fura-2FF to monitor changes in cytosolic calcium concentrations. The neurons were exposure to $5\mu\text{M}$ ionomycin, a calcium ionophore, where indicated. The increase in calcium was compensated by both the $\text{Na}^+/\text{Ca}^{2+}$ exchanger (NCX) in the forward mode and mitochondrial calcium accumulation. In panel B, Na^+ was replaced with NMDG^+ preventing the NCX from functioning resulting in immediate calcium dysregulation upon ionomycin addition. This indicates the need for the forward mode of the NCX. $1\mu\text{M}$ MK801 (C), $50\mu\text{M}$ memantine (D), and $200\mu\text{M}$ AP-5 had not affect on calcium signal. Fura-2FF signal was expressed in F_{340}/F_{380} ratio after background subtraction.

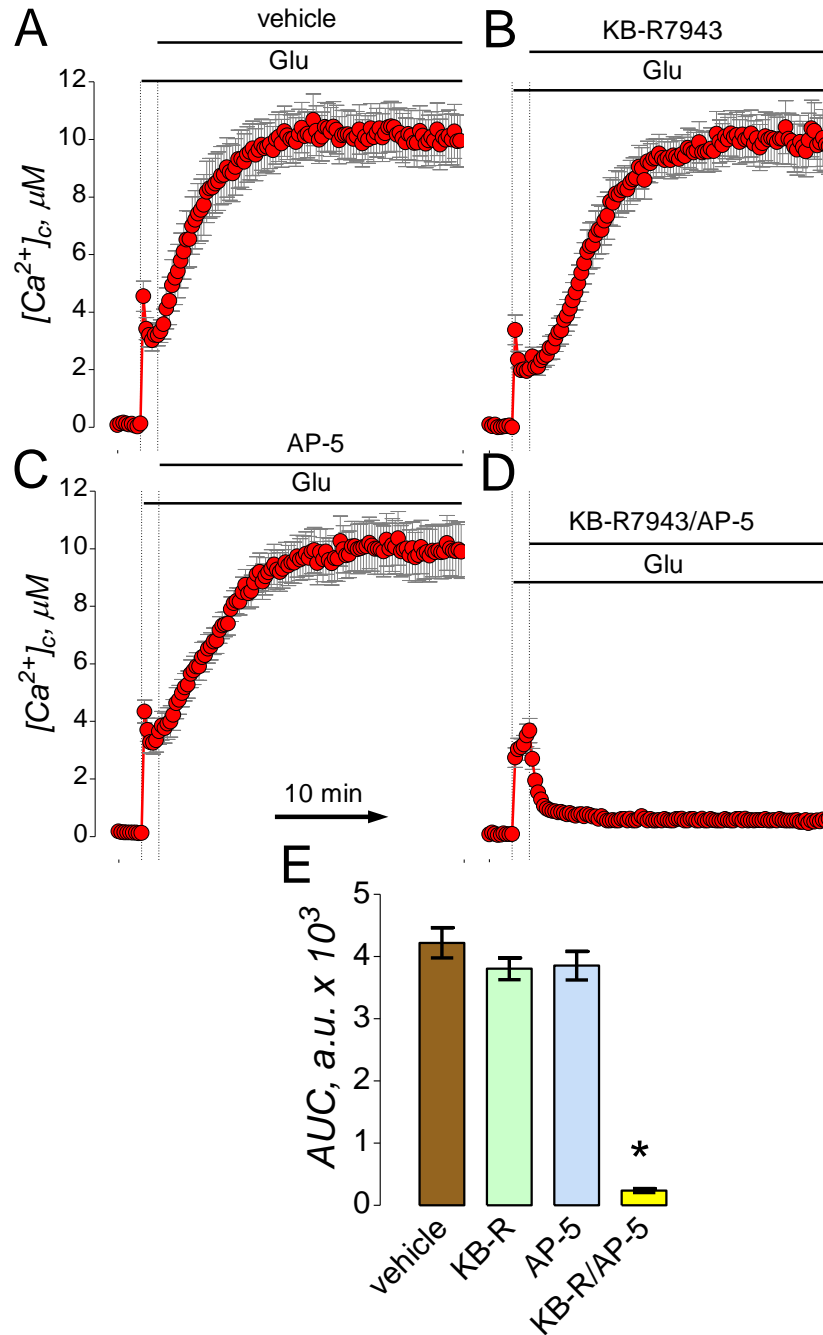


Figure 48. **Glutamate-induced sustained elevation in $[Ca^{2+}]_c$ is inhibited by a combination of KB-R7943 and AP-5 but not by individual inhibitors applied separately.** In A-D, cultured hippocampal neurons were exposed to 25μM glutamate (Glu, plus 10μM glycine). Where indicated, 10μM KB-R7943 or 200μM AP-5, or a combination of 10μM KB-R7943 and 20μM AP-5 were applied. The time scale shown in panel C is applicable to all traces in A, B, and D. In E, statistical analysis of glutamate-induced $[Ca^{2+}]_c$ changes over time in dependence on the presence of different inhibitors. Data are mean±SEM, * $p < 0.01$ compared to vehicle, n=3.

($3.6 \pm 0.05 \mu\text{M}$). Therefore, $10 \mu\text{M}$ KB-R7943 could not inhibit NMDA receptor completely. NMDA receptor inhibition with $200 \mu\text{M}$ AP-5 also failed to prevent DCD (Figure 48C). However, the combined application of $10 \mu\text{M}$ KB-R7943 and $20 \mu\text{M}$ AP-5 completely prevented DCD (Figure 48D). Thus, inhibition of only one of Ca^{2+} entry mechanisms, either NMDA receptor with AP-5 or NCX_{rev} with KB-R7943, was not sufficient to protect neurons against DCD.

Similar to AP-5, memantine at low concentrations fails to inhibit the reverse mode of the NCX, $\text{IC}_{50} = 17.7 \pm 0.1 \mu\text{M}$. Thus, we hypothesized that memantine at $10 \mu\text{M}$ should fail to prevent glutamate-induced calcium dysregulation, and that similar to AP-5, the KB-R7943 should restore that inhibition. In these experiments, we used $10 \mu\text{M}$ memantine, which is below the IC_{50} for NCX_{rev} but still completely inhibits the NMDA receptor. In Figure 49 memantine was applied 90 seconds after glutamate exposure, memantine failed to completely prevent glutamate-induced Ca^{2+} dysregulation (Figure 49A and B). However, similar to AP-5, the combination of $10 \mu\text{M}$ KB-R7943 and $10 \mu\text{M}$ memantine completely inhibited calcium dysregulation (Figure 49D).

KB-R7943 has off-target effects that might confound the results obtained with this drug (Brustovetsky *et al.*, 2011). Therefore, we looked for alternative approaches to turn off NCX_{rev} . To achieve this, we replaced Na^+ by NMDG^+ in the bath solution and released cytosolic Na^+ by applying $5 \mu\text{M}$ gramicidin thus completely eliminating the Na^+ gradient across the plasma membrane. This stopped NCX operation in both forward and reverse modes. Under these conditions glutamate produced instantaneous calcium dysregulation apparently

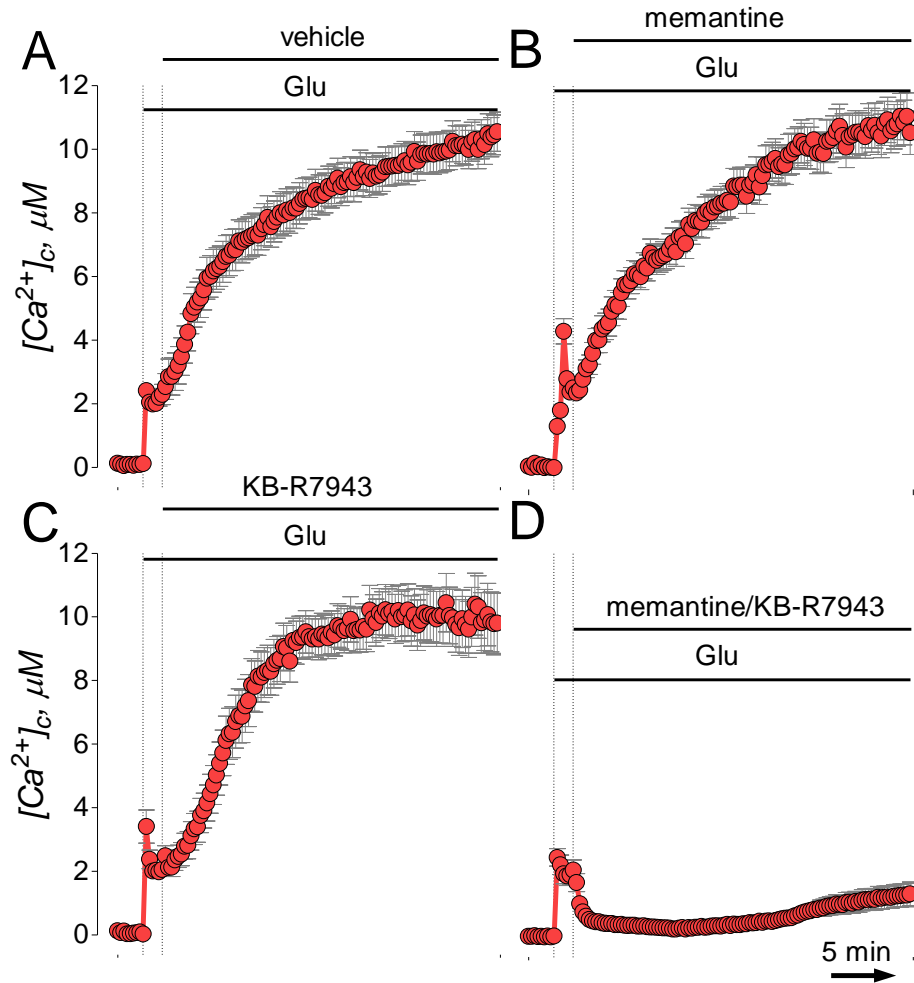


Figure 49. **Glutamate-induced sustained elevation in $[Ca^{2+}]_c$ is inhibited by a combination of KB-R7943 and memantine (10 μM) but not by individual inhibitors applied separately.** In A-D, cultured hippocampal neurons were exposed to 25 μM glutamate (Glu, plus 10 μM glycine). Where indicated, 10 μM KB-R7943 or 10 μM memantine, or a combination of 10 μM KB-R7943 and 10 μM memantine were applied. The time scale shown in panel D is applicable to all traces in A, B, and D. Data are mean \pm SEM. (note: Memantine at 10 μM inhibits the NMDA receptor but fails to inhibit the reverse mode of the Na^+/Ca^{2+} exchanger.)

due to a failure of NCX to extrude Ca^{2+} from the cytosol (Figure 50A). Importantly, now AP-5 (20 μM) readily inhibited glutamate-induced calcium dysregulation (Figure 50B). This observation confirms that both NMDA receptor and NCX_{rev} have to be inhibited to prevent glutamate-induced calcium dysregulation and supports our hypothesis that both NMDA receptor and NCX_{rev} contribute to DCD.

Our experiments with the Na^+ -sensitive fluorescent dye SBFI demonstrated that glutamate produced an increase in $[\text{Na}^+]_c$ (Figure 25). None of the tested NMDA receptor inhibitors prevented or attenuated this $[\text{Na}^+]_c$ increase suggesting an alternative route for Na^+ influx into cells. Recently, it has been shown that Na^+/H^+ exchanger (NHE) plays a central role in $[\text{Na}^+]_c$ increase in neurons following oxygen/glucose deprivation (Luo *et al.*, 2005). In our experiments, 5-(N-ethyl-N-isopropyl)amiloride (EIPA, 10 μM), an inhibitor of NHE (Vigne *et al.*, 1983), significantly attenuated glutamate-induced increase in $[\text{Na}^+]_c$ (Figure 51 A,B,D). The glutamate-induced changes in $[\text{Na}^+]_c$ over time were quantitatively assessed by calculating the AUC (Figure 50D) as it has been done previously for $[\text{Ca}^{2+}]_c$ changes (Chang *et al.*, 2006). In these experiments we used Na^+ -sensitive fluorescent dye Sodium GreenTM because EIPA interferes with SBFI measurements (Zhang & Melvin, 1996). Similar to experiments with SBFI (Figure 25B), MK801 failed to prevent or diminish glutamate-induced increase in $[\text{Na}^+]_c$ (Figure 51C).

Next, we tested whether EIPA (10 μM) inhibited NMDA receptor and NCX_{rev} and found that neither NMDA-induced nor gramicidin-induced increases

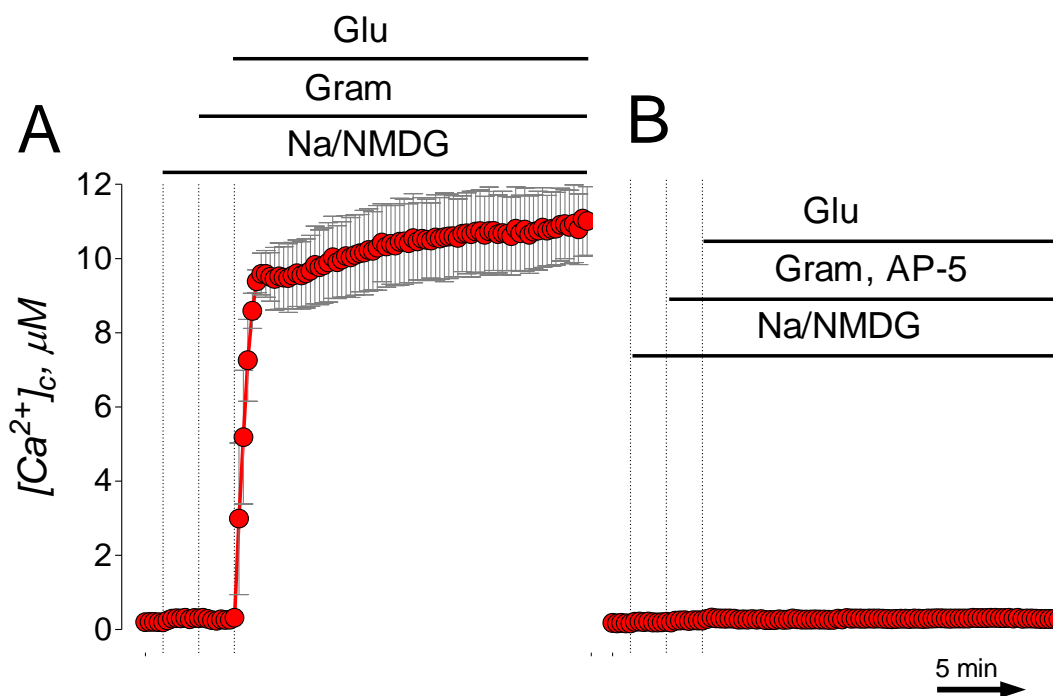


Figure 50. **Inhibition of forward and reverse Na^+/Ca^{2+} exchanger by eliminating Na^+ gradient across the plasma membrane permits complete inhibition of glutamate-induced calcium dysregulation by AP-5.** In A and B, where indicated, Na^+ in the bath solution was replaced by NMDG $^+$ (-Na/+NMDG). Then, neurons were treated with 5 μM gramicidin (Gram) to release cytosolic Na^+ . After that, neurons were exposed to 25 μM glutamate (Glu, plus 10 μM glycine) without (A) or with 20 μM AP-5 (B). In these experiments, bath solution was supplemented with 5 μM nifedipine and 1 mM ouabain. The time scale shown in panel B is applicable to the trace in A.

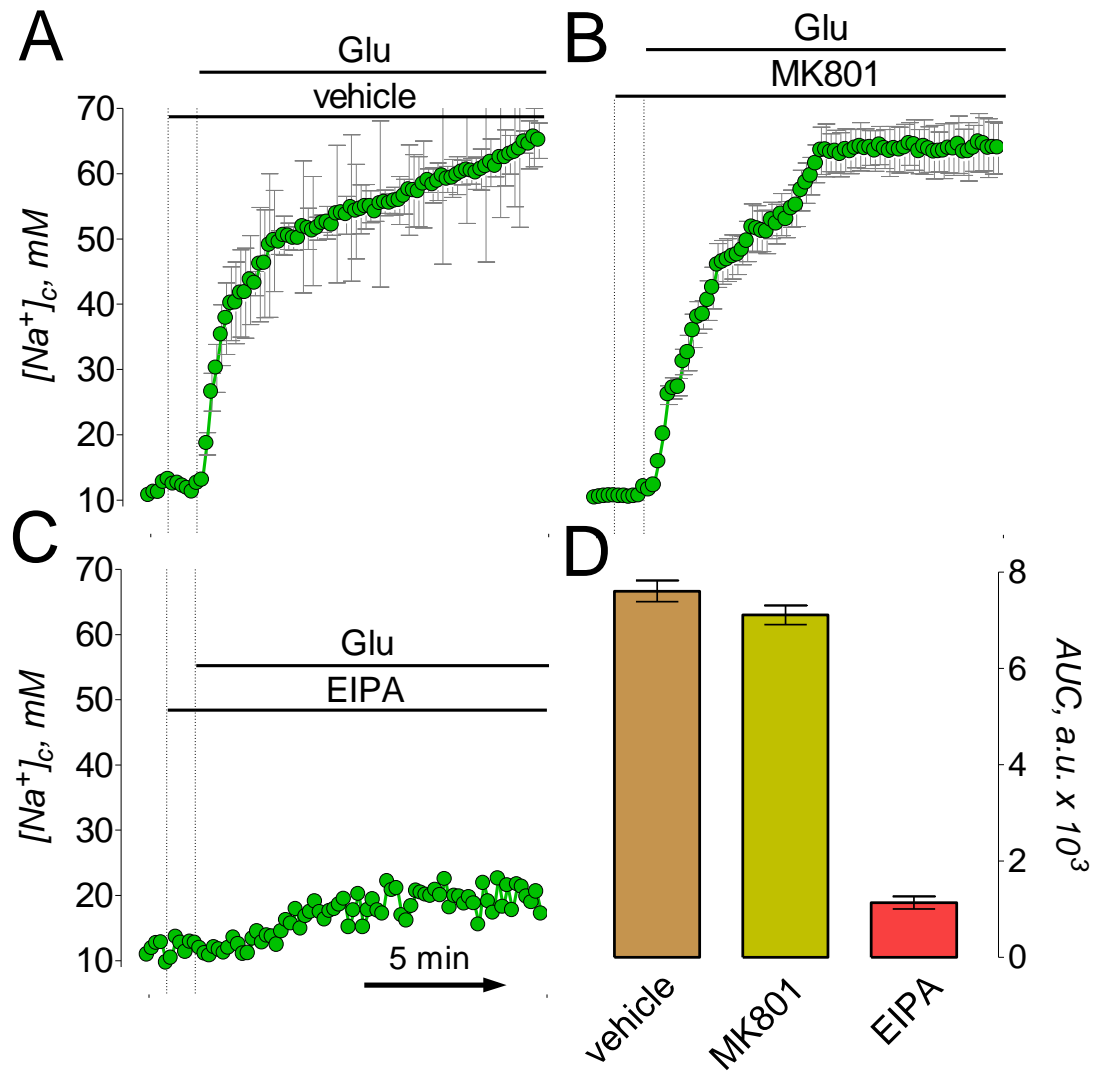


Figure 51. **EIPA but not MK801 inhibit the increase in $[Na^+]_c$ induced by glutamate.** In A-C, the changes in $[Na^+]_c$ were monitored by following Sodium GreenTM fluorescence F_{480} . Neurons were exposed to 25 μ M glutamate (Glu, plus 10 μ M glycine). Where indicated, neurons were treated with 10 μ M MK801 (B) or 10 μ M EIPA (C). The time scale shown in panel B is applicable to traces in A and C. In D, statistical analysis of glutamate-induced $[Na^+]_c$ changes over time in dependence on the presence of MK801 and EIPA. Data are mean \pm SEM, * p <0.01 compared to vehicle, n=3.

in $[Ca^{2+}]_c$ were affected by EIPA (Figure 52), suggesting that EIPA at the used concentration inhibited neither NMDA receptor nor NCX_{rev} . Because the reversal of NCX requires an increase in $[Na^+]_c$, we hypothesized that inhibiting $[Na^+]_c$ increase with EIPA should indirectly inhibit Ca^{2+} influx via NCX_{rev} and thus EIPA could substitute for KB-R7943 in the combination with AP-5 (Figure 48D). Indeed, whereas EIPA and AP-5 alone failed to prevent or attenuate glutamate-induced DCD (Figure 53A-C), their combination completely prevented DCD (Figure 53D). In these experiments, the EIPA was applied to neurons prior to glutamate to prevent $[Na^+]_c$ increase. Thus, using three different experimental approaches to shut-off NCX_{rev} we demonstrated that DCD in cultured hippocampal neurons exposed to glutamate depended on both NMDA receptor and NCX_{rev} , and that both mechanisms had to be inhibited to protect neurons against glutamate-induced delayed calcium dysregulation.

D. Does ifenprodil inhibit both the NMDA receptor and the reverse mode of the Na^+/Ca^{2+} exchanger?

The presented data suggest that both NMDA receptor and NCX_{rev} contribute to DCD in neurons exposed to glutamate and, consequently, both Ca^{2+} influx mechanisms have to be inhibited to prevent DCD (Brittain *et al.*, 2012). Ifenprodil inhibits DCD in young neurons exposed to glutamate (Stanika *et al.*, 2009). This effect was attributed to ifenprodil-mediated inhibition of NR2B-NMDA receptors. However, whether ifenprodil inhibits NCX_{rev} is unknown. In the

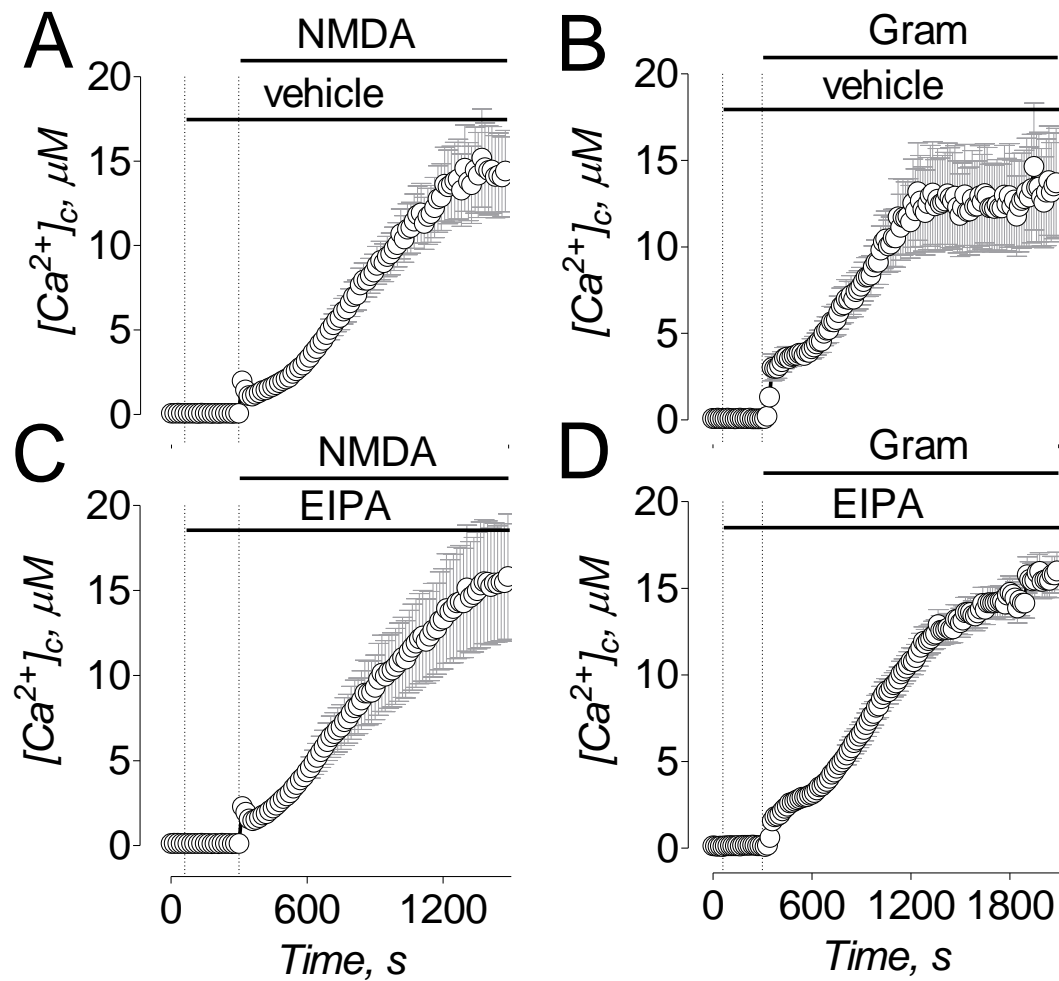


Figure 52. **EIPA did not affect NMDA- and gramicidin-induced increases in $[Ca^{2+}]_c$.** In A-D, measurements of $[Ca^{2+}]_c$ in hippocampal neurons loaded with a Ca^{2+} -sensitive fluorescent dye Fluo-4FF. The traces show mean \pm SEM. In A and C, where indicated 30 μM NMDA and 10 μM EIPA was added. In B and D, where indicated 5 μM gramicidin and 10 μM EIPA was added. In these experiments, the bath solution was supplemented with 5 μM nifedipine and 1 mM ouabain. The time scale shown in panel C is applicable to panel A; the time scale shown in panel D is applicable to panel B.

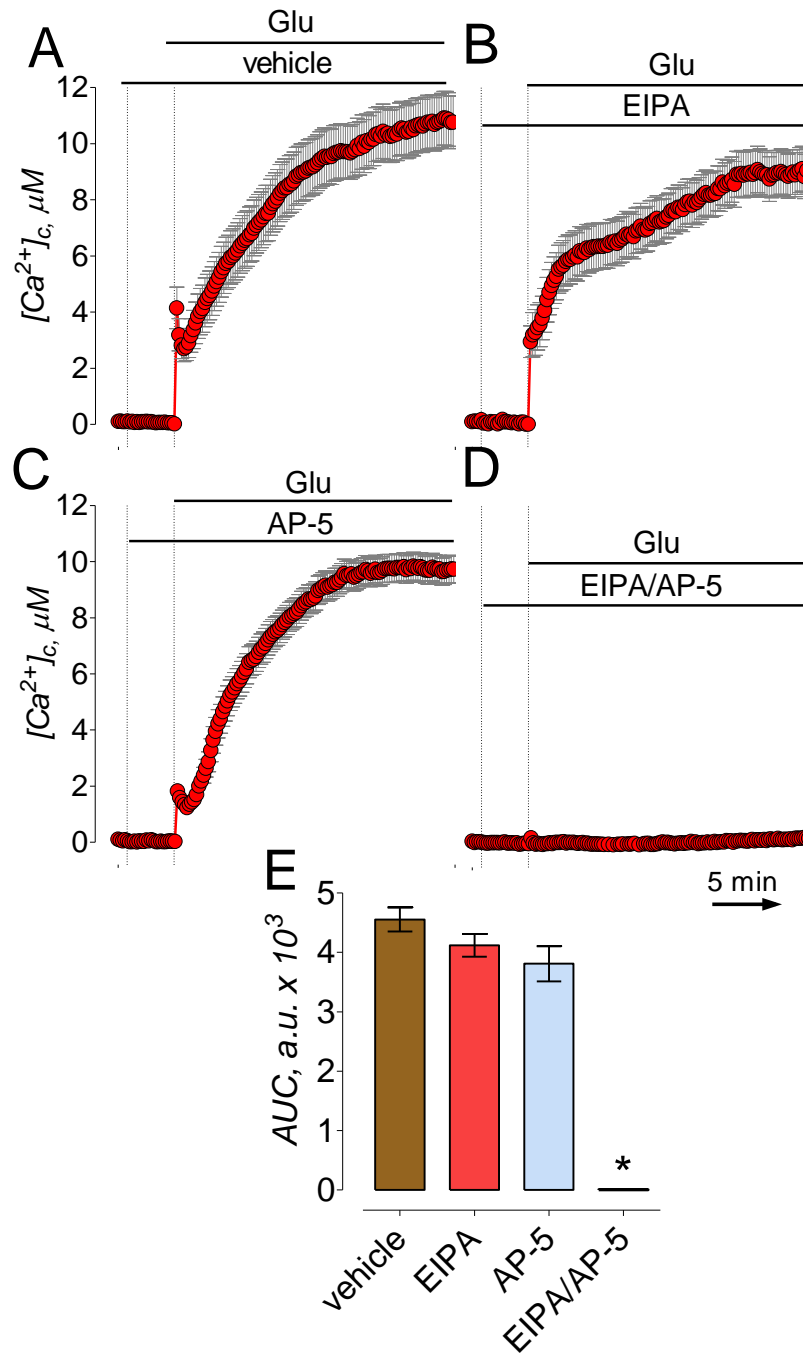


Figure 53. **Glutamate-induced sustained elevation in $[Ca^{2+}]_c$ is inhibited by a combination of EIPA and AP-5 but not by individual inhibitors applied separately.** In A-D, cultured hippocampal neurons were exposed to 25μM glutamate (Glu, plus 10μM glycine). Where indicated, 10μM EIPA (B) or 200μM AP-5 (C), or a combination of 10μM EIPA and 20μM AP-5 (D) were applied. The time scale shown in panel D is applicable to all traces in A-C. In E, statistical analysis of glutamate-induced $[Ca^{2+}]_c$ changes over time in dependence on the presence of different inhibitors. Data are mean±SEM, * $p < 0.01$ compared to vehicle, $n=3$.

present study, we hypothesized that ifenprodil, in addition to antagonizing NR2B-NMDA receptor, also inhibits NCX_{rev} .

1. Ifenprodil and PEAQX, selective NMDA receptor antagonists, differentially block calcium influx induced by NMDA

First, we determined the efficacy and potency of ifenprodil, an NR2B-selective NMDA receptor antagonist (Williams, 1993), and PEAQX, an NR2A-selective NMDA receptor antagonist (Auberson *et al.*, 2002), to inhibit NMDA-induced increase in $[Ca^{2+}]_c$ in “younger” and “older” neurons that differ in the expression of NR2A and NR2B subunits (Brewer *et al.*, 2007; Stanika *et al.*, 2009). In these experiments, we used two 30-second NMDA (30 μ M, plus 10 μ M glycine) pulses. The inhibitors or vehicle were applied 5 minutes before the second NMDA pulse and the amplitude of $[Ca^{2+}]_c$ increase was compared to $[Ca^{2+}]_c$ increase in response to the first NMDA pulse. In “younger” neurons (6-8 DIV), ifenprodil (1 μ M) completely inhibited the increase in $[Ca^{2+}]_c$ induced by NMDA (Figure 54A,B) with an $IC_{50}=0.11\pm 0.07\mu$ M (Figure 55A,B) whereas PEAQX failed to inhibit the NMDA-induced increase in $[Ca^{2+}]_c$ (Figure 54C,D and Figure 55C,D). In “older” neurons (13-16 DIV), ifenprodil (50 μ M) and PEAQX (5 μ M) applied separately only partly (45-55%) inhibited NMDA-induced increases in $[Ca^{2+}]_c$ (Figure 56A-C) with $IC_{50}=0.29\pm 0.14\mu$ M and $0.13\pm 0.04\mu$ M, respectively (Figure 57). However, if applied simultaneously, even at lower concentrations, ifenprodil (1 μ M) and PEAQX (0.1 μ M) inhibited NMDA-induced increases in $[Ca^{2+}]_c$ (Figure 56D). This inhibition of the NMDA effect correlated with the

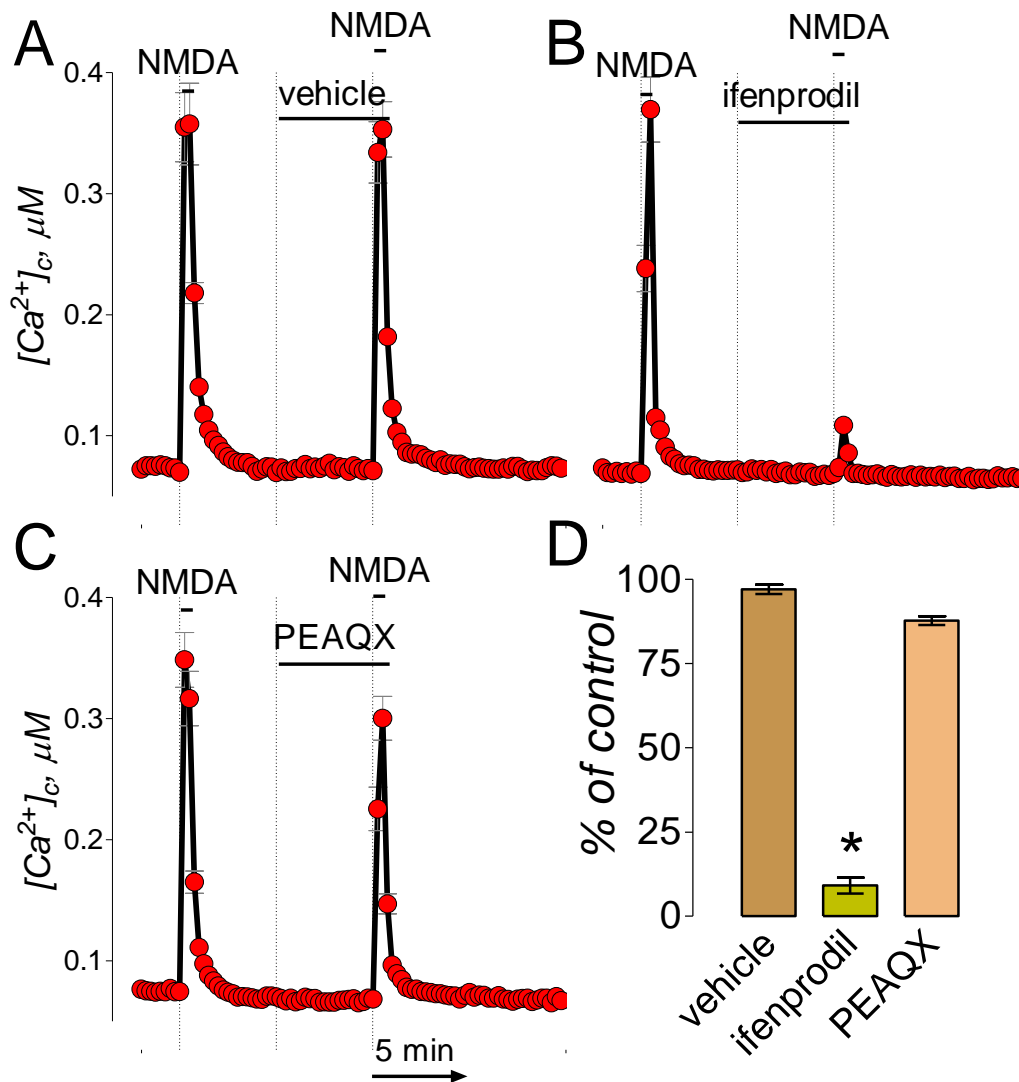


Figure 54. In “younger” neurons (6-8 DIV), ifenprodil completely inhibits Ca^{2+} influx induced by NMDA. The bath solution was supplemented with 1 μM tetrodotoxin and 5 μM nifedipine. Neurons were loaded with 2.6 μM Fura-2-AM. In A-C, where indicated, vehicle (0.2% DMSO), ifenprodil (1 μM) or PEAQX (5 μM) were applied. NMDA (30 μM , plus 10 μM glycine) was applied twice for 30 seconds as indicated. The Ca^{2+} influx into neurons was evaluated by measuring amplitude of the increases in $[Ca^{2+}]_c$. $[Ca^{2+}]_c$ was calculated using the Grynkiewicz method (Grynkiewicz *et al.*, 1985). The time scale shown in panel C is applicable to traces in A and B. In D, statistical analysis of the Ca^{2+} influx inhibition. Data are mean \pm SEM, * $p < 0.01$ compared to vehicle, $n = 3$.

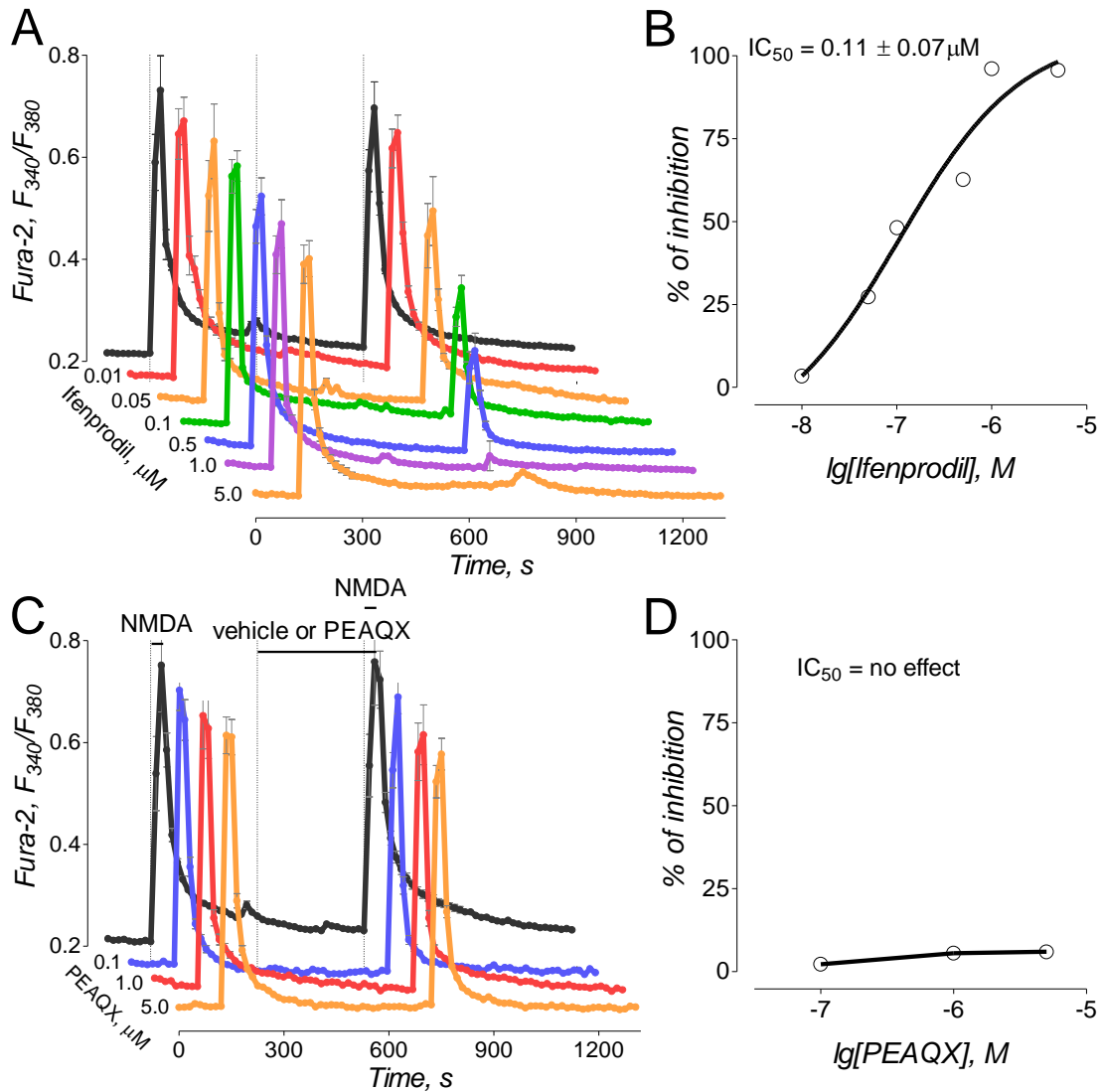


Figure 55. In younger neurons, ifenprodil completely inhibits NMDA-induced increase in cytosolic Ca^{2+} whereas PEAQX was without effect. Neurons were loaded with $2.6 \mu M$ Fura-2-AM. Traces are averages \pm SEM from individual experiments ($n=18-25$ neurons per experiment) performed in triplicate. The bath solution was supplemented with $1 \mu M$ tetrodotoxin and $5 \mu M$ nifedipine. Where indicated, vehicle (0.2% DMSO, black trace) or various concentrations of ifenprodil ($0.01-5 \mu M$) or PEAQX ($0.1-5 \mu M$) were applied. NMDA ($30 \mu M$, plus $10 \mu M$ glycine) was applied twice for 30 seconds as indicated. The activity of NMDA receptors was evaluated by measuring amplitude of the increases in Fura-2 F_{340}/F_{380} ratio triggered by the second application of NMDA. The dose-dependence graph was plotted, and IC_{50} was calculated using GraphPad Prism[®] 4.0 (GraphPad Software Inc., San Diego, CA).

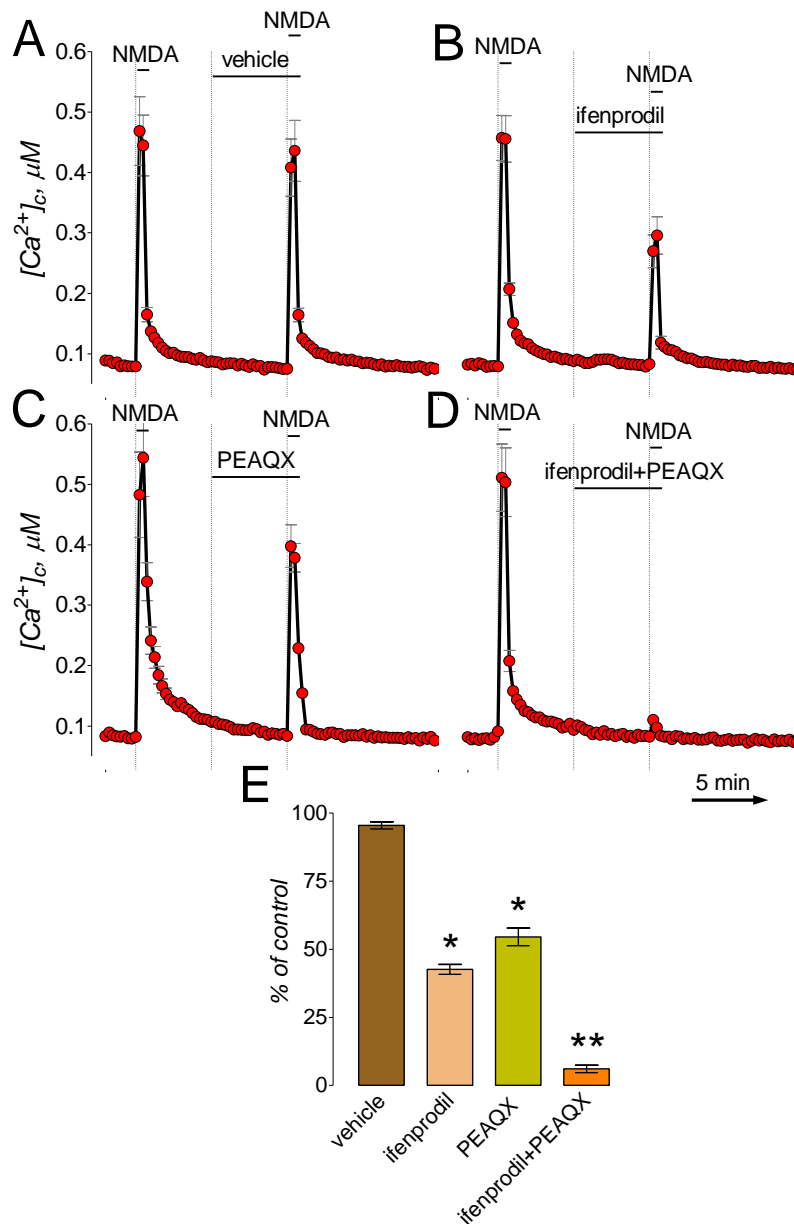


Figure 56. In “older” neurons (13-16 DIV), ifenprodil and PEAQX partially inhibits Ca^{2+} influx induced by NMDA. Combined application of ifenprodil and PEAQX completely block the $[Ca^{2+}]_c$ increase. The bath solution was supplemented with 1 μM tetrodotoxin and 5 μM nifedipine. Neurons were loaded with 2.6 μM Fura-2-AM. Where indicated, (A.) vehicle (0.2% DMSO), ifenprodil (50 μM), PEAQX (5 μM), or the combination of both ifenprodil (1 μM) and PEAQX (0.1 μM). NMDA (30 μM , plus 10 μM glycine) was applied twice for 30 seconds as indicated. The Ca^{2+} influx into neurons was evaluated by measuring amplitude of the increases in $[Ca^{2+}]_c$. $[Ca^{2+}]_c$ was calculated using the Grynkiewicz method (Grynkiewicz *et al.*, 1985). The time scale shown in panel D is applicable to traces in A-C. In E, statistical analysis of the Ca^{2+} influx inhibition. Data are mean \pm SEM, * $p < 0.05$, ** $p < 0.01$ compared to vehicle, $n = 3$.

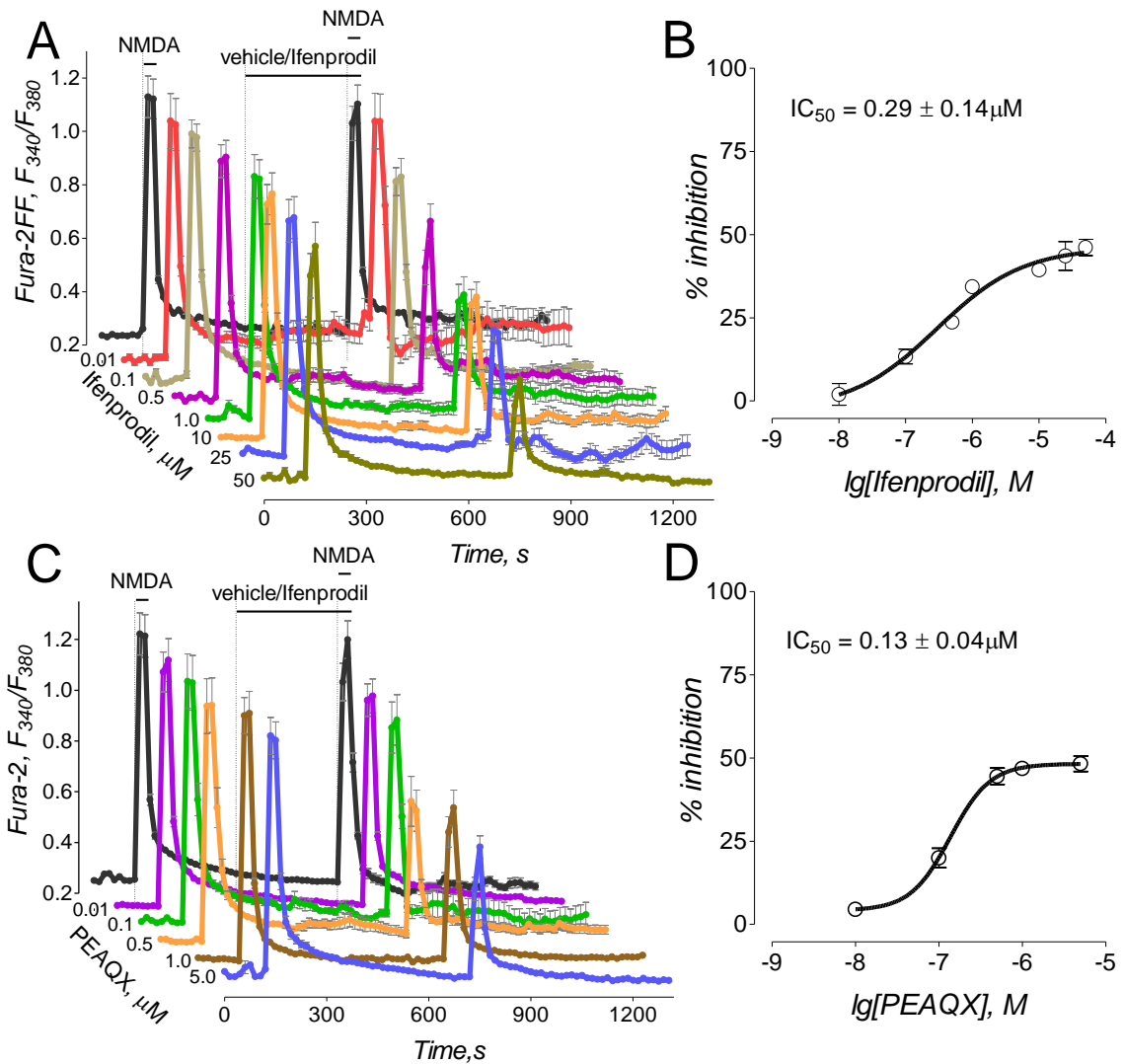


Figure 57. In older neurons, ifenprodil and PEAQX partially inhibit NMDA-induced increase in cytosolic Ca^{2+} . Neurons were loaded with $2.6 \mu\text{M}$ Fura-2-AM. Traces are averages \pm SEM from individual experiments ($n=18-25$ neurons per experiment) performed in triplicate. The bath solution was supplemented with $1 \mu\text{M}$ tetrodotoxin and $5 \mu\text{M}$ nifedipine. Where indicated, vehicle (0.2% DMSO, black trace) or various concentrations of ifenprodil ($0.01-50 \mu\text{M}$) or PEAQX ($0.01-5 \mu\text{M}$) were applied. NMDA ($30 \mu\text{M}$, plus $10 \mu\text{M}$ glycine) was applied twice for 30 seconds as indicated. The activity of NMDA receptors was evaluated by measuring amplitude of the increases in Fura-2 F_{340}/F_{380} ratio triggered by the second application of NMDA. The dose-dependence graph was plotted, and IC_{50} was calculated using GraphPad Prism[®] 4.0 (GraphPad Software Inc., San Diego, CA).

expression of NR2A and NR2B subunits in “younger” and “older” neurons used in our experiments (Figure 58). Consistent with previously reported results (Stanika *et al.*, 2009), expression of NR2B in younger “neurons” was much higher compared to NR2A (Figure 58). In addition, in “younger” neurons, expression of NR2A was much lower compared to “older” neurons (Figure 58), consistent with earlier published data (Brewer *et al.*, 2007). This may explain why ifenprodil alone was effective in inhibiting the NMDA effect in “younger” neurons (Figure 54A, B) and why both inhibitors, ifenprodil and PEAQX, were necessary to inhibit the NMDA effect in “older” neurons (Figure 56D).

2. Ifenprodil and PEAQX, selective NMDA receptor antagonists, differentially block calcium influx induced by glutamate

The NMDA receptor is one of the major Ca^{2+} influx pathways contributing to DCD in neurons exposed to glutamate (Tymianski *et al.*, 1993b). Consistent with the high efficacy in inhibiting NMDA receptors in “younger” neurons, ifenprodil (1 μM), added 90 seconds after glutamate, completely prevented DCD (Figure 59A, B). PEAQX (5 μM), on the other hand, was ineffective (Figure 59C,D). In “older” neurons, both ifenprodil (50 μM) and PEAQX (5 μM) applied separately slightly slowed down the increases in $[\text{Ca}^{2+}]_c$ (Figure 60A-C). However, applied together, even at 50-fold lower concentrations, ifenprodil (1 μM) and PEAQX (0.1 μM) completely prevented DCD (Figure 60D). These results suggest that inhibition of both NR2A- and NR2B- containing NMDA receptors is necessary and sufficient to prevent glutamate-induced DCD.

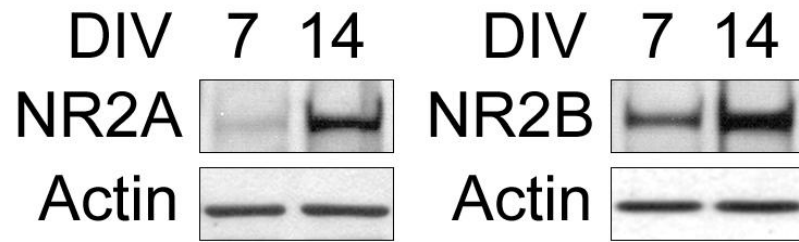


Figure 58. **NR2A and NR2B expression in cultured hippocampal neurons at 7 and 14 DIV.** Neurons from postnatal day 1 rat pups were grown in culture for 7 or 14 days. Actin was used as a loading control.

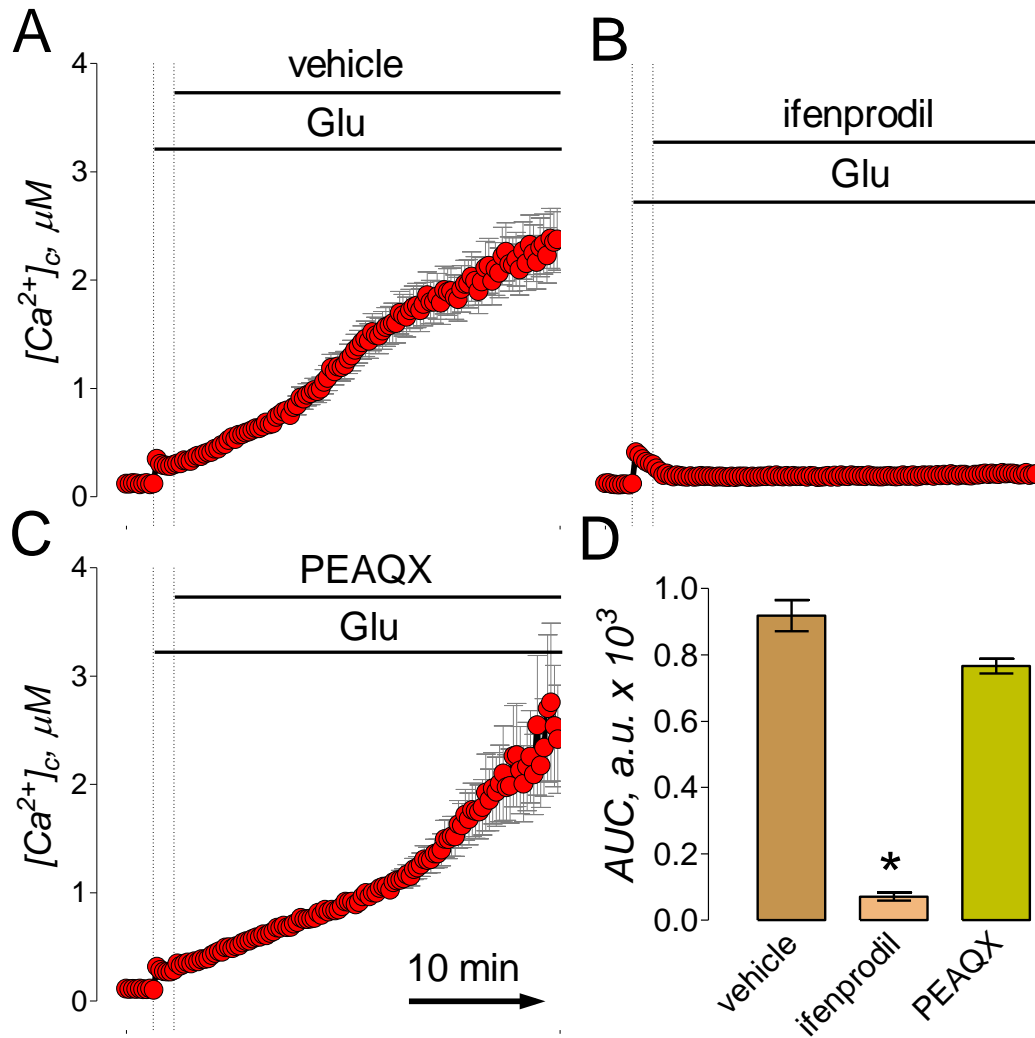


Figure 59. In “younger” neurons (6-8 DIV), ifenprodil but not PEAQX inhibit glutamate-induced sustained elevation in $[Ca^{2+}]_c$. Neurons were loaded with 2.6 μM Fura-2FF-AM. In A-C, neurons were exposed to 100 μM glutamate (Glu, plus 10 μM glycine). Where indicated, 1 μM ifenprodil or 5 μM PEAQX were applied. The time scale shown in panel C is applicable to traces in A and B. In D, statistical analysis of glutamate-induced $[Ca^{2+}]_c$ changes over time. Here and in other figures, glutamate-induced changes in $[Ca^{2+}]_c$ over time were analyzed by using the area under the curve (AUC) as it has been done previously (Chang *et al.*, 2006). Data are mean \pm SEM, * $p < 0.01$ compared to vehicle, $n = 3$.

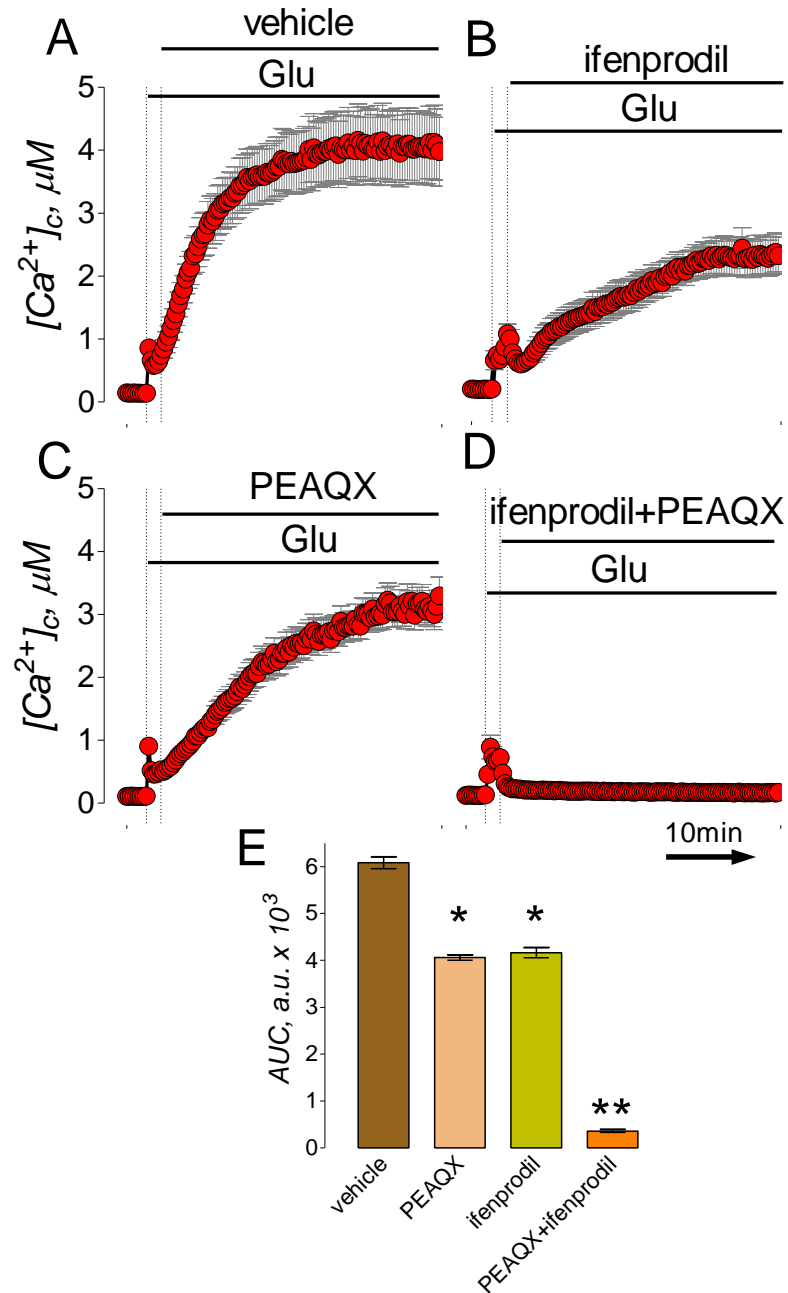


Figure 60. In “older” neurons (13-16 DIV), the combination of ifenprodil and PEAQX but not individual inhibitors applied separately completely prevent glutamate-induced sustained elevation in $[Ca^{2+}]_c$. Neurons were loaded with 2.6 μM Fura-2FF-AM. In A-D, neurons were exposed to 25 μM glutamate (Glu, plus 10 μM glycine). Where indicated, vehicle (0.2% DMSO), 50 μM ifenprodil or 5 μM PEAQX, or a combination of 1 μM ifenprodil and 0.1 μM PEAQX were applied. The time scale shown in panel D is applicable to traces in A-C. In E, statistical analysis of glutamate-induced $[Ca^{2+}]_c$ changes over time. Data are mean \pm SEM, * $p < 0.05$, ** $p < 0.01$ compared to vehicle, $n=3$.

3. Ifenprodil, an NR2B-containing NMDA receptor antagonist, inhibits the reverse mode of the Na⁺/Ca²⁺ exchanger

Previously in this thesis, data were presented showing both NMDA receptor and NCX_{rev} significantly contributed to DCD in hippocampal neurons exposed to glutamate and that inhibition of only NMDA receptor or NCX_{rev} was not sufficient to prevent DCD (Brittain *et al.*, 2012). This apparently contradicts our conclusion based on the results obtained with ifenprodil and PEAQX (see above). To resolve this contradiction, we performed experiments aimed at clarification of the mechanisms of ifenprodil and PEAQX effects. First, we confirmed that inhibition of NMDA receptor alone is not sufficient to prevent DCD. Indeed, AP-5 (20μM), a potent NMDA receptor antagonist, completely inhibited NMDA-induced increase in [Ca²⁺]_c (Figure 61A,B) but failed to inhibit NCX_{rev} (Figure 61C-F) and prevent glutamate-induced DCD in neurons (Figure 61G,H). In these experiments, NCX reversal was induced either by gramicidin (Newell *et al.*, 2007), an ionophore for monovalent cations (Myers & Haydon, 1972), or by reversing Na⁺ gradient across the plasma membrane by substituting external Na⁺ for equimolar N-methyl-D-glucamine (NMDG⁺) (Wu *et al.*, 2008). AP-5 failure to prevent glutamate-induced DCD suggests that NMDA receptor inhibition is not enough to prevent DCD. Furthermore, this suggests that the failure to prevent DCD could be due to a failure to inhibit NCX_{rev}. Consequently, the next question was whether ifenprodil and/or PEAQX inhibit NCX_{rev}.

To investigate the effect of ifenprodil and PEAQX on NCX_{rev}, we induced NCX reversal using either gramicidin application (Newell *et al.*, 2007) or

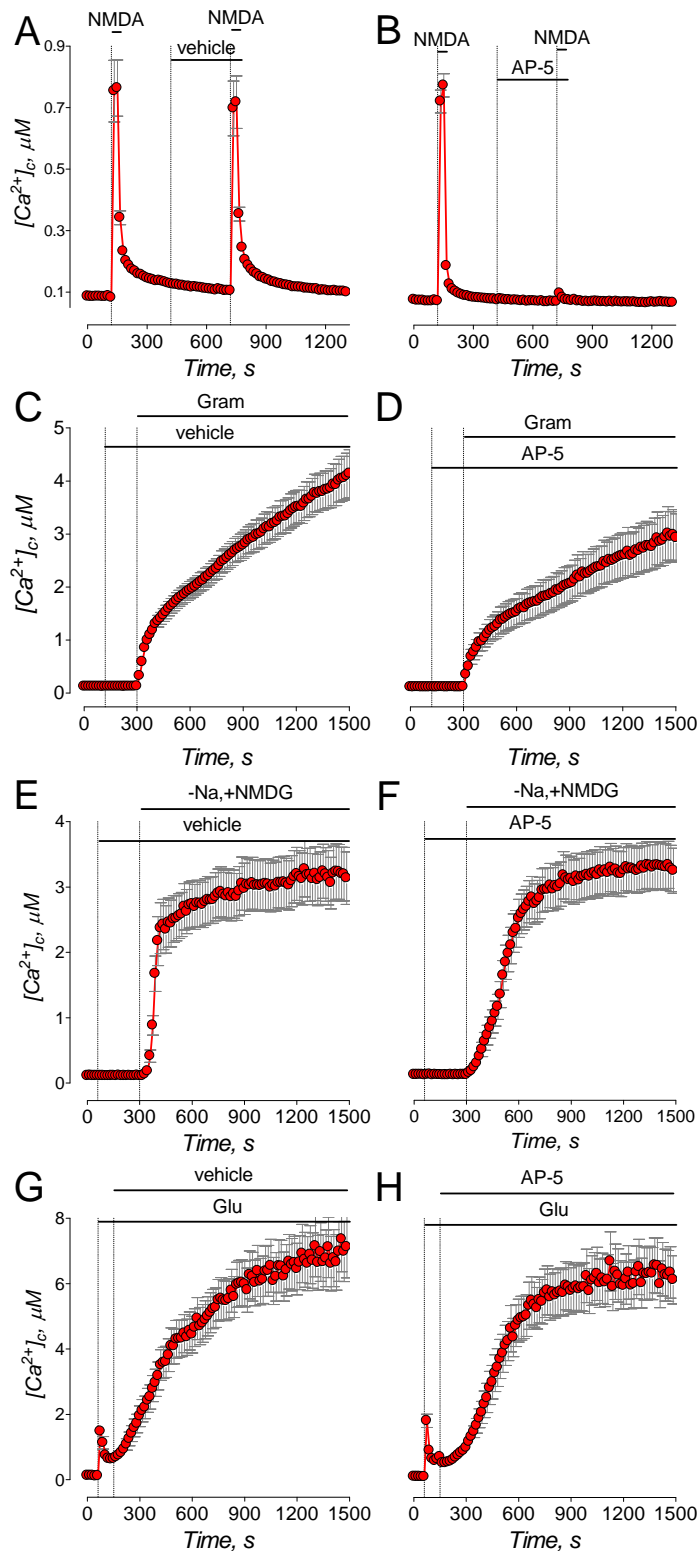


Figure 61. AP-5 inhibits NMDA-induced $[Ca^{2+}]_c$ increase (A,B) but fails to inhibit $[Ca^{2+}]_c$ increases mediated by the reverse Na^+/Ca^{2+} exchanger (C-F) or prevent glutamate-induced Ca^{2+} dysregulation (G,H). Neurons were loaded with $2.6\mu M$ Fura-2FF-AM. In A and B, where indicated, neurons were treated with NMDA ($30\mu M$, plus $10\mu M$ glycine), AP-5 ($20\mu M$), or vehicle (0.2% DMSO). In C and D, where indicated, neurons were treated with gramicidin (Gram, $5\mu M$), AP-5 ($200\mu M$) or vehicle (0.2% DMSO). In E and F, where indicated, NaCl in the bath solution was replaced by equimolar NMDG and neurons were treated with AP-5 ($200\mu M$). In C-F, bath solution was supplemented with $1\mu M$ tetrodotoxin, $5\mu M$ nifedipine, and 1 mM ouabain. In G and H, where indicated, neurons were treated with glutamate (Glu, $25\mu M$, plus $10\mu M$ glycine), AP-5 ($200\mu M$), or vehicle (0.2% DMSO).

Na⁺/NMDG⁺ replacement (Wu *et al.*, 2008). Previously, we showed that gramicidin depolarized plasma membrane, induced the release of endogenous glutamate in the low micromolar range, and increased both cytosolic Na⁺ concentration ([Na⁺]_c) and [Ca²⁺]_c (Brittain *et al.*, 2012). The Na⁺/NMDG⁺ replacement also led to a minuscule release of endogenous glutamate (1.8±0.3μM, n=6, versus 0.18±0.07μM before Na⁺/NMDG⁺ replacement, n=11, *p*<0.001). In addition, Na⁺/NMDG⁺ replacement decreased [Na⁺]_c, and increased [Ca²⁺]_c (Figure 42). The increase in [Ca²⁺]_c induced by Na⁺/NMDG⁺ replacement depended on elevation of [Na⁺]_c induced by pre-incubation with ouabain (1 mM) consistent with the reported earlier requirement for ouabain pre-treatment to reverse NCX by Na⁺/NMDG⁺ replacement (Wu *et al.*, 2008). Without ouabain, Na⁺/NMDG⁺ replacement did not produce an increase in [Ca²⁺]_c (Figure 42).

Next, we tested whether ifenprodil and PEAQX inhibit NCX_{rev}. In contrast to AP-5, ifenprodil prevented both gramicidin- and Na⁺/NMDG⁺- induced increases in [Ca²⁺]_c (Figure 62A,B and E,F) suggesting that in addition to NR2B-NMDA receptor inhibition, ifenprodil also inhibited NCX_{rev}. PEAQX, similar to AP-5, was ineffective in preventing gramicidin- and Na⁺/NMDG⁺-induced increases in [Ca²⁺]_c (Figure 62C,G).

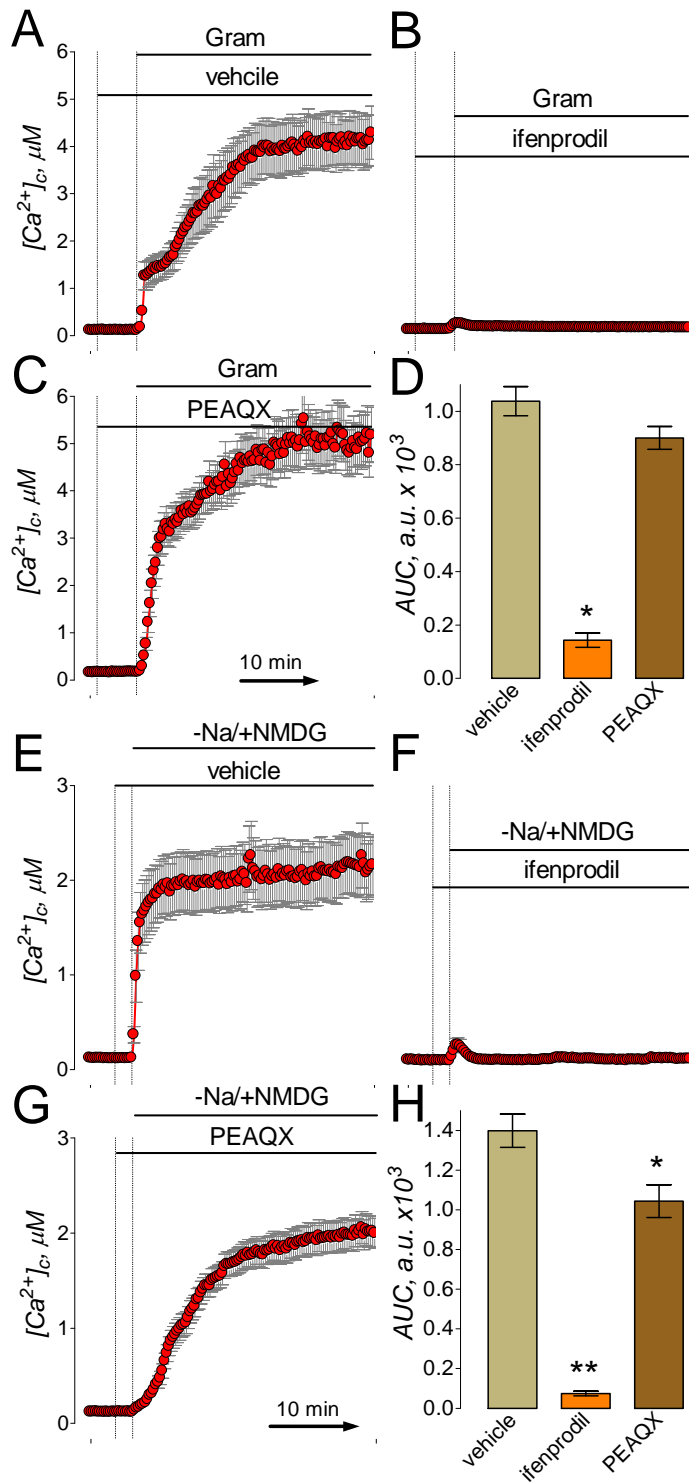


Figure 62. **Ifenprodil but not PEAQX inhibit the increases in $[Ca^{2+}]_i$ mediated by reversal of Na^+/Ca^{2+} exchanger triggered by gramicidin or by $Na^+/NMDG$ replacement.** Neurons were loaded with 2.6 μ M Fura-2FF-AM. In A-C, where indicated, neurons were treated with 5 μ M gramicidin (Gram), 1 μ M ifenprodil, or 5 μ M PEAQX. In E-G, where indicated, NaCl in the bath solution was substituted for equimolar NMDG⁺ and neurons were treated with 1 μ M ifenprodil, or 5 μ M PEAQX. In all experiments, the bath solution was supplemented with 1 μ M tetrodotoxin, 5 μ M nifedipine, and 1 mM ouabain. The time scale shown in panel C is applicable to traces in A and B. The time scale shown in panel G is applicable to traces in E and F. In D, statistical analysis of gramicidin-induced $[Ca^{2+}]_i$ changes over time. Data are mean \pm SEM, * p <0.01 compared to vehicle, n=3. In H, statistical analysis of $Na^+/NMDG^+$ -induced $[Ca^{2+}]_i$ changes over time. Data are mean \pm SEM, * p <0.05, ** p <0.01 compared to vehicle, n=3.

IV. DISCUSSION

The delayed calcium dysregulation is a critical event in glutamate excitotoxicity and it is causally linked to neuronal death induced by glutamate (Manev *et al.*, 1989; Tymianski *et al.*, 1993b; Tymianski *et al.*, 1993c). Several studies have shown a link between the sustained increase in cytosolic calcium and neuronal death, for this reason the focus of this thesis is on the mechanism of calcium dysregulation rather than neuronal death.

This sustained elevation in $[Ca^{2+}]_c$ represents a serious toxicity for neurons due to possible activation of various degradation enzymes such as Ca^{2+} -dependent proteases (e.g. calpains) (Bano *et al.*, 2005; Brustovetsky *et al.*, 2010) and phospholipases (Farooqui *et al.*, 2006). Accordingly, prevention or attenuation of delayed calcium dysregulation is considered a promising strategy to alleviate the consequences of prolonged glutamate exposure (Tymianski *et al.*, 1993a; Tymianski *et al.*, 1994). Understanding of the mechanisms contributing to this calcium dysregulation, therefore is of paramount importance.

A. Inhibition of the reverse mode of the Na^+/Ca^{2+} exchanger alone fails to prevent glutamate-induced delayed calcium dysregulation

It has been proposed that the reversal of NCX could significantly contribute to Ca^{2+} influx into neurons and thus promote calcium dysregulation under conditions of prolonged glutamate exposure and/or oxygen/glucose deprivation (Kiedrowski *et al.*, 1994; Hoyt *et al.*, 1998). Therefore, inhibitors of NCX_{rev} attract great attention as research tools as well as potentially valuable

therapeutic agents. Despite new additions to the panel of NCX_{rev} inhibitors (SEA0400, YM-244769, SN-6) (Matsuda *et al.*, 2001; Iwamoto & Kita, 2006; Watanabe *et al.*, 2006), KB-R7943 remains the most popular pharmacological agent used to attenuate NCX_{rev} activity in different experimental settings (Namekata *et al.*, 2006; Kiedrowski, 2007; Chen *et al.*, 2007; Dietz *et al.*, 2007; Araujo *et al.*, 2007; Wu *et al.*, 2008). Similar to many other pharmacological agents, KB-R7943 has some confounding off-target effects that might affect the interpretation of experimental results and KB-R7943 applicability. For example, in addition to inhibiting NCX_{rev}, KB-R7943 was reported to inhibit L-type of voltage gated Ca²⁺ channels (Ouardouz *et al.*, 2005), TRP channels (Kraft, 2007), NMDA receptors (Sobolevsky & Khodorov, 1999), and mitochondrial Ca²⁺ uptake (Santo-Domingo *et al.*, 2007). In this thesis, we present the first evidence that KB-R7943 inhibits mitochondrial Complex I and that this inhibition might influence neuronal response to excitotoxic glutamate. In addition, using electrophysiological patch-clamp technique and calcium imaging, we unequivocally demonstrated that KB-R7943 attenuated NMDA-induced increases in [Ca²⁺]_c and blocked ion current via the NMDA receptor. Our observations indicate that KB-R7943 indeed inhibits the NMDA receptor, and thus, our data support conclusions made in an earlier electrophysiological study (Sobolevsky & Khodorov, 1999). With all of these important off-target effects that could affect calcium dysregulation, it is hard to interpret the exact mechanism of action of KB-R7943. Thus, determinations made using this drug are in question.

1. Glutamate exposure results in “uncoupling” of the respiratory chain and oxidative phosphorylation

In the cell, up to 80% of NAD(P)H is located in mitochondria (Duchen & Biscoe, 1992). The increase in NAD(P)H concentration takes place when NAD(P)H oxidation is slowed by suppressing the electron flow through the respiratory chain. FCCP depolarizes mitochondria, accelerating electron flow in the respiratory chain and leading to NAD(P)H oxidation. NAD(P)⁺ does not fluoresce (Chance & Williams, 1956); we therefore observe a decrease in fluorescence following addition of FCCP. On the other hand, KCN, an inhibitor of cytochrome oxidase (Complex IV), stops electron flow in the entire respiratory chain, leading to recovery of NAD(P)H signal through the citric acid cycle.

Glutamate could stimulate NAD(P)H oxidation by different mechanisms. Glutamate causes massive Na⁺ influx into neurons, increasing Na⁺/K⁺-ATPase activity and ADP production. In turn, augmented ADP production stimulates oxidative phosphorylation. Oligomycin inhibits ATP synthase, so NAD(P)H increase induced by oligomycin reflects oxidation coupled with ATP synthesis.

Alternatively, massive influx of Ca²⁺ induced by glutamate could cause uncoupling of oxidative phosphorylation due to activation of the permeability transition pore (Bernardi *et al.*, 2006) or Ca²⁺ cycling across the inner mitochondrial membrane (Carafoli, 1979). The failure of oligomycin to recover NAD(P)H following glutamate application in the Ca²⁺-containing bath solution supports this scenario. In contrast, robust oligomycin-induced recovery of NAD(P)H in Ca²⁺-free bath solution indicates tight coupling of oxidative

phosphorylation and suggests a key role of Ca^{2+} in the uncoupling of oxidative phosphorylation in neurons exposed to glutamate.

This series of experiment is important in that it gives us insight into the bioenergetics consequences resulting from this influx of calcium. The mitochondria become damaged due to calcium dysregulation resulting in their failure to maintain a high membrane potential and thus most likely not able to produce ATP. The loss of ATP produce would also contribute to the overall neuronal death that occurs due excitotoxic events.

Also worth noting, the concentration found during experiments where neuronal cultures are deprived of oxygen and glucose, extracellular glutamate rises from $0.1\mu\text{M}$ to between 1.5 and $2.5\mu\text{M}$ within 60 minutes (Goldberg & Choi, 1993). Glutamate levels have also been measured in the cerebral spinal fluid of patients following a stroke and measure between 2 and $8\mu\text{M}$ (Benveniste *et al.*, 1984; Castillo *et al.*, 1999; Lancelot *et al.*, 1997). This is consistent with what is shown in Figure 39. Similar to the condition in this figure, during oxygen glucose deprivation the forward mode of the NCX would be shut off due to lose of the sodium gradient. Thus, the neurons would be sensitive to low concentrations of glutamate. However, the concentration of glutamate used throughout this thesis was $25\mu\text{M}$ (plus $10\mu\text{M}$ glycine). The reason that such a high concentration of glutamate was used was twofold. The first reason is that in most case the sodium gradient was not disrupted prior to the start of the experiment. If the neurons are exposed to $1\mu\text{M}$ glutamate (plus $10\mu\text{M}$ glycine) without disrupting the sodium gradient no calcium dysregulation is observed. Thus, high

concentrations of glutamate are needed to induce DCD. The second reason is that all of the experiments in this thesis are performed at room temperature, 25°C. That is significantly lower than body temperature, 37°C. At room temperature reaction occur much slower than at body temperature. Thus to experimental induce DCD at room temperature a higher concentration of glutamate is need.

2. KB-R7943 inhibits Complex I on the mitochondrial respiratory chain

An increase in NAD(P)H fluorescence induced by KB-R7943 in our experiments indicated a reduction of NAD(P)⁺ into NAD(P)H. The similarity between the effects of KB-R7943 and rotenone, an inhibitor of Complex I, suggested that KB-R7943 could inhibit Complex I as well. However, oligomycin, an inhibitor of ATP synthase, also increased NAD(P)H under resting conditions. This raised the question whether KB-R7943 inhibited Complex I, ATP synthase, or both. The answer to this question comes from the observation that KB-R7943, similar to rotenone and in contrast to oligomycin, greatly suppressed the effects of glutamate, FCCP, and KCN. This strongly suggested that KB-R7943 inhibited Complex I in neuronal mitochondria.

The possibility of rotenone having off-target effect and the result we observe is due to another mechanism and not Complex I inhibition is of concern. However we have shown similar indication of KB-R7943 inhibiting Complex I in the experiments with isolated brain mitochondria fueled with succinate in which

KB-R7943 failed to affect State 3 respiration (in the presence of ADP), ruled out inhibition of ATP synthase and also suggested Complex I inhibition.

Despite KB-R7943-induced inhibition of Complex I, mitochondrial depolarization did not occur immediately after KB-R7943 exposure, presumably due to a very low proton permeability of the inner mitochondrial membrane in live neurons. A slight increase in proton permeability induced by an ultra-low concentration of the protonophore FCCP, nontoxic on its own for membrane potential, produced rapid depolarization in the presence of KB-R7943. This suggested that the ability of mitochondria to compensate for an increased H^+ influx back into the matrix by increasing H^+ extrusion via proton pumps of the respiratory chain was diminished by KB-R7943. Importantly, the effect of KB-R7943 on mitochondrial membrane potential was Ca^{2+} -independent and could be observed in the Ca^{2+} -free medium as well. This suggests that KB-R7943 is directly affecting Complex I and calcium influx only accelerates the damage. Furthermore, if the initial influx of calcium through the NMDA receptor could be prevented, short exposure of KB-R7943 may not be harmful to the neuron.

3. Experiments with isolated mitochondria confirm that KB-R7943 inhibits Complex I on the respiratory chain and thus, depolarize the mitochondria and reduced its ability to accumulate calcium

The increase in NAD(P)H autofluorescence produced with KB-R7943 suggested inhibition of Complex I. However, the same effect on NAD(P)H fluorescence could also be produced by inhibition of Complex III or IV. Isolated

brain mitochondria were instrumental in distinguishing between these possibilities. With isolated mitochondria, we chose oxidative substrates, which are oxidized either by Complex I (malate plus glutamate or malate plus pyruvate) or by Complex II (succinate). Since, KB-R7943 selectively inhibited mitochondrial respiration, produced mitochondrial depolarization, and suppressed mitochondrial Ca^{2+} uptake when mitochondria oxidized Complex I substrates but not succinate, a Complex II substrate, this shows that KB-R7943 specifically inhibited Complex I but did not inhibit other components of the respiratory chain (e.g. Complexes II, III, or IV) or mitochondrial Ca^{2+} uniporter. In fact, a recovery of Ca^{2+} uptake with succinate suggested that KB-R7943 might inhibit the Ca^{2+} uptake by limiting the amount of energy available for Ca^{2+} transport rather than directly inhibiting the Ca^{2+} uniporter (Santo-Domingo *et al.*, 2007). The experiments with isolated mitochondria corroborated the conclusion regarding the mechanism of KB-R7943 action on mitochondrial membrane potential and calcium handling in cultured hippocampal neurons.

As we demonstrated, Complex I inhibition decreases mitochondrial capacity to generate membrane potential thus limiting the ability of mitochondria to contribute to clearance of elevated cytosolic Ca^{2+} . This explains why KB-R7943 accelerated the onset of delayed calcium dysregulation in the experiments with neurons exposed to 25 μM glutamate. On the other hand, in the experiments with 100 μM glutamate, the effect of KB-R7943 on delayed calcium dysregulation was less pronounced probably because the onset of delayed calcium dysregulation was very rapid. Under these conditions, mitochondria

apparently became injured and lost their ability to accumulate Ca^{2+} very quickly even in the absence of KB-R7943. Interestingly, the indirect inhibition of mitochondrial Ca^{2+} uptake due to mild mitochondrial depolarization with KB-R7943 might protect mitochondria from irreversible damage imposed by excessive Ca^{2+} accumulation and this could be protective for the whole neuron. Previously, a transient depolarization of neuronal mitochondria with FCCP leading to inhibition of mitochondrial Ca^{2+} uptake was found to be neuroprotective in the experiments with excitotoxic glutamate applied to cultured neurons (Stout *et al.*, 1998). In our previous study, KB-R7943 protected the ability of cultured neurons to recover low $[\text{Ca}^{2+}]_c$ after glutamate removal (Storozhevych *et al.*, 2010) suggesting that KB-R7943 prevented mitochondrial injury and preserved neuronal mitochondria for Ca^{2+} accumulation in the post-glutamate period. This supports the idea that prevention of mitochondrial Ca^{2+} overload could be neuroprotective in the experimental model of glutamate excitotoxicity (Stout *et al.*, 1998).

Overall this research showed KB-R7943 disrupting mitochondrial membrane potential in whole cell experiments with Rhodamine 123 and NAD(P)H redox state experiments, and specifically that it inhibits Complex I using isolated mitochondria membrane potential, oxygen consumption experiments, and calcium accumulation experiments. Using different approaches to confirm this result, we strengthened our argument for the conclusion that KB-R7943 does inhibit Complex I on the mitochondrial electron transport chain. Also by using multiple experiment methods we counter any

weakness with each individual approach by confirming the same results with another method. This was done throughout this thesis, using multiple methods to confirm our results.

B. Inhibition of the NMDA receptor alone fails to prevent glutamate-induced delayed calcium dysregulation, but simultaneous inhibition of both the NMDA receptor and the reverse mode of the $\text{Na}^+/\text{Ca}^{2+}$ exchanger strongly prevent this phenomenon

The NMDA-subtype of glutamate ionotropic receptors (NMDA receptor) is considered the major route for Ca^{2+} entry in neurons exposed to glutamate (Tymianski *et al.*, 1993b). In our previous study, we found that the NMDA receptor inhibitor, MK801, applied to neurons shortly after glutamate, completely prevented delayed calcium dysregulation (DCD) (Brustovetsky *et al.*, 2010). This finding supports the major role of NMDA receptor in delayed calcium dysregulation and apparently rejects the NCX_{rev} hypothesis. However, it is known that during glutamate exposure conditions are favorable for the reverse NCX. Thus, the complete inhibition of DCD with NMDA receptor inhibition does not take into account calcium influx through NCX_{rev} .

In this thesis, we found that the strong protection against delayed calcium dysregulation evoked by MK801 and memantine depended on inhibition of both NMDA receptor and NCX_{rev} whereas inefficiency of either AP-5 or KB-R7943 alone to protect against delayed calcium dysregulation correlated with their respective inability to inhibit either NCX_{rev} or NMDA receptors. Thus, for the first

time, we demonstrated that both NMDA receptors and NCX_{rev} play essential role in glutamate-induced delayed calcium dysregulation. Our results unify the NMDA receptor and NCX_{rev} hypotheses of delayed calcium dysregulation and explain the inefficiency of separate NMDA receptor and NCX_{rev} inhibition in preventing delayed calcium dysregulation. We also demonstrated for the first time that the NMDA receptor antagonists, MK801 and memantine, are also potent NCX_{rev} inhibitors. Importantly, the forward mode of NCX was not affected by these antagonists because the forward mode of the NCX is essential in maintaining low $[Ca^{2+}]_c$. The findings of this study add a new perspective to our understanding of the mechanisms of glutamate-induced delayed calcium dysregulation and provide a rationale for the inconsistency in neuroprotection afforded by different NMDA receptor antagonists. In conclusion, the NMDA receptor antagonists that inhibit both calcium influx mechanisms (NMDA receptor and NCX_{rev}) completely prevented glutamate-induced DCD.

The prolonged exposure of neurons to glutamate causes overstimulation of glutamate receptors and produces a massive Ca^{2+} influx and significant elevation of $[Ca^{2+}]_c$ (Tymianski *et al.*, 1993b). Incoming Ca^{2+} can be extruded from the cytosol by Ca^{2+} -ATPase in the plasma membrane or by NCX operating in the forward mode (Guerini *et al.*, 2005). In addition, Ca^{2+} can be taken up by mitochondria (Bernardi, 1999). The Ca^{2+} -ATPase has low transport capacity (Tymianski *et al.*, 1993b), and therefore cannot compensate for the massive Ca^{2+} influx into neurons triggered by glutamate. The NCX, on the other hand, has a much greater Ca^{2+} transport capacity and therefore can more effectively clear

elevated Ca^{2+} (Carafoli *et al.*, 2001). However, glutamate-induced increase in $[\text{Na}^+]_c$ and plasma membrane depolarization lead to a reversal of NCX that instead of extruding Ca^{2+} brings more Ca^{2+} into the cell (Kiedrowski *et al.*, 1994). In the cell, mitochondria play a significant role in clearing the elevated cytosolic Ca^{2+} (Herrington *et al.*, 1996). However, mitochondrial Ca^{2+} uptake capacity is limited because of induction of the permeability transition pore (PTP) that precludes further Ca^{2+} accumulation (Chalmers & Nicholls, 2003; Li *et al.*, 2009). Inhibition of the PTP induction by cyclosporine A or its non-immunosuppressive derivatives or by genetic ablation of the mitochondrial cyclophilin D defers calcium dysregulation and increases resistance of neurons to glutamate toxicity but cannot reliably protect neurons from delayed calcium dysregulation and cell death (Li *et al.*, 2009; Brustovetsky *et al.*, 2009). On the other hand, the extracellular space is practically an infinite source of Ca^{2+} and, therefore, attenuating Ca^{2+} entry from the outside of the cell seems the most effective way to protect neurons exposed to glutamate rather than maintaining function of calcium reducing mechanisms. However, this requires precise knowledge about Ca^{2+} entry routes into neurons exposed to glutamate and warrants extensive research in this direction.

In our study, inhibition of NMDA receptor and NCX_{rev} appeared to be sufficient for preventing delayed calcium dysregulation and, therefore, we were focused on these mechanisms of Ca^{2+} influx in neurons exposed to glutamate. The stimulation of ionotropic glutamate receptors results in plasma membrane depolarization, resulting in elimination of the voltage-dependent Mg^{2+} block of

NMDA receptor, and thus maintains NMDA receptor activity, permitting continuous divalent cation influx (Nowak *et al.*, 1984; Planells-Cases *et al.*, 2006). However, in electrophysiological experiments the NMDA receptor is rapidly inactivated due to Ca^{2+} -induced actin depolymerization (Legendre *et al.*, 1993; Rosenmund & Westbrook, 1993) and therefore its role in delayed calcium dysregulation remains questionable. In addition to the NMDA receptor, the NCX_{rev} significantly contributes to delayed calcium dysregulation by bringing Ca^{2+} into the cytosol in exchange for cytosolic Na^+ (Kiedrowski *et al.*, 1994; Hoyt *et al.*, 1998). This conclusion is based on the observations that glutamate considerably increases $[\text{Na}^+]_c$ and depolarizes neurons, thus predisposing cells for NCX reversal. However, the extent to which NCX_{rev} contributed to delayed calcium dysregulation in neurons exposed to glutamate had not been completely elucidated. It was also not completely clear which of these two mechanisms - Ca^{2+} influx via NMDA receptor or via NCX_{rev} - plays the major role in delayed calcium dysregulation. The data presented in this thesis increases our understanding of the importance both of these mechanisms, and that either is sufficient to produce calcium dysregulation.

1. MK801 and memantine inhibit both the NMDA receptor and the reverse mode of the $\text{Na}^+/\text{Ca}^{2+}$ exchanger and thus, prevent glutamate-induced delayed Ca^{2+} dysregulation

In our previous study (Brustovetsky *et al.*, 2010), MK801, a noncompetitive NMDA receptor inhibitor, prevented glutamate-induced delayed

calcium dysregulation, consistent with the results from others (Stanika *et al.*, 2009). These data suggested that NMDA receptor plays a key role in delayed calcium dysregulation. At the same time, these data strongly argued against NCX_{rev} involvement in glutamate-induced delayed calcium dysregulation because MK801 is considered a selective NMDA receptor inhibitor. In this thesis, for the first time we present evidence that MK801 as well as memantine, both noncompetitive NMDA receptor antagonists (Huettner & Bean, 1988; Chen *et al.*, 1992), do in fact inhibit NCX_{rev}, whereas AP-5, a competitive NMDA receptor inhibitor, did not. Moreover, inhibition of only one mechanism of Ca²⁺ entry into neurons - either NMDA receptor or NCX_{rev} - appeared to be insufficient to prevent delayed calcium dysregulation, suggesting that both NMDA receptor and NCX_{rev} play essential roles in the collapse of calcium homeostasis in neurons exposed to excitotoxic glutamate. Consequently our results provide the first evidence showing that simultaneous inhibition of both of these calcium influx mechanisms must be accomplished to have any meaning reduction in glutamate-induced calcium dysregulation.

2. Tested NMDA receptor antagonists produce mixed results concerning the NMDA receptor importance in glutamate-induced delayed calcium dysregulation

Inhibition of sustained elevation in [Ca²⁺]_c correlates with increased survival rate of neurons exposed to excitotoxic insult (Kaku *et al.*, 1993). For example, MK801 added after a short exposure to glutamate protected neurons from excitotoxic cell death (Brustovetsky *et al.*, 2004), emphasizing NMDA

receptor involvement in excitotoxicity. Memantine also has been successfully used in experiments to attenuate ischemia/reperfusion brain damage associated with excitotoxicity (Chen *et al.*, 1992; Volbracht *et al.*, 2006). In contrast to MK801 and memantine, AP-5, a competitive inhibitor of NMDA receptor, has been shown to be only moderately effective on both reduction in glutamate-induced calcium dysregulation and in neuroprotection against glutamate excitotoxicity (Levy & Lipton, 1990). Based on our data, this differential neuroprotective efficacy of NMDA receptor inhibitors could be due to the difference in their ability to inhibit NCX_{rev}.

3. The reverse mode of the Na⁺/Ca²⁺ exchanger is sufficient to produce glutamate-induced delayed Ca²⁺ dysregulation

The NCX_{rev} plays an important role not only in glutamate-induced delayed calcium dysregulation and excitotoxicity in neurons (Kiedrowski *et al.*, 1994; Hoyt *et al.*, 1998), but also in other pathological conditions such as ischemia/reperfusion heart injury (Ohtsuka *et al.*, 2004; Feng *et al.*, 2006) and traumatic spinal cord injury (Li *et al.*, 2000). This exemplifies a significant need for potent and efficacious NCX_{rev} inhibitors. However, since the introduction of KB-R7943 in 1996 (Iwamoto *et al.*, 1996), only a few NCX_{rev} inhibitors have been developed (Annunziato *et al.*, 2004; Watanabe *et al.*, 2006), warranting a more intense search for new NCX_{rev} inhibitors. Our study serendipitously adds MK801 and memantine to the list of NCX_{rev} inhibitors. Both MK801 and memantine appeared to be potent and efficacious in inhibiting NCX_{rev} in neurons. It is likely

that these agents will be also effective in inhibiting NCX_{rev} in other cells (e.g. cardiomyocytes) and hence could be helpful not only in protecting neurons but other cells as well. This is important because our research has not only shown the poor specificity of the NCX_{rev} inhibitor KB-R7943, but it has also provided evidence of that the NCX_{rev} activity in fact can result in DCD. Thus finding new ways to prevent the calcium influx through the NCX_{rev} is an integral part of preventing glutamate-induced calcium dysregulation.

C. Ifenprodil inhibits both the N2R-containing NMDA receptor and the reverse mode of the $\text{Na}^+/\text{Ca}^{2+}$ exchanger confirming our hypothesis that both routes of Ca^{2+} influx are sufficient for producing glutamate-induced delayed calcium dysregulation

The NMDA receptor is one of the major routes for Ca^{2+} influx in glutamate-exposed neurons (Tymianski *et al.*, 1993b) and inhibition of NMDA receptor increases survival of neurons *in vitro* (Brustovetsky *et al.*, 2004). However, strong inhibition of glutamate neurotransmission with high-affinity NMDA receptor antagonists such as MK801 leads to unacceptable side-effects (Lipton, 2006). In contrast, ifenprodil, an activity-dependent NMDA receptor antagonist, effectively inhibits NMDA receptors activated by high concentrations of glutamate and, at the same time, retains the basal level of glutamate neurotransmission and is therefore considered to be a more promising and clinically relevant neuroprotector (Kew *et al.*, 1996).

1. Ifenprodil and PEAQX, NR2B- and NR2A- containing NMDA receptor antagonists, respectively, have differential inhibitor abilities depending on age of neurons

In our experiments with “younger” (6-8 DIV) glutamate-treated neurons that predominantly express NR2B subunits, ifenprodil alone completely inhibited NMDA-induced increases in $[Ca^{2+}]_c$ and prevented delayed calcium dysregulation according to its selectivity to NR2B-containing NMDA receptors (Kew *et al.*, 1996). Predictably, in “older” (12-14 DIV) glutamate-treated neurons that express greater amount of NR2A subunits, ifenprodil alone appeared to be less effective. Only combined inhibition of NR2A-containing NMDA receptors with PEAQX and NR2B-containing NMDA receptors with ifenprodil completely inhibited NMDA-induced increase in $[Ca^{2+}]_c$ and prevented glutamate-induced delayed calcium dysregulation, emphasizing the important role of both NR2A- and NR2B-containing subtypes of NMDA receptors in the collapse of Ca^{2+} homeostasis in neurons exposed to excitotoxic glutamate.

2. Ifenprodil, not PEAQX, inhibit the reverse mode of the Na^+/Ca^{2+} exchanger

In addition to NMDA receptor, Ca^{2+} influx via NCX_{rev} significantly contributes to glutamate-induced delayed calcium dysregulation (Hoyt *et al.*, 1998; Kiedrowski, 1999). Above, we provided evidence that inhibition of only the NMDA receptor was insufficient to prevent delayed calcium dysregulation and that NCX_{rev} inhibition is required to protect neurons against glutamate-induced delayed calcium dysregulation (Brittain *et al.*, 2012). We then provided evidence

that ifenprodil alone (with “younger” neurons) or in combination with PEAQX (with “older” neurons) completely prevented glutamate induced delayed calcium dysregulation. Consequently, we hypothesized that ifenprodil in addition to NMDA receptor also inhibits NCX_{rev} . The experiments described in this thesis suggest that ifenprodil indeed inhibits NCX_{rev} . This is significant because our research has shown that only inhibiting a single calcium influx mechanism is insufficient in preventing delayed calcium dysregulation. Thus the addition inhibitor affect on the NCX_{rev} is extremely beneficial.

In the forward mode, the NCX mediates an exchange of 1 intracellular Ca^{2+} for 3 extracellular Na^+ ions driven by Na^+ concentration gradient across the plasma membrane and facilitated by plasma membrane potential (Blaustein & Lederer, 1999). Plasma membrane depolarization and collapse of the Na^+ gradient lead to NCX reversal. Both, the loss of the Na^+ gradient and membrane depolarization take place following glutamate exposure, resulting in NCX reversal and massive Ca^{2+} influx into neurons (Czyz & Kiedrowski, 2002; Kiedrowski *et al.*, 1994). However, because the NMDA receptor also significantly contributes to glutamate-induced, sustained elevation in $[\text{Ca}^{2+}]_c$ (Tymianski *et al.*, 1993b), it is difficult to determine the exact target(s) of the pharmacological agents in experiments with neurons exposed to glutamate. Accordingly, to test whether ifenprodil inhibits NCX_{rev} , we used two experimental approaches that did not involve application of exogenous glutamate. In our experiments, the reversal of NCX was triggered by collapse of Na^+ gradient across the plasma membrane and plasma membrane depolarization induced by gramicidin, a monovalent

cation ionophore that does not transport Ca^{2+} (Czyz & Kiedrowski, 2002). However, gramicidin could damage mitochondria (Luvisetto & Azzone, 1989; Rottenberg & Koeppe, 1989) involved in Ca^{2+} buffering in neurons (Wang & Thayer, 1996; White & Reynolds, 1997). To circumvent this potentially confounding variable, NCX reversal was triggered by $\text{Na}^+/\text{NMDG}^+$ -replacement in the bath solution (Wu *et al.*, 2008). Both gramicidin and $\text{Na}^+/\text{NMDG}^+$ replacement produced an increase in $[\text{Ca}^{2+}]_c$ that was inhibited by ifenprodil; indicating that ifenprodil is an effective inhibitor of the reverse mode of the NCX. Both manipulations led to the release of endogenous glutamate in low micromolar concentration range probably due to reversal of Na^+ -glutamate co-transporter. This might contribute to the increase in $[\text{Ca}^{2+}]_c$ due to Ca^{2+} influx via activated NMDA receptor, particularly, under conditions when the forward mode of NCX is shut down due to elimination or reversal of Na^+ gradient across the plasma membrane. We used GPT, which converts glutamate and pyruvate into α -ketoglutarate and alanine (Matthews *et al.*, 2000; Matthews *et al.*, 2003), to prevent the increase in glutamate concentration in the bath solution induced by gramicidin (Brittain *et al.*, 2012) and to prevent the increase in external glutamate following $\text{Na}^+/\text{NMDG}^+$ replacement. In both cases, GPT prevented the rises in glutamate concentration in the bath solution but failed to prevent the increases in $[\text{Ca}^{2+}]_c$. This suggests that the gramicidin- and $\text{Na}^+/\text{NMDG}^+$ -induced increases in $[\text{Ca}^{2+}]_c$ were not due to NMDA receptor stimulation by the released endogenous glutamate. This conclusion is supported by the fact that AP-5, a potent NMDA receptor inhibitor, failed to inhibit $[\text{Ca}^{2+}]_c$ increases induced by gramicidin or

Na⁺/NMDG⁺ replacement. On the other hand, in the experiments with Na⁺/NMDG⁺ replacement, the magnitude of [Ca²⁺]_c elevations depended on [Na⁺]_c and became significantly increased with increasing [Na⁺]_c in the presence of ouabain, an inhibitor of Na⁺/K⁺-ATPase. The similar dependence was reported earlier (Wu *et al.*, 2008). This suggests that the mechanism of Na⁺/NMDG⁺-induced increase in [Ca²⁺]_c most likely utilized the reverse Na⁺ gradient. Taken together, our results suggest that the reversal of NCX is the most likely mechanism of the increases in [Ca²⁺]_c induced by gramicidin or Na⁺/NMDG⁺ replacement. Consequently, inhibition of these [Ca²⁺]_c increases with ifenprodil strongly suggests that ifenprodil inhibits NCX_{rev} whereas the lack of inhibition with PEAQX indicates that this agent does not inhibit NCX_{rev}. Ifenprodil's ability to inhibit NCX_{rev} is not unique among NMDA receptor antagonists. In this thesis, we found evidence that MK801 and memantine, noncompetitive inhibitors of NMDA receptor, most likely also inhibit NCX_{rev} in hippocampal neurons (Brittain *et al.*, 2012). Recently, PPADS, a P2X receptor antagonist, was found to inhibit the NCX_{rev} in guinea pig airway smooth muscle (Flores-Soto *et al.*, 2012).

3. Ifenprodil inhibit both the NMDA receptor and the reverse mode of the Na⁺/Ca²⁺ exchanger confirms results suggesting that both Ca²⁺ influx routes are sufficient to produce glutamate-induced delayed calcium dysregulation

The ability of ifenprodil alone or in combination with PEAQX to prevent glutamate-induced delayed calcium dysregulation in neurons correlates with ifenprodil's efficacy to inhibit NCX_{rev}. It is conceivable that other neuroprotective

agents, used against glutamate excitotoxicity and originally aimed at different molecular targets, may also exert neuroprotection, at least in part, by inhibiting NCX_{rev}. Accordingly, further studies are necessary to investigate the ability of different neuroprotective agents to inhibit NCX_{rev}. The results presented in this thesis improve our understanding of the mechanisms of ifenprodil neuroprotective action and support our hypothesis about significant contribution of both NMDA receptor and NCX_{rev} in glutamate-induced delayed calcium dysregulation in neurons.

V. SUMMARY AND CONCLUSIONS

The results of this thesis research can be summarized by the following statements:

1. Preventing the reverse mode of the $\text{Na}^+/\text{Ca}^{2+}$ exchanger alone fails to prevent glutamate-induced delayed calcium dysregulation.
2. KB-R7943 inhibits not only the reverse mode of the $\text{Na}^+/\text{Ca}^{2+}$ exchanger, but also NMDA receptor and Complex I in the respiratory chain, resulting in mitochondrial depolarization and failure of mitochondrial Ca^{2+} accumulation.
3. Inhibiting the NMDA receptor alone fails to prevent delayed Ca^{2+} dysregulation induced by prolonged glutamate exposure.
4. MK801 and memantine, non-competitive NMDA receptor antagonists, completely prevent glutamate-induced delayed calcium dysregulation by completely inhibiting both the NMDA receptor and the reverse mode of the $\text{Na}^+/\text{Ca}^{2+}$ exchanger.
5. AP-5, a competitive NMDA receptor antagonist, or KB-R7943, a reverse mode of the $\text{Na}^+/\text{Ca}^{2+}$ exchanger antagonist, alone fail to prevent delayed Ca^{2+} dysregulation, but the combination of both of these antagonists completely prevent glutamate-induced delayed calcium dysregulation.
6. Ifenprodil blocks both NR2B-containing NMDA receptors and the reverse mode of the $\text{Na}^+/\text{Ca}^{2+}$ exchanger, but only completely prevents glutamate-induced delayed Ca^{2+} dysregulation in combination with PEAQX, an NR2A-containing NMDA receptor inhibitor.

In conclusion, here for the first time we presented strong evidence suggesting that KB-R7943 inhibits Complex I in the mitochondrial respiratory chain. This could contribute to mitochondrial depolarization, limit Ca^{2+} uptake by this organelle, and thus preserve mitochondria from the Ca^{2+} -induced damage in neurons exposed to excitotoxic glutamate. In turn, preventing mitochondrial damage could facilitate recovery of calcium homeostasis and promote neuronal survival in a post-glutamate period. Our data also indicate that in addition to inhibition of the mitochondrial Complex I and NCX_{rev} , KB-R7943 inhibits NMDA receptor. Therefore, the whole spectrum of KB-R7943 effects has to be considered while interpreting the results obtained with this popular pharmacological agent.

Also, we demonstrated for the first time that both NMDA receptor and NCX_{rev} significantly contribute to delayed calcium dysregulation in glutamate-treated neurons. We found that strong protection against delayed calcium dysregulation evoked by MK801 and memantine correlates with strong inhibition of both NMDA receptor and NCX_{rev} , whereas inefficiency of AP-5 and KB-R7943 to protect against delayed calcium dysregulation correlates with their low efficacy to inhibit either NCX_{rev} or NMDA receptor. Thus, our results unify NMDA receptor and NCX_{rev} hypotheses of delayed calcium dysregulation and explain inefficiency of separate NMDA receptor and NCX_{rev} inhibition in preventing delayed calcium dysregulation and protecting neurons against glutamate excitotoxicity. Also, this research concluded that several important NMDA receptor antagonists - MK801, memantine, and ifenprodil - had off-target inhibitor effects on the reverse mode of

the Na⁺/Ca²⁺ exchanger. This data significantly broaden our understanding of the mechanism of action regarding these antagonists, and thus, will help to correctly interpret results obtained with these widely used pharmacological agents.

Further research is needed to confirm the predictive strength of the overall conclusion of this thesis regarding dual calcium influx mechanisms leading to glutamate-induced DCD. Other NMDA receptor antagonists and NCX_{rev} inhibitors need to be tested for off-target effect affecting the other route of calcium influx. It appears that chemical structure of these inhibitors may have a role in determining if the antagonist blocks both pathways. Structure analysis and receptor modeling may be helpful in determining this relationship. Furthermore, the overall conclusion needs to be tested *in vivo* to determine if it translate from a cellular assay to a whole animal.

VI. REFERENCES

- AARTS,M., IIHARA,K., WEI,W.L., XIONG,Z.G., ARUNDINE,M., CERWINSKI,W., MACDONALD,J.F. & TYMIANSKI,M. (2003). A key role for TRPM7 channels in anoxic neuronal death. *Cell*, 115, 863-877.
- AHA. (2007). American Heart Association. Heart Disease and Stroke Statistics - 2007 Update. Dallas, Texas: American Heart Association.
- AMRAN,M.S., HOMMA,N. & HASHIMOTO,K. (2003). Pharmacology of KB-R7943: a Na⁺-Ca²⁺ exchange inhibitor. *Cardiovasc. Drug Rev.*, 21, 255-276.
- ANNUNZIATO,L., PIGNATARO,G. & DI RENZO,G.F. (2004). Pharmacology of brain Na⁺/Ca²⁺ exchanger: from molecular biology to therapeutic perspectives. *Pharmacol. Rev.*, 56, 633-654.
- ARAUJO,I.M., CARREIRA,B.P., PEREIRA,T., SANTOS,P.F., SOULET,D., INACIO,A., BAHR,B.A., CARVALHO,A.P., AMBROSIO,A.F. & CARVALHO,C.M. (2007). Changes in calcium dynamics following the reversal of the sodium-calcium exchanger have a key role in AMPA receptor-mediated neurodegeneration via calpain activation in hippocampal neurons. *Cell Death. Differ.*, 14, 1635-1646.
- AUBERSON,Y.P., ALLGEIER,H., BISCHOFF,S., LINGENHOEHL,K., MORETTI,R. & SCHMUTZ,M. (2002). 5-Phosphonomethylquinolinediones as competitive NMDA receptor antagonists with a preference for the human 1A/2A, rather than 1A/2B receptor composition. *Bioorg. Med. Chem. Lett.*, 12, 1099-1102.
- AVKIRAN,M. (2001). Protection of the ischaemic myocardium by Na⁺/H⁺ exchange inhibitors: potential mechanisms of action. *Basic Res. Cardiol.*, 96, 306-311.
- BAINES,C.P., KAISER,R.A., PURCELL,N.H., BLAIR,N.S., OSINSKA,H., HAMBLETON,M.A., BRUNSKILL,E.W., SAYEN,M.R., GOTTLIEB,R.A., DORN,G.W., ROBBINS,J. & MOKENTIN,J.D. (2005). Loss of cyclophilin D reveals a critical role for mitochondrial permeability transition in cell death. *Nature*, 434, 658-662.
- BAKER,P.F. & GLITSCH,H.G. (1973). Does metabolic energy participate directly in the Na⁺-dependent extrusion of Ca²⁺ -Ca²⁺ ions from squid giant axons? *J. Physiol*, 233, 44P-46P.
- BAKER,P.F., MEVES,H. & RIDGWAY,E.B. (1973). Calcium entry in response to maintained depolarization of squid axons. *J. Physiol*, 231, 527-548.

- BANO,D., YOUNG,K.W., GUERIN,C.J., LEFEUVRE,R., ROTHWELL,N.J., NALDINI,L., RIZZUTO,R., CARAFOLI,E. & NICOTERA,P. (2005). Cleavage of the plasma membrane Na⁺/Ca²⁺ exchanger in excitotoxicity. *Cell*, 120, 275-285.
- BARTH,A.L. & MALENKA,R.C. (2001). NMDA receptor EPSC kinetics do not regulate the critical period for LTP at thalamocortical synapses. *Nat. Neurosci.*, 4, 235-236.
- BEARDSLEY,P.M., HAYES,B.A. & BALSTER,R.L. (1990). The self-administration of MK-801 can depend upon drug-reinforcement history, and its discriminative stimulus properties are phencyclidine-like in rhesus monkeys. *J. Pharmacol. Exp. Ther.*, 252, 953-959.
- BELLOCCHIO,E.E., REIMER,R.J., FREMEAU,R.T., JR. & EDWARDS,R.H. (2000). Uptake of glutamate into synaptic vesicles by an inorganic phosphate transporter. *Science*, 289, 957-960.
- BENVENISTE,H., DREJER,J., SCHOUSBOE,A. & DIEMER,N.H. (1984). Elevation of the extracellular concentrations of glutamate and aspartate in rat hippocampus during transient cerebral ischemia monitored by intracerebral microdialysis. *J. Neurochem.*, 43, 1369-1374.
- BERBERICH,S., PUNNAKKAL,P., JENSEN,V., PAWLAK,V., SEEBURG,P.H., HVALBY,O. & KOHR,G. (2005). Lack of NMDA receptor subtype selectivity for hippocampal long-term potentiation. *J. Neurosci.*, 25, 6907-6910.
- BERNARDI,P. (1999). Mitochondrial transport of cations: channels, exchangers, and permeability transition. *Physiol Rev.*, 79, 1127-1155.
- BERNARDI,P., KRAUSKOPF,A., BASSO,E., PETRONILLI,V., BLALCHY-DYSON,E., DI LISA,F. & FORTE,M.A. (2006). The mitochondrial permeability transition from in vitro artifact to disease target. *FEBS J.*, 273, 2077-2099.
- BERNARDI,P. & PETRONILLI,V. (1996). The permeability transition pore as a mitochondrial calcium release channel: a critical appraisal. *J. Bioenerg. Biomembr.*, 28, 131-138.
- BEVENSEE,M.O., WEED,R.A. & BORON,W.F. (1997). Intracellular pH regulation in cultured astrocytes from rat hippocampus. I. Role Of HCO₃⁻. *J. Gen. Physiol.*, 110, 453-465.
- BINDOKAS,V.P. & MILLER,R.J. (1995). Excitotoxic degeneration is initiated at non-random sites in cultured rat cerebellar neurons. *J. Neurosci.*, 15, 6999-7011.
- BLAUSTEIN,M.P. & LEDERER,W.J. (1999). Sodium/calcium exchange: its physiological implications. *Physiol Rev.*, 79, 763-854.

BONDE,C., NORABERG,J., NOER,H. & ZIMMER,J. (2005). Ionotropic glutamate receptors and glutamate transporters are involved in necrotic neuronal cell death induced by oxygen-glucose deprivation of hippocampal slice cultures. *Neuroscience*, 136, 779-794.

BONVENTRE,J.V. (1997). Roles of phospholipases A2 in brain cell and tissue injury associated with ischemia and excitotoxicity. *J. Lipid Mediat. Cell Signal.*, 17, 71-79.

BORTOLOTTO,Z.A., CLARKE,V.R., DELANY,C.M., PARRY,M.C., SMOLDERS,I., VIGNES,M., HO,K.H., MIU,P., BRINTON,B.T., FANTASKE,R., OGDEN,A., GATES,M., ORNSTEIN,P.L., LODGE,D., BLEAKMAN,D. & COLLINGRIDGE,G.L. (1999). Kainate receptors are involved in synaptic plasticity. *Nature*, 402, 297-301.

BRADFORD,M.M. (1976). A rapid and sensitive method for the quantitation of microgram quantities of protein utilizing the principle of protein-dye binding. *Anal. Biochem.*, 72, 248-254.

BRAMLETT,H.M. & DIETRICH,W.D. (2004). Pathophysiology of cerebral ischemia and brain trauma: similarities and differences. *J. Cereb. Blood Flow Metab*, 24, 133-150.

BREDER,J., SABELHAUS,C.F., OPITZ,T., REYMANN,K.G. & SCHRODER,U.H. (2000). Inhibition of different pathways influencing Na(+) homeostasis protects organotypic hippocampal slice cultures from hypoxic/hypoglycemic injury. *Neuropharmacology*, 39, 1779-1787.

BREWER,L.D., THIBAUT,O., STATON,J., THIBAUT,V., ROGERS,J.T., GARCIA-RAMOS,G., KRANER,S., LANDFIELD,P.W. & PORTER,N.M. (2007). Increased vulnerability of hippocampal neurons with age in culture: temporal association with increases in NMDA receptor current, NR2A subunit expression and recruitment of L-type calcium channels. *Brain Res.*, 1151, 20-31.

BRITAIN,M.K., BRUSTOVETSKY,T., SHEETS,P.L., BRITAIN,J.M., KHANNA,R., CUMMINS,T.R. & BRUSTOVETSKY,N. (2012). Delayed calcium dysregulation in neurons requires both the NMDA receptor and the reverse Na(+)/Ca(2+) exchanger. *Neurobiol. Dis.*

BROEKEMEIER,K.M., DEMPSEY,M.E. & PFEIFFER,D.R. (1989). Cyclosporin A is a potent inhibitor of the inner membrane permeability transition in liver mitochondria. *J. Biol. Chem.*, 264, 7826-7830.

BRUSTOVETSKY,N., BRUSTOVETSKY,T., PURL,K.J., CAPANO,M., CROMPTON,M. & DUBINSKY,J.M. (2003). Increased susceptibility of striatal mitochondria to calcium-induced permeability transition. *J. Neurosci.*, 23, 4858-4867.

- BRUSTOVETSKY,N., JEMMERSON,R. & DUBINSKY,J.M. (2002). Calcium-induced Cytochrome c release from rat brain mitochondria is altered by digitonin. *Neurosci. Lett.*, 332, 91-94.
- BRUSTOVETSKY,T., BOLSHAKOV,A. & BRUSTOVETSKY,N. (2010). Calpain activation and Na⁺/Ca²⁺ exchanger degradation occur downstream of calcium deregulation in hippocampal neurons exposed to excitotoxic glutamate. *J. Neurosci. Res.*, 88, 1317-1328.
- BRUSTOVETSKY,T., BRITAIN,M.K., SHEETS,P.L., CUMMINS,T.R., PINELIS,V. & BRUSTOVETSKY,N. (2011). KB-R7943, an inhibitor of the reverse Na⁺ /Ca²⁺ exchanger, blocks N-methyl-D-aspartate receptor and inhibits mitochondrial Complex I. *Br. J. Pharmacol.*, 162, 255-270.
- BRUSTOVETSKY,T., LI,V. & BRUSTOVETSKY,N. (2009). Stimulation of glutamate receptors in cultured hippocampal neurons causes Ca²⁺-dependent mitochondrial contraction. *Cell Calcium*, 46, 18-29.
- BRUSTOVETSKY,T., PURL,K., YOUNG,A., SHIMIZU,K. & DUBINSKY,J.M. (2004). Dearth of glutamate transporters contributes to striatal excitotoxicity. *Exp. Neurol.*, 189, 222-230.
- BRYANT,H.E., SCHULTZ,N., THOMAS,H.D., PARKER,K.M., FLOWER,D., LOPEZ,E., KYLE,S., MEUTH,M., CURTIN,N.J. & HELLEDAY,T. (2005). Specific killing of BRCA2-deficient tumours with inhibitors of poly(ADP-ribose) polymerase. *Nature*, 434, 913-917.
- BUCANA,C., SAIKI,I. & NAYAR,R. (1986). Uptake and accumulation of the vital dye hydroethidine in neoplastic cells. *J. Histochem. Cytochem.*, 34, 1109-1115.
- BUDD,S.L. & NICHOLLS,D.G. (1996). Mitochondria, calcium regulation, and acute glutamate excitotoxicity in cultured cerebellar granule cells. *J. Neurochem.*, 67, 2282-2291.
- BUKI,A., OKONKWO,D.O., WANG,K.K. & POVLISHOCK,J.T. (2000). Cytochrome c release and caspase activation in traumatic axonal injury. *J. Neurosci.*, 20, 2825-2834.
- BUTCHER,S.P., HENSHALL,D.C., TERAMURA,Y., IWASAKI,K. & SHARKEY,J. (1997). Neuroprotective actions of FK506 in experimental stroke: in vivo evidence against an antiexcitotoxic mechanism. *J. Neurosci.*, 17, 6939-6946.
- CARAFOLI,E. (1979). The calcium cycle of mitochondria. *FEBS Lett.*, 104, 1-5.
- CARAFOLI,E., SANTELLA,L., BRANCA,D. & BRINI,M. (2001). Generation, control, and processing of cellular calcium signals. *Crit Rev. Biochem. Mol. Biol.*, 36, 107-260.

- CARLEZON,W.A., JR. & WISE,R.A. (1996). Rewarding actions of phencyclidine and related drugs in nucleus accumbens shell and frontal cortex. *J. Neurosci.*, 16, 3112-3122.
- CASTILHO,R.F., WARD,M.W. & NICHOLLS,D.G. (1999). Oxidative stress, mitochondrial function, and acute glutamate excitotoxicity in cultured cerebellar granule cells. *J. Neurochem.*, 72, 1394-1401.
- CASTILLO,J., DAVALOS,A. & NOYA,M. (1997). Progression of ischaemic stroke and excitotoxic aminoacids. *Lancet*, 349, 79-83.
- CASTILLO,J., DAVALOS,A. & NOYA,M. (1999). Aggravation of acute ischemic stroke by hyperthermia is related to an excitotoxic mechanism. *Cerebrovasc. Dis.*, 9, 22-27.
- CHALMERS,S. & NICHOLLS,D.G. (2003). The relationship between free and total calcium concentrations in the matrix of liver and brain mitochondria. *J. Biol. Chem.*, 278, 19062-19070.
- CHAN,S.L. & MATTSON,M.P. (1999). Caspase and calpain substrates: roles in synaptic plasticity and cell death. *J. Neurosci. Res.*, 58, 167-190.
- CHANCE,B. & WILLIAMS,G.R. (1956). The respiratory chain and oxidative phosphorylation. *Adv. Enzymol. Relat Subj. Biochem.*, 17, 65-134.
- CHANG,D.T., RINTOUL,G.L., PANDIPATI,S. & REYNOLDS,I.J. (2006). Mutant huntingtin aggregates impair mitochondrial movement and trafficking in cortical neurons. *Neurobiol. Dis.*, 22, 388-400.
- CHEN,H., KINTNER,D.B., JONES,M., MATSUDA,T., BABA,A., KIEDROWSKI,L. & SUN,D. (2007). AMPA-mediated excitotoxicity in oligodendrocytes: role for Na(+)-K(+)-Cl(-) co-transport and reversal of Na(+)/Ca(2+) exchanger. *J. Neurochem.*, 102, 1783-1795.
- CHEN,H.S., PELLEGRINI,J.W., AGGARWAL,S.K., LEI,S.Z., WARACH,S., JENSEN,F.E. & LIPTON,S.A. (1992). Open-channel block of N-methyl-D-aspartate (NMDA) responses by memantine: therapeutic advantage against NMDA receptor-mediated neurotoxicity. *J. Neurosci.*, 12, 4427-4436.
- CHINOPOULOS,C. & ADAM-VIZI,V. (2006). Calcium, mitochondria and oxidative stress in neuronal pathology. Novel aspects of an enduring theme. *FEBS J.*, 273, 433-450.
- CHINOPOULOS,C., GERENCSEK,A.A., DOCZI,J., FISKUM,G. & ADAM-VIZI,V. (2004). Inhibition of glutamate-induced delayed calcium deregulation by 2-APB and La³⁺ in cultured cortical neurones. *J. Neurochem.*, 91, 471-483.

- CHINOPOULOS,C., STARKOV,A.A. & FISKUM,G. (2003). Cyclosporin A-insensitive permeability transition in brain mitochondria: inhibition by 2-aminoethoxydiphenyl borate. *J. Biol. Chem.*, 278, 27382-27389.
- CHOI,D.W. (1985). Glutamate neurotoxicity in cortical cell culture is calcium dependent. *Neurosci. Lett.*, 58, 293-297.
- CHOI,D.W. (1987). Ionic dependence of glutamate neurotoxicity. *J. Neurosci.*, 7, 369-379.
- CHOI,D.W. (1988). Glutamate neurotoxicity and diseases of the nervous system. *Neuron*, 1, 623-634.
- CHOI,D.W. (1996). Ischemia-induced neuronal apoptosis. *Curr. Opin. Neurobiol.*, 6, 667-672.
- CHOI,D.W. & HARTLEY,D.M. (1993). Calcium and glutamate-induced cortical neuronal death. *Res Publ. Assoc. Res Nerv. Ment. Dis.*, 71, 23-34.
- CHOI,D.W., MAULUCCI-GEDDE,M. & KRIEGSTEIN,A.R. (1987). Glutamate neurotoxicity in cortical cell culture. *J. Neurosci.*, 7, 357-368.
- CLEMENTS,J.D. & WESTBROOK,G.L. (1994). Kinetics of AP5 dissociation from NMDA receptors: evidence for two identical cooperative binding sites. *J. Neurophysiol.*, 71, 2566-2569.
- CLIFFORD,D.B., ZORUMSKI,C.F. & OLNEY,J.W. (1989). Ketamine and MK-801 prevent degeneration of thalamic neurons induced by focal cortical seizures. *Exp. Neurol.*, 105, 272-279.
- COAN,E.J., SAYWOOD,W. & COLLINGRIDGE,G.L. (1987). MK-801 blocks NMDA receptor-mediated synaptic transmission and long term potentiation in rat hippocampal slices. *Neurosci. Lett.*, 80, 111-114.
- CONVERY,M.K. & HANCOX,J.C. (1999). Comparison of Na⁺-Ca²⁺ exchange current elicited from isolated rabbit ventricular myocytes by voltage ramp and step protocols. *Pflugers Arch.*, 437, 944-954.
- CORBETT,J. (2007). Memantine/Gabapentin for the treatment of congenital nystagmus. *Curr. Neurol. Neurosci. Rep.*, 7, 395-396.
- COUNILLON,L. & POUYSSEGUER,J. (2000). The expanding family of eucaryotic Na⁽⁺⁾/H⁽⁺⁾ exchangers. *J. Biol. Chem.*, 275, 1-4.
- CZYZ,A., BARANAUSKAS,G. & KIEDROWSKI,L. (2002). Instrumental role of Na⁺ in NMDA excitotoxicity in glucose-deprived and depolarized cerebellar granule cells. *J. Neurochem.*, 81, 379-389.

- CZYZ,A. & KIEDROWSKI,L. (2002). In depolarized and glucose-deprived neurons, Na⁺ influx reverses plasmalemmal K⁺-dependent and K⁺-independent Na⁺/Ca²⁺ exchangers and contributes to NMDA excitotoxicity. *J. Neurochem.*, 83, 1321-1328.
- DAVALOS,A., CASTILLO,J., SERENA,J. & NOYA,M. (1997). Duration of glutamate release after acute ischemic stroke. *Stroke*, 28, 708-710.
- DELLDOT ET AL. (2007). Electron Transport Chain.
- DI,L.F., MENABO,R., CANTON,M., BARILE,M. & BERNARDI,P. (2001). Opening of the mitochondrial permeability transition pore causes depletion of mitochondrial and cytosolic NAD⁺ and is a causative event in the death of myocytes in postischemic reperfusion of the heart. *J. Biol. Chem.*, 276, 2571-2575.
- DIETZ,R.M., KIEDROWSKI,L. & SHUTTLEWORTH,C.W. (2007). Contribution of Na⁽⁺⁾/Ca⁽²⁺⁾ exchange to excessive Ca⁽²⁺⁾ loading in dendrites and somata of CA1 neurons in acute slice. *Hippocampus*, 17, 1049-1059.
- DINGLEDINE,R., BORGES,K., BOWIE,D. & TRAYNELIS,S.F. (1999). The glutamate receptor ion channels. *Pharmacol. Rev.*, 51, 7-61.
- DIPOLO,R. & BEAUGE,L. (2006). Sodium/calcium exchanger: influence of metabolic regulation on ion carrier interactions. *Physiol Rev.*, 86, 155-203.
- DU,L., ZHANG,X., HAN,Y.Y., BURKE,N.A., KOCHANNEK,P.M., WATKINS,S.C., GRAHAM,S.H., CARCILLO,J.A., SZABO,C. & CLARK,R.S. (2003). Intra-mitochondrial poly(ADP-ribosylation) contributes to NAD⁺ depletion and cell death induced by oxidative stress. *J. Biol. Chem.*, 278, 18426-18433.
- DUAN,Y., GROSS,R.A. & SHEU,S.S. (2007). Ca²⁺-dependent generation of mitochondrial reactive oxygen species serves as a signal for poly(ADP-ribose) polymerase-1 activation during glutamate excitotoxicity. *J. Physiol*, 585, 741-758.
- DUBINSKY,J.M. (1993). Intracellular calcium levels during the period of delayed excitotoxicity. *Journal of Neuroscience*, 13, 623-631.
- DUBINSKY,J.M., KRISTAL,B.S. & ELIZONDO-FOURNIER,M. (1995). An obligate role for oxygen in the early stages of glutamate-induced, delayed neuronal death. *J. Neurosci.*, 15, 7071-7078.
- DUCHEN,M.R. & BISCOE,T.J. (1992). Mitochondrial function in type I cells isolated from rabbit arterial chemoreceptors. *J. Physiol*, 450, 13-31.
- ENGLAND,P.J. (1986). Intracellular calcium receptor mechanisms. *Br. Med. Bull.*, 42, 375-383.

- ERUSLANOV,E. & KUSMARTSEV,S. (2010). Identification of ROS using oxidized DCFDA and flow-cytometry. *Methods Mol. Biol.*, 594, 57-72.
- FAROOQUI,A.A., ONG,W.Y. & HORROCKS,L.A. (2006). Inhibitors of brain phospholipase A2 activity: their neuropharmacological effects and therapeutic importance for the treatment of neurologic disorders. *Pharmacol. Rev.*, 58, 591-620.
- FENG,N.C., SATOH,H., URUSHIDA,T., KATOH,H., TERADA,H., WATANABE,Y. & HAYASHI,H. (2006). A selective inhibitor of Na⁺/Ca²⁺ exchanger, SEA0400, preserves cardiac function and high-energy phosphates against ischemia/reperfusion injury. *J. Cardiovasc. Pharmacol.*, 47, 263-270.
- FLINT,A.C., MAISCH,U.S., WEISHAUPT,J.H., KRIEGSTEIN,A.R. & MONYER,H. (1997). NR2A subunit expression shortens NMDA receptor synaptic currents in developing neocortex. *J. Neurosci.*, 17, 2469-2476.
- FLORES-SOTO,E., REYES-GARCIA,J., SOMMER,B., CHAVEZ,J., BARAJAS-LOPEZ,C. & MONTANO,L.M. (2012). PPADS, a P2X receptor antagonist, as a novel inhibitor of the reverse mode of the Na/Ca(2) exchanger in guinea pig airway smooth muscle. *Eur. J. Pharmacol.*, 674, 439-444.
- FRIZELLE,P.A., CHEN,P.E. & WYLLIE,D.J. (2006). Equilibrium constants for (R)-[(S)-1-(4-bromo-phenyl)-ethylamino]-(2,3-dioxo-1,2,3,4-tetrahydroquinoxalin-5-yl)-methyl]-phosphonic acid (NVP-AAM077) acting at recombinant NR1/NR2A and NR1/NR2B N-methyl-D-aspartate receptors: Implications for studies of synaptic transmission. *Mol. Pharmacol.*, 70, 1022-1032.
- FROMHERZ,P., HUBENER,G., KUHN,B. & HINNER,M.J. (2008). ANNINE-6plus, a voltage-sensitive dye with good solubility, strong membrane binding and high sensitivity. *Eur. Biophys. J.*, 37, 509-514.
- GEE,K.R., BROWN,K.A., CHEN,W.N., BISHOP-STEWART,J., GRAY,D. & JOHNSON,I. (2000). Chemical and physiological characterization of fluo-4 Ca(2+)-indicator dyes. *Cell Calcium*, 27, 97-106.
- GOEBEL,D.J. & POOSCH,M.S. (1999). NMDA receptor subunit gene expression in the rat brain: a quantitative analysis of endogenous mRNA levels of NR1Com, NR2A, NR2B, NR2C, NR2D and NR3A. *Brain Res. Mol. Brain Res.*, 69, 164-170.
- GOLDBERG,M.P. & CHOI,D.W. (1993). Combined oxygen and glucose deprivation in cortical cell culture: calcium-dependent and calcium-independent mechanisms of neuronal injury. *J. Neurosci.*, 13, 3510-3524.
- GOLL,D.E., THOMPSON,V.F., LI,H., WEI,W. & CONG,J. (2003). The calpain system. *Physiol Rev.*, 83, 731-801.

- GOYAL,S., VANDEN,H.G. & ARONSON,P.S. (2003). Renal expression of novel Na⁺/H⁺ exchanger isoform NHE8. *Am. J. Physiol Renal Physiol*, 284, F467-F473.
- GREWER,C., GAMEIRO,A., ZHANG,Z., TAO,Z., BRAAMS,S. & RAUEN,T. (2008). Glutamate forward and reverse transport: from molecular mechanism to transporter-mediated release after ischemia. *IUBMB. Life*, 60, 609-619.
- GRYNKIEWICZ,G., POENIE,M. & TSIEN,R.Y. (1985). A new generation of Ca²⁺ indicators with greatly improved fluorescence properties. *J. Biol. Chem.*, 260, 3440-3450.
- GUERINI,D., COLETTI,L. & CARAFOLI,E. (2005). Exporting calcium from cells. *Cell Calcium*, 38, 281-289.
- GWAG,B.J., LEE,Y.A., KO,S.Y., LEE,M.J., IM,D.S., YUN,B.S., LIM,H.R., PARK,S.M., BYUN,H.Y., SON,S.J., KWON,H.J., LEE,J.Y., CHO,J.Y., WON,S.J., KIM,K.W., AHN,Y.M., MOON,H.S., LEE,H.U., YOON,S.H., NOH,J.H., CHUNG,J.M. & CHO,S.I. (2007). Marked prevention of ischemic brain injury by Neu2000, an NMDA antagonist and antioxidant derived from aspirin and sulfasalazine. *J. Cereb. Blood Flow Metab*, 27, 1142-1151.
- HABLITZ,J.J. (1982). Conductance changes induced by DL-homocysteic acid and N-methyl-DL-aspartic acid in hippocampal neurons. *Brain Res.*, 247, 149-153.
- HALESTRAP,A.P. & DAVIDSON,A.M. (1990). Inhibition of Ca²⁺(+)-induced large-amplitude swelling of liver and heart mitochondria by cyclosporin is probably caused by the inhibitor binding to mitochondrial-matrix peptidyl-prolyl cis-trans isomerase and preventing it interacting with the adenine nucleotide translocase. *Biochem. J.*, 268, 153-160.
- HANSSON,M.J., MATTIASSON,G., MANSSON,R., KARLSSON,J., KEEP,M.F., WALDMEIER,P., RUEGG,U.T., DUMONT,J.M., BESSEGHIR,K. & ELMER,E. (2004). The nonimmunosuppressive cyclosporin analogs NIM811 and UNIL025 display nanomolar potencies on permeability transition in brain-derived mitochondria. *J. Bioenerg. Biomembr.*, 36, 407-413.
- HAROOTUNIAN,A.T., KAO,J.P., ECKERT,B.K. & TSIEN,R.Y. (1989). Fluorescence ratio imaging of cytosolic free Na⁺ in individual fibroblasts and lymphocytes. *J. Biol. Chem.*, 264, 19458-19467.
- HARTLEY,Z. & DUBINSKY,J.M. (1993). Changes in intracellular pH associated with glutamate excitotoxicity. *Journal of Neuroscience*, 13, 4690-4699.
- HATEFI,Y. (1985). The mitochondrial electron transport and oxidative phosphorylation system. *Annu. Rev. Biochem.*, 54, 1015-1069.

- HAYASHI,T. (1954). Effects of Sodium Glutamate on the Nervous System. *Keio Journal of Medicine*, 3, 183-192.
- HAZELL,A.S. (2007). Excitotoxic mechanisms in stroke: an update of concepts and treatment strategies. *Neurochem. Int.*, 50, 941-953.
- HERBERG,L.J. & ROSE,I.C. (1989). The effect of MK-801 and other antagonists of NMDA-type glutamate receptors on brain-stimulation reward. *Psychopharmacology (Berl)*, 99, 87-90.
- HERRINGTON,J., PARK,Y.B., BABCOCK,D.F. & HILLE,B. (1996). Dominant role of mitochondria in clearance of large Ca²⁺ loads from rat adrenal chromaffin cells. *Neuron*, 16, 219-228.
- HOLLMANN,M., BOULTER,J., MARON,C., BEASLEY,L., SULLIVAN,J., PECHT,G. & HEINEMANN,S. (1993). Zinc potentiates agonist-induced currents at certain splice variants of the NMDA receptor. *Neuron*, 10, 943-954.
- HONORE,T., LAURIDSEN,J. & KROGSGAARD-LARSEN,P. (1982). The binding of [3H]AMPA, a structural analogue of glutamic acid, to rat brain membranes. *J. Neurochem.*, 38, 173-178.
- HOU,S.T. & MACMANUS,J.P. (2002). Molecular mechanisms of cerebral ischemia-induced neuronal death. *Int. Rev. Cytol.*, 221, 93-148.
- HOYT,K.R., ARDEN,S.R., AIZENMAN,E. & REYNOLDS,I.J. (1998). Reverse Na⁺/Ca²⁺ exchange contributes to glutamate-induced intracellular Ca²⁺ concentration increases in cultured rat forebrain neurons. *Mol. Pharmacol.*, 53, 742-749.
- HUETTNER,J.E. (2003). Kainate receptors and synaptic transmission. *Prog. Neurobiol.*, 70, 387-407.
- HUETTNER,J.E. & BEAN,B.P. (1988). Block of N-methyl-D-aspartate-activated current by the anticonvulsant MK-801: selective binding to open channels. *Proc. Natl. Acad. Sci. U. S. A*, 85, 1307-1311.
- IKONOMIDOU,C., BOSCH,F., MIKSA,M., BITTIGAU,P., VOCKLER,J., DIKRANIAN,K., TENKOVA,T.I., STEFOVSKA,V., TURSKI,L. & OLNEY,J.W. (1999). Blockade of NMDA receptors and apoptotic neurodegeneration in the developing brain. *Science*, 283, 70-74.
- ISHII,T., MORIYOSHI,K., SUGIHARA,H., SAKURADA,K., KADOTANI,H., YOKOI,M., AKAZAWA,C., SHIGEMOTO,R., MIZUNO,N., MASU,M. & . (1993). Molecular characterization of the family of the N-methyl-D-aspartate receptor subunits. *J. Biol. Chem.*, 268, 2836-2843.

- IWAMOTO,T. & KITA,S. (2006). YM-244769, a novel Na⁺/Ca²⁺ exchange inhibitor that preferentially inhibits NCX3, efficiently protects against hypoxia/reoxygenation-induced SH-SY5Y neuronal cell damage. *Mol. Pharmacol.*, 70, 2075-2083.
- IWAMOTO,T., WATANO,T. & SHIGEKAWA,M. (1996). A novel isothioureia derivative selectively inhibits the reverse mode of Na⁺/Ca²⁺ exchange in cells expressing NCX1. *J. Biol. Chem.*, 271, 22391-22397.
- JANSSENS,N. & LESAGE,A.S. (2001). Glutamate receptor subunit expression in primary neuronal and secondary glial cultures. *J. Neurochem.*, 77, 1457-1474.
- JEFFS,G.J., MELONI,B.P., SOKOLOW,S., HERCHUELZ,A., SCHURMANS,S. & KNUCKEY,N.W. (2007). NCX3 knockout mice exhibit increased hippocampal CA1 and CA2 neuronal damage compared to wild-type mice following global cerebral ischemia. *Exp. Neurol.*
- JOHNSON,J.W. & ASCHER,P. (1987). Glycine potentiates the NMDA response in cultured mouse brain neurons. *Nature*, 325, 529-531.
- KAKU,D.A., GIFFARD,R.G. & CHOI,D.W. (1993). Neuroprotective effects of glutamate antagonists and extracellular acidity. *Science*, 260, 1516-1518.
- KARMAZYN,M., GAN,X.T., HUMPHREYS,R.A., YOSHIDA,H. & KUSUMOTO,K. (1999). The myocardial Na⁽⁺⁾-H⁽⁺⁾ exchange: structure, regulation, and its role in heart disease. *Circ. Res.*, 85, 777-786.
- KASS,I.S. & LIPTON,P. (1986). Calcium and long-term transmission damage following anoxia in dentate gyrus and CA1 regions of the rat hippocampal slice. *J. Physiol*, 378, 313-334.
- KEW,J.N., TRUBE,G. & KEMP,J.A. (1996). A novel mechanism of activity-dependent NMDA receptor antagonism describes the effect of ifenprodil in rat cultured cortical neurones. *J. Physiol*, 497 (Pt 3), 761-772.
- KIEDROWSKI,L. (1999). N-methyl-D-aspartate excitotoxicity: relationships among plasma membrane potential, Na⁽⁺⁾/Ca⁽²⁺⁾ exchange, mitochondrial Ca⁽²⁺⁾ overload, and cytoplasmic concentrations of Ca⁽²⁺⁾, H⁽⁺⁾, and K⁽⁺⁾. *Mol. Pharmacol.*, 56, 619-632.
- KIEDROWSKI,L. (2004). High activity of K⁺-dependent plasmalemmal Na⁺/Ca²⁺ exchangers in hippocampal CA1 neurons. *Neuroreport*, 15, 2113-2116.
- KIEDROWSKI,L. (2007). NCX and NCKX operation in ischemic neurons. *Ann. N. Y. Acad. Sci.*, 1099, 383-395.

- KIEDROWSKI,L., BROOKER,G., COSTA,E. & WROBLEWSKI,J.T. (1994). Glutamate impairs neuronal calcium extrusion while reducing sodium gradient. *Neuron*, 12, 295-300.
- KIEDROWSKI,L. & COSTA,E. (1995). Glutamate-induced destabilization of intracellular calcium concentration homeostasis in cultured cerebellar granule cells: role of mitochondria in calcium buffering. *Mol. Pharmacol.*, 47, 140-147.
- KIEDROWSKI,L., CZYZ,A., BARANAUSKAS,G., LI,X.F. & LYTTON,J. (2004). Differential contribution of plasmalemmal Na/Ca exchange isoforms to sodium-dependent calcium influx and NMDA excitotoxicity in depolarized neurons. *J. Neurochem.*, 90, 117-128.
- KIM,A., KERCHNER,G. & CHIO,D. (2010). Blocking Excitotoxicity.In *CNS Neuroprotection*. ed. Marcoux,F. & Chio,D. pp. 3-36. New York: Springer.
- KIM,D.Y., KIM,S.H., CHOI,H.B., MIN,C. & GWAG,B.J. (2001). High abundance of GluR1 mRNA and reduced Q/R editing of GluR2 mRNA in individual NADPH-diaphorase neurons. *Mol. Cell Neurosci.*, 17, 1025-1033.
- KIMURA,J., MIYAMAE,S. & NOMA,A. (1987). Identification of sodium-calcium exchange current in single ventricular cells of guinea-pig. *J. Physiol*, 384, 199-222.
- KINTNER,D.B., CHEN,X., CURRIE,J., CHANANA,V., FERRAZZANO,P., BABA,A., MATSUDA,T., COHEN,M., ORLOWSKI,J., CHIU,S.Y., TAUNTON,J. & SUN,D. (2010). Excessive Na⁺/H⁺ exchange in disruption of dendritic Na⁺ and Ca²⁺ homeostasis and mitochondrial dysfunction following in vitro ischemia. *J. Biol. Chem.*, 285, 35155-35168.
- KINTNER,D.B., SU,G., LENART,B., BALLARD,A.J., MEYER,J.W., NG,L.L., SHULL,G.E. & SUN,D. (2004). Increased tolerance to oxygen and glucose deprivation in astrocytes from Na⁽⁺⁾/H⁽⁺⁾ exchanger isoform 1 null mice. *Am. J. Physiol Cell Physiol*, 287, C12-C21.
- KIRISCHUK,S., KETTENMANN,H. & VERKHRATSKY,A. (2007). Membrane currents and cytoplasmic sodium transients generated by glutamate transport in Bergmann glial cells. *Pflugers Arch.*, 454, 245-252.
- KORNHUBER,J., BORMANN,J., RETZ,W., HUBERS,M. & RIEDERER,P. (1989). Memantine displaces [3H]MK-801 at therapeutic concentrations in postmortem human frontal cortex. *Eur. J. Pharmacol.*, 166, 589-590.
- KRAFT,R. (2007). The Na⁺/Ca²⁺ exchange inhibitor KB-R7943 potently blocks TRPC channels. *Biochem. Biophys. Res. Commun.*, 361, 230-236.
- KUBIN,R. & FLETCHER,A. (1982). Fluorescence quantum yield of some rhodamine dye. *Journal of Luminescence*, 27, 456-462.

KUSHNAREVA,Y.E., WILEY,S.E., WARD,M.W., ANDREYEV,A.Y. & MURPHY,A.N. (2005). Excitotoxic injury to mitochondria isolated from cultured neurons. *J. Biol. Chem.*, 280, 28894-28902.

KWAK,S. & WEISS,J.H. (2006). Calcium-permeable AMPA channels in neurodegenerative disease and ischemia. *Curr. Opin. Neurobiol.*, 16, 281-287.

LANCELOT,E., REVAUD,M.L., BOULU,R.G., PLOTKINE,M. & CALLEBERT,J. (1997). alpha-Phenyl-N-tert-butyl nitron attenuates excitotoxicity in rat striatum by preventing hydroxyl radical accumulation. *Free Radic. Biol. Med.*, 23, 1031-1034.

LEBRUN,B., SAKAITANI,M., SHIMAMOTO,K., YASUDA-KAMATANI,Y. & NAKAJIMA,T. (1997). New beta-hydroxyaspartate derivatives are competitive blockers for the bovine glutamate/aspartate transporter. *J. Biol. Chem.*, 272, 20336-20339.

LEE,S.H., KIM,M.H., PARK,K.H., EARM,Y.E. & HO,W.K. (2002). K⁺-dependent Na⁺/Ca²⁺ exchange is a major Ca²⁺ clearance mechanism in axon terminals of rat neurohypophysis. *J. Neurosci.*, 22, 6891-6899.

LEGENDRE,P., ROSENMUND,C. & WESTBROOK,G.L. (1993). Inactivation of NMDA channels in cultured hippocampal neurons by intracellular calcium. *J. Neurosci.*, 13, 674-684.

LEHNINGER,A.L., NELSON,D.L. & COX,M.M. (1993). *Principles of Biochemistry*. New York: Worth Publishers.

LESTER,R.A., CLEMENTS,J.D., WESTBROOK,G.L. & JAHR,C.E. (1990). Channel kinetics determine the time course of NMDA receptor-mediated synaptic currents. *Nature*, 346, 565-567.

LEVY,D.I. & LIPTON,S.A. (1990). Comparison of delayed administration of competitive and uncompetitive antagonists in preventing NMDA receptor-mediated neuronal death. *Neurology*, 40, 852-855.

LI,S., JIANG,Q. & STYS,P.K. (2000). Important role of reverse Na⁽⁺⁾-Ca⁽²⁺⁾ exchange in spinal cord white matter injury at physiological temperature. *J. Neurophysiol.*, 84, 1116-1119.

LI,T., BRUSTOVETSKY,T., ANTONSSON,B. & BRUSTOVETSKY,N. (2008). Oligomeric BAX induces mitochondrial permeability transition and complete cytochrome c release without oxidative stress. *Biochim. Biophys. Acta*, 1777, 1409-1421.

LI,V., BRUSTOVETSKY,T. & BRUSTOVETSKY,N. (2009). Role of cyclophilin D-dependent mitochondrial permeability transition in glutamate-induced calcium deregulation and excitotoxic neuronal death. *Exp. Neurol.*, 218, 171-182.

- LIPTON,S.A. (2004). Failures and successes of NMDA receptor antagonists: molecular basis for the use of open-channel blockers like memantine in the treatment of acute and chronic neurologic insults. *NeuroRx*, 1, 101-110.
- LIPTON,S.A. (2006). Paradigm shift in neuroprotection by NMDA receptor blockade: memantine and beyond. *Nat. Rev. Drug Discov.*, 5, 160-170.
- LIU,J., FARMER,J.D., JR., LANE,W.S., FRIEDMAN,J., WEISSMAN,I. & SCHREIBER,S.L. (1991). Calcineurin is a common target of cyclophilin-cyclosporin A and FKBP-FK506 complexes. *Cell*, 66, 807-815.
- LIU,X.B., MURRAY,K.D. & JONES,E.G. (2004). Switching of NMDA receptor 2A and 2B subunits at thalamic and cortical synapses during early postnatal development. *J. Neurosci.*, 24, 8885-8895.
- LU,H.C., GONZALEZ,E. & CRAIR,M.C. (2001). Barrel cortex critical period plasticity is independent of changes in NMDA receptor subunit composition. *Neuron*, 32, 619-634.
- LUCAS,D.R. & NEWHOUSE,J.P. (1957). The effects of nutritional and endocrine factors on an inherited retinal degeneration in the mouse. *AMA. Arch. Ophthalmol.*, 57, 224-235.
- LUO,J., CHEN,H., KINTNER,D.B., SHULL,G.E. & SUN,D. (2005). Decreased neuronal death in Na⁺/H⁺ exchanger isoform 1-null mice after in vitro and in vivo ischemia. *J. Neurosci.*, 25, 11256-11268.
- LUO,J., WANG,Y., CHEN,H., KINTNER,D.B., CRAMER,S.W., GERDTS,J.K., CHEN,X., SHULL,G.E., PHILIPSON,K.D. & SUN,D. (2007a). A concerted role of Na⁽⁺⁾-K⁽⁺⁾-Cl⁽⁻⁾ cotransporter and Na⁽⁺⁾/Ca⁽²⁺⁾ exchanger in ischemic damage. *J. Cereb. Blood Flow Metab*, 1-10.
- LUO,J., WANG,Y., CHEN,X., CHEN,H., KINTNER,D.B., SHULL,G.E., PHILIPSON,K.D. & SUN,D. (2007b). Increased tolerance to ischemic neuronal damage by knockdown of Na⁺-Ca²⁺ exchanger isoform 1. *Ann. N. Y. Acad. Sci.*, 1099, 292-305.
- LUVISETTO,S. & AZZONE,G.F. (1989). Nature of proton cycling during gramicidin uncoupling of oxidative phosphorylation. *Biochemistry*, 28, 1100-1108.
- LYTTON,J., LI,X.F., DONG,H. & KRAEV,A. (2002). K⁺-dependent Na⁺/Ca²⁺ exchangers in the brain. *Ann. N. Y. Acad. Sci.*, 976, 382-393.
- MACDERMOTT,A.B., MAYER,M.L., WESTBROOK,G.L., SMITH,S.J. & BARKER,J.L. (1986). NMDA-receptor activation increases cytoplasmic calcium concentration in cultured spinal cord neurones. *Nature*, 321, 519-522.

- MACGREGOR,D.G., AVSHALUMOV,M.V. & RICE,M.E. (2003). Brain edema induced by in vitro ischemia: causal factors and neuroprotection. *J. Neurochem.*, 85, 1402-1411.
- MANEV,H., FAVARON,M., GUIDOTTI,A. & COSTA,E. (1989). Delayed increase of Ca²⁺ influx elicited by glutamate: role in neuronal death. *Mol. Pharmacol.*, 36, 106-112.
- MATSUDA,T., ARAKAWA,N., TAKUMA,K., KISHIDA,Y., KAWASAKI,Y., SAKAUE,M., TAKAHASHI,K., TAKAHASHI,T., SUZUKI,T., OTA,T., HAMANO-TAKAHASHI,A., ONISHI,M., TANAKA,Y., KAMEO,K. & BABA,A. (2001). SEA0400, a novel and selective inhibitor of the Na⁺-Ca²⁺ exchanger, attenuates reperfusion injury in the in vitro and in vivo cerebral ischemic models. *J. Pharmacol. Exp. Ther.*, 298, 249-256.
- MATTHEWS,C.C., ZIELKE,H.R., PARKS,D.A. & FISHMAN,P.S. (2003). Glutamate-pyruvate transaminase protects against glutamate toxicity in hippocampal slices. *Brain Res.*, 978, 59-64.
- MATTHEWS,C.C., ZIELKE,H.R., WOLLACK,J.B. & FISHMAN,P.S. (2000). Enzymatic degradation protects neurons from glutamate excitotoxicity. *J. Neurochem.*, 75, 1045-1052.
- MATTHEWS,E.K. (1986). Calcium and membrane permeability. *Br. Med. Bull.*, 42, 391-397.
- MAYER,M.L. (2005). Glutamate receptor ion channels. *Curr. Opin. Neurobiol.*, 15, 282-288.
- MAYER,M.L. & WESTBROOK,G.L. (1987). Permeation and block of N-methyl-D-aspartic acid receptor channels by divalent cations in mouse cultured central neurones. *J. Physiol*, 394, 501-527.
- MAYER-GROSS,W. & WALKER,J.W. (1947). Effect of 1(+)glutamic acid in hypoglycaemia. *Nature*, 160, 334.
- MCBAIN,C.J. & MAYER,M.L. (1994). N-methyl-D-aspartic acid receptor structure and function. *Physiol Rev.*, 74, 723-760.
- MCENTEE,W.J. & CROOK,T.H. (1993). Glutamate: its role in learning, memory, and the aging brain. *Psychopharmacology (Berl)*, 111, 391-401.
- MINELLI,A., CASTALDO,P., GOBBI,P., SALUCCI,S., MAGI,S. & AMOROSO,S. (2007). Cellular and subcellular localization of Na⁺-Ca²⁺ exchanger protein isoforms, NCX1, NCX2, and NCX3 in cerebral cortex and hippocampus of adult rat. *Cell Calcium*, 41, 221-234.

- MIYAWAKI,A., LLOPIS,J., HEIM,R., MCCAFFERY,J.M., ADAMS,J.A., IKURA,M. & TSIEN,R.Y. (1997). Fluorescent indicators for Ca²⁺ based on green fluorescent proteins and calmodulin. *Nature*, 388, 882-887.
- MONYER,H., BURNASHEV,N., LAURIE,D.J., SAKMANN,B. & SEEBURG,P.H. (1994). Developmental and regional expression in the rat brain and functional properties of four NMDA receptors. *Neuron*, 12, 529-540.
- MORRIS,R.G. (1989). Synaptic plasticity and learning: selective impairment of learning rats and blockade of long-term potentiation in vivo by the N-methyl-D-aspartate receptor antagonist AP5. *J. Neurosci.*, 9, 3040-3057.
- MOTT,D.D., DOHERTY,J.J., ZHANG,S., WASHBURN,M.S., FENDLEY,M.J., LYUBOSLAVSKY,P., TRAYNELIS,S.F. & DINGLEDINE,R. (1998). Phenylethanolamines inhibit NMDA receptors by enhancing proton inhibition. *Nat. Neurosci.*, 1, 659-667.
- MOUNT,C. & DOWNTON,C. (2006). Alzheimer disease: progress or profit? *Nat. Med.*, 12, 780-784.
- MYERS,V.B. & HAYDON,D.A. (1972). Ion transfer across lipid membranes in the presence of gramicidin A. II. The ion selectivity. *Biochim. Biophys. Acta*, 274, 313-322.
- NAMEKATA,I., KAWANISHI,T., IIDA-TANAKA,N., TANAKA,H. & SHIGENOBU,K. (2006). Quantitative fluorescence measurement of cardiac Na⁺/Ca²⁺ exchanger inhibition by kinetic analysis in stably transfected HEK293 cells. *J. Pharmacol. Sci.*, 101, 356-360.
- NEWELL,E.W., STANLEY,E.F. & SCHLICHTER,L.C. (2007). Reversed Na⁺/Ca²⁺ exchange contributes to Ca²⁺ influx and respiratory burst in microglia. *Channels (Austin.)*, 1, 366-376.
- NICHOLLS,D.G. (1986). Intracellular calcium homeostasis. *Br. Med. Bull.*, 42, 353-358.
- NICHOLLS,D.G. (2004). Mitochondrial dysfunction and glutamate excitotoxicity studied in primary neuronal cultures. *Curr. Mol. Med.*, 4, 149-177.
- NICHOLLS,D.G. & BUDD,S.L. (1998). Mitochondria and neuronal glutamate excitotoxicity. *Biochim. Biophys. Acta*, 1366, 97-112.
- NICHOLLS,D.G. & BUDD,S.L. (2000). Mitochondria and neuronal survival. *Physiol Rev.*, 80, 315-360.

- NIEMINEN,A.L., PETRIE,T.G., LEMASTERS,J.J. & SELMAN,W.R. (1996). Cyclosporin A delays mitochondrial depolarization induced by N-methyl-D-aspartate in cortical neurons: evidence of the mitochondrial permeability transition. *Neuroscience*, 75, 993-997.
- NIXON,R.A. (2003). The calpains in aging and aging-related diseases. *Ageing Res. Rev.*, 2, 407-418.
- NOWAK,L., BREGESTOVSKI,P., ASCHER,P., HERBET,A. & PROCHIANTZ,A. (1984). Magnesium gates glutamate-activated channels in mouse central neurones. *Nature*, 307, 462-465.
- OESTREICHER,A.B., VAN DEN BERGH,S.G. & SLATER,E.C. (1969). The inhibition by 2,4-dinitrophenol of the removal of oxaloacetate formed by the oxidation of succinate by rat-liver and -heart mitochondria. *Biochim. Biophys. Acta*, 180, 45-55.
- OHTSUKA,M., TAKANO,H., SUZUKI,M., ZOU,Y., AKAZAWA,H., TAMAGAWA,M., WAKIMOTO,K., NAKAYA,H. & KOMURO,I. (2004). Role of Na⁺-Ca²⁺ exchanger in myocardial ischemia/reperfusion injury: evaluation using a heterozygous Na⁺-Ca²⁺ exchanger knockout mouse model. *Biochem. Biophys. Res Commun.*, 314, 849-853.
- OKUBO,Y., SEKIYA,H., NAMIKI,S., SAKAMOTO,H., IINUMA,S., YAMASAKI,M., WATANABE,M., HIROSE,K. & IINO,M. (2010). Imaging extrasynaptic glutamate dynamics in the brain. *Proc. Natl. Acad. Sci. U. S. A*, 107, 6526-6531.
- OLNEY,J.W. (1969). Brain lesions, obesity, and other disturbances in mice treated with monosodium glutamate. *Science*, 164, 719-721.
- OLNEY,J.W., ADAMO,N.J. & RATNER,A. (1971). Monosodium glutamate effects. *Science*, 172, 294.
- OLNEY,J.W. & HO,O.L. (1970). Brain damage in infant mice following oral intake of glutamate, aspartate or cysteine. *Nature*, 227, 609-611.
- OLNEY,J.W., LABRUYERE,J. & PRICE,M.T. (1989). Pathological changes induced in cerebrocortical neurons by phencyclidine and related drugs. *Science*, 244, 1360-1362.
- OLNEY,J.W. & SHARPE,L.G. (1969). Brain lesions in an infant rhesus monkey treated with monosodium glutamate. *Science*, 166, 386-388.
- ORLOWSKI,J. & GRINSTEIN,S. (1997). Na⁺/H⁺ exchangers of mammalian cells. *J. Biol. Chem.*, 272, 22373-22376.

OUARDOUZ,M., ZAMPONI,G.W., BARR,W., KIEDROWSKI,L. & STYS,P.K. (2005). Protection of ischemic rat spinal cord white matter: Dual action of KB-R7943 on Na⁺/Ca²⁺ exchange and L-type Ca²⁺ channels. *Neuropharmacology*, 48, 566-575.

PALMADA,M. & CENTELLES,J.J. (1998). Excitatory amino acid neurotransmission. Pathways for metabolism, storage and reuptake of glutamate in brain. *Front Biosci.*, 3, d701-d718.

PESHAVARIYA,H.M., DUSTING,G.J. & SELEMIDIS,S. (2007). Analysis of dihydroethidium fluorescence for the detection of intracellular and extracellular superoxide produced by NADPH oxidase. *Free Radic. Res.*, 41, 699-712.

PITT,D., WERNER,P. & RAINE,C.S. (2000). Glutamate excitotoxicity in a model of multiple sclerosis. *Nat. Med.*, 6, 67-70.

PIVOVAROVA,N.B., NGUYEN,H.V., WINTERS,C.A., BRANTNER,C.A., SMITH,C.L. & ANDREWS,S.B. (2004). Excitotoxic calcium overload in a subpopulation of mitochondria triggers delayed death in hippocampal neurons. *J. Neurosci.*, 24, 5611-5622.

PLANELLS-CASES,R., LERMA,J. & FERRER-MONTIEL,A. (2006). Pharmacological intervention at ionotropic glutamate receptor complexes. *Curr. Pharm. Des.*, 12, 3583-3596.

PLATT,S.R. (2007). The role of glutamate in central nervous system health and disease--a review. *Vet. J.*, 173, 278-286.

PRICE,J., WAELSCH,H. & PUTNAM,T. (1943). dl-Glutamic Acid Hydrochloride in treatment of Petit Mal and Psychomotor Seizures. *The Journal of the American Medical Association*, 122, 1153-1156.

RAJESH,K.G., SASAGURI,S., SUZUKI,R. & MAEDA,H. (2003). Antioxidant MCI-186 inhibits mitochondrial permeability transition pore and upregulates Bcl-2 expression. *Am. J. Physiol Heart Circ. Physiol*, 285, H2171-H2178.

REICHLING,D.B. & MACDERMOTT,A.B. (1991). Lanthanum actions on excitatory amino acid-gated currents and voltage-gated calcium currents in rat dorsal horn neurons. *J. Physiol*, 441, 199-218.

REPPPEL,M., SASSE,P., MALAN,D., NGUEMO,F., REUTER,H., BLOCH,W., HESCHELER,J. & FLEISCHMANN,B.K. (2007). Functional expression of the Na⁺/Ca²⁺ exchanger in the embryonic mouse heart. *J. Mol. Cell Cardiol.*, 42, 121-132.

REYNOLDS,I.J. & MILLER,R.J. (1989). Ifenprodil is a novel type of N-methyl-D-aspartate receptor antagonist: interaction with polyamines. *Mol. Pharmacol.*, 36, 758-765.

- RINK,T.J., TSIEN,R.Y. & POZZAN,T. (1982). Cytoplasmic pH and free Mg²⁺ in lymphocytes. *J. Cell Biol.*, 95, 189-196.
- ROBINSON,D.M. & KEATING,G.M. (2006). Memantine: a review of its use in Alzheimer's disease. *Drugs*, 66, 1515-1534.
- ROGAWSKI,M.A. & WENK,G.L. (2003). The neuropharmacological basis for the use of memantine in the treatment of Alzheimer's disease. *CNS. Drug Rev.*, 9, 275-308.
- ROSENMUND,C., STERN-BACH,Y. & STEVENS,C.F. (1998). The tetrameric structure of a glutamate receptor channel. *Science*, 280, 1596-1599.
- ROSENMUND,C. & WESTBROOK,G.L. (1993). Calcium-induced actin depolymerization reduces NMDA channel activity. *Neuron*, 10, 805-814.
- ROTTENBERG,H. & KOEPPE,R.E. (1989). Mechanism of uncoupling of oxidative phosphorylation by gramicidin. *Biochemistry*, 28, 4355-4360.
- RUIZ,F., ALVAREZ,G., RAMOS,M., HERNANDEZ,M., BOGONEZ,E. & SATRUSTEGUI,J. (2000). Cyclosporin A targets involved in protection against glutamate excitotoxicity. *Eur. J. Pharmacol.*, 404, 29-39.
- RUNG,J.P., CARLSSON,A., RYDEN,M.K. & CARLSSON,M.L. (2005). (+)-MK-801 induced social withdrawal in rats; a model for negative symptoms of schizophrenia. *Prog. Neuropsychopharmacol. Biol. Psychiatry*, 29, 827-832.
- SACCO,R.L., CHONG,J.Y., PRABHAKARAN,S. & ELKIND,M.S. (2007). Experimental treatments for acute ischaemic stroke. *Lancet*, 369, 331-341.
- SAKAUE,M., NAKAMURA,H., KANEKO,I., KAWASAKI,Y., ARAKAWA,N., HASHIMOTO,H., KOYAMA,Y., BABA,A. & MATSUDA,T. (2000). Na⁽⁺⁾-Ca⁽²⁺⁾ exchanger isoforms in rat neuronal preparations: different changes in their expression during postnatal development. *Brain Res*, 881, 212-216.
- SALINSKA,E., DANYSZ,W. & LAZAREWICZ,J.W. (2005). The role of excitotoxicity in neurodegeneration. *Folia Neuropathol.*, 43, 322-339.
- SANTO-DOMINGO,J., VAY,L., HERNANDEZ-SANMIGUEL,E., LOBATON,C.D., MORENO,A., MONTERO,M. & ALVAREZ,J. (2007). The plasma membrane Na⁺/Ca²⁺ exchange inhibitor KB-R7943 is also a potent inhibitor of the mitochondrial Ca²⁺ uniporter. *Br. J. Pharmacol.*, 151, 647-654.
- SCHIFITTO,G., NAVIA,B.A., YIANNOUTSOS,C.T., MARRA,C.M., CHANG,L., ERNST,T., JARVIK,J.G., MILLER,E.N., SINGER,E.J., ELLIS,R.J., KOLSON,D.L., SIMPSON,D., NATH,A., BERGER,J., SHRIVER,S.L., MILLAR,L.L., COLQUHOUN,D., LENKINSKI,R., GONZALEZ,R.G. & LIPTON,S.A. (2007).

Memantine and HIV-associated cognitive impairment: a neuropsychological and proton magnetic resonance spectroscopy study. *AIDS*, 21, 1877-1886.

SCHINZEL,A.C., TAKEUCHI,O., HUANG,Z., FISHER,J.K., ZHOU,Z., RUBENS,J., HETZ,C., DANIAL,N.N., MOSKOWITZ,M.A. & KORSMEYER,S.J. (2005). Cyclophilin D is a component of mitochondrial permeability transition and mediates neuronal cell death after focal cerebral ischemia. *Proc. Natl. Acad. Sci. U. S. A*, 102, 12005-12010.

SCHNEIDER,D., GERHARDT,E., BOCK,J., MULLER,M.M., WOLBURG,H., LANG,F. & SCHULZ,J.B. (2004). Intracellular acidification by inhibition of the Na⁺/H⁺-exchanger leads to caspase-independent death of cerebellar granule neurons resembling paraptosis. *Cell Death. Differ.*, 11, 760-770.

SCHONFELD,P. & REISER,G. (2007). Ca²⁺ storage capacity of rat brain mitochondria declines during the postnatal development without change in ROS production capacity. *Antioxid. Redox. Signal.*, 9, 191-199.

SCHRODER,U.H., BREDER,J., SABELHAUS,C.F. & REYMANN,K.G. (1999). The novel Na⁺/Ca²⁺ exchange inhibitor KB-R7943 protects CA1 neurons in rat hippocampal slices against hypoxic/hypoglycemic injury. *Neuropharmacology*, 38, 319-321.

SECONDO,A., STAIANO,R.I., SCORZIELLO,A., SIRABELLA,R., BOSCIA,F., ADORNETTO,A., VALSECCHI,V., MOLINARO,P., CANZONIERO,L.M., DI RENZO,G. & ANNUNZIATO,L. (2007). BHK cells transfected with NCX3 are more resistant to hypoxia followed by reoxygenation than those transfected with NCX1 and NCX2: Possible relationship with mitochondrial membrane potential. *Cell Calcium*, 42, 521-535.

SHALBUYEVA,N., BRUSTOVETSKY,T. & BRUSTOVETSKY,N. (2007). Lithium desensitizes brain mitochondria to calcium, antagonizes permeability transition, and diminishes cytochrome C release. *J. Biol. Chem.*, 282, 18057-18068.

SHI,S.H., HAYASHI,Y., PETRALIA,R.S., ZAMAN,S.H., WENTHOLD,R.J., SVOBODA,K. & MALINOW,R. (1999). Rapid spine delivery and redistribution of AMPA receptors after synaptic NMDA receptor activation. *Science*, 284, 1811-1816.

SIMON,R.P., SWAN,J.H., GRIFFITHS,T. & MELDRUM,B.S. (1984). Blockade of N-methyl-D-aspartate receptors may protect against ischemic damage in the brain. *Science*, 226, 850-852.

SMALL,D.L. & BUCHAN,A.M. (1997). NMDA antagonists: their role in neuroprotection. *Int. Rev. Neurobiol.*, 40, 137-171.

SMITH,G.L., ELLIOTT,E.E., KETTLEWELL,S., CURRIE,S. & QUINN,F.R. (2006). Na(+)/Ca(2+) exchanger expression and function in a rabbit model of myocardial infarction. *J. Cardiovasc. Electrophysiol.*, 17 Suppl 1, S57-S63.

SOBOLEVSKY,A.I. & KHODOROV,B.I. (1999). Blockade of NMDA channels in acutely isolated rat hippocampal neurons by the Na⁺/Ca²⁺ exchange inhibitor KB-R7943. *Neuropharmacology*, 38, 1235-1242.

SONG,I. & HUGANIR,R.L. (2002). Regulation of AMPA receptors during synaptic plasticity. *Trends Neurosci.*, 25, 578-588.

STANIKA,R.I., PIVOVAROVA,N.B., BRANTNER,C.A., WATTS,C.A., WINTERS,C.A. & ANDREWS,S.B. (2009). Coupling diverse routes of calcium entry to mitochondrial dysfunction and glutamate excitotoxicity. *Proc. Natl. Acad. Sci. U. S. A.*, 106, 9854-9859.

STEPHENSON,F.A. (2006). Structure and trafficking of NMDA and GABA_A receptors. *Biochem. Soc. Trans.*, 34, 877-881.

STOROZHEVYKH,T.P., SENILOVA,Y.E., BRUSTOVETSKY,T., PINELIS,V.G. & BRUSTOVETSKY,N. (2010). Neuroprotective effect of KB-R7943 against glutamate excitotoxicity is related to mild mitochondrial depolarization. *Neurochem. Res.*, 35, 323-335.

STOUT,A.K., RAPHAEL,H.M., KANTEREWICZ,B.I., KLANN,E. & REYNOLDS,I.J. (1998). Glutamate-induced neuron death requires mitochondrial calcium uptake. *Nat. Neurosci.*, 1, 366-373.

SUN,L., SHIPLEY,M.T. & LIDOW,M.S. (2000). Expression of NR1, NR2A-D, and NR3 subunits of the NMDA receptor in the cerebral cortex and olfactory bulb of adult rat. *Synapse*, 35, 212-221.

THAYER,S.A. & MILLER,R.J. (1990). Regulation of the intracellular free calcium concentration in single rat dorsal root ganglion neurones in vitro. *J. Physiol*, 425, 85-115.

THURNEYSEN,T., NICOLL,D.A., PHILIPSON,K.D. & PORZIG,H. (2002a). Immunohistochemical detection of the sodium-calcium exchanger in rat hippocampus cultures using subtype-specific antibodies. *Ann. N. Y. Acad. Sci.*, 976, 367-375.

THURNEYSEN,T., NICOLL,D.A., PHILIPSON,K.D. & PORZIG,H. (2002b). Sodium/calcium exchanger subtypes NCX1, NCX2 and NCX3 show cell-specific expression in rat hippocampus cultures. *Brain Res Mol. Brain Res*, 107, 145-156.

TRAPP,S., LUCKERMANN,M., KAILA,K. & BALLANYI,K. (1996). Acidosis of hippocampal neurones mediated by a plasmalemmal Ca²⁺/H⁺ pump. *Neuroreport*, 7, 2000-2004.

- TSUZUKI,K., MOCHIZUKI,S., IINO,M., MORI,H., MISHINA,M. & OZAWA,S. (1994). Ion permeation properties of the cloned mouse epsilon 2/zeta 1 NMDA receptor channel. *Brain Res Mol. Brain Res*, 26, 37-46.
- TYMIANSKI,M., CHARLTON,M.P., CARLEN,P.L. & TATOR,C.H. (1993a). Secondary Ca²⁺ overload indicates early neuronal injury which precedes staining with viability indicators. *Brain Res*, 607, 319-323.
- TYMIANSKI,M., CHARLTON,M.P., CARLEN,P.L. & TATOR,C.H. (1993b). Source specificity of early calcium neurotoxicity in cultured embryonic spinal neurons. *J. Neurosci.*, 13, 2085-2104.
- TYMIANSKI,M., CHARLTON,M.P., CARLEN,P.L. & TATOR,C.H. (1994). Properties of neuroprotective cell-permeant Ca²⁺ chelators: effects on [Ca²⁺]_i and glutamate neurotoxicity in vitro. *J. Neurophysiol.*, 72, 1973-1992.
- TYMIANSKI,M., WALLACE,M.C., SPIGELMAN,I., UNO,M., CARLEN,P.L., TATOR,C.H. & CHARLTON,M.P. (1993c). Cell-permeant Ca²⁺ chelators reduce early excitotoxic and ischemic neuronal injury in vitro and in vivo. *Neuron*, 11, 221-235.
- VIGNE,P., FRELIN,C., CRAGOE,E.J., JR. & LAZDUNSKI,M. (1983). Ethylisopropyl-amiloride: a new and highly potent derivative of amiloride for the inhibition of the Na⁺/H⁺ exchange system in various cell types. *Biochem. Biophys. Res. Commun.*, 116, 86-90.
- VILLOSLADA,P., ARRONDO,G., SEPULCRE,J., ALEGRE,M. & ARTIEDA,J. (2009). Memantine induces reversible neurologic impairment in patients with MS. *Neurology*, 72, 1630-1633.
- VOLBRACHT,C., VAN,B.J., ZHU,C., BLOMGREN,K. & LEIST,M. (2006). Neuroprotective properties of memantine in different in vitro and in vivo models of excitotoxicity. *Eur. J. Neurosci.*, 23, 2611-2622.
- WALDMEIER,P.C., FELDTRAUER,J.J., QIAN,T. & LEMASTERS,J.J. (2002). Inhibition of the mitochondrial permeability transition by the nonimmunosuppressive cyclosporin derivative NIM811. *Mol. Pharmacol.*, 62, 22-29.
- WANG,G.J., RANDALL,R.D. & THAYER,S.A. (1994). Glutamate-induced intracellular acidification of cultured hippocampal neurons demonstrates altered energy metabolism resulting from Ca²⁺ loads. *J. Neurophysiol.*, 72, 2563-2569.
- WANG,G.J. & THAYER,S.A. (1996). Sequestration of glutamate-induced Ca²⁺ loads by mitochondria in cultured rat hippocampal neurons. *J. Neurophysiol.*, 76, 1611-1621.

- WANG,Y., BRITAIN,J.M., WILSON,S.M., HINGTGEN,C.M. & KHANNA,R. (2010). ALTERED CALCIUM CURRENTS AND AXONAL GROWTH IN Nf1 HAPLOINSUFFICIENT MICE. *Transl. Neurosci.*, 1, 106-114.
- WATANABE,Y. & KIMURA,J. (2000). Inhibitory effect of amiodarone on Na(+)/Ca(2+) exchange current in guinea-pig cardiac myocytes. *Br. J. Pharmacol.*, 131, 80-84.
- WATANABE,Y., KOIDE,Y. & KIMURA,J. (2006). Topics on the Na⁺/Ca²⁺ exchanger: pharmacological characterization of Na⁺/Ca²⁺ exchanger inhibitors. *J. Pharmacol. Sci.*, 102, 7-16.
- WEIL-MALHERBE,H. (1950). Significance of glutamic acid for the metabolism of nervous tissue. *Physiol Rev.*, 30, 549-568.
- WHITE,R.J. & REYNOLDS,I.J. (1996). Mitochondrial depolarization in glutamate-stimulated neurons: an early signal specific to excitotoxin exposure. *J. Neurosci.*, 16, 5688-5697.
- WHITE,R.J. & REYNOLDS,I.J. (1997). Mitochondria accumulate Ca²⁺ following intense glutamate stimulation of cultured rat forebrain neurones. *J. Physiol*, 498 (Pt 1), 31-47.
- WILLIAMS,K. (1993). Ifenprodil discriminates subtypes of the N-methyl-D-aspartate receptor: selectivity and mechanisms at recombinant heteromeric receptors. *Mol. Pharmacol.*, 44, 851-859.
- WOLF,J.A., STYS,P.K., LUSARDI,T., MEANEY,D. & SMITH,D.H. (2001). Traumatic axonal injury induces calcium influx modulated by tetrodotoxin-sensitive sodium channels. *J. Neurosci.*, 21, 1923-1930.
- WON,S.J., KIM,D.Y. & GWAG,B.J. (2002). Cellular and molecular pathways of ischemic neuronal death. *J. Biochem. Mol. Biol.*, 35, 67-86.
- WU,M.L., CHEN,J.H., CHEN,W.H., CHEN,Y.J. & CHU,K.C. (1999). Novel role of the Ca(2+)-ATPase in NMDA-induced intracellular acidification. *Am. J. Physiol*, 277, C717-C727.
- WU,M.P., KAO,L.S., LIAO,H.T. & PAN,C.Y. (2008). Reverse mode Na⁺/Ca²⁺ exchangers trigger the release of Ca²⁺ from intracellular Ca²⁺ stores in cultured rat embryonic cortical neurons. *Brain Res.*, 1201, 41-51.
- XIONG,Z.G., ZHU,X.M., CHU,X.P., MINAMI,M., HEY,J., WEI,W.L., MACDONALD,J.F., WEMMIE,J.A., PRICE,M.P., WELSH,M.J. & SIMON,R.P. (2004). Neuroprotection in ischemia: blocking calcium-permeable acid-sensing ion channels. *Cell*, 118, 687-698.

- XU,W., WONG,T.P., CHERY,N., GAERTNER,T., WANG,Y.T. & BAUDRY,M. (2007). Calpain-mediated mGluR1alpha truncation: a key step in excitotoxicity. *Neuron*, 53, 399-412.
- YAMAGUCHI,K. & OHMORI,H. (1990). Voltage-gated and chemically gated ionic channels in the cultured cochlear ganglion neurone of the chick. *J. Physiol*, 420, 185-206.
- YAMAGUCHI,S., DONEVAN,S.D. & ROGAWSKI,M.A. (1993). Anticonvulsant activity of AMPA/kainate antagonists: comparison of GYKI 52466 and NBOX in maximal electroshock and chemoconvulsant seizure models. *Epilepsy Res.*, 15, 179-184.
- YAO,H., MA,E., GU,X.Q. & HADDAD,G.G. (1999). Intracellular pH regulation of CA1 neurons in Na(+)/H(+) isoform 1 mutant mice. *J. Clin. Invest*, 104, 637-645.
- YU,S.P. & CHOI,D.W. (1997). Na(+)-Ca²⁺ exchange currents in cortical neurons: concomitant forward and reverse operation and effect of glutamate. *Eur. J. Neurosci.*, 9, 1273-1281.
- YUAN,Z., CAI,T., TIAN,J., IVANOV,A.V., GIOVANNUCCI,D.R. & XIE,Z. (2005). Na/K-ATPase tethers phospholipase C and IP3 receptor into a calcium-regulatory complex. *Mol. Biol. Cell*, 16, 4034-4045.
- ZHANG,G.H. & MELVIN,J.E. (1996). Na⁺-dependent release of Mg²⁺ from an intracellular pool in rat sublingual mucous acini. *J. Biol. Chem.*, 271, 29067-29072.
- ZIMMERMAN,F.T., BURGEMEISTER,B.B. & PUTNAM,T.J. (1947). A group study of the effect of glutamic acid upon mental functioning in children and adolescents. *Psychosom. Med.*, 9, 175-183.
- ZIMMERMAN,F.T., BURGEMEISTER,B.B. & PUTNAM,T.J. (1948). The ceiling effect of glutamic acid upon intelligence in children and in adolescents. *Am. J. Psychiatry*, 104, 593-599.
- ZORATTI,M. & SZABO,I. (1995). The mitochondrial permeability transition. *Biochim. Biophys. Acta*, 1241, 139-176.

CURRICULUM VITAE

Matthew K. Brittain

Education:

Indiana University, Indianapolis, IN

Doctor of Philosophy in Toxicology.....2012

Dissertation: "The role of the NMDA receptor and reverse sodium calcium exchanger in calcium dysregulation in glutamate exposed neurons"

University of Southern Indiana, Evansville, IN

B.S. Chemistry, American Chemical Society (ACS) certified.....2005

- Research, Innovation, Scholarship, and Creativity Fellowship: 2004, 2005
 - research grant for lab supplies and travel expenses for scientific conferences
- minor in Psychology

University of Southern Indiana, Evansville, IN

B.S. Biology.....2005

Honors, Awards, and Fellowships:

- American Heart Association pre-doctoral fellowship 10PRE4300005
(Midwest affiliate)

PROFESSIONAL AFFILIATIONS:

- Society for Neuroscience (SfN), student member 2009-present
- Society of Toxicology (SOT), student member 2010-present

PUBLICATIONS, PRESENTATIONS, AND ABSTRACTS:

- Ifenprodil, a NR2B-selective antagonist of the NMDA receptor, inhibits reverse $\text{Na}^+/\text{Ca}^{2+}$ exchanger in neurons. Brittain MK, Brustovetsky T, Brustovetsky N., *Manuscript accepted, Neuropharmacology*.
- Simultaneous inhibition of NMDA receptor and reverse $\text{Na}^+/\text{Ca}^{2+}$ exchanger is required to prevent glutamate-induced calcium dysregulation in hippocampal neurons. Brittain MK, Brustovetsky T, Sheets PL, Cummins TR, Brustovetsky N., abstract/poster presentation, SfN National Meeting, Washington DC. Nov 2011.
- Delayed calcium dysregulation in neurons requires both NMDA receptor and the reverse $\text{Na}^+/\text{Ca}^{2+}$ exchanger. Brittain MK, Brustovetsky T, Sheets PL, Brittain JM, Khanna R, Cummins TR, Brustovetsky N., *Neurobiol Dis.*, 2012; 46(1): 109-117.
- KB-R7943, an inhibitor of the reverse $\text{Na}^+/\text{Ca}^{2+}$ exchanger, blocks N-methyl-D-aspartate receptor and inhibits mitochondrial complex I. Brustovetsky T, Brittain MK, Sheets PL, Cummins TR, Pinelis V, Brustovetsky N., *Br J Pharmacol*. 2011 Jan;162(1):255-70.
- KB-R7943, an inhibitor of the reverse $\text{Na}^+/\text{Ca}^{2+}$ exchanger, inhibits Complex I in the mitochondrial respiratory chain and blocks N-methyl-D-

aspartate receptor. Brittain MK, Brustovetsky T, Sheets PL, Cummins TR, Brustovetsky N., abstract/poster presentation, SfN National Meeting, San Diego, CA. Nov 2010.

- Role of reverse $\text{Na}^+/\text{Ca}^{2+}$ exchange in sustained elevation of cytosolic Ca^{2+} in hippocampal neurons exposed to glutamate. Brittain MK, Brustovetsky T, Sheets PL, Cummins TR, Brustovetsky N., abstract/poster presentation, SfN National Meeting, Chicago, IL. Oct 2009.
- Undergraduate Abstracts and Presentations
 - National Conference on Undergraduate Research (NCUR), Lexington, VA. April 2005 - poster presentation.
 - Actin filament formation changes during the Aphanoplasmodial and Coralloid Plasmodial stages of *Stemonitis flavogenita* life cycle. Brittain MK, Collins J., Publication: 2005 edition of NCUR.
 - ACS National Meeting, Philadelphia, PA: Aug '04 and San Diego, CA: Mar '05 - abstract/poster presentation